Exploring Therapeutic Opportunities Against Gain-of-Function-Mutant P53 Harboring Cancer Cells Through Regulation of Protein Homeostatic Machinery

THESIS

Submitted in partial fulfillment

of the requirements for the degree of

DOCTOR OF PHILOSOPHY
by

Ms. Heena Saini

2015PHXF0402P

Under the Supervision of

Prof. Rajdeep Chowdhury

&

Co-Supervision of

Prof. Shibasish Chowdhury

BITS Pilani
Pilani | Dubai | Goa | Hyderabad
BIRLA INSTITUTE OF TECHNOLOGY AND SCIENCE
PILANI

2021

Table of contents

BIRLA INSTITUTE OF TECHNOLOGY AND SCIENCE,

PILANI

CERTIFICATE

This is to certify that the thesis entitled **"Exploring Therapeutic Opportunities Against Gain-of-Function-Mutant P53 Harboring Cancer Cells Through Regulation of Protein Homeostatic Machinery"** and submitted by **Ms. Heena Saini** ID No**. 2015PHXF0402P** for award of Ph.D. of the institute embodies original work done by her under my supervision.

Signature of the Supervisor:

Prof. Rajdeep Chowdhury

Associate Professor

Department of Biological Sciences

Birla Institute of Technology and Science,

Pilani

Pilani campus, Rajasthan

Signature of the Co-Supervisor:

Prof. Shibasish Chowdhury

Associate Professor

Department of Biological Sciences

Birla Institute of Technology and Science,

Pilani

Pilani campus, Rajasthan

Date: 13. 08. 21

Acknowledgment

One of the delights of completing my research work is to look over the journey and remember everyone who has supported me along this long but satisfying road. I would, hereby, like to express my gratitude towards all those people who have helped me during my Ph.D. tenure and without whose support completing this work would be impossible.

First and foremost, I want to thank my Ph.D. supervisor Prof. Rajdeep Chowdhury and co-supervisor Prof. Shibasish Chowdhury, Department of Biological Sciences, BITS-Pilani, Pilani Campus. I owe them sincere gratitude for providing me the opportunity to work under their supervision. Their guidance, encouragement, and stimulating discussions were indispensable for the successful completion of this thesis. I appreciate all their contributions of time, ideas, and motivation to make my Ph.D. experience productive and learning. I am thankful to my DAC members, Dr. Sudeshna Mukherjee, Department of Biological Sciences, BITS-Pilani, Pilani Campus, and Prof. Sandhya Mehrotra, Department of Biological Sciences, BITS-Pilani, K.K. Birla Goa Campus for their constructive evaluation of the research work. I especially thank Dr. Sudeshna Mukherjee for being a pillar of support. I strongly feel that she has helped me in inculcating a strong attitude towards life and I will always keep learning from her.

With due respect, I acknowledge Prof. Souvik Bhattacharyya, Vice-Chancellor, BITS Pilani, and Prof. Sudhirkumar Barai, Director, BITS Pilani, Pilani campus for providing me the infrastructure to carry out the research in their premier institute, BITS-Pilani, Pilani Campus. I also thank Prof. Jitendra Panwar, Associate Dean, AGSRD, Prof. Shibasish Chowdhury Convener, Departmental Research Committee, Prof. P.N. Jha, Former HOD, Department of Biological Sciences, Prof. P.R. Deepa, HOD, Department of Biological Sciences, BITS Pilani for their timely guidance and support regarding the academic formalities throughout the thesis work. I would also like to acknowledge the faculties at BITS-Pilani for letting me

use their lab facilities and providing a critical review of my work in the presentations I gave in the institute. I especially thank Prof. A.K Das and Dr. Syamantak Majumder, Department of Biological Sciences for always listening to my doubts and providing me solutions with an enthusiastic and smiling face. I acknowledge Prof. A.K. Das for asking about my well-being every time we meet. I owe a special thanks to the non-teaching staff, especially Mukesh Ji, for providing me with the pre-requisites for my experiments. I thank DBT, BITS-Pilani, and CSIR for providing me research fellowship.

It was my privilege to have seniors like Dr. Zarna Pala, Dr. Gagandeep Singh Saggu, Dr. Anuradha, Dr. Vajir Malik, Dr. Vikram, Dr. Vidushi, Ms. Shraddha, Mr. Sandeep, Ms. Poonam, Mr. Vikas, Ms. Tripti who have guided me and helped me whenever I was stuck.

I would like to thank my lab seniors cum friends Dr. Subhra Dash and Dr. Leena Fageria who were a great source of inspiration and encouragement. I owe them heartfelt gratitude for being there with me in all ups and downs of my professional or personal life. In them, I have earned friends for life. I am also grateful to my labmates Ms. Abhilasha, Ms. Ankita Daiya, Ms. Ankita Sharma, Mr. Anirudha Sahu, Ms. Propanna Bandyopadhyay, Ms. Mahima Chaudhary, Ms. Subhashree Chatterjee who have helped me in innumerable ways. All the doubts they have asked me helped me be a better researcher and a good team player. I cannot thank them enough for all the respect, love, and care they have showered on me. I would always cherish the time that I have spent with them.

I would also like to take the opportunity to thank Mr. Sumukh, Mr. Raghav, Ms. Niyati, Ms. Ashima, Mr. Yash, Mr. Ramakrishnan, Ms. Sonia, Ms. Hansa, Mr. Shreyas, Ms. Harshita, Ms. Swarnima, Ms. Smita, Mr. Ashish, Ms. Aastha, Ms. Swati, Ms. Swetha, Ms. Nidhi, Mr. Shobham who with their helping attitude and fun-filled discussions have always made the time spent in the lab even more cherished. I would also like to thank the thesis students Mr. Lohitesh, Ms. Sukanya, Ms. Ifrah, Ms. Vishakha, Ms. Shivangi, Ms. Tejasvini, Ms. Srinidhi,

and Ms. Sanhita who were always ready to help me in all the possible ways. Their all-time ready-to-work attitude kept me motivated enough to work hard. The journey of Ph.D. became fun and stimulating with them. A special thanks to my friends and batchmates, Dr. Heema, Dr. Nisha, Dr. Kishan Italiya, Dr. Krishna, Dr. Zeeshan, Mr. Shahid, Mr. Ginson, Ms. Neelam, Ms. Pracheta for making this journey memorable. They have always been my hangout buddies whenever I needed a break from my experiments. I may not be able to write all the names here but there were many students at BITS-Pilani who have helped me throughout and I shall always be indebted for their help.

I express my heartfelt thanks to Dr. Neeru Saini and her lab members- Dr. Ravindresh, Dr. Yogita Adlakha, Dr. Vikas Yadav, Dr. Richa Dubey, Dr. Richa Singh, Dr. Shruti Chowdhary, Dr. Pallavi Varshney, Mr. Sachin Kumar who taught me numerous techniques during my stay in CSIR-IGIB. They made me realize that I can do research.

My list of acknowledgments will be incomplete without special mention of my family, who has been there from the beginning till the end and made this experience more fulfilling by providing me support and motivation from time to time. I feel blessed for having parents like my Mummy and Papa. The unconditional love and support of my brother Isht and Sunny and my bhabhi cum sisters Megha and Nikita is beyond expression in words. I also feel grateful to have an understanding and supportive in-law. Their faith and love have not just made this journey easy for me but it has been an inspiration for every girl who wants to pursue her career even after getting married.

Words are not enough to express my feelings for Dr. Pankaj Saini, my husband (truly my better half) for his unconditional love and constant support. Without him, this journey would have been impossible.

Above all, I owe my continuing gratitude to the almighty for everything.

Heena Saini

Abstract

Cancer is one of the leading causes of death worldwide. Among the top occurring cancers, lung cancer is the second most prevalent; and it shares the highest cancer mortality rate across the world. Reportedly, non-small cell lung carcinoma (NSCLC) comprises more than 85% of the lung cancer burden and develops through progressive genomic alterations. These genomic alterations are often associated with disease pathogenesis and hindrance to first-line treatment therapy. Therefore, understanding the alterations and designing appropriate strategies to curb their deleterious effect is important from the perspective of cancer therapeutics.

In this study, we initially analyzed the NSCLC patient data from the publicly available cancer database. Interestingly, we observed that the tumor suppressor- p53 is amongst the top mutated genes in NSCLC patients. Importantly, mutations in p53 decreased the survival probability of NSCLC patients in comparison to patients bearing wild-type (WT) -p53. Herein, it is well known that acquisition of mutation at a specific locus in P53 often imparts this key protein with a gain of function (GOF) property classically absent in its WT form. Intriguingly, the GOF-P53 can impart a contrasting pro-tumorigenic function. This signifies the importance of studying GOF mutations in P53 and its relevance in NSCLC progression. We further observed that in NSCLCs, P53 is prone to missense mutations, and the probability of harboring a GOF-R273H-P53 mutation is considerably high. Therefore, to understand the molecular effects imparted by this GOF-P53 and design appropriate therapeutic strategies, in this study, we prepared a stably transfected R273H-P53 *in vitro* model in H1299 cells (P53 null NSCLCs) and compared its characteristics with empty vector (EV) or WT-P53 transfected cells. Interestingly, the presence of R273H-P53 resulted in decreased sensitivity to chemotherapeutic agents, like cisplatin, not only in NSCLCs but also in other cancer types establishing its role in therapy resistance. The fact that P53 protein turnover is controlled by the ubiquitin proteasomal system (UPS), and importantly GOF-P53 proteins are reported to have

higher stability resulting in an increased half-life can provide a therapeutic opportunity based on interference of protein degradation. We hypothesized that proteasome inhibitors (PIs) might induce pronounced proteotoxic stress in cells with R273H-P53 by over-accumulated protein response. The R273H-P53 harboring H1299 cells showed sensitivity to PI treatment and it simultaneously resulted in compensatory activation of the other cellular homeostatic and protein turnover process-autophagy. Importantly, an induction of autophagy increased PI-induced cytotoxicity. In this context, we observed that autophagy enhancement along with PI, played a pro-death role *via* enhancement of cellular reactive oxygen species (ROS) and through ERK signaling in the R273H-P53 harboring NSCLC cells. These results demonstrate a probable strategy of sensitizing R273H-P53 harboring cancer cells by exploiting the crosstalk between UPS and autophagy.

To understand the effect of GOF-P53 on cellular transcriptomic expression pattern, we extracted RNA sequencing and ChiP-seq data available over web source for H1299 cells transfected with R273H-P53. Further analysis revealed an increased expression of the potent transcription factor-TEAD1, the binding partner of Yes-associated protein (YAP) and its downstream targets. In addition to the above, through *in vitro* analysis, we observed that a feedback loop exists between GOF-P53 and YAP in NSCLC cells regulating cellular proliferation. Therefore, a therapeutic strategy that can attenuate the effect of both these proteins can be critical to inhibition of NSCLC proliferation. Importantly, GOF-P53 and YAP were found to have intense crosstalk with autophagy. We, therefore, decided to inhibit autophagy in NSCLC cells and observe its impact on cellular proliferation. Interestingly, as we treated NSCLC cells with the autophagy inhibitor- CQ, it resulted in a considerable growth arrest. This was accompanied by a CQ-induced cytoplasmic co-localization of GOF-P53 and YAP proteins. This might be attributed to the non-dividing state of the CQ exposed cells. Importantly, a withdrawal of CQ from the culture medium resulted in reversal of features, characterized by decreased cytoplasmic accumulation of GOF-P53/YAP and resumption of cellular proliferative ability suggesting a transitory effect imparted by CQ. We, therefore assume that CQ has

a growth inhibitory effect on NSCLC cells, however, to our understanding its effects observed in the R273H-P53 harboring NSCLC cells might not be restricted exclusively to its autophagy inhibitory role, but can be resultant of autophagy-independent effects as well.

Given the importance of UPS and autophagy in the regulation of cellular homeostasis we further decided to explore the effect of an FDA-approved drug – Verteporfin (VP), known to have an autophagy inhibitory function. It is reported that VP results in impairment of P62 function, a protein critical to autophagy, through induction of high molecular weight oligomerization of P62 protein. We primarily selected two different GOF-P53 cancer cell types- GOF-R156P-P53 harboring osteosarcoma cells (HOS) and R273H-P53 harboring NSCLC cells for our analysis of VP-induced effects. Interestingly, VP exposure resulted in a ROS-dependent high molecular weight (HMW) band formation of not only P62 but also of P53 protein, more predominantly of GOF-P53 protein. This was associated with dose-dependent cellular cytotoxicity as well. Importantly, we demonstrated that VP exposure resulted in autophagy disruption at multiple steps, from inhibiting phagophore formation to inducing lysosomal instability. The VP-induced effects were further enhanced by addition of a proteasomal inhibitor, leading to increased ROS and aggravated cytotoxicity.

Overall, our study establishes the importance of GOF-P53 in cancer cells. It establishes its association with drug insensitivity. We further propose strategies to sensitize GOF-P53 harboring cells based on interference of cellular protein turnover machinery- autophagy and UPS. This can lead to the development of advanced therapy against drug-resistant cancer cells.

List of figures

List of tables

List of abbreviations

ALLN: N-acetyl-leu-leu-norleucinal

AO: Acridine orange

ATG: Autophagy related genes

Baf: Bafilomycin

CDK: Cyclin-dependent kinases

CMA: Chaperone mediated autophagy

CQ: Chloroquine diphosphate

DCFDA: 2′ 7′ –Dichlorofluorescin diacetate

ECM: Extracellular matrix

EGFR: Epidermal growth factor receptor

ERK1 and ERK2: Extracellular signal-regulated kinases 1 and 2

EV: Empty vector

FDA: Food and drug administration

GFP: Green fluorescent protein

GOF: Gain of function

HSP: Heat shock protein

HMW: High molecular weight

HOS: Human osteosarcoma

LAMP 1: Lysosomal associated membrane protein 1

LAMP-2A: Lysosomal associated membrane protein 2A

LC3B-II: Microtubule-associated protein light chain 3-II

LMP: Lysosomal membrane permeabilization

LTR: Lysotracker red

MDC: Monodansylcadaverine

mTOR: mammalian target of rapamycin

MTT: 3-(4,5-dimethylthiazol-2-yl)-2,5-di-phenyltetrazolium bromide

Mut: Mutant

NAC: N-acetyl cysteine

NSCLC: Non-small cell lung carcinoma

OS: Osteosarcoma

PB1: Phox and Bem1p-1

PCNA: Proliferating cell nuclear antigen

PI: Proteasome inhibitor

PFT-α: Pifithrin-alpha

Rab7: Ras-related protein-7

Rapa: Rapamycin

RFP: Red fluorescent protein

ROS: Reactive oxygen species

SEM: Scanning electron microscope

SS: Serum starvation

TFEB: Transcription factor EB

Ub: Ubiquitin

UPS: Ubiquitin proteasomal system

VP: Verteporfin

WHO: World Health Organization

WT: Wild-type

YAP: Yes-associated protein

Chapter-1

Introduction

1.1 Cancer

Cancer is a generic term broadly used for a large group of diseases that can affect almost the entire body. Unlike normal cells, the hallmark of cancer cells includes abnormal growth, uncontrolled proliferation of cells, ability to migrate away from its tissue of origin, escaping growth suppressors, induction of angiogenesis, immune evasion, and resistance to apoptosis **(Fig. 1.1).** Nevertheless, genomic alterations are considered a critical factor to accelerate cancer pathogenesis [1, 2]. According to the World Health Organization (WHO), cancer is among the topmost causes of death worldwide. As per the latest Globocan 2020 data, there were an estimated 19.3 million new cases and 10.0 million cancer deaths across the board. An approximate 50% increase in the cancer burden has been predicted between 2020 and 2040. [3, 4]

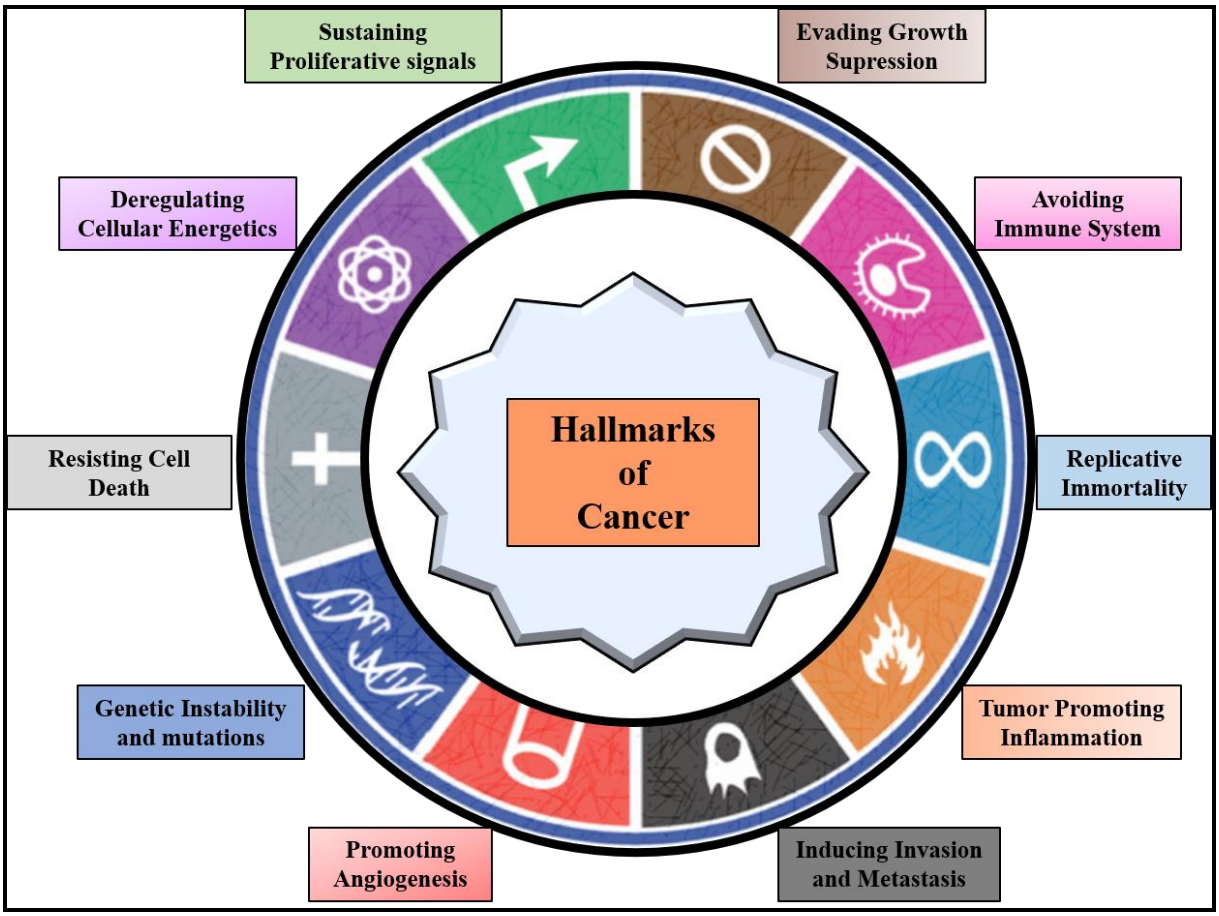

Figure 1.1. Hallmarks of a cancer cell. A cancer cell is characterized by abnormalities in various biological processes including genomic instability, escaping cellular death, metastasis, and immortalized replication leading to the ineffectiveness of major therapies and poor prognosis.

Amongst all cancers, lung cancer is the second most prominent cancer (11.6 % of the total cases)

however, shares the highest cancer mortality rate (18.4% of the total cancer deaths) worldwide **(Fig 1.2)**. Lung cancer is the abnormal proliferation of otherwise healthy cells in either or both of the lungs that effects a person's ability to breathe [3, 4]. Lung cancer is broadly divided into two categories: **small-cell lung carcinoma** (SCLC) which is the most aggressive type of lung cancer; it grows and spreads very fast and tend to be discovered at a very advanced stage, and **non-small cell lung carcinoma** (NSCLC) which is the most common type of lung cancer, found in smokers and non-smokers. NSCLC comprises about 85% of the lung cancer cases, while SCLC accounts for the remaining 15% [5].

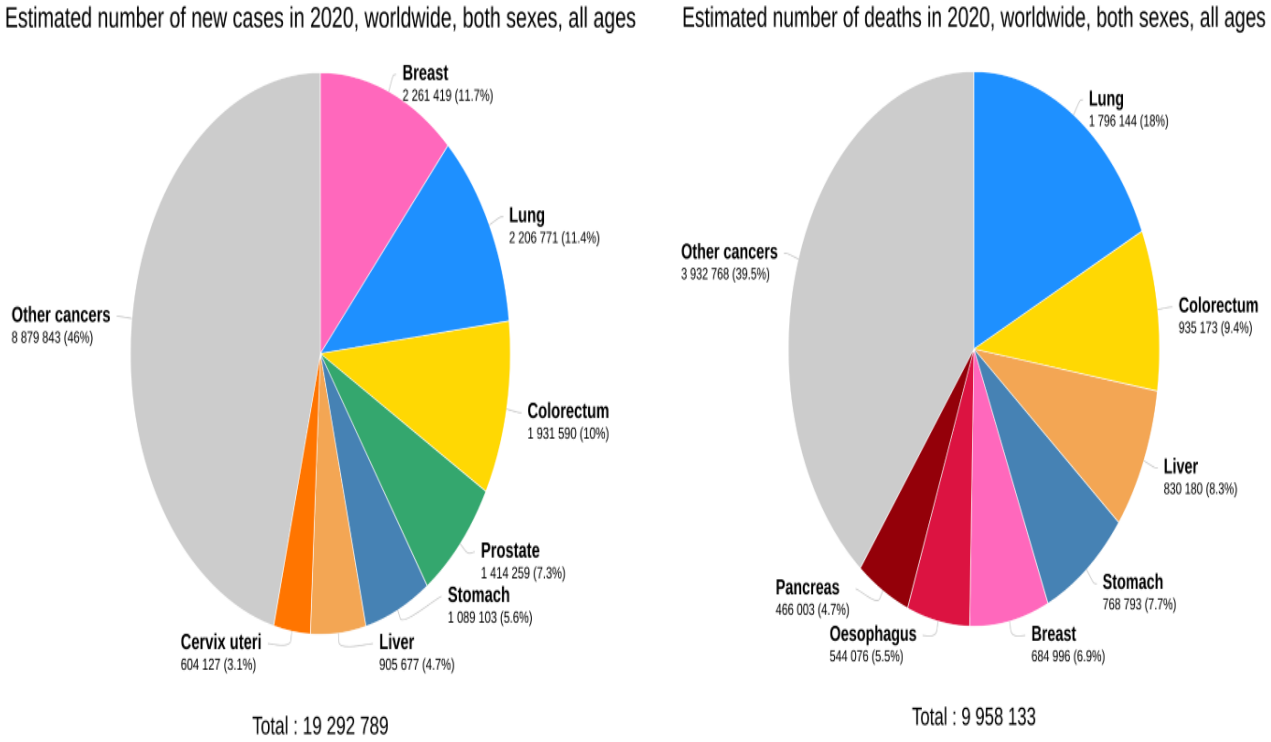

Figure 1.2. Cancer burden in 2020. Pie Chart depicting the estimated number of new cancer cases and estimated deaths worldwide. Source: Globocan 2020 (http://gco.iarc.fr)

This has been widely reported that genetic mutations in critical genes play an indispensable role in cancer occurrence and progression. As per the cancer genome atlas data, lung adenocarcinoma patients exhibit a high rate of somatic mutations, 18 statistically significant genetic mutations including TP53, KRAS, KEAP1, STK11, EGFR, NF1, and BRAF have been found. Similarly, in squamous cell carcinoma patients, the significant mutation count is 11 including TP53, CDKN2A, PTEN, PIK3CA, KEAP1, NOTCH1, and RB1. Interestingly, about 90% of these mutations occur in the TP53 gene [5, 6].

1.2 P53: The guardian of the genome

The P53 protein was first identified in 1979, by two independent groups which reported the association of a 53K Da protein with the simian virus 40 (SV40) large T-antigen [7, 8]. For the next ten years, P53 was believed to be an oncogene whose protein expression is too high in transformed cells, a characteristic that was not observed in normal tissue [9, 10]. However, by 1989, several pieces of evidence came into light suggesting the tumor-suppressive role of WT-P53. It was then identified that the early set of experiments reporting a P53 induced transformation of primary cells were performed with a mutated version of P53 isolated from the tumor cells [11-13]. Hence, only mutant P53 could induce cellular transformation [12], inversely, WT-P53 could inhibit transformation by several means [14].

1.2.1 Structure of P53

The p53 gene is located on the short arm of human chromosome 17 at the locus 17p13. The gene spans 20kb which comprises 11 exons, where, exon 1 is non-coding and there is a large first intron of 10kb between exon 1 and exon2. The p53 gene encodes a 393-amino acid protein.

The coding sequence of p53 contains five domains that are highly conserved in vertebrates [15]. Based on structural and functional analysis, these domains **(Fig. 1.3)** are coined as:

The transactivation (TA) domain. The TA region of the p53 gene is required for P53 transcriptional activity. MDM2 can bind to this region of P53 and repress its transcriptional activity.

The proline-rich domain (40-92 amino acid) is involved in P53 dependent apoptosis [16].

The DNA binding domain (DBD, the core domain) is spanned between 101-306 amino acids. This domain binds to the P53 consensus DNA sequence that consist of two PuPuPuC(A/T)(A/T)GPyPyPy decamers separated by a 0 to 14 base pair spacer [(A) adenine; (T) thymine; (C) cytosine; (G) guanine; (Pu) purine; (Py) pyrimidine] [17, 18]. P53 can bind to specific genes with a consensus P53 response element and either transactivate or trans-repress it. The majority of missense mutations including ‘hot spot’ mutations that occur with unusually high frequency are clustered within this conserved domain [19].

The oligomerization domain spanned between 307-355 amino acid is essentially required for the formation of P53 dimer or tetramer which is important for sequence-specific DNA-binding of P53. It

also contains a nuclear export signal [20].

C-terminal regulatory domain. It is a basic domain that can bind to DNA without sequence specificity.

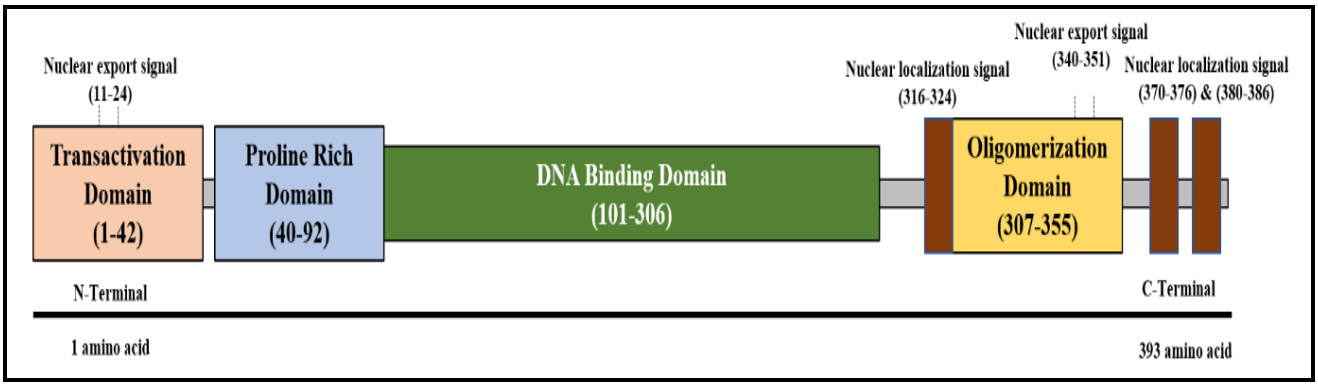

Figure 1.3. The P53 structure. P53 is a 393 amino acid protein. Based on function, P53 is divided into five major domains along with nuclear export or localization signals.

1.2.2 Stabilization of P53

P53 is usually found at low levels due to its short half-life in normal cells. However, DNA damage caused by genotoxic stress phosphorylates P53, enhances its stability, and increases protein accumulation [21]. In turn, stabilization of P53 is caused by dissociation of P53 from MDM2 [22]. MDM2 targets P53 for proteasomal degradation. However, both ionizing radiation (IR) and UV light-induced phosphorylation of P53 at Ser-20 weakens its association with MDM2. ARF, an alternative reading frame protein encoded by INK4 binds with MDM2 and prevents P53 from ubiquitination and degradation hence increasing its stability [23]. The C-terminal lysine residues are reported to be acetylated by histone acetyl transferases (HATs) which induce P53 stabilization and activation [24].

1.2.3. Function of P53

The WT-P53 has several tumor-suppressing roles which made this protein the "Guardian of the genome". WT-P53 is reported to regulate a myriad of genes and possess the following important function in tumor suppression:

Cell cycle arrest: As mentioned earlier, the DNA damage activates the P53 protein which halts the cell cycle to allow for DNA repair. P53 downstream target gene, $p21^{waf1/cip1}$, is a cyclin-dependent kinase inhibitor (CKI) which arrests the cells in the G1 phase by inhibiting the phosphorylation of

retinoblastoma [25]. Another, P53 target and CKI, GADD45 is responsible for either UV or methyl methanesulfonate (MMS)-induced, but not IR-induced G2/ M arrest of the cell cycle [26]. Wild type P53 is also involved in senescence and DNA repair.

Apoptosis: The WT-P53 is involved in both, extrinsic or intrinsic apoptosis, when the damaged DNA is not repaired. WT-P53 has been reported to control several apoptosis-related proteins. For example, P53 transcribes the Bax gene, which forms a pro-apoptotic protein, while it represses the expression of anti-apoptotic protein, Bcl-2 [27]. WT-P53 also upregulates several other pro-apoptotic proteins like the insulin-like growth factor binding protein IGF-BP3, PUMA, killer/DR5, and FAS/APOL [28].

Invasion or metastasis inhibition: The WT-P53 partly controls the genes that block extra cellular matrix (ECM) degradation. For example, P53 regulates PAI1 which inhibits urokinase-type plasminogen activator (u-PA). U-PA is mainly involved in the activation of plasmin, which degrades ECM proteins. Certain WT-P53 targets like KAI1 and Nm23-Hl are known to inhibit metastasis [29].

1.2.4 Mutation in P53

The p53 gene is one of the most frequent targets for genetic alterations in human cancer. Mutation of p53 generally occurs by deletion or insertion of amino acid, truncation, point mutation, or loss of heterozygosity in which the wild-type allele is deleted. Interestingly, a vast majority of P53 mutations lead to the production of the full-length protein, mostly with only a single amino acid substitution known as missense mutations [30]. A vast majority of these missense mutations localized at the central most conserved region of P53 known as the DNA binding domain. There are well-established '**hot-spot** mutants at residues 175, 245, 248, 249, 273, or 282 of P53 protein with unusually high frequency that localize in DBD of P53 [19].

These P53 mutations are roughly divided into two structural subgroups:

DNA contact mutants affect the residues that are directly involved in sequence-specific DNA contact and don't alter the overall conformation of the P53 molecule. Examples of DNA contact mutation include R273H-P53 [31].

Conformational mutants are the ones that lead to either partial or complete removal of WT-P53 conformation of DBD, exposing the otherwise buried residues and interfaces. Such mutants are exemplified by R175H-P53 [31].

In principle, as shown in **figure 1.4**, there are three mechanisms that contribute to P53 mutation-mediated outcome that helps in tumor progression [32, 33].

First, **loss of WT-P53** mediated tumor suppressor function; if both alleles are mutated or if the remaining wild-type allele is lost.

Second, many mutant P53 isoforms can induce **dominant-negative** inhibition of WT-P53, mostly through mixed tetramer formation which is incapable of DNA binding and transactivation.

Third, several mutant P53 proteins might possess activities of their own that are often absent in WT-P53 and can contribute to various oncogenic functions. Such activities are commonly known as **gain-of-function (GOF)**. In this regard, GOF can be exemplified as unlike WT-P53, the GOF-P53 binds and inactivate the P53 family proteins-P63 and P73.

Several germline P53 mutations are also present that are known to cause a genetic disorder "**Li Fraumeni syndrome** (LFS)". This syndrome results in the onset of malignant tumors like breast cancer, sarcomas, and other neoplasms early in life [28].

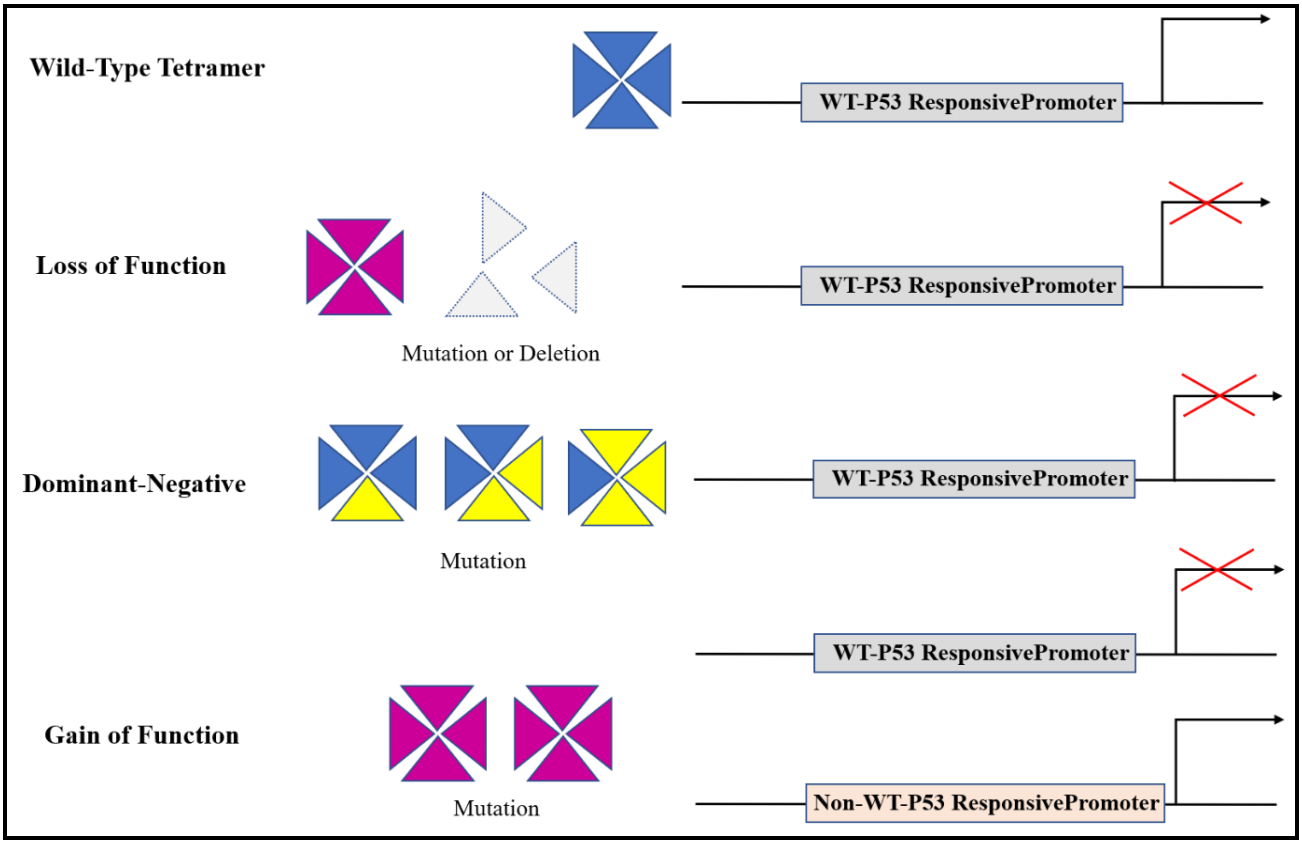

Figure 1.4. Mutant-P53 mediated mechanism of inhibiting WT function. Different mechanisms for disrupting WT-P53 mediated transactivation of tumor-suppressive genes.

1.2.5 Role of mutant P53 in cancer progression

Acquisition of mutation imparts P53 with several oncogenic functions. Few of such well-known mutation-induced functions of P53 have been shown in **figure 1.5** and are discussed in detail below:

1.2.5.1 Mutant P53 and genomic instability

An increased genomic instability indicated by an obvious variation in chromosome structure and number is a major hallmark of cancer progression. Mutant P53 is reportedly involved in transmitting genomic instability in human cancer by disrupting the normal spindle checkpoint control and thus increases the number of cells with polyploid genomes [34]. It is noteworthy that P73 can replace WT-P53 in P53-deficient cells and can maintain genome stability by suppressing aneuploidy and polyploidy [35]. However, removal of P73 by excess mutant P53 results in the accumulation of cells with polyploidy and thus facilitate cancer progression. Mutant P53 can interact with nuclease Mre11 and suppresses the recruitment of MRN complex to DNA double-stranded break damage site which further inactivates ATM, the damage sensor and impairs the G2/M checkpoint [36].

1.2.5.2 Mutant P53 and drug resistance

Mutant P53 proteins are expressed at high frequency in human cancer and are associated with drug resistance and poor clinical prognosis [30]. As reported, R175H-P53 enhances MRP1 expression and induces doxorubicin resistance [37]; mutant P53 is also known to activate NF-κB pathway or NRF2 expression and resulted in drug resistance [38, 39]. Certain mutant P53 proteins are reported to inhibit procaspase-3 levels or caspase-9 levels. Also, P63/73-dependent induction of Bax and Noxa failed to contribute insensitivity in mutant P53 harboring cells [40-42]. Unlike WT-P53, mutant P53 has also been reported to activate cancer stem cell markers and enhance the radio or chemo resistance [43]. Mutant P53 is also reported to downregulate miR-223 expression and a consequent increase of stathmin-1, an oncoprotein known to confer resistance to chemotherapeutic drugs [44].

1.2.5.3 Mutant P53 and metastasis

Metastasis is another “hallmark of cancer” and contributes to most cancer-associated deaths. Mutant P53 is reported to enhance the expression of several epithelial to mesenchymal transition (EMT) related markers like ZEB1, SLUG, TWIST1 by transcriptional, post-translational, and epigenetic modifications [45-47]. Mutant P53 is known to inhibit MDM2 mediated degradation of SLUG that resulted in high SLUG expression and low E-cadherin expression [46]. Gene expression profiling

studies revealed that mutant p53 co-operates with oncogenic RAS to induce gene clusters of chemokines, interleukins, and ECM-related molecules which are majorly involved in tumor progression and invasion [30]. Also, as reported, mutant P53 represses the miR-130b expression, which negatively regulates ZEB1 and hence promotes metastasis [45].

1.2.5.4 Mutant P53 and cell proliferation

Burgeoning reports are suggesting the role of mutant P53 in promoting the limitless replicative potential and insensitivity towards several anti-growth signals. Mutant P53 is reported to physically interact with nuclear transcription factor Y (NF-Y) and recruits the hippo pathway effector, YAP to activate certain cell cycle genes including cyclin A, cyclin B, cdk1, and cdc25C [48, 49]. Another report on mutant P53-YAP and TEAD trimeric transcriptional complex suggested the induction of circular RNA, circ PVT1 which further enhances the expression of proliferation genes like, AURKA and MKI67 [50]. Mutant P53 is also known to target key chromatin regulators like methyltransferases (MLL1 and MLL2) and acetyltransferase (MOZ) to enhance cell proliferation by increasing active histone modifications (H3K4me3 and H3K9ac) [51]. Additionally, mutant P53 regulates miR-271a expression, promotes EGF-induced ERK1/2 activation, and facilitates cell proliferation and tumorigenesis [52].

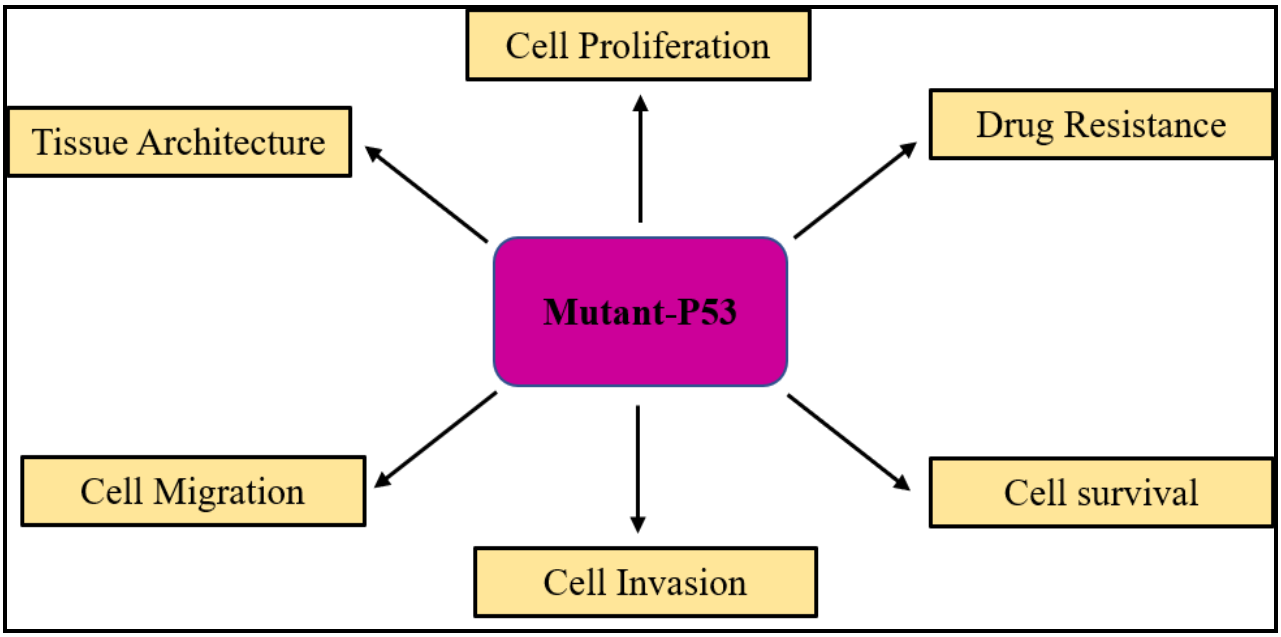

Figure 1.5. Role of mutant P53 in tumor progression. Mutant P53 enhances drug resistance, cell survival, cell migration, cell proliferation, cell invasion leading to the growth and progression of tumor cells.

1.2.6 Stabilization of mutant P53 in cancer

Under normal conditions, WT-P53 is a very short-lived protein however, a missense mutation leads to the production of a prolonged half-life P53 protein [53]. Unlike WT-P53, mutant P53 proteins poorly regulate MDM2 induction and are reported to escape MDM2 mediated proteasomal degradation [54]. This leads to the mutant P53 accumulation inside the cells. However, contrasting reports are suggesting mutant P53 is susceptible to MDM2 mediated degradation and there must be other mechanisms enabling P53 stabilization in tumor cells [55]. Mutant P53 has also been reported to associate with molecular chaperons, like HSP90 to attain stabilization during tumor-associated stress [56]. In line with this, inhibition of HSP90 has been reported to degrade certain mutant P53 proteins [57]. Additionally, mutant P53 proteins interact with HSP70 that inhibits its ubiquitination and MDM2 mediated proteasomal degradation, and promote stable aggregation of mutant P53 [58].

1.2.7 Mutant P53 interacting partners

WT-P53 acts mostly as a transcription factor, however, several studies have described the gain-of-function activities of mutant P53 mediated through non-transcriptional processes **(Fig 1.6)**.

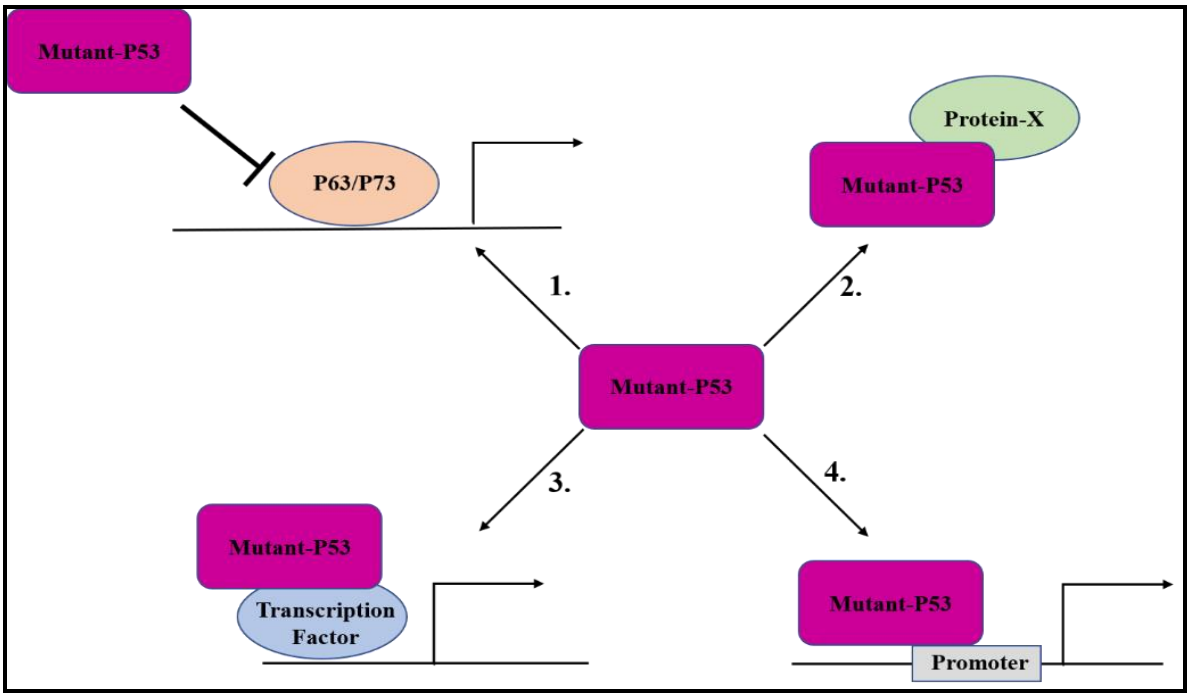

Figure 1.6. Mechanism of mutant P53 mediated GOF activity. Mutant P53 can induce GOF either by interacting with other proteins or directly or indirectly targeting the activation of several genes involved in tumorigenesis.

As the acquisition of mutation allows P53 to interact with several proteins. Two cellular proteins P42 and P38, are reported to be specifically associated with mutant P53 but not WT-P53 in a cell cycle-specific manner and helps in promoting cell growth [59]. In another study, mutant P53 has been shown to interact with MBP1, which is an oncogene and is responsible for enhanced neoplastic transformation and tumor growth [60]. Mutant P53 is also reported to physically interact with promyelocytic leukemia (PML) protein which facilitates the transcriptional activity of mutant P53 [61]. The prolyl isomerase Pin1 is also known to interact with mutant P53 and promote migration and invasion of breast cancer cells [62]. Mutant P53 but not WT-P53 is also reported to interact with other P53 family proteins P63/P73 and inhibits their activity [35]. A few of the more prominent examples of proteins forming a complex with mutant P53 in humans (H) or mice (M) is described in **Table 1.1.**

Table.1.1 List of mutant P53 interacting proteins.

Protein	Missense Mutation	Species	Disease	Cell Line	Reference
Sp1	R248W	H	Pancreatic Cancer	MIA PaCa-2	[63]
	R280K	H	Breast Cancer	MDA-MB-231	[63]
Ets1/Ets2	R175H/R273H/ R248Q/R248W	H	Embryonic Kidney	HEK293T	[64]
	R248W	H	LFS	MDAH087	[65]
	R248W	H	Pancreatic Cancer	MIA-PaCa-2	[65]
	R273H	H	Breast Cancer	MDA-MB-468	[64]
YAP1	C194D	H	Breast Cancer	T47D	[66]
	H193L	H	Head and Neck	CAL27	[66]
	R175H	H	Cancer	H1299	[66]
	R175H	H	Lung Cancer	SKBr3	[66]
	R248L	H	Breast Cancer	FaDu	[66]
	R273H	H	Head and Neck	H1299	[66]
	R273H	H	Cancer	PANC-1	[66]
	R273H	H	Lung Cancer	MDA-MB-468	[66]
	R273H, P309S	H	Pancreatic Cancer	SW-480	[66]
	R280K	H	Breast Cancer	MDA-MB-231	[66]
			Colon Cancer		
			Breast Cancer		
NF-Y	R175H	H	Breast Cancer	SKBr3	[67]
	R249S	H	Breast Cancer	BT-549	[68]
	R273H	H	Glioblastoma	U373	[69]

	R273H	H	Glioblastoma	SNB19	[69]
	R273H	H	Colon Cancer	HT-29	[67]
	R273H, P309S	H	Colon Cancer	SW-480	[67]
	R280K	H	Breast Cancer	MDA-MB-231	[68]
CBP	R273H	H	Glioblastoma	U373	[69]
	R273H	H	Glioblastoma	SNB19	[69]
VDR	R175H	H	Breast Cancer	SKBr3	[70]
	R248W	H	LFS	MDAH087	[65]
	R248W	H	Pancreatic Cancer	MIA-PaCa-2	[65]
SREBP	R273H	H	Breast Cancer	MDA-MB-468	[71]
E2F1	R175H	H	Lung Cancer	H1299	[72]
P63/P73	H179Y/R282W	H	Keratinocytes	HACAT	[73]
	R110P/E258V/ R175H/R282W	H	Osteosarcoma	SaOS-2	[74]
	R175H	M	Fibroblasts	MEFs	[73]
	R280K	H	Breast Cancer	MDA-MB-231	[73]
Smad2/Smad3	H17Y/R282W	H	Keratinocytes	HACAT	[73]
	R175H	M	Fibroblasts	MEFs	[73]
	R175H/R273H/ R248W/R282W	H	Lung Cancer	H1299	[75]
Nrf2	M237I	H	Breast Cancer	SUM149PT	[68]
	R175H	H	Breast Cancer	HCC1395	[68]
	R249S	H	Breast Cancer	BT-549	[68]
	R273H	H	Breast Cancer	MDA-MB-468	[68]
	R280K	H	Breast Cancer	MDA-MB-231	[68]
STAT3	R273H	H	Breast Cancer	MDA-MB-468	[68]
	R280K	H	Breast Cancer	MDA-MB-231	[68]

1.2.8 Mutant P53 and gene regulation

Like WT-P53, mutant P53 has also been known for the transactivation of myriad genes. As reported, the transactivation domain of P53 is critical for the oncogenic functions of mutant P53. While the WT-P53 transactivate genes involved in apoptosis, senescence, cell cycle arrest, mutant P53 transactivate genes involved in cancer progression. A few of the key genes regulated by mutant P53 have been implicated in **Table 1.2.**

Table1.2. List of genes regulated by mutant P53

Category	Gene	Mutant	Reference
Anti-Apoptosis	NF-κB2	R175H, R273H, D281G	[38]
(or Chemoresistance)	ABCB1	R175H, R248Q, D281G	[76]
	BCL2L1	R273H	[77]
Cell-Proliferation	MYC	V143A, R175H, R273H, R248W, D281G	[78]
	MAP2K3	R175H, R273H, R280K	[77]
	IGF1R	R175H, R248W, R273H	[77]
	CCNA2	R175H, L194F, R273H	[48]
	EGFR	V143A, R175H, R248W, R273H, D281G	[79]
Metabolism	ACAT2	R273H	[80]
	HMGCR	R273H	[80]
	MVT	R273H, R280K	[80]
	DHCR24	R175H, R273H	[80]
Cell-Cell Signalling	MMP3	R175H	[81]
	ITGA6	D281G	[38]
GTPase Activity	ARHGDIA	R175H, R273H	[77]
	DEPDC1	R280K, R273H	[62]
	WDR67	R280K, R273H	[62]
Cytoskeleton	KIF20A	R175H, R273H	[77]
	EPB41L4B	R280K, R273H	[62]
mRNA Processing	CPSF6	R280K, R273H	[62]
RNA stability	ID4	R175H, R273H	[82]

1.2.9 Mutant P53 interacting protein-YAP

Numerous studies have revealed the crucial cross-talk between mutant P53 and YAP in cancer progression. YAP is a downstream effector of the hippo signaling pathway which regulates the organ size in a normal scenario. When hippo signaling is activated, YAP is phosphorylated at Ser127 and Ser89, respectively, creating a 14-3-3σ binding site and consequent YAP cytoplasmic retention. Moreover, Lats1/2 induced phosphorylation at Ser381 and Ser311 trigger ubiquitin-mediated proteasome degradation [83]. However, when hippo signaling is off, YAP and its ortholog TAZ localize to the nucleus and leads to the activation of the TEAD family transcription factors that control the organ size and growth [84]. YAP/TAZ activation is also regulated by cell-cell contact as high cell density leads to YAP phosphorylation and cytoplasmic retention [85]. Nuclear YAP is reported to induce p21, Bax, and caspase-3 expression and inhibit BCL-2 and BCL-xl in a P53 dependent way. YAP is shown to induce transcription of WT-P53 which in turn binds to the YAP promoter and activates its transcription in a positive feedback manner suggesting YAP and WT-P53

sustain each other to impart apoptosis and drug resistance [86]. Also, YAP is known to stabilize P73 by preventing its nuclear export and degradation, and together they are reported to induce transcription of pro-apoptotic genes such as PUMA and p53AIP1 [87].

Strikingly, dysregulation of YAP/TAZ expression is reported to promote tumor growth, proliferation, and metastasis *via* transcription of genes involved in cell growth including connective tissue growth factor (CTGF) [88], amphiregulin (AREG) [89], cysteine-rich angiogenic inducer 61 (Cyr61) [90], Axl [91], birc-5 [92], ankyrin repeat domain 1 (ANKRD1) [93]. YAP/TAZ also regulates the expression of several genes involved in cell cycle progression, cyclin A2 (CCNA2) [94], cyclin B1 (CCNB1) [49], and cancer drug resistance, ATP-binding cassette sub-family G member 2 (ABCG2) [95]. Studies from different groups have shown that YAP induces tumorigenic traits including growth factor independent proliferation, cancer metastasis, and drug resistance in most solid cancer types including ovarian, esophageal, pancreatic, liver, colon, lung, and breast cancers [96-100]. Interestingly, YAP is reported to physically interact with mutant P53 proteins to enable GOF [101] and enhances the pro-proliferative transcriptional activity of mutant P53 [49]. YAP and mutant P53 proteins are reported to form a complex with NF-Y onto the regulatory region of CCNA, CCNB, and CDK1 genes and enhance their transcription which leads to increased cell proliferation [102].

Earlier studies have also demonstrated, an increase in the mevalonate pathway mediated malignant phenotype is mediated by mutant P53 induced activation of SREBPs. Indeed, this phenomenon increases the YAP/TAZ oncogenic activity such as enhanced cell proliferation and self-renewal in breast cancer cells [103]. As discussed early, concerning WT-P53 cells YAP interacts with P73 and induce anti-tumorigenic activity, however, in mutant P53 context YAP is no more able to induce tumor suppressor instead binds to mutant P53 and enhances its oncogenic functions with consequently increased cell proliferation, invasion, and chemoresistance in cancer cells [103]. Also, a high expression of YAP targets in presence of mutant P53 results in a poor prognosis of cancer patients than in presence of WT-P53 [104].

1.2.10 Mutant P53 and therapeutic approach

Since more than 50% of human cancers possess a mutation in the p53 gene and rely on it for pro-oncogenic functions, it makes mutant P53 an ideal target for cancer therapy. There are several drugs in pre-clinical studies or clinical trials to target mutant P53 however, no therapeutic regimen has yet been clinically approved. Repurposing of food and drug administration (FDA) approved drugs can also be explored as an option. Several therapeutic strategies have been reported to target mutant P53

and are categorized as below.

1.2.10.1 Restoring wild type conformation and transcriptional activity

CP-31398: CP-31398 is the first reported small molecule known to restore wild type function of some P53 mutants. CP-31398 is reported to refold mutant P53 and impart anti-tumor activity [105]. Although CP-31398 is known to inhibit tumor growth *in vivo*, however, it showed to have a complex mechanism of action with multiple targets as it also affects the WT-P53 or P53-null cells [105]. As listed at clinicaltrials.gov no ongoing clinical trials are reported for CP-31398.

APR-246: APR-246 is a methylated analog of PRIMA-1, which can restore wild-type function of mutant P53 [105]. APR-246 covalently binds to the core domain of mutant P53, enhances its thermostability, and contributes to the refolding of mutant P53 to wild-type conformation enabling the re-induction of WT-P53 target genes such as cdkn1a [106]. APR-246 has imposed a tumor-suppressive effect on mutant P53 expressing tumor cells of different origins hence considered as a promising first-in-class mutant P53 targeting drug [107]. Several phase II clinical trials have used APR-246 in combination with other chemotherapeutic drugs like carboplatin (NCT02098343), azacytidine (NCT03072043), 5-fluorouracil, and cisplatin (NCT02999893) to target different stringent cancers.

COTI-2: COTI-2, a novel thiosemicarbazone derivative that promotes refolding and DNA binding of mutant P53 resulting in reactivation of several WT-P53 genes like cdkn1a, puma, and noxa [108]. COTI-2 induced apoptosis or senescence is reported to progress with the involvement of MAPK and mTOR [109]. Phase I trial of COTI-2 as therapy in tumors with mutant P53 is in progress (NCT02433626).

1.2.10.2 Targeting mutant P53 degradation

Ganetespib: As discussed earlier, hyper-stabilization of mutant P53 is largely responsible for its dominant-negative and oncogenic GOF activities, hence therapy leading to mutant P53 degradation can help to target the tumor cells. Since HSP90 imparts stability to mutant P53 hence 17AAG and Ganetespib, HSP90 inhibitors, have been studied to degrade mutant P53 and kill mutant P53 cancer cells [110]. Ganetespib is reported to be more efficient with 50-fold more potency in comparison to 17AAG [111]. Phase II clinical trials with Ganetespib have not shown an overall effective result in monotherapy or combination however, positive results were obtained for subgroups of patients hence an extensive clinical trial is needed.

SAHA: Histone deacetylase (HDAC) inhibitors are another group of molecules reported to reduce the levels of mutant P53. SAHA (suberoylanilide hydroxamic acid) is an FDA-approved HDAC inhibitor for the treatment of T cell lymphomas. Notably, SAHA exhibits preferential cytotoxicity for mutant P53, rather than WT-P53 and null P53 cancer cells in different human cancers [112]. SAHA is reported to inhibit the HDAC6-HSP90 chaperone axis hence could destabilize mutant P53 [57]. Also, it inhibits the mutant P53 transcription through HDAC8 [113]. Additionally, it strongly sensitizes the mutant P53 harboring cancer cells to chemotherapies.

1.2.10.3 Inducing synthetic lethality

MK-1775: Since, the mutant P53 harboring tumor cells abrogate the G1/S cell cycle checkpoint and enter the S phase with damaged DNA, makes the G2/M checkpoint very important to maintain genomic stability. In line with this, inactivation of the G2/M checkpoint would result in unscheduled mitotic entry and lead to mitotic catastrophe [114]. This synthetic lethality can be used as an ideal opportunity to target cancer cells with mutant P53. MK-1775 is a specific inhibitor of Wee-1, a tyrosine kinase involved in G2/M cell cycle arrest, reported showing anti-tumor activities in cancer cells with mutant P53. It is reported to enhance the efficacy of other chemotherapeutic drugs like cisplatin, vorinostat in cancer cells harboring mutant P53 however, shows minimal response towards WT-P53 cancer cells [115, 116]. This drug is in Phase-II clinical trials for combination therapy in ovarian cancer (NCT01357161).

1.2.10.4 Genetic approach to target mutant p53

CRISPR/Cas9 and RNAi: CRISPR/Cas9-based genome editing could result in a straightforward therapeutic strategy to target mutant P53 harboring tumor cells. This technique has been used to replace mutant p53 with a functional copy that led to the successful restoration of WT-p53 genotype and phenotype [117]. However, there are high chances of genomic instability hence the specificity and in vivo efficacy need an in-depth study.

1.2.10.5 Small peptides

Small peptides are used to restore WT-P53 activity, either by restabilizing mutant P53 or by inhibiting the aggregation of mutant P53. In this context, ReACp53, a cell-penetrating peptide inhibitor of mutant P53's aggregation, is reported to show a promising anti-cancer effect in ovarian and prostate cancer [118, 119].

1.2.10.6 Immunotherapy

Although mutant P53 is reported to escape MDM2 mediated degradation, it can still be degraded through various MDM2 independent and proteasome or autophagy-dependent pathways. Degradation of mutant P53 generates peptides that can be presented on the tumor cell surface by major histocompatibility complex-I (MHC-I), hence could serve as a therapeutic target for immunotherapy [120]. An engineered T cell receptor-like (TCRL) antibody P1C1TM is reported to be specific for WT-P53 peptide and can differentiate it from mutant P53 peptide [121]. These findings can enable the efficient antibody-dependent targeting of mutant P53 harboring cancer cells and induction of cytotoxicity.

1.3 Protein homeostasis machinery

Since the acquisition of mutation imparts stability to mutant P53 protein and enhances its half-life, therefore regulating protein homeostasis could maintain the turnover of mutant P53 inside the cell. The main cellular quality control for cells comprises the maintenance of balance between the damaged and unwanted proteins and organelles inside the cell. This balance is maintained by two major homeostasis machinery: Ubiquitin proteasomal system (UPS) and autophagy. These two machineries play a very important role in cancer progression and suppression [122].

1.3.1 Ubiquitin proteasomal system (UPS)

Ubiquitin-proteasome-mediated degradation is extremely efficient for degrading short-lived proteins, soluble unfolded/misfolded proteins, and polypeptides [123]. As shown in **figure 1.7**, this mode of degradation involves the addition of ubiquitin (Ub), a small protein specific to certain lysine residues on the target proteins. Ubiquitin covalently attaches to the target protein in a cascade of events involving three enzymes. Firstly, ATP-dependent Ub activation occurs with the help of the E1 enzyme, followed by the transfer of a Ub thioester to a Ub-conjugating enzyme, E2, then an isopeptide bond making a polyubiquitin chain is formed catalyzed by Ub E3 ligases [124].

The polyubiquitin chain formation involves seven lysine residues (K6, K11, K27, K29, K33, K48, or K63) in the Ub protein. K48-linked ubiquitin chain formation is known to be involved in proteasomal degradation, however, K11 or K63 chains or single ubiquitin moieties are associated with non-proteolytic functions and K63-linked ubiquitin chains are involved in autophagic elimination [122].

The ultimate protein degradation complex is 26S proteasome, consisting of 20S proteasome, the core complex, and the 19S proteasome cap, the regulatory complex. The 20S proteasome is a barrel-shaped structure with two outer rings of α subunits to regulate the entry of unfolded proteins and two middle rings of β subunits harboring proteolytic activity. The α subunits guide the unfolded substrate to catalytic cleavage which occurs in the β subunit with the help of several peptidases [125]. The new amino acid so formed after the recycling of proteins is reused by the cells to synthesize new proteins. Additionally, the 19S cap structure further regulates the internalization of ubiquitinated proteins. The central Rpt ring at the 19S cap is responsible for substrate binding and unfolding. It also regulates the substrate transfer through the channel [126]. Notably, ubiquitination is a reversible phenomenon as certain proteases, deubiquitinating enzymes (DUBs) removes the ubiquitin from the substrates and disassemble polyubiquitin chains [122].

UPS is reported to be involved in the regulation of many cellular processes, like transcription, cell cycle progression, DNA repair, protein quality control, cell stress, and apoptosis. As exemplified, cell cycle regulation relies on sequential formation and degradation of cell cycle proteins like cyclins [127]. Also, during apoptosis survivin undergo ubiquitin ligase XIAP mediated UPS degradation [128].

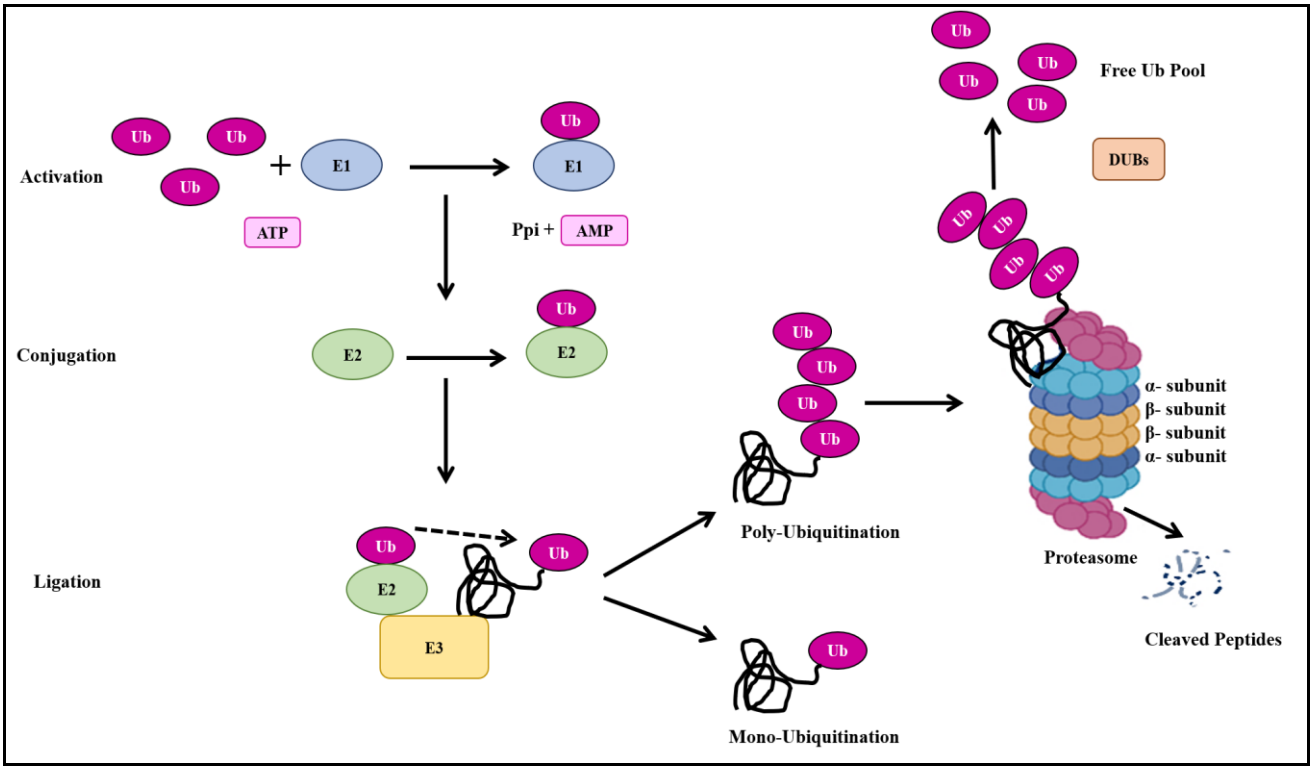

Figure 1.7. Diagrammatic representation of UPS. UPS mediated degradation of proteins involve ubiquitination by different enzymes, where E1 activates the ubiquitin and transfer it to E2 enzyme

which further polyubiquitinate the target protein with the help of E3 enzyme. The polyubiquitinated protein then passes through the proteasome for degradation.

1.3.1.1 UPS and cancer

Ubiquitin ligase, E3 is known to play a very important role in the regulation of several cellular processes including proliferation and differentiation via recognizing, interacting, and ubiquitinating the key cellular proteins. The type of ubiquitin chain formed decides the fate of the ubiquitinated substrate to either go for proteasomal degradation or display altered subcellular localization or suffer a compromised interaction with functional protein complexes. Hence, deregulation of E3 activity can result in several human pathologies including cancer as it can lead to either accelerated degradation of tumor-suppressive proteins or accumulation of tumor-promoting proteins [129]. The abnormal protein accumulation could be related to mutations that alter the recognition of protein by E3 ligase as observed with mutant P53 and MDM2 [129]. However, there are very few clinical trials reported for E3 ligase inhibiting compounds because of the dual role of an E3 ligase in cancer progression.

Depending on the type of proteins being degraded or not degraded, UPS can impart oncogenic effects. Proteasome can degrade several proteins with a tumor-suppressive role however an oncoprotein can escape out proteasomal degradation procedure. In such a condition, treating the cancer cells with proteasomal inhibitors has been observed to give some positive results. As inhibiting proteasome can save tumor suppressor proteins from degradation which can increase their duration inside the cells and can enhance their tumor-suppressive activity. Similarly, a proteasomal inhibitor would increase the aggregation of oncoproteins that evade the degradation procedure already. Aggregation of proteins beyond a limit would result in cytotoxic stress and hence result in cell sensitization. As depicted in **figure 1.8,** proteasome inhibitors have been reported to induce several outcomes. A wide range of proteasome inhibitors have been reported to date, a few of them have been discussed below.

Bortezomib belongs to the peptide boronate class of proteasomal inhibitor have been known to form tetrahedral adducts with the N-terminal Thr1 of the catalytic β subunits of the proteasome [130]. Bortezomib is reported to stabilize two crucial negative regulators of the cell cycle, $P27^{KIP1}$, and P53, well-known proteasome substrates [131]. Bortezomib treatment has been reported to accumulate pro-apoptotic protein Bax, thereby inducing apoptosis [132]. However, there are reports for Bortezomib resistance probably mediated by a mutation in the proteasomal β5 subunit which impairs the bortezomib binding [132].

MG132 belongs to peptide aldehyde-based proteasome inhibitors**.** These compounds are known to form a covalent hemiacetal bond with the hydroxyl group of the N-terminal threonine (Thr1) in the catalytic β subunit, thereby inhibiting proteasomal activity [130]. MG132 is among the first proteasome inhibitors developed. It is a potent proteasome inhibitor and reported to induce apoptosis in many cancer cells [133].

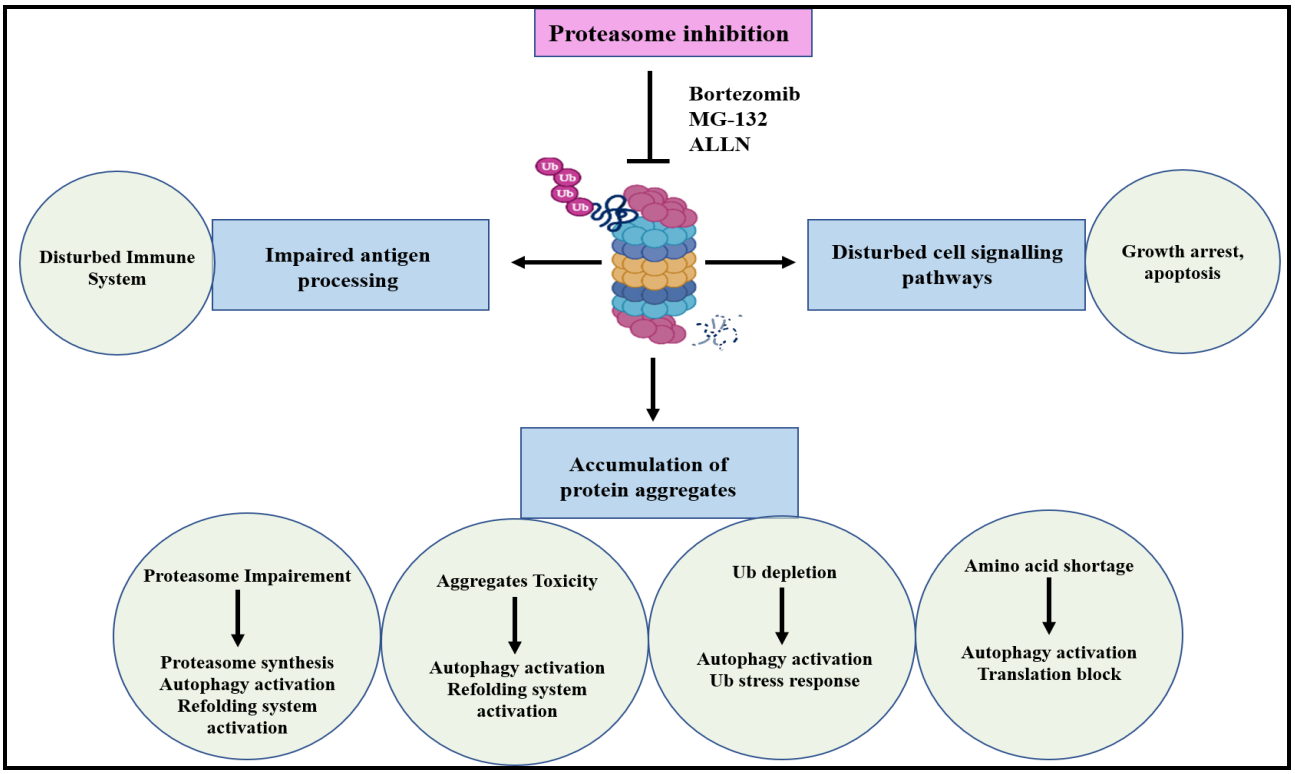

Figure 1.8. Outcomes of proteasome inhibition. Inhibition of proteasomal activity by various pharmacological agents can lead to several cellular consequences including impairment of antigen processing, accumulation of aggregates, and disturbance in several cell signaling pathways.

1.3.2 Autophagy

Autophagy is a highly conserved process known to recycle cellular macromolecules and damaged organelles, thus maintaining cellular homeostasis **(Fig 1.9)**. Unlike UPS, autophagy is known to degrade long-lived proteins, insoluble protein aggregates, and dysfunctional organelles like degenerated mitochondria [134]. Normal physiological condition maintains the basal level of autophagy however, under stress e.g amino acid deprivation, serum starvation or growth factor deprivation, hypoxia, exposure to various chemicals or toxins autophagy is activated to meet the metabolic demand of the cell. Its regulation is controlled by numerous proteins as dysregulation of autophagy could lead to several disorders such as cancer, autoimmunity, neurodegeneration, and

aging [122].

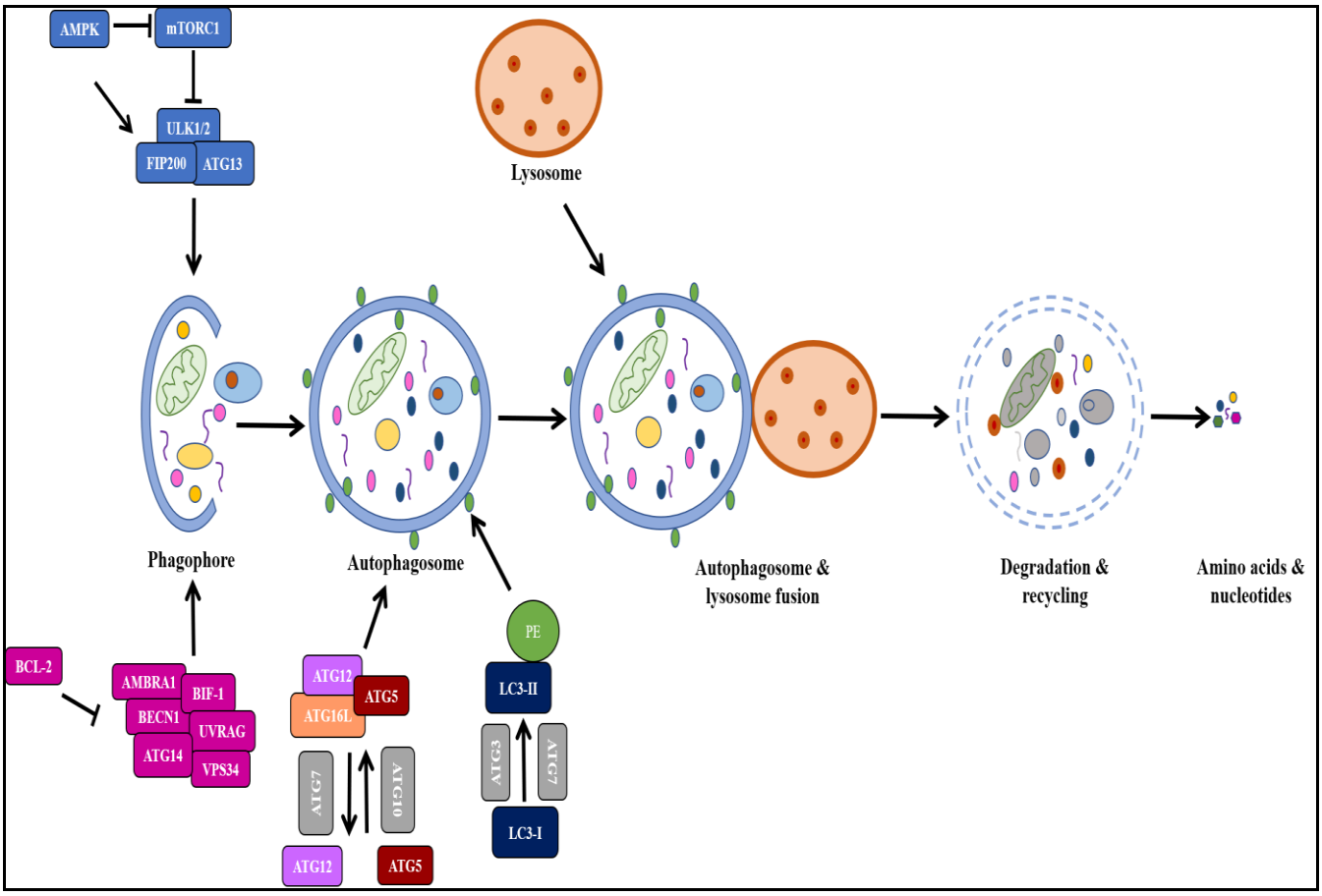

Figure 1.9. Schematic representation of autophagy. Autophagy is one of the important mechanisms involved in maintaining cellular homeostasis. It involves several steps to degrade the cargo beginning from phagophore formation followed by elongation of membrane and formation of autophagosome, the double-membrane structure. Later, it fuses with the lysosome where the degradation process happens with the help of digestive enzymes.

1.3.2.1 Types of autophagy

As shown in **figure 1.10,** autophagy is broadly divided into the following categories based on their mechanism of translocating the cargo to lysosomes.

Macroautophagy: Referred as autophagy, is the highly studied and well-characterized type. During this process, the cargoes are typically engulfed in a membrane-bound vesicle, autophagosome, followed by its fusion with lysosomes for subsequent enzymatic degradation [122]. Under normal physiological conditions, mTORC1 is known to impair autophagy through the inactivation of the ULK1/2 autophagy complex. However, upon stress signal, mTORC1 is inhibited and ULK1/2

phosphorylates itself and ATG-13 and FIP200, leading to autophagy activation [135]. The process of autophagy starts with membrane nucleation and phagophore formation which is controlled by PI3K complex, including VPS34 and the regulatory protein Beclin1 [136]. Further, the elongation of the isolated membrane relies on two conjugation systems. Firstly, autophagy-related gene 12 (ATG-12) is covalently conjugated to ATG-5 protein through ATG-7 (E1-like) and ATG-10 (E2-like) proteins. Then, ATG16L1 protein is recruited to this dimer and forms a large complex (ATG12-5-16L1) which serves as an E3 ligase, conjugating lipid molecules (like phosphatidylethanolamine) to ATG-8 orthologs MAP1LC3, GATE16, GABARAP. These lipid conjugated proteins play a very crucial role in the elongation, expansion, and closure of autophagosome membranes [137]. Lastly, the autophagosome fuses with late endosomes or lysosomes with the help of proteins like LAMP-2, SNAREs, RABs. Following this, lysosomal hydrolase-dependent degradation takes place [138].

Selective autophagy: Macroautophagy engulfs targets in a non-selective manner however, several selective forms of autophagy have been reported in recent years. This type of autophagy mainly degrades endoplasmic reticulum via reticulogy [139], ribosomes via ribophagy [140], cytoplasmic protein aggregates via aggrephagy [141], pathogenic intracellular invaders [142], mitochondria via mitophagy [143], peroxisomes via pexophagy [144] and even certain free proteins and RNAs [145]. This mechanism helps a cell to control several organelles, eliminate dysfunctional components and potentially harmful aggregates and invaders.

Microautophagy: This type of autophagy doesn’t typically require the formation of an autophagosome. Cargoes are directly engulfed by the membrane with the help of Rab7, several ATGs, and ESCRT machinery proteins [146].

Chaperone mediated autophagy (CMA): This is a special class of autophagy where a protein must possess a KFERQ motif to be eligible for CMA degradation. This motif is then recognized by a chaperone, HSC-70 which further translocates the CMA substrate to lysosomes via LAMP-2a protein [147].

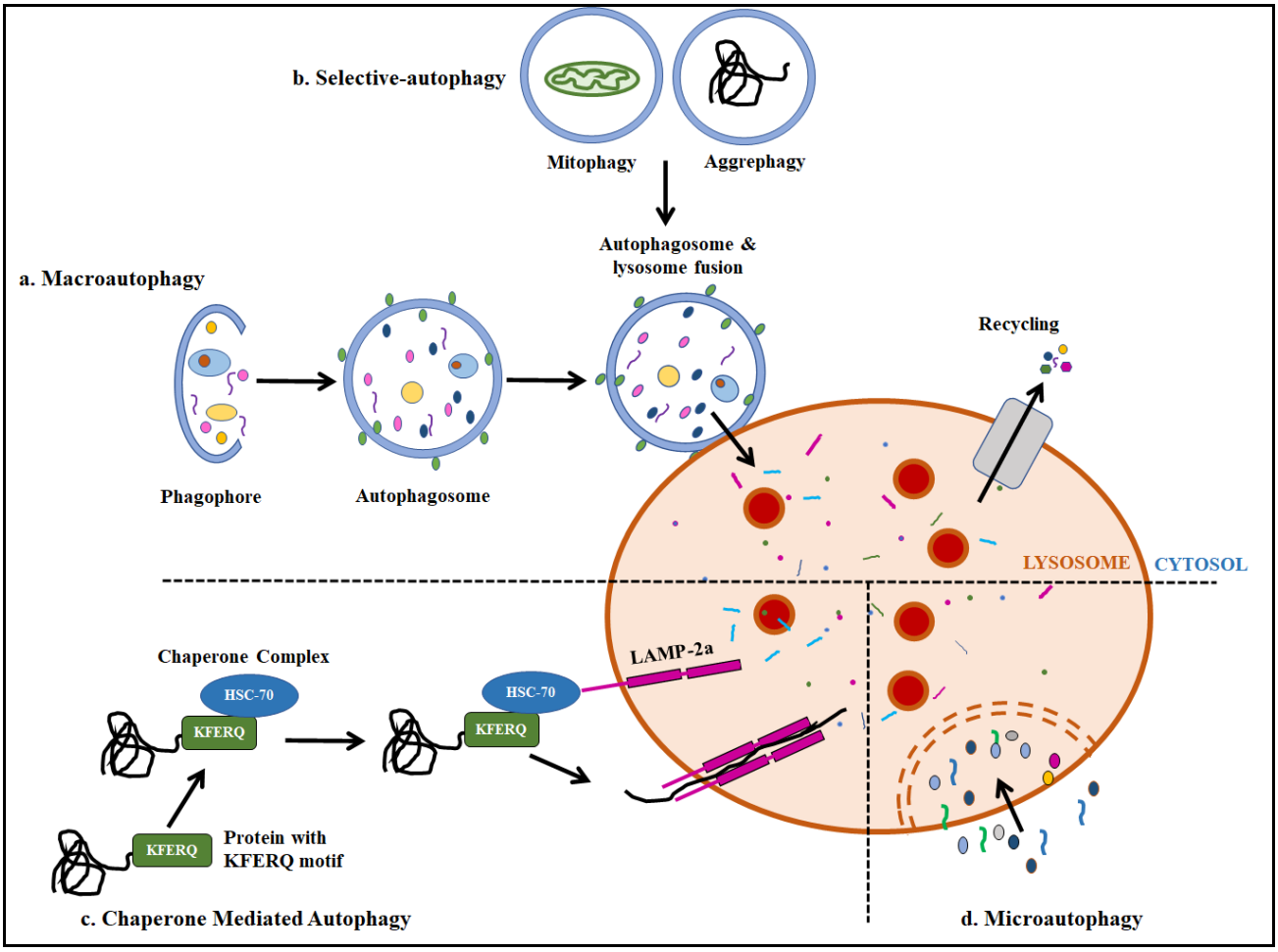

Figure 1.10. Diagrammatic representation of types of autophagy. Autophagy is broadly divided into four categories based on the type of cargo to be degraded and the kind of degradation mechanism involved.

1.3.2.2 Bipolar nature of autophagy in cancer

Autophagy is widely reported for its complex and bipolar role in cancer progression **(Fig 1.11)**. As studied, the cancer type, stage, and genetic context decide the autophagy-dependent fate of tumor cells. Autophagy is known as a quality control process as it exerts a cytoprotective effect by eliminating misfolded proteins and damaged organelles hence limits the chances of cancer progression. Inversely, there are reports on utilizing the stress-mitigating properties of autophagy by cancer cells to meet the heightened metabolic demand for rapid proliferation [148].

1.3.2.2.1 Tumor-suppressive role of autophagy

Autophagy has been known to play a crucial role in tumor suppression as impairment of autophagy is reported to induce instability, tumorigenesis, and malignant transformation. Beclin1, an important

autophagy-promoting protein is well established for its tumor-inhibitory role. Several reports are suggesting that the loss of Beclin-1 can develop tumors not only in mice but in several human cancers including breast, ovarian, and prostate [148]. Also, mice lacking ATG-5 and ATG-7 have been shown to experience mitochondrial damage and oxidative stress which led to the development of liver tumors. [149]. In another report, mice with ATG-4 deficiency have been shown to possess chemically induced fibrosarcoma [150]. Notably, autophagy inhibition-mediated accumulation of aggregated P62 is reported to cause cytotoxicity, oxidative stress, and DNA damage which is associated with poor prognosis in several cancers [151]. Additionally, dysregulating PI3K/Akt signaling or loss of tumor suppressor PTEN has been reported to be a probable cause of decreased autophagy in cancer cells [148]. Conclusively, autophagy suppresses tumor initiation but an impairment may lead to tumorigenesis, hence plays an important role in cancer progression.

1.3.2.2.2 Tumor-promoting role of autophagy

Many established tumors have been demonstrated to utilize autophagy to meet the high metabolic demands of proliferating tumor cells to avoid metabolic stress-induced necrosis. Also, the recycled amino acids post lysosomal degradation have been reported to be utilized by tumor cells to fuel their elevated metabolism. Additionally, during, poor oxygen supply, HIF-1α dependent and independent autophagy is induced, which contributes to tumor survival [152]. This suggested an obvious apoptotic tumor cell death post pharmacological inhibition of autophagy or genetic knockdown of essential autophagy genes. In corroboration to this, genetic studies in mice have reported a reduced growth of mammary tumors post FIP200 deletion [153]. Interestingly, cancers possessing activating HRAS or KRAS mutations are known to be autophagy addicted and inhibition of autophagy by various means has shown tumor regression in such cancers [150]. Thus, by enhancing stress tolerance and meeting the heightened metabolic demand of tumor cells, autophagy is well-regarded as a mechanism for tumor cell survival.

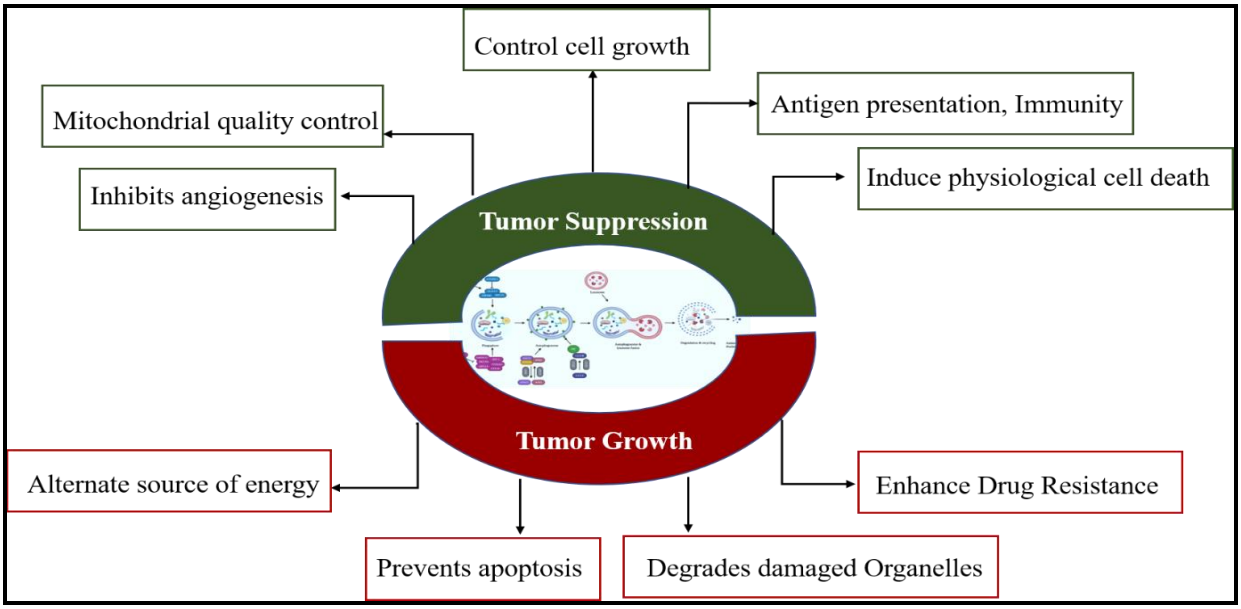

Figure 1.11. Depicting dual role of autophagy in cancer progression. Autophagy can either enhance cancer by increasing drug resistance or by providing an alternate source of energy or can inhibit cancer by initiating apoptosis and by controlling the tumor growth.

1.3.2.3 Targeting autophagy for cancer therapeutics

As discussed already, autophagy plays a paradoxical role in tumor progression hence, the strategy to target autophagy can have a deep therapeutic impact on cancer therapy in future.

1.3.2.3.1 Autophagy inhibitors

Since enhanced autophagy has been established as a mechanism involved in tumor cell survival and acquired drug-resistance hence, inhibition of autophagy has been extensively demonstrated to sensitize tumor cells to anticancer therapy. Many reports are suggesting the use of small-molecule inhibitors of autophagy alone or in combination with anti-cancer drugs to target many stringent cancers. Deletion of ATG-5, ATG-7, or Beclin-1 genes has been reported to revert the acquired tamoxifen resistance in breast cancer cells [154]. As reported, a combined treatment of autophagy inhibitor 3-MA along with trastuzumab has been shown to enhance the potency of chemotherapy in HER2-positive breast cancer cells [155]. In another study, high-level autophagy was observed to be associated with cisplatin resistance in ovarian cancer cells and interestingly, an ATG-5 deletion resulted in apoptotic cell death [156]. CQ is an anti-malarial drug known to inhibit autophagosome-lysosome fusion [157]. HIF-1α induced autophagy has been shown to induce resistance towards anti-angiogenesis drug bevacizumab in glioblastoma cells, which can be reverted either by ATG-7

deletion or CQ treatment [158]. Presently, Chloroquine (CQ) /Hydroxychloroquine (HCQ) is the only autophagy inhibitor approved by the FDA for clinical trials. Also, autophagy inhibition either by 3-MA or Beclin-1 deletion has been reported to sensitize hepatocellular carcinoma cells to chemotherapy. Similarly, CQ treatment in colorectal cancer cells has been shown to induce sensitization towards chemotherapy drugs [148]. All these findings suggest autophagy inhibitors when used along with anti-cancer drugs, enhances the cancer cell sensitization, eventually inhibiting tumor survival. These findings hold great clinical importance in designing novel therapy because acquired drug resistance is the biggest bottleneck in cancer chemotherapy

1.3.2.3.2 Autophagy inducers

An excessive autophagy induction post cytotoxic drug treatment or through autophagy inducers could also result in autophagic cell death. In line with this, temsirolimus and everolimus, analogs of mTOR inhibitor rapamycin have been shown to induce antiproliferative effect by inducing cell cycle arrest and excessive autophagy, leading to tumor cell death in mantle cell lymphoma and acute lymphoblastic leukemia [148]. Also, a combinatorial treatment of anti-cancer drug temozolomide with dasatinib induced autophagy-dependent apoptotic cell death in drug-resistant Glioblastoma cells [159]. Similarly, HDAC inhibitors have also been known to show anti-cancer effects by inducing autophagy [160]. Rapamycin-induced decreased VEGF production and inhibited downstream signaling is reported to be one of the successful therapeutic interventions in terms of its anti-angiogenesis role [161].

Although, the autophagy inhibitors either alone or in combination with chemotherapeutic drugs are already in clinical trials, however, excessive autophagy induced cell death and contradicting role of autophagy in tumor suppression should also be considered for therapy. With regards to autophagy induction-based therapy, more attention is required to understand the importance of using autophagy inducers based on cancer progression. Importantly, more focus is required on an understanding of autophagy modulation to achieve better clinical outcomes.

1.3.3 Cross talk between UPS and autophagy

The UPS and autophagy are the two major independent and evolutionarily conserved homeostasis machineries in eukaryotes. Many studies have revealed their connections and cross-talks in modulating the cellular process **(Fig. 1.12**).

1.3.3.1 Compensatory balance between the two degradative pathways

To maintain homeostasis, the cellular cargo that accumulates post inhibition of one degradation pathway needs to be cleared by other systems. It has been observed, UPS and autophagy have functional connections as inhibition of one led to compensatory activation of another pathway. In this regard, inhibition of UPS by bortezomib was observed to enhance autophagy by increasing the expression of ATG-5 and ATG-7 [122]. Additionally, treatment with MG-132, another proteasomal inhibitor was shown to decrease cell proliferation and stimulate autophagy through upregulation of Beclin-1 and LC3 [162].

Similarly, pharmacological and genetic inhibition of autophagy was observed to enhance the UPS activity via increasing PSMB5, proteasome β5 subunit levels in colon cancer cells [122]. Another study showed increased chymotrypsin-like activity of proteasome post 3-MA mediated autophagy block in cultured neonatal rat ventricular myocytes (NRVMs) [163].

Also, autophagy inhibition is correlated with accumulated ubiquitinated proteins in many cases. In corroboration to this, independent studies with ATG-5 or ATG-7 knock-out mice, have shown accumulated ubiquitinated conjugates in the brain and liver of the animals [122]. In another study, autophagy inhibition through siRNA-mediated knockdown of ATG-7 and ATG-12 led to impairment of UPS and accumulation of several UPS substrates like P53 and β-catenin [164].

In summary, both the degradation pathways work in a compensatory manner yet an ideal compensation mechanism does not always achieve and largely depends on cell types, cellular and environmental conditions, and targeted protein.

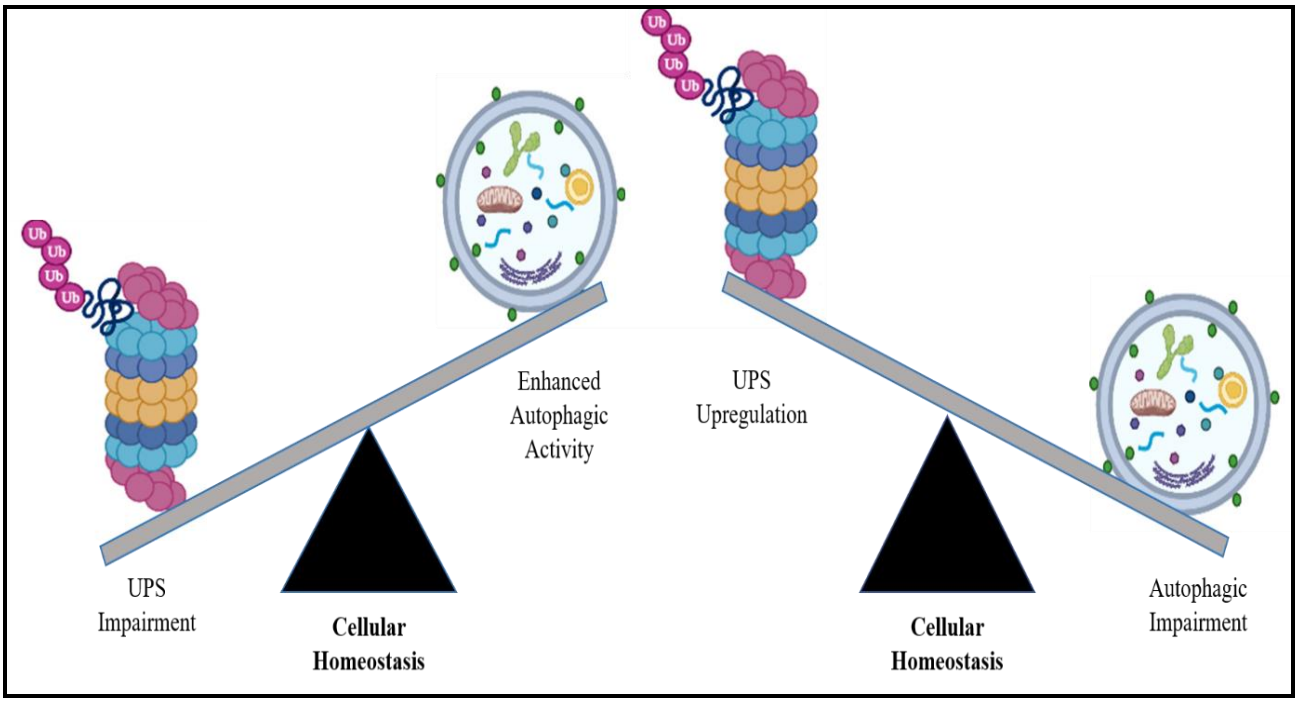

Figure 1.12. Illustrating the balance between cellular homeostasis. To maintain balanced cellular homeostasis, UPS and autophagy work in a compensatory manner as impairment of one lead to activation of another.

1.3.3.2 Interplay between the UPS-autophagy: selective clearance of cytosolic proteins

Several soluble proteins with a folding problem are known to be recognized by chaperons and are instructed towards UPS for degradation. In this regard, CHIP (E3 ligase), an HSP70 and HSP90 interactor, was found to be responsible for K48-linked ubiquitin chain addition to unfolded/misfolded proteins. Further, BAG1 has been shown to interact with the HSP70 complex and further induce proteasomal degradation of target proteins [122]. Inversely, aggregated insoluble proteins are directed for autophagy-mediated clearance. For this process, aggregated proteins first form aggresomes with the help of proteins like HDAC6, ubiquitinated by different E3 ligases, like CHIP, Parkin, HRD1. Post aggresome formation, adaptor proteins P62 and NBR1 directly recruit ubiquitinated aggregates to autophagosomes [122].

1.3.3.3 Mutually controlled proteolytic degradation of UPS or autophagy components

Earlier we have discussed the complimentary yet independent mechanism of two degradation pathways. However, reports are suggesting their mutual coordination in proteolytic degradation. In this regard, a plant-based study has revealed the selective autophagy (proteaphagy) mediated degradation of 26S proteasomes [165]. Amino acid starvation has been reported to enhance

ubiquitination of 19S proteasome cap components and resulted in their P62-mediated recruitment to autophagosomes [166]. Interestingly, plant and yeast proteasomes have been observed to localize in proteasomal storage granules (PSGs), to avoid autophagic degradation during carbon or nitrogen starvation [167].

1.3.4 P53 and protein homeostasis

Levels of WT-P53 are usually maintained by MDM2 (E3 ligase) mediated ubiquitination that targets P53 for proteasomal degradation. However, mutant P53 being more stabilized evade MDM2 mediated degradation but is reported to be highly ubiquitinated in an MDM2 independent manner. One of the ubiquitin ligases reported in this regard is CHIP (C terminus of Hsc70-interacting protein) which has the capability of mutant P53 ubiquitination and degradation. Interestingly, although MDM2 failed to degrade mutant P53 directly, it is reported to induce mutant P53 degradation independent of its E3 ligase activity [55].

In the past decades, many groups have shown the impact of P53 on macroautophagy. There are reports for WT-P53 to act as a pro-autophagic factor in human cancers as it increases the transcription of various genes with autophagy regulatory functions including AMPK activation, mTOR inhibition, suppression of PI3K activity, promoting ULK1/2 and ATG-7 expression, transactivating DRAM1 that affects multiple stages of autophagy[168]. Notably, autophagy-inducing functions of WT-P53 are mostly involved in tumor suppression under stress conditions like hypoxia, starvation, or DNA damage as autophagy assist to cope with different cellular stress. However, the cytosolic pool of WT-P53 in normal conditions is known to inhibit autophagy by inhibition of AMPK or in turn activating mTOR [169], by inducing TIGAR-dependent glycolysis and ROS [170]. A similar mechanism was observed in selective autophagy for mitochondrial clearance as nuclear WT-P53 has been reported to promote mitophagy by transactivating the Pink, involved in the degradation of impaired mitochondria however, cytosolic P53 was observed in mitophagy inhibition by directly binding with Parkin, preventing its translocation to damaged mitochondria [171].

Unlike WT-P53 which possesses a dual role in autophagy induction, mutant P53 is mostly reported to regulate the suppressive role. As evident from a previous study where ectopic overexpression of 22 mutant variants in colon cancer resulted in suppressed autophagy. However, a few of them showed no change [172]. This was supported with the study performed later, where R175H-P53 and R273H-P53 were reported to suppress the formation of autophagic vesicles and their lysosomal fusion by transcriptionally repressing the important autophagy genes such as Beclin1, DRAM1,

ATG12 [173]. Nevertheless, mutant P53 has also been reported to inhibit autophagy independent of transcriptional regulation. As reported, unlike WT-P53 certain mutant P53 proteins failed to form a complex with Bcl-2 or Bcl-XL, thus cancer cells with mutant P53 sustain the Beclin1 and Bcl-2 inhibitory interactions [174]. Additionally, by stimulating mTOR, mutant P53 has also been reported to suppress the Beclin1 functionality.

Since autophagy can sustain tumor metabolism and mutant P53 encourages the adaptations to nutrient deprivation, it is reasonable that certain P53 mutations may stimulate autophagy to meet up the energy demand of cancer cells. In support of this, a recent report on 113 colorectal cancer specimens has shown a significant association of high LC3B levels with mutant P53 protein expression pattern in ~35% of the patients [175]. Similarly, additional signaling, mutation, or epigenetic changes might abrogate the mutant P53 dependent autophagy suppression. For instance, cancer cells with activating HRAS or KRAS mutations have been known to induce autophagy, regardless of mutant P53 presence [176]. Thus, mutant P53 might contribute to autophagy stimulation in a cell type, context, or cancer stage-dependent manner.

Conclusively, the role of mutant P53 in autophagy regulation is complex and context-dependent. Further, since mutant P53 is stabilized inside the tumor cell, designing strategies to promote autophagic degradation of mutant P53 seems an attractive anti-cancer approach.

1.4 Gaps in research

The p53 gene has been implicated in multiple cancers due to loss of its tumor-suppressive property, a consequence of frequent mutations. Interestingly, specific missense mutations at a particular locus in the p53 gene often result in an acquisition of gain of function (GOF) to the translated protein, hitherto absent in its wild type form. Hence, the GOF-P53 is often associated with a pro-tumorigenic role which is in contrast to properties of its wild-type form. In this regard, lung cancer, especially non-small cell lung carcinoma (NSCLC) registers the highest cancer mortality rate worldwide and was found to harbor a high percentage of p53 mutations often associated with poor patient survival. Initial data also shows that of all the GOF-mutations, R273H is amongst the top prevalent missense mutations observed in NSCLCs. However, the relevance of P53 status is often neglected in the current clinical therapeutic strategies for the treatment of cancers. This hence warrants consideration of important factors like, the type of P53 mutation, site of mutation, the crosstalk of mutant P53 proteins with other proteins or intracellular pathways, and thereafter experimental analysis and selection of an appropriate therapeutic strategy that can effectively sensitize cells with GOF-P53. However, though P53 is an extensively studied molecule worldwide, yet, there is dearth of relevant literature portraying strategies to successfully attenuate GOF-P53 mediated effects. It is reported that the acquisition of GOF mutation imparts additional stability to the P53 protein thus endowing it with a time window for promoting its GOF-like activities. The procedure of stabilization and degradation of WT-P53 is well established, but the understanding of mutant P53 in this regard is under-explored. As we are aware, the cellular protein turnover is often regulated by machineries like the ubiquitin proteasomal system (UPS) and autophagy; however, the crosstalk of GOF-P53 with the cellular protein turnover system and its implications in therapy is poorly elucidated. Further, a host of proteins in the intra-cellular milieu can interact with the GOF-P53 in a context and cell type-dependent manner dictating an array of GOF-like activities. Therefore, there is an urgent need to harness knowledge regarding these interactions of GOF-P53 within the disease context and identify a probable vulnerability that can be exploited to efficiently ablate its GOF effects. Given the number of variables, further understanding the mechanism of action of GOF-P53 is required to translate the information into an appropriate therapy. In this context, dissecting the crosstalk of GOF-P53 with other proteins and pathways regulated by them becomes critical. Deciphering the details of these interactions can provide cues to appropriate sensitization of GOF-P53 harboring cancer cells and can be translated into the future development of novel and effective protective regimens. **Figure 1.13** represents a few of the gaps in existing research.

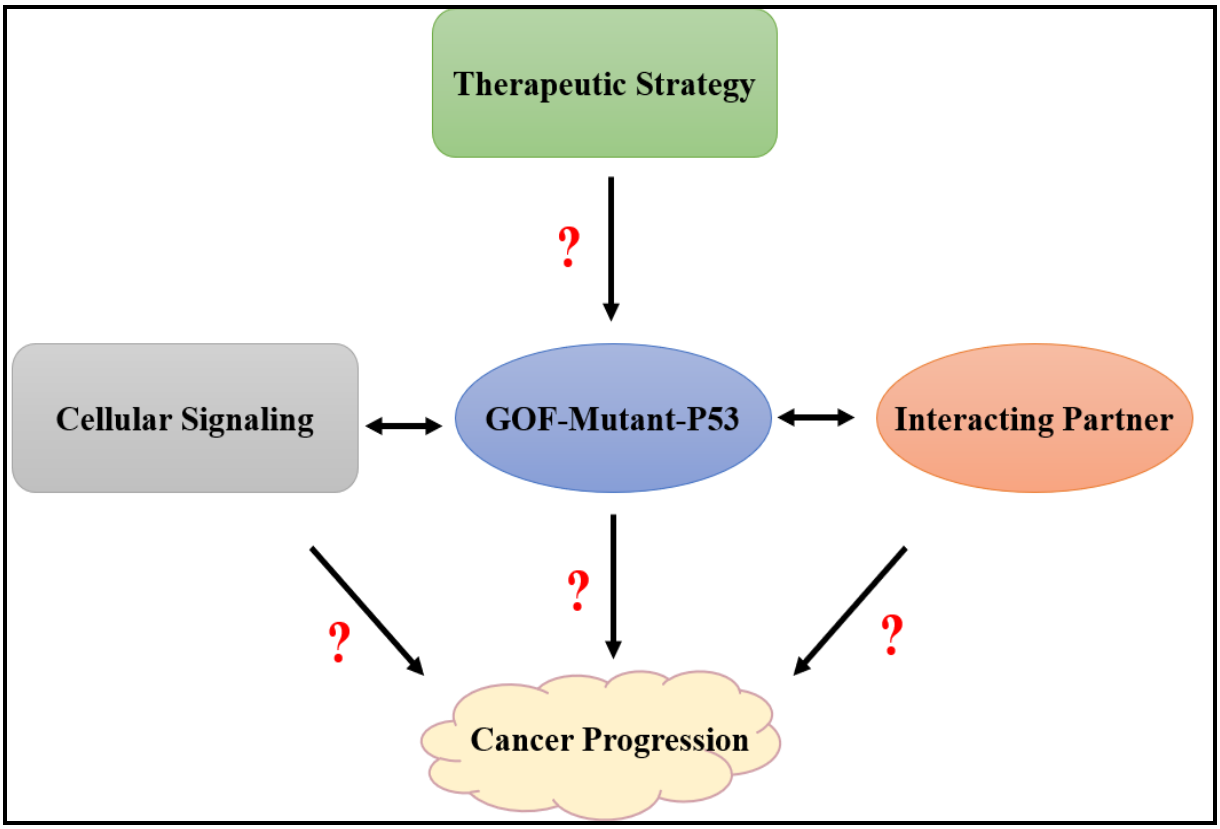

Figure 1.13. Schematic representation of gaps in existing research

1.5 The objective of the research:

1. Elucidating prevalence of GOF-P53 mutation in cancer, analysis of drug sensitivity in GOF-P53 harboring cancer cells.

2. Exploring the crosstalk between GOF-P53 and cellular homeostatic machineries - ubiquitin proteasomal system and autophagy.

3. Design of appropriate therapeutic strategies against tumor cells harboring GOF-mutant P53 based on the understanding of its crosstalk with protein homeostatic machineries.

Chapter-2

Materials and Methods

2.1 Materials

2.1.1 Chemicals

ALLN (#sc-221236), pifithrin-alpha (PFT-*α*, #sc-45050), and rapamycin (Rapa, #sc-3504A) were purchased from santa-cruz biotechnology. Cisplatin (#232120) was obtained from MERCK. Verteporfin (#SML0534-5MG), 2′,7′-dichlorofluorescin diacetate (DCFDA, # D6883), monodansylcadaverine (MDC, # D4008), chloroquine (#C6528), propidium iodide (PI; #P4864), RIPA buffer (#R0278), acridine orange (AO, #A9231) were purchased from sigma; N-Acetyl-L-cysteine (NAC, #47866) and 3-(4, 5-dimethylthiazol-2-yl)-2,5-di-phenyltetrazolium bromide (MTT, #33611) were obtained from SRL. Bafilomycin A1 (#11038) was purchased from cayman chemicals. Geneticin (G418, # 10131-035), FITC conjugated annexin V (#A13199), Annexin V binding buffer (#V13246), and Lysotracker green DND-26 (# L7526), Lysotracker red DND-99 (LTR, # L7528), Enhanced chemiluminescence (ECL, #32,106), Antifade mountant (4′-6-diamidino-2-phenylindole, #P36962), mammalian Beta-galactosidase assay kit (#75707), and PVDF membrane (#88518) were procured from thermo fisher scientific. Lipofectamine 3000 was from Invitrogen (#L3000-001). The MAPK inhibitor, U0126, was obtained from cell signaling technology (CST, USA). Plasmid GFP-RFP-LC3 was kindly provided by Dr. Sovan Sarkar (Birmingham Fellow, University of Birmingham). Ub GFP (#11,928), mRFP Ub (#11,935), FLAG pcDNA3 (#20011), pcDNA FLAG YAP1 (#18881), 8XGTIIC luciferase (#34615), pCMV-Neo-Bam P53 WT (#16434), pCMV-Neo-Bam P53 R273H (#16439), and pCMV-Neo-Bam Empty Vector (# 16440) plasmids were procured from addgene. siRNA-P53 (#106140), siYAP (#107951), and siATG-5 (#137766) were obtained from ambion.

2.1.2 Instruments

The major instruments used for the wet-lab experiments are enlisted below in **Table 2.1**.

Table 2.1 List of major instruments used.

Name of Instrument	**Company**
Laminar airflow	MAC
Inverted Microscope	Olympus
Fluorescent Microscope/Apotome	Zeiss

Confocal Microscope	Zeiss
Scanning Electron Microscope	Thermo fisher scientific
Multiskan GO microplate spectrophotometer	Thermo fisher scientific
Cooling Centrifuge	Thermo fisher scientific
Vertical/ Horizontal gel electrophoresis unit	Bio-Rad
Semi-dry transfer apparatus	Bio-Rad
Real-time PCR	Bio-Rad
Thermocycler	Bio-Rad
Chemi Doc/Gel Doc	Bio-Rad
Luminometer	Promega
Flow Cytometer	Beckman Coulter

2.2 Methods

2.2.1 *In silico* analysis

The initial analysis for P53 and other mutation frequency in NSCLC patients was done using the program and tools made available online at cBioportal (cBioPortal for Cancer Genomics) [177, 178]. The transcriptomic data of lung cancer patients was extracted from the GDC portal and autophagy genes were segregated using a KEGG mapper. The human protein atlas (Search: The Human Protein Atlas) was used to check the 5-year survival of NSCLC patients [179]. The transcriptomic data of osteosarcoma patients were extracted from the GEO database of NCBI, which can be accessed through GEO accession ID GSE99671 [180]. Differentially expressed transcripts between the osteosarcoma tumor sample and their tissue-matched control were identified using DESeq2 software [181]. The transcripts with a p-value ≤ 0.05 were considered significantly differentially expressed. The resultant transcripts were then imported to cytoscapeV3.7.2 for highlighting the regulatory

network consisting of differentially expressed transcripts. A Cytoscape plugin, clueGO, was used to integrate gene ontology (GO) terms and KEGG pathways, which created a functionally organized GO/pathway term network [182].

2.2.2 Cell culture

The non-small cell lung carcinoma cell line, H1299 (P53-null), was a kind gift from Dr. Sanjeev Das (NII, New Delhi). Breast cancer cells- MCF-7 (WT-P53) and MDA-MB-468 (R273H-P53), Human osteosarcoma cells- HOS (R156P-P53) were procured from NCCS (Pune, India); HCT116 (P53-null) and HCT116 (WT P53) cells were obtained from Wogan Lab (MIT, USA); HT-29 and SW480 (R273H-P53) cells were a gift from Dr. Susanta Roychoudhury, IICB-Kolkata. Cells were cultured at 37°C, 5% CO_2 in medium supplemented with 10% fetal bovine serum and 1% penicillin-streptomycin mixture. Cells were grown to 70-80% confluency before treatments. Trypsin-EDTA solution (0.05%) was used for the detachment of cells.

2.2.3 Plasmid isolation and verification

P53 plasmids with wild-type P53 (WT-P53), GOF-P53 (R175H-P53, R248W-P53, R249S-P53, and R273H-P53), and empty vector (EV) were received in the form of culture-stabs. They were processed as follows:

1. Bacteria were streaked on antibiotic-supplemented LB agar plates. Colonies were allowed to grow overnight at 37°C.
2. A single-grown colony was taken and inoculated in antibiotic-supplemented LB media. The culture was allowed to grow in a bacterial hood at 37°C with continuous shaking.
3. The plasmid was isolated using Qiagen midi prep kit. The isolated plasmid was then quantified and checked for impurities through a spectrophotometer.
4. The isolated plasmid was digested with restriction digestion enzymes specific to the cloned insert. The digested plasmid was then checked over agarose gel electrophoresis to confirm the size of the backbone and insert. **Figure 2.1** represents the agarose gel image for undigested and digested plasmids.

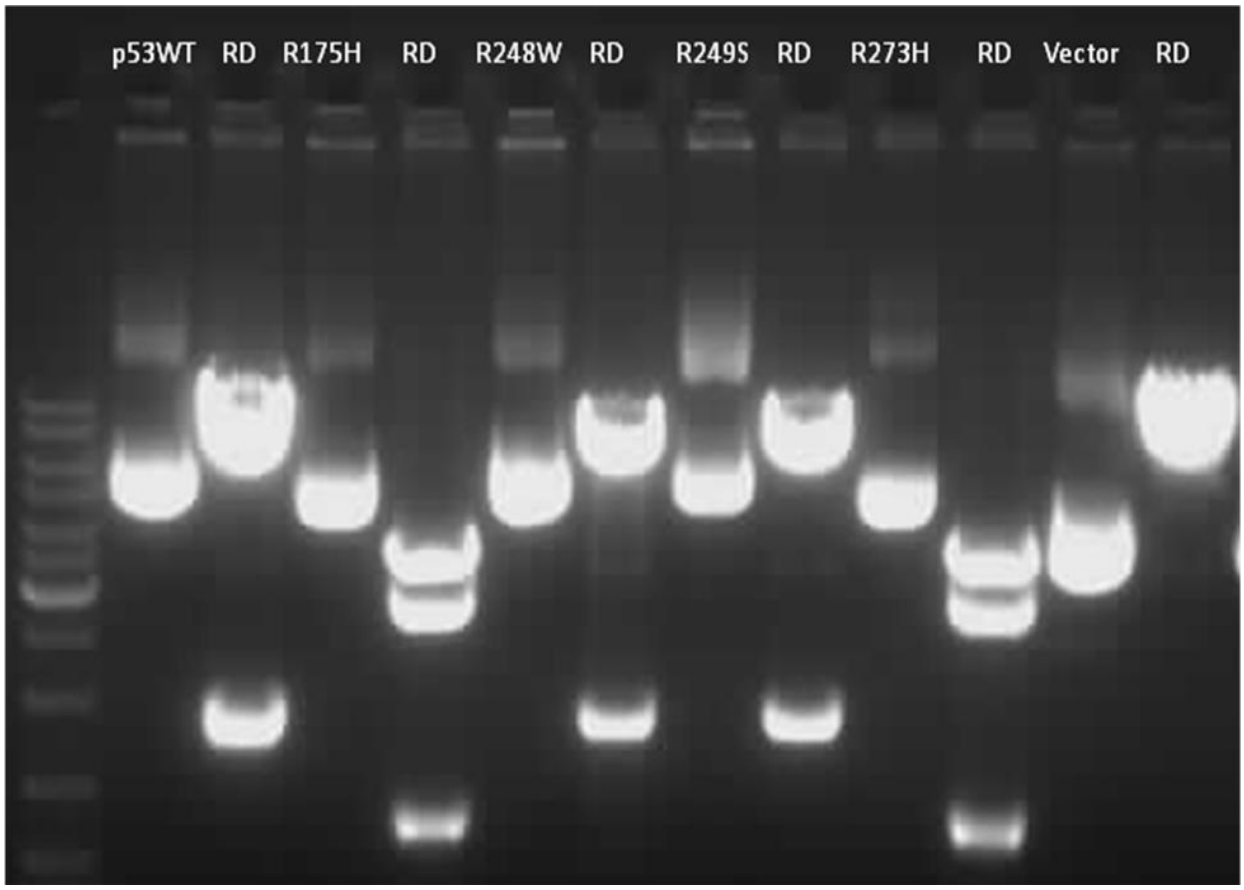

Figure 2.1. A representative figure from restriction digestion of the different P53 plasmids. P53 (WT-P53), GOF-P53 (R175H-P53, R248W-P53, R249S-P53, and R273H-P53), and empty vector (EV) plasmids were run on agarose gel in undigested and restricted digested form to confirm the size of the insert. Here RD stands for restriction digestion.

5. Further, plasmids were sent for DNA sequencing to verify key regions of the plasmid. For this, P53 specific primer was designed through Primer3 software. The following primer was used for amplification - forward- 5' TGGCCATCTACAAGCAGTCA -3' and reverse 5' GATTCTCTTCCTCTGTGCGC -3'. The amplified DNA sequence was then compared to the online available addgene plasmid sequence using clustal W sequence alignment.

Comparing WT-P53 sequence

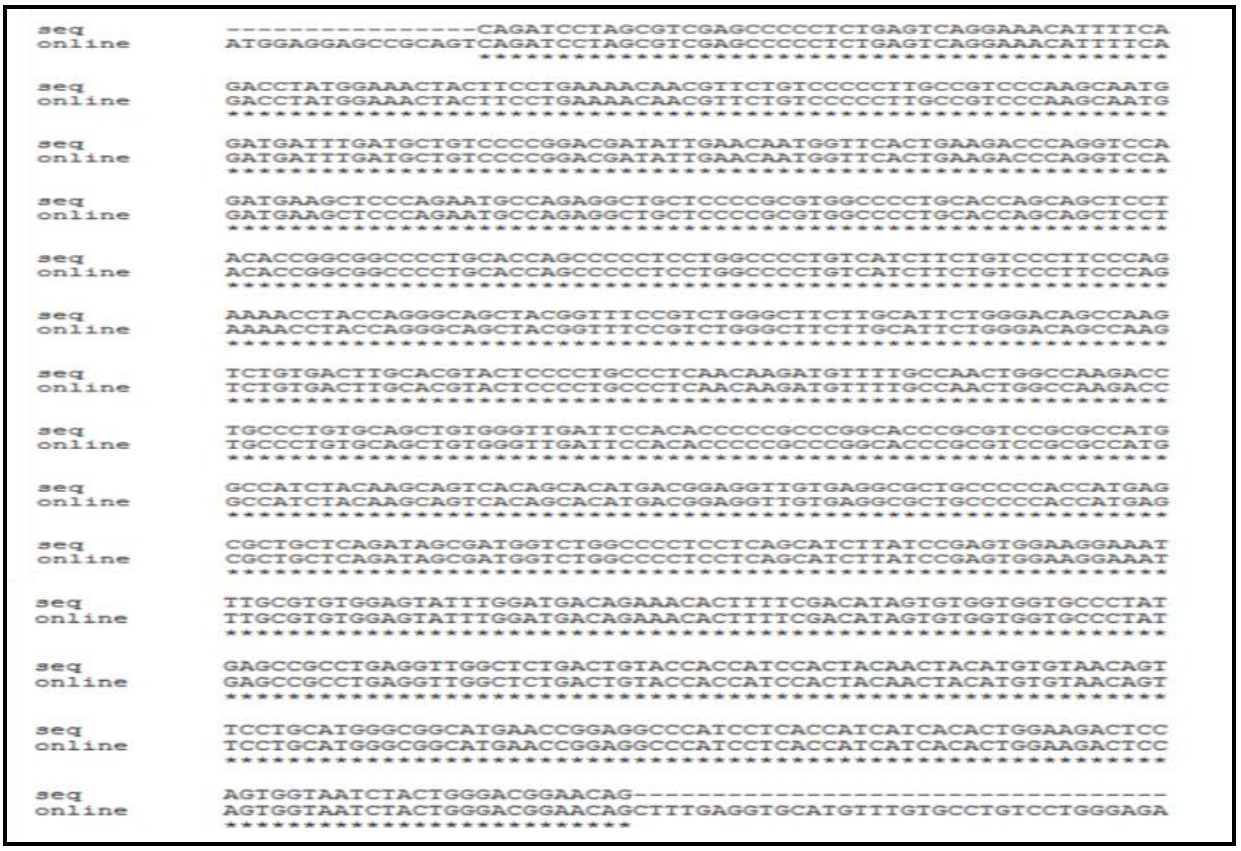

Comparing R175H-P53 sequence

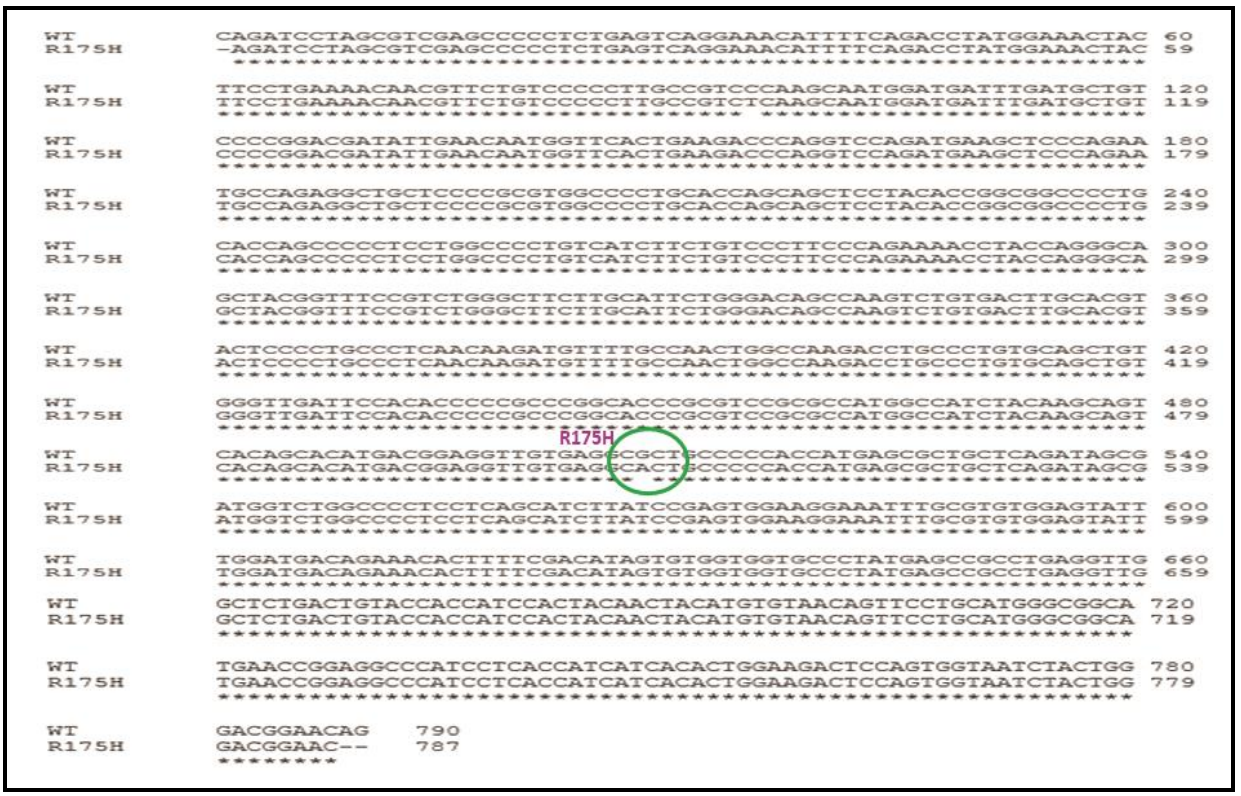

Comparing R248W-P53 sequence

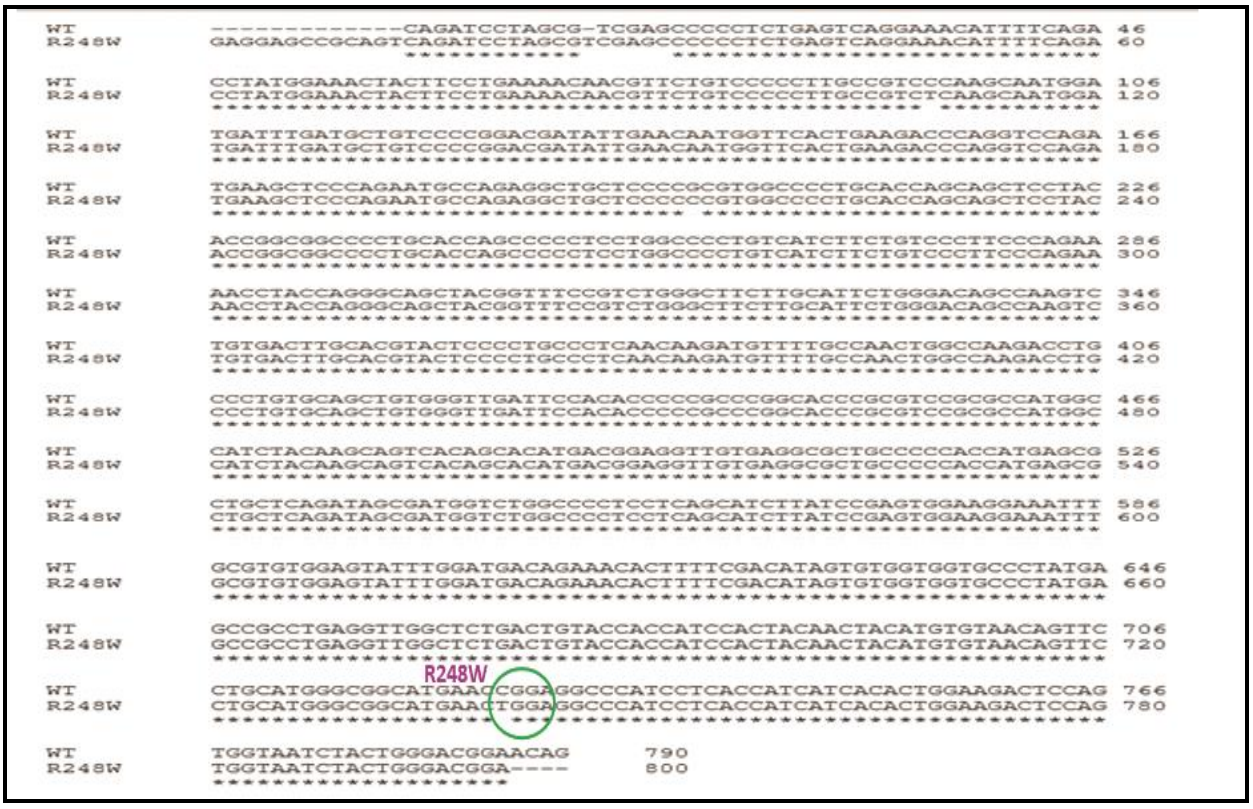

Comparing R249S-P53 sequence

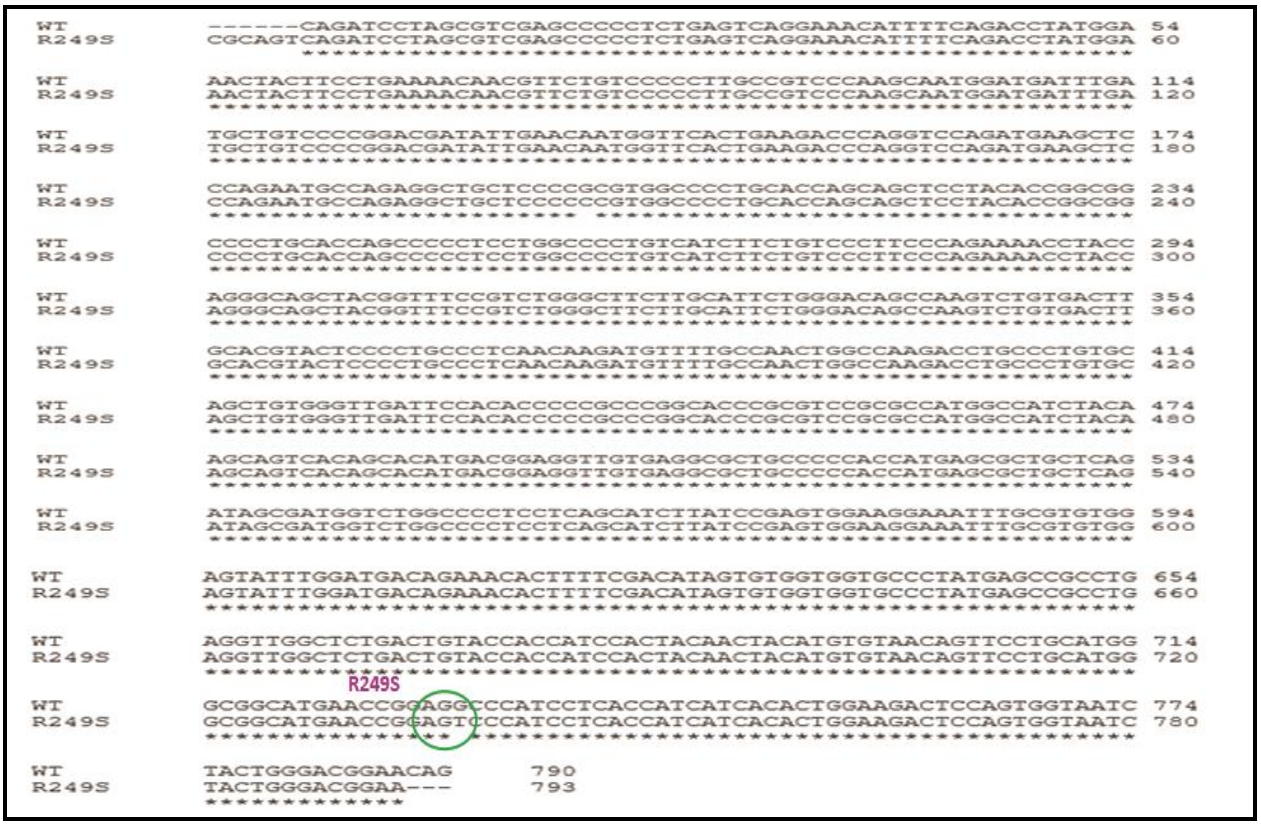

Comparing R273H-P53 sequence

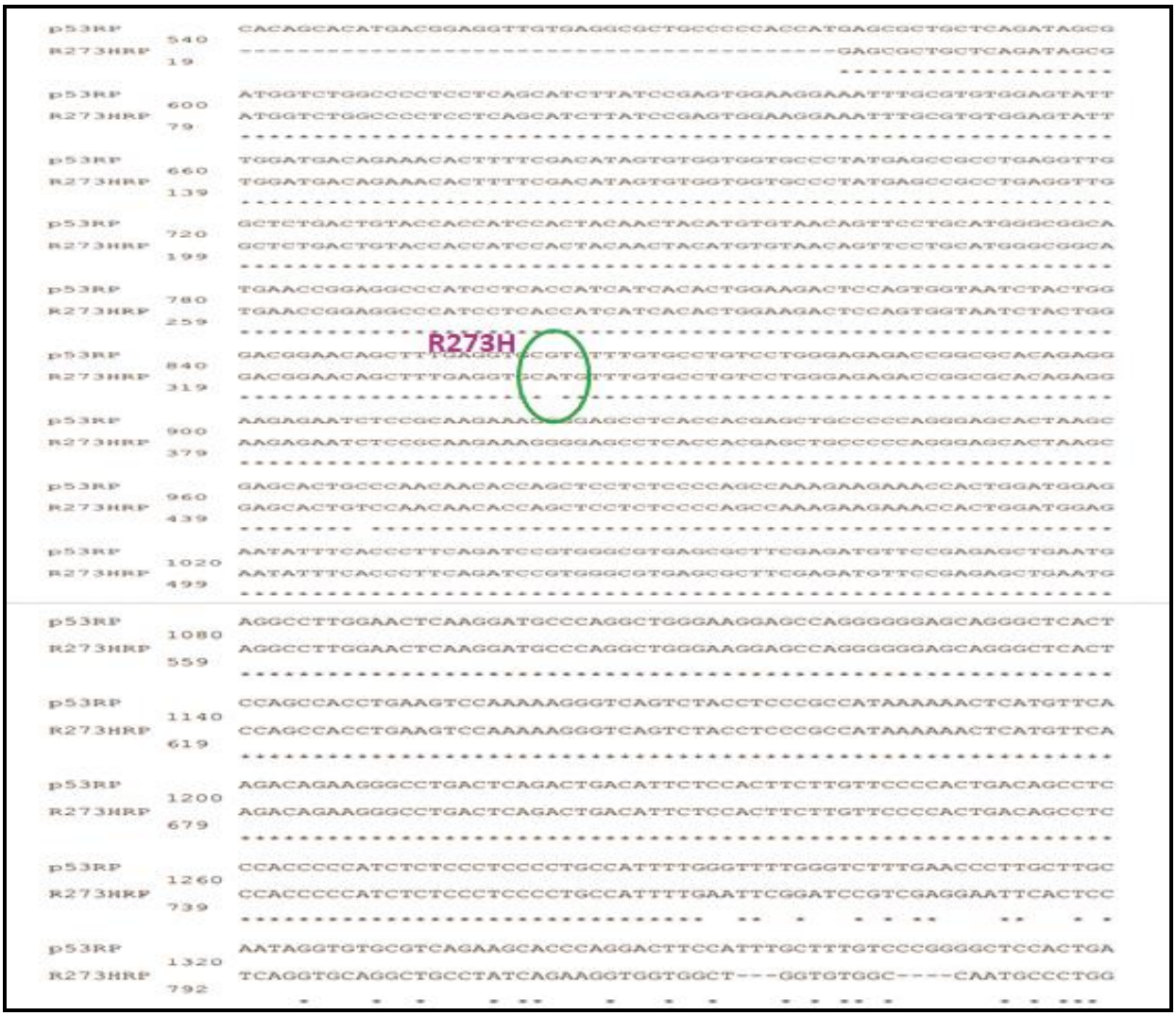

6. Post verification, bacterial glycerol stocks were prepared and stored at -80°C.

2.2.4 Preparation of stably transfected cells expressing WT-P53, R273H-P53, EV control, and GFP-RFP-LC3 plasmids

P53 null H1299 cells were cultured in a six-well plate and transfected with either 2 μg of pCMV-Neo-Bam P53-WT or pCMV-Neo-Bam P53-R273H or pCMV-Neo-Bam Empty Vector (EV) or GFP-RFP-LC3 purified plasmid with lipofectamine 3000 according to manufacturer's instructions. Around 24-hour (h) after transfection, the cells were transferred to a 10 cm dish and selected for transfection positivity by geneticin (G418, 600 μg/ml) selection. Transfected cells were maintained for several days under G418 pressure. Non surviving cells were washed off with PBS and fresh media with G418 was added. This was done until the cell colonies were obtained **(Fig. 2.2).** Random colonies were selected and allowed to grow in a new culture dish under G418 pressure. Cells were

grown until confluency and then stable transfection of WT-P53 or R273H-P53 vector was confirmed by immunoblotting against P53 antibody **(Fig. 2.3).** Successful stable transfection of the GFP-RFP-LC3 plasmid was confirmed by fluorescent detection of GFP and RFP fluorescence in surviving cells **(Fig. 2.4.i and ii).**

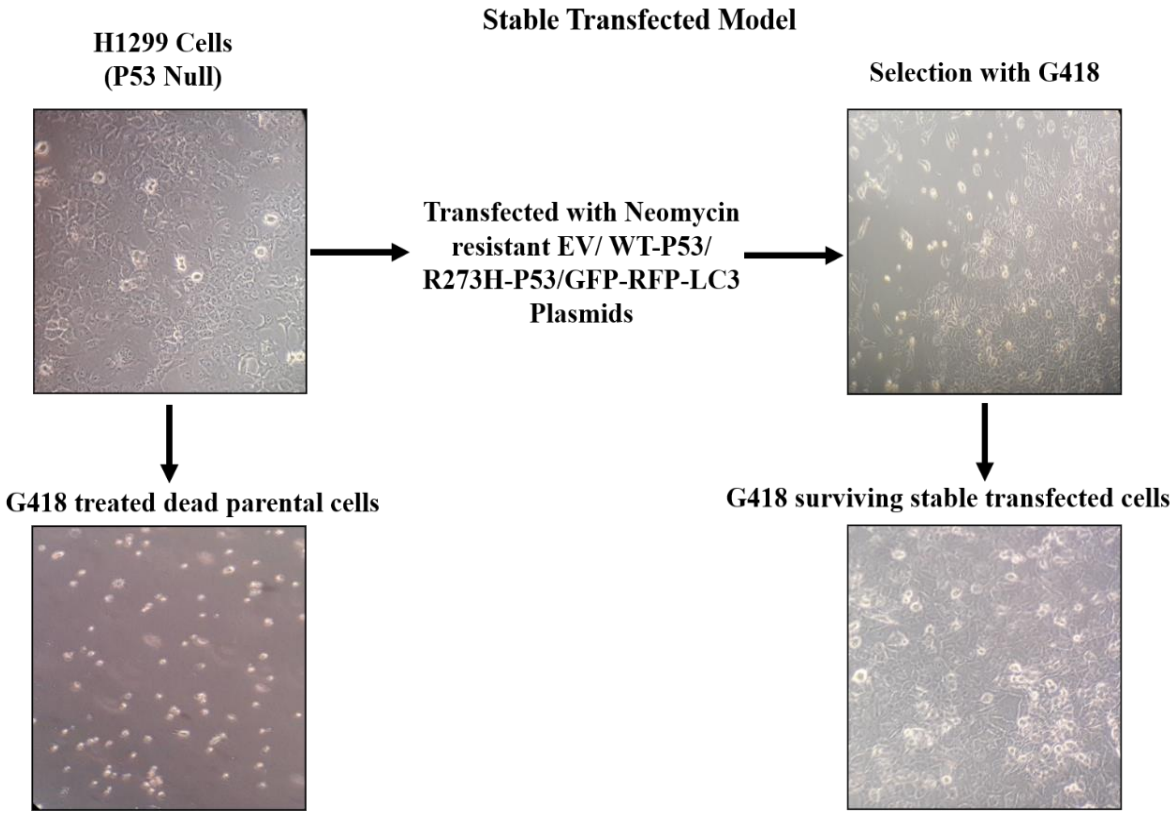

Figure 2.2. Schematic representation of preparing stably transfected cells. P53 null H1299 cells were transfected with specific plasmid and transfected cells were selected using G418 pressure.

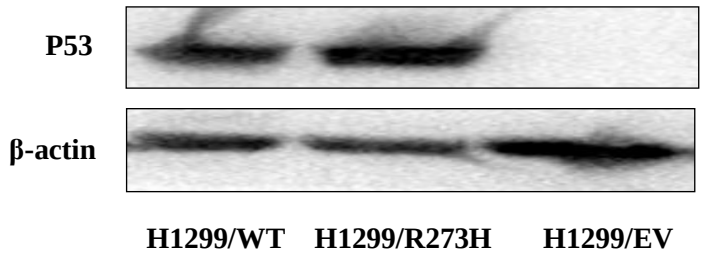

Figure 2.3. Verification of P53 stable transfected model through immunoblotting. Protein from stably transfected H1299 cells was quantified and immunoblotted with P53 antibody to confirm the presence of the transfected plasmid.

i. **ii.**

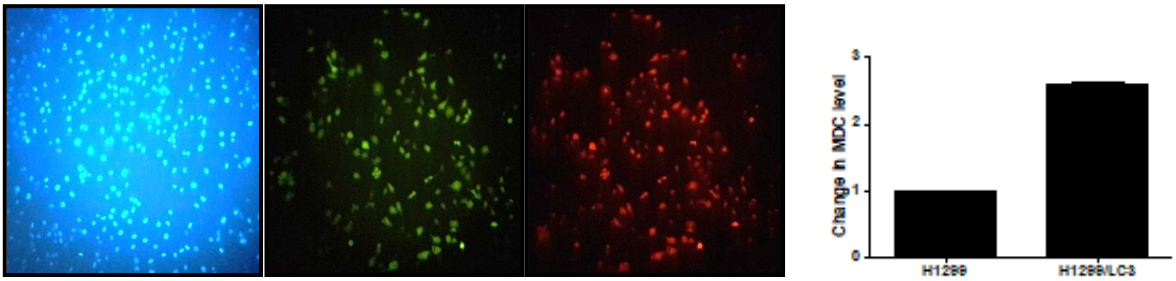

Figure 2.4. Verification of GFP-RFP-LC3 stable transfection. (i) Fluorescence microscope image to detect the presence of GFP and RFP fluorescence in stably transfected cells. **(ii)** MDC level measured by fluorimetry to detect the probable autophagosomes in GFP-RFP-LC3 expressing stably transfected cells.

2.2.5 Cell viability assay

In vitro cell viability assay was performed using 3-(4,5-dimethylthiazol-2-yl)-2,5-di-phenyltetrazolium bromide (MTT), following methods previously described in Chowdhury et al's work [183]. Briefly, cells were cultured in 96-well plates till they attain 70–80% confluency. Cells were then treated with specific compounds for a stipulated period. Following that, MTT was added to each well and incubated for 4 h. Formazan crystals formed by live cells were dissolved in DMSO, and readings were captured at 570 nm with a differential filter of 630 nm by multiskan GO microplate spectrophotometer. Untreated samples served as control. Percentage of viable cells was calculated using the following formula: viability (%) = (mean absorbance value of drug-treated cells)/ (mean absorbance value of the control) x 100.

2.2.6 Verteporfin uptake analysis

After treatment with VP, cells were harvested at 1800 rpm, 8 min. To the pellet, 500 µl PBS was added and centrifuged at 3000 rpm for 5 min. An equal volume of 100% acetonitrile was added, and cells were kept at vortex at medium speed for 30 min. This suspension was then centrifuged at 5000 rpm at room temperature (RT) for 10 min. The supernatant was collected in fresh eppendorf and 100 µl of this was added to the wells of 96 well plate and absorbance was taken at 436 nm in multiskan plate reader. A standard curve was plotted by taking the absorbance of the drug directly and then uptake in cells was analyzed using the equation.

2.2.7 Measurement of caspase-3 activity

Caspase-3 colorimetric protease assay kit (Invitrogen) was used to measure caspase-3 activity following the procedure described elsewhere [183]. For measurement of caspase activity, cells were seeded in a 6-well plate and exposed to desired drugs for a specific period. Thereafter, the protein was extracted using RIPA buffer; concentration was determined by bradford assay and then an equal amount (60 μg) of protein was added to microtiter plates with the caspase-3 substrate (Ac-DEVD-pNA). The concentration of the p-nitroaniline (pNA) released from the substrate was calculated from the absorbance values at 405 nm.

2.2.8 Analysis of DNA fragmentation

Apoptosis was evaluated by fragmented genomic DNA forming DNA ladders (short fragments of ~200 base pairs) on agarose gel [184]. To analyze DNA ladder formation, P53 null and R273H-P53 cells were seeded in 6 cm dishes at a density of 5×10^5 cells/plate and treated with cisplatin for 48 h. DNA was extracted using invitrogen apoptotic DNA ladder detection kit and ladder formation was analyzed on 1% agarose gel. A DNA marker was run parallel to the samples.

2.2.9 Transient transfection

Cells were seeded at a density of 70%. The next day, cells were kept in incomplete media for 45 mins and then transfected with specific siRNA (40 nM) or plasmid (2 µg) using Lipofectamine 3000 reagent (Invitrogen, USA), as per the manufacturer's instructions. After 4-6 h of transfection, complete media was added to the cells, treated with the required drug. Cells were then incubated for the desired time before proceeding for further experiment.

2.2.10 RNA isolation and real-time PCR

TRIzol reagent ((Sigma, #T9424) was used to isolate total cellular RNA, and cDNA was synthesized using GeneSure First Strand cDNA synthesis kit (Genetix # PGK162-B) with random hexamers as per the manufacturer's instructions. cDNA templates were amplified for specific genes **(Table 2.2)** in CFX connect real-time PCR system (BioRad) and detected using SYBR Green (BioRad #170-8882AP). GAPDH was amplified as a control. The relative RNA expression was calculated using Pfaffl's method [185].

Table 2.2. List of primers used for real time PCR.

Gene name	Forward primer (5’ to 3’)	Reverse primer (5’ to 3’)
gapdh	GCACCGTCAAGGCTGAGAAC	TGGTGAAGACGCCAGTGGA
abcb1	GGGATGGTCAGTGTTGATGGA	GCTATCGTGGTGGCAAACAATA
vimentin	TCTACGAGGAGGAGATGCGG	GGTCAAGACGTGCCAGAGAC
n-cadherin	CGAATGGATGAAAGACCCATCC	GGAGCCACTGCCTTCATAGTCAA
p53	TATGGCGGGAGGTAGACTGA	CCAGCCAAAGAAGAAACCA
yap	TAGCCCTGCGTAGCCAGTTA	TCATGCTTAGTCCACTGTCTGT
atg-5	GCAGATGGACAGTTGCACACA	TTTCCCCATCTTCAGGATCAA
cyr61	ATGGTCCCAGTGCTCAAAGA	GGGCCGGTATTTCTTCACAC
ctgf	CAAGGGCCTCTTCTGTGACT	ACGTGCACTGGTACTTGCAG
malat1	AGGCGTTGTGCGTAGAGGA	GGATTTTTACCAACCACTCGC
ki67	GACAGTACCGCAGATGACTC	TACGTCCAGCATGTTCTGAGG
pcna	TCACAGGGCAGTGTCTTCATT	GGGTGACTGTAGCTGGGAAT

2.2.11 Annexin V/Propidium Iodide (PI) staining

Cells were seeded in a 6 well plate till they reach 70 % confluency. The following day, cells were treated with the desired drug for a required period. Thereafter, the cells were harvested, washed with PBS, and re-suspended in 500 µl of 1X Annexin binding buffer. To detect the percentage of apoptotic cells, Annexin V/PI was added to cells and incubated for 20 min in the dark. Flow cytometric (Cytoflex, Beckmann Coulter) analysis was performed and the acquired data was analyzed using CytExpert software. To detect both early and late apoptotic cells, the percentage of cells in the lower and upper right (LR and UR) quadrant representative of only Annexin V and both Annexin V-PI positive cells, respectively, were counted. The percentage of apoptotic cells is represented through a bar graph.

2.2.12 Cell cycle assay

For DNA content analysis, cells were seeded in a 6 well plate and grown overnight. After the required treatment, the cells were harvested, washed with PBS, and centrifuged at 2000 rpm for 5 min at 4ºC. The pellet was then re-suspended in 100 µl of PBS and 900 µl of ice-cold 70% ethanol, used as a fixative. The fixed cells were incubated at -20ºC overnight. The next day, cells were centrifuged and the pellet was re-suspended in 450 µl PBS with 10 µl of propidium iodide (PI; 2 mg/ml) containing solution [183]. The samples were then incubated in dark for 10 min and acquisition was performed through a flow cytometer (Cytoflex, Beckmann Coulter) and data analysis was done using CytExpert software.

2.2.13 Luciferase assay

Cells were seeded in a 6 well plate and transfected with 8XGTIIC luciferase plasmid as discussed in the transfection section. After 6 hours, the drug was added to the cells and incubated for desired time. Post incubation, media was discarded and PBS wash was given. Luciferase assay was performed using a luciferase assay kit (# E1500, Promega) as discussed in the manufacturer's protocol. Briefly, 1X cell culture lysis reagent was added to the cells. Cells were scraped and transferred to a fresh eppendorf. Brief centrifugation was done to pellet the debris and supernatant was transferred to a new eppendorf. Luciferase assay reagent (LAR) was prepared by adding luciferase assay buffer to the vial of lyophilized luciferase assay substrate. 20 µl of cell lysate was mixed with 100 µl of luciferase assay reagent and the light produced was measured immediately using a luminometer.

2.2.14 Acridine orange (AO) staining

For the determination of lysosomal permeabilization, cells were seeded in 6 well plate and grown to 70-80 % confluency. The following day, cells were treated with the desired drug for a specific period. Thereafter, the cells were harvested, centrifuged for 10 min, washed with PBS, and re-suspended in fresh media. After that, AO was added (final concentration: 0.5 µg/ml), followed by incubation in the dark for 20 min. Cells were washed with PBS and re-suspended in fresh media. The samples were then acquired using a flow cytometer (Cytoflex, Beckmann Coulter) and analysis of acquired data was performed using CytExpert software. Percentage reduction in red fluorescence is represented through a bar graph.

2.2.15 Monodansylcadaverine (MDC) staining of autophagic vacuoles

MDC, an autophagolysosomal marker, was used to analyze autophagy induction. Cells were grown over coverslips and the following day drug treatment was made. Post incubation, cells were loaded with 0.05 mM MDC and kept in the dark for 10 min at 37°C. Thereafter, the coverslips with cells were washed and mounted with antifade DAPI. MDC punctate dots were analyzed under a fluorescence microscope. For fluorimetric measurements, cells were grown in a 6-well plate. After treatment, cells were labeled with MDC for 10 min followed by PBS wash and then collected in 10 mM Tris-HCl (pH 8.0) containing 0.1% Triton X-100 [20, 21]. Intracellular MDC was assessed by fluorescence photometry (excitation 380 nm and emission 525 nm) on a microplate reader (Fluoroskan Ascent™). Change in MDC fluorescence with respect to control is expressed as fold change.

2.2.16 Lysotracker staining of acidic vesicles

Lysotracker green (LTG) or Lysotracker red (LTR) constituting a fluorophore linked to a weak base is a fluorescent acidotropic probe, used for labelling and tracking acidic organelles in live cells. Cells were cultured overnight on coverslips and then exposed to different concentrations of drugs. After treatment, the media was removed, cells were washed with PBS, and thereafter LTG/ LTR was added (0.05 μM). Cells were then incubated for 20 min in a CO_2 incubator. The solution was aspirated, and slides were prepared. The cells were observed under a fluorescence microscope (Zeiss, Axio Scope A1).

2.2.17 Immunofluorescence microscopy

Cells were seeded on coverslips and then treated with the drug as indicated. Cells were then washed with PBS and fixed with 100 % methanol at -20 °C for 10 min. After multiple PBS washes, blocking was done in 2.5 % bovine serum albumin (BSA) for 60 min. The cells were incubated with primary antibody (1:1000 dilution in 2.5 % BSA) overnight at 4 °C, washed twice with PBS, and then incubated with FITC/TRITC conjugated secondary antibody (1:1000 in 2.5 % BSA) for 60 min. Coverslips were mounted on slides using antifade DAPI and viewed under a fluorescent microscope (Zeiss, Axio Scope A1, or Axio Observer.Z1/7). Images were analyzed using Zen 2.3 SP1 software.

2.2.18 Phalloidin staining

Post drug treatment, cells were washed with PBS. Cells were fixed in 2% paraformaldehyde for 10 mins in dark at room temperature. Multiple PBS wash was given and cells were exposed to 0.2% Triton X100 solution for 2 minutes at room temperature. Multiple PBS wash was given and cells were incubated with Phalloidin stain (1:2000 in 1% BSA) in dark for 1 hour at room temperature. After PBS washes, the coverslip was stained with DAPI and slide was prepared. Images were viewed under a confocal microscope (LSM 880, AxioObserver). Images were analyzed using Zen 2.3 SP1 software.

2.2.19 Scanning electron microscopy

Cells were seeded over a coverslip and drug treatment was given. Post incubation with the drug, media was discarded and PBS washes were given. Cells were then fixed with 4 % formaldehyde in dark for 8 mins at room temperature. Multiple PBS wash was given and cells were then treated with ethanol in gradient (25 %, 50 %, 75 %, and 100 %) for 1 min in each solution. Post 100 % ethanol dip, cells were air-dried. A conductive gold coating of coverslip was done and microscopy was performed using FEI-Apreo-S-SEM.

2.2.20 Beta-galactosidase activity

Cells were seeded in 96 well plate, allowed to reach 70 % confluency and drug treatment was given. Galactosidase activity was thereafter measured following the manufacturer's instruction (Thermo Fisher Scientific, # 75707). Briefly, cells were washed with PBS, and 100 µl of β-galactosidase assay reagent was added. The plate was incubated for 37 ºC for 30 min in dark; reaction was stopped by addition of 100 µl of stop solution and absorbance was measured at 405 nm (Fluoroskan Ascent).

2.2.21 Measurement of intracellular ROS

The 2, 7-dichlorofluorescein diacetate (H2DCF-DA) was used to estimate the ROS levels. The H2DCF-DA passively enters the cell, where it reacts with ROS to form the highly fluorescent compound dichloro-fluorescein (DCF) that can be detected using a fluorescent plate reader. Briefly, the cells were seeded in 96-well plates and exposed to treatments. NAC, a ROS scavenger (20 mM), was added 1 h before treatment. After treatment, the cells were washed with PBS and then incubated in 100 μl of working solution (10 μM) of DCFDA at 37 °C for 30 min. Fluorescence was measured using a microplate reader (Fluoroskan Ascent) at 485 nm excitation and 530 nm emission [184].

2.2.22 Immunoblotting

Immunoblotting was performed following protocols described elsewhere [186]. Cells were grown in 10 cm dishes. Following treatment, cells were lysed in RIPA buffer (Sigma), and the protein concentration was estimated using bradford reagent. Then, 5X gel loading dye was added to the lysates followed by heat denaturation (100 °C for 10 min). Proteins were then loaded in denaturing polyacrylamide gels and transferred to polyvinylidene fluoride membranes. Skimmed milk (5%) was used for blocking. The blots were probed or re-probed with specific primary and secondary antibodies (**Table 2.3 & 2.4)** and detected using enhanced chemiluminescence detection on ChemiDoc (Bio-Rad) [187]. GAPDH or *β*-actin (dilution 1:2000) was used as a loading control. Wherever required, the blots were cut to probe with different antibodies against proteins of different molecular weights. Expression was quantitated using ImageJ and analyzed through Graph-pad Prism software.

Table 2.3 List of primary antibodies used

Antibodies	Catalogue No.
ATG-5	CST; D5F5U #12994
ATG-3	CST; #3415
LC3B-II	CST; D11 #3868S
Beclin-1	CST; D40C5 #3495
phospho-MAPK (ERK1/2)	CST; #4370
Rab-7	CST; D95F2 #9367
LAMP-1	CST; D2D11 #9091S
TFEB	CST; D2O7D #37785S
Caspase-3	CST; D3R6Y #14220
YAP/TAZ	CST; D24E4 #8418S
P53	SCBT; DO-1 #sc-126
β-actin	SCBT; AC-15 #sc69879
GAPDH	SCBT; G-9 #sc-365062

YAP	SCBT; 63.7 #sc-101199
HSC70	SCBT; B-6 #sc-7298
HSP70	Biobharti; #BB-AB0210
P62	Biobharti; #BB-AB0130
LAMP-2A	Abcam; #Ab18528

Table 2.4 List of secondary antibodies used

Antibodies	**Catalogue No.**
anti-mouse	CST; #7076S
anti-rabbit	CST; #7074P2
Antimouse IgG-FITC antibody	Sigma; #F0257
Antirabbiit IgG-TRITC antibody	SCBT; #sc-3917

2.2.23 Statistical Analysis

The obtained data was analyzed using Graph-pad Prism software version 5.0. The effect of treatment in comparison to control was statistically determined using one-way or two-way ANOVA. The Bonferroni method was used to analyze multiple comparisons. Throughout the text, the representative images are of experiments done in multiples. Data are represented in mean ± SEM. If p-value was more than 0.05, then the difference was considered not significant (ns); whereas, if p-value was ≤ 0.05 it was considered significant and denoted by symbols * or # or $ or @; if p-value ≤ 0.01 then denoted by ** / ## / $$/@@ and if p-value ≤ 0.001 then denoted by *** / ### / $$$ / @@@.

Chapter-3

Gain of function mutant P53 inculcates drug insensitivity in NSCLC cells; a proteasomal inhibitor treatment coupled to autophagy induction can be a potential sensitization strategy

3.1 Overview

Lung cancer is one of the most prominent cancers (11.6 % of the total cases) and shares the highest cancer mortality rate (18.4% of the total cancer deaths) worldwide [3]. As per WHO classification, lung cancer is divided into small-cell lung carcinoma (SCLC) and non-small cell lung carcinoma (NSCLC), of which NSCLC comprises about 85% of lung cancer cases. In India, more than one million new cases arise every year with a burgeoning incidence of NSCLC reported annually. The traditional treatment approach against NSCLC has altered over the past few years with the approval of targeted therapy against epidermal growth factor receptor (EGFR) [188, 189]. Currently, the choice of targeted therapy extends to other targets as well, like, ALK, ROS1, and RET [190-193]. Although targeted therapy has improved NSCLC patient prognosis, however, the response is generally short-term and most prone to either on or off-target resistance [194]. Therefore, there is an urgent need to explore novel molecular factors, which can be exploited to overcome the hurdles of current therapy.

In more than 50% of cancer patients, p53 is arguably the most frequent target for genetic alterations which is associated with poor prognosis and relatively enhanced chemoresistance [195]. Accumulating evidences show that a vast majority of P53 mutations are missense that results in the production of a stable, full-length mutated protein carrying only a single amino acid substitution. These mutations not only annul P53's tumor-suppressive function but also in certain instances can endow mutant proteins with neomorphic properties described as a mutant gain of function (GOF)-P53 which can contribute actively to various stages of tumor progression and increased resistance to chemotherapy. In this regard, the central DNA-binding domain of P53 spans the most conserved region composed of a vast number of these missense mutations and among these the hot spot residues occur with unusually high frequency [19, 196, 197]. P53 missense mutations can generally be classified as DNA contact (or class I) mutants, like R273H-P53, which normally make direct contact with target DNA sequences and conformational (or class II) mutants, like R175H-P53, which disrupt the structure of the P53 protein partially or completely, thus its function [31, 32]. R175H-P53 and R273H-P53, being the most frequently occurring GOF mutations in cancer cells, were observed to induce resistance to chemotherapeutic agents in multiple cancer cell types [36, 198]. Interestingly, few reports suggest that, unlike WT-53, mutant P53 can escape MDM2-dependent proteasomal degradation, and hence accumulate stimulating the oncogenic effect [54]. Hence, how to effectively promote degradation of GOF-P53 and sensitize cancer cells or mitigiate drug resistance, is still an open-ended question. We hypothesized that the regulation of cellular protein homeostatic

machineries might be useful.

In this context, autophagy is a well-established self-degradation process that degrades and recycles numerous intracellular cytoplasmic constituents, including proteins to maintain homeostasis. However, in a cancerous state, autophagy is known to play a paradoxical role by either inhibiting tumor progression or promoting tumor cell survival and later stages of cancer progression [199]. Also, substantial evidence shows that different forms of autophagy, for example, macroautophagy and chaperone-mediated autophagy, are implicated in the depletion of stable, mutant P53 isoforms [200]. However, functional involvement of mutant P53 in the regulation of autophagy and in turn being regulated by the cellular degradation system and identification of associated molecular mechanisms governing it are still incompletely understood. A growing number of studies also suggest that both intra-cellular degradation pathways, for example, ubiquitin proteasome system (UPS), and autophagy are mechanistically and functionally linked, such that blockage to either one can led to upregulation of the other in a way that remains yet to be fully clarified [201]. For example, proteasomal inhibition can enhance the load of misfolded proteins and can trigger autophagy as a compensatory mechanism for their degradation [202]. However, autophagy, serving as an essential mechanism to cope with cellular stresses, may directly contribute to the survival of cancer cells exposed to proteasomal inhibitors and, hence, in consequence, might reduce the effectiveness of therapy. Importantly, inhibition of autophagic flux after induction of pro-survival autophagy has often been utilized as a strategy to sensitize multiple cancer cell types [187]. However, conversely, an over-activation of autophagy can also act as a bonafide death inducer or death effector, upstream of other death pathways, like apoptosis [203]. Based on the above considerations, we believe that appropriate tinkering of protein homeostatic processes, like UPS and/or autophagy in cancer cells harboring GOF-P53 can dictate its cell fate.

In this study, we analyzed publicly available NSCLC patient datasets and observed that p53 is the top mutated gene in lung cancer as well, with GOF-R273H being amongst the most predominant ones. Taking this into consideration, in this study, we exposed R273H-P53 cells to proteasomal inhibitor ALLN and observed its effect on autophagy. ROS-dependent autophagy was found to be induced in the R273H-P53 cells, which acted as a pro-death mechanism. Furthermore, we observed that R273H-P53 serves to mitigate cell death induced by autophagy in the lung cancer H1299 cells. Our study provides novel insights into modes of sensitization of resistant NSCLC cells harboring R273H-P53.

3.2 Results

3.2.1 The frequency of p53 mutation is high in NSCLC patients

Mutations play a critical role in the development of cancers including NSCLC. It is postulated that with an increase in mutational burden, the number of driver mutations promoting cancer also increases [204]. Hence, we were interested in exploring the prevalent mutations and their frequency in NSCLC. We selected six projects from cBioportal encompassing 1963 samples of NSCLC patients and compared the total number of mutations. The top 15 genes mutated in NSCLC are presented in **figure 3.2.1a**; this included multiple genes like, EGFR, KRAS which are currently targeted in NSCLCs or other cancers [188, 189, 205]. Importantly, the tumor suppressor- p53 was found to harbor the highest mutational frequency (67%) **(Fig. 3.2.1b)** and was found to co-occur significantly with other druggable targets in NSCLCs **(Table 3.1)**. Notably, the median months' survival (MMS) of patients with p53 mutation was highly comparable with the survival of patients with mutations in other druggable genes implicating the significance of p53 mutation in the pathogenesis of NSCLCs **(Fig. 3.2.1c)**. To understand the consequences of a p53 mutation we analyzed the mortality rate between NSCLC patients with and without p53 mutation; importantly, the mortality rate in patients with a mutation in p53 was a striking 2.77-fold higher **(Fig. 3.2.1d)**. Further analysis into the classification of mutations revealed an increased incidence of missense mutations in p53 with a higher probabilistic occurrence of a mutation at 273 amino acid position (R273H) in NSCLC patients **(Fig. 3.2.1e)**. Importantly, an R273H mutation imparts GOF function to the P53 protein. The above analysis warrants the importance of studying p53 mutations, especially R273H in NSCLC progression.

Table 3.1 Tendency of mutant p53 to occur with other druggable mutations in NSCLC

Gene 1	Gene 2	p=-value	Tendency
TP53	**ALK**	**<0.001 ***	**Co-occurrence**
TP53	**BRAF**	**0.014 ***	**Co-occurrence**
TP53	**ROS1**	**0.014 ***	**Co-occurrence**
TP53	**EGFR**	**0.183**	**Mutual exclusivity**

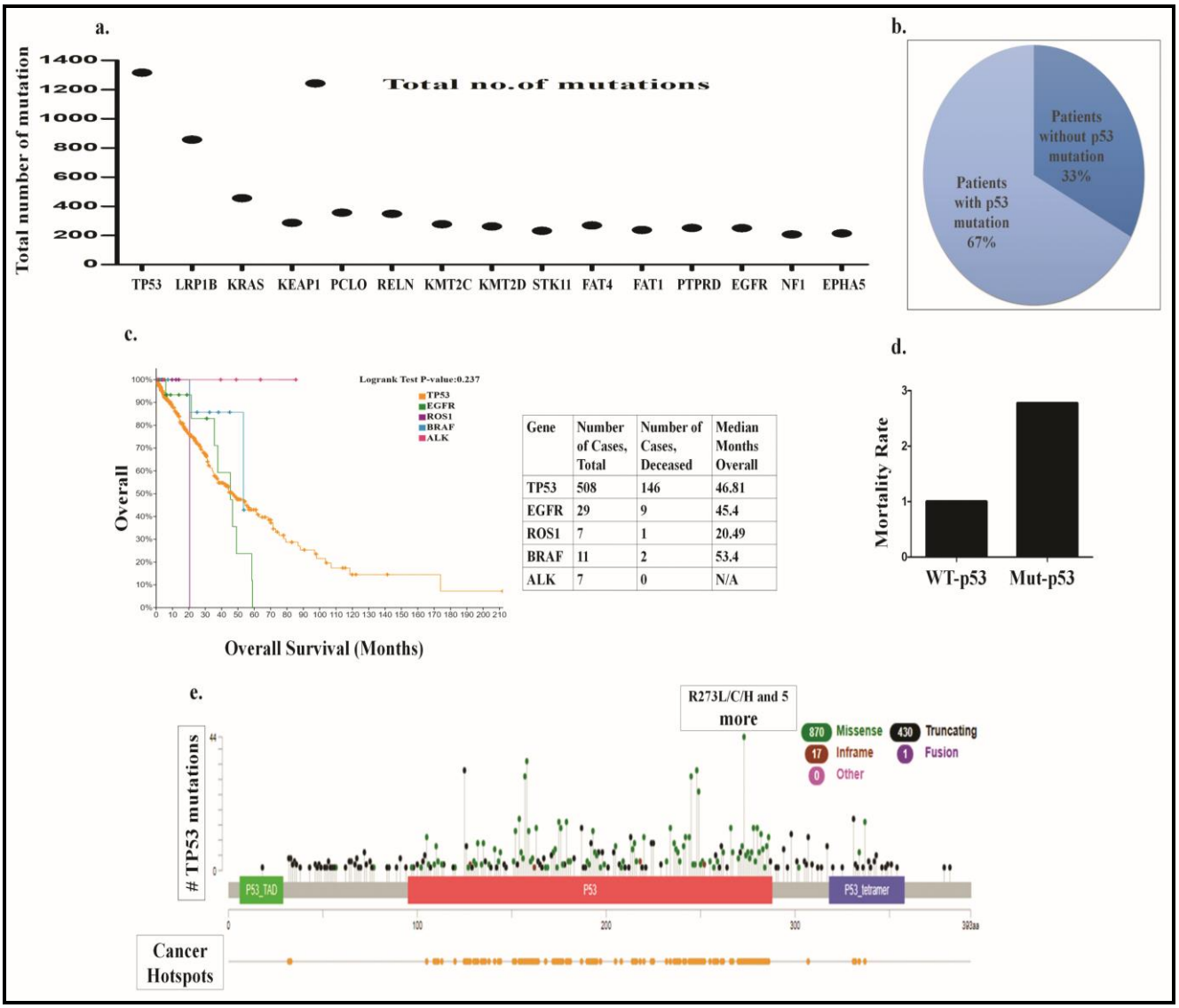

Figure 3.2.1. Prevalence of p53 mutation in NSCLCs and its association with prognosis. a Graph representing top 15 mutated genes in NSCLC patients. **b** Pie chart showing probability of p53 mutation in NSCLC patients. **c** Survival curve representing median month survival of NSCLC patients with p53 mutation or mutation in other druggable targets. **d** Bar graph showing relation between p53 mutation and mortality of NSCLC patients. **e** Graph representing the types of P53 mutations and their prevalence.

3.2.2. R273H-P53 cells exhibit decreased drug sensitivity compared to null or WT-P53 cells

In NSCLC patients, P53 status shows no prognostic significance in the absence of adjuvant chemotherapy; however, after undergoing treatment with cisplatin, a reduced disease-free interval and overall survival are seen bearing a GOF-P53 protein [206]. Given the importance of GOF-P53 in NSCLCs, in this study, we prepared a stable transfected R273H-P53 NSCLC cell model aimed at understanding *the modus operandi* of resistance and develop an effective strategy for sensitizing

GOF-P53 cells, which is elusive till date. P53 null H1299 cell line was stable transfected with empty vector (EV), WT-P53, or R273H-P53. Stable transfection was confirmed by immunoblotting against the P53 antibody **(Supplementary Fig. 3a)**. The cells were then exposed to varying concentrations of cisplatin (standard chemotherapy for NSCLC patients) for 48 h. Similarly, other cancer cell types possessing WT-P53 (MCF7), P53-null (HCT116), or R273H-P53 (MDA-MB-468, HT-29, and SW480) were also exposed to various doses of cisplatin. Interestingly, in all the cell types studied, GOF-P53 cells showed significantly decreased sensitivity to cisplatin compared to WT-P53 harboring cells demonstrating resistance **(Fig. 3.2.2a.i-iii)**. Importantly, R273H-P53 cells showed less sensitivity to cisplatin compared to either parental H1299 P53 null cells or EV stable transfected cells **(Fig. 3.2.2ai, Supplementary Fig. 3b-c)**; the sensitivity of EV cells to cisplatin was comparable to null cells. We hence compared caspase-3 activity upon cisplatin treatment between H1299 P53-null (15 μM ~ IC-50) and R273H-P53 (30 μM ~ IC-50) cells through ELISA based method. As expected, R273H-P53 cells showed significantly decreased enzymatic activity compared to the P53 null cell type **(Fig. 3.2.2b)**. Similar results were obtained in the DNA fragmentation study **(Fig. 3.2.2c)**. Since R273H-P53 cells showed a marked increase in resistance compared to null or WT-P53 cell types, we further confirmed it by analyzing mRNA expression of ABCB1, which showed a substantially increased expression upon cisplatin treatment in R273H-P53 stable transfected cells compared to control **(Fig. 3.2.2d)**. Based on the above experimental evidence, it is clear that R273H-P53 cells show resistance to cisplatin, compared to null or WT-P53 cells. However, to analyze that the resistance is a generalized phenomenon across multiple drug types or is purely specific to cisplatin, we evaluated cross-resistance of R273H-P53 cells to other conventionally used anticancer drugs like 5-FU. As evident from **figure 3.2.2e**, R273H-P53 cells were less sensitive to 5-FU as well. Collectively, these observations suggest that P53-null cells acquire drug-resistant characteristics upon stable transfection of R273H-P53 vector in NSCLC cells.

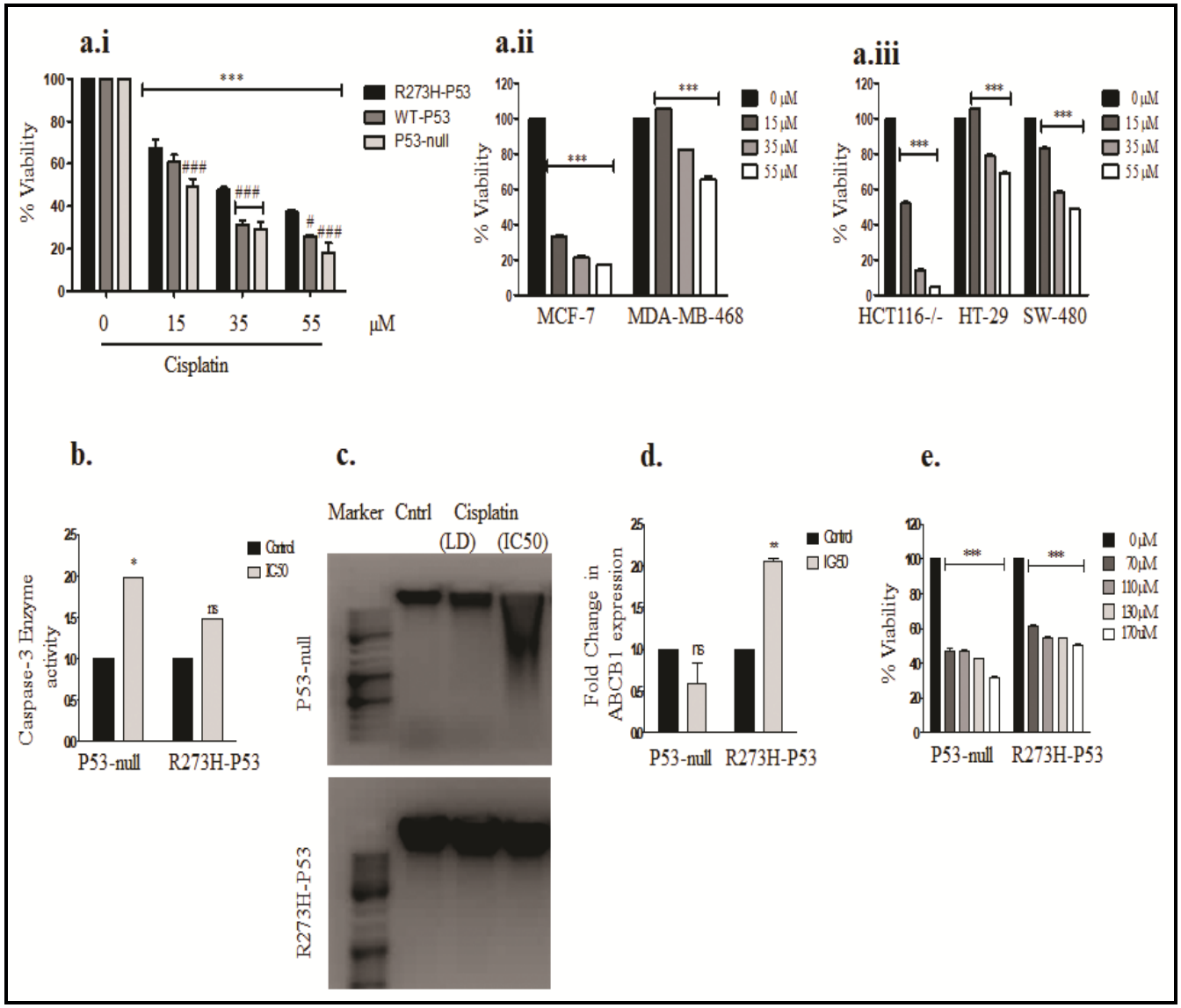

Figure 3.2.2. R273H-P53 mutation imparts drug insensitivity. a Cell lines with varied P53 status were exposed to different doses of cisplatin. Cell viability was analyzed after 48 h of treatment through MTT assay. Untreated samples were taken as control. '*' and '#' indicates a significant difference compared to untreated cells and R273H-P53 cells, respectively. **b** Fold change in caspase-3 enzyme activity was measured following cisplatin treatment at IC-50 dose for 48 h in H1299 (P53-null) and H1299-R273H-P53 stable transfected cells. The level of caspase-3 activity in untreated control was taken as an arbitrary unit '1'. **c** DNA fragmentation was measured on an agarose gel. P53-null and R273H-P53 cells were treated with cisplatin at a low dose (LD) and IC-50 dose for 48 h; DNA was extracted and run on an agarose gel. A DNA marker was run alongside the samples. **d** Real-time PCR showing expression of ABCB1 mRNA levels upon exposure of P53-null and R273H-P53 cells to cisplatin (IC-50) for 48 h. **e** P53-null and R273H-P53 cells were given different doses of 5-FU and cross-resistance was analyzed through MTT assay. '*' indicates a significant difference

compared to untreated cells.

3.2.3 Proteasome inhibitor imparts cell sensitization in P53 positive cells

Targeting the proteasomal degradation pathway is increasingly getting recognized as a promising strategy for cancer therapy [207-209]. WT-P53 protein is primarily degraded by the UPS pathway; however, mutations in P53 might stabilize this protein and inhibit MDM2 interaction, thereby preventing degradation [210-212]. However, reports are suggesting that several "hot-spot" P53 mutants like R175H, R248W, or R273H remain sensitive to ubiquitin-mediated degradation [213]. We assumed that proteasomal degradation of GOF-P53 might be context-dependent and shows increased bias towards the nature of the inhibitor used. We used ALLN, a well-known proteasome inhibitor that is known to induce apoptosis by accumulated protein response. ALLN was chosen over the widely used proteasomal inhibitor, bortezomib because the effects of ALLN are relatively less explored and the use of bortezomib has recently been challenged by severe adverse side effects and resistance [214]. Exposure of ALLN (5 and 10 μM) for 48 h showed more cell deaths in WT-P53/R273H-P53 transfected cells than null **(Fig. 3.2.3a)** or EV transfected cells **(Supplementary Fig. 3d)**. Similar results were obtained when cells were treated with another proteasomal inhibitor, MG132 (data not shown). Interestingly, R273H-P53 cells in comparison to WT-P53 showed decreased sensitivity to proteasomal inhibition as well **(Fig. 3.2.3a-b)** as evident from cell viability assay or apoptosis assay by annexin V and propidium iodide staining. Importantly, unlike the response to conventionally used drugs like cisplatin, both WT-P53 and R273H-P53 cells were more sensitive than the parental null or EV cells, suggesting that the presence of P53 protein provides a therapeutic advantage to targeting strategies based on interference of protein degradation. Nuclear staining by DAPI in R273H cells showing fragmented nucleus, as depicted in **figure 3.2.3c**, further confirmed cell sensitization on ALLN treatment. Overall, the above results highlight the importance of targeting the protein degradation machinery in P53 positive cells, though an adjuvant therapy might be essential for R273H-P53 cells as they are more resistant than WT-P53 cells to cell death by protein overload.

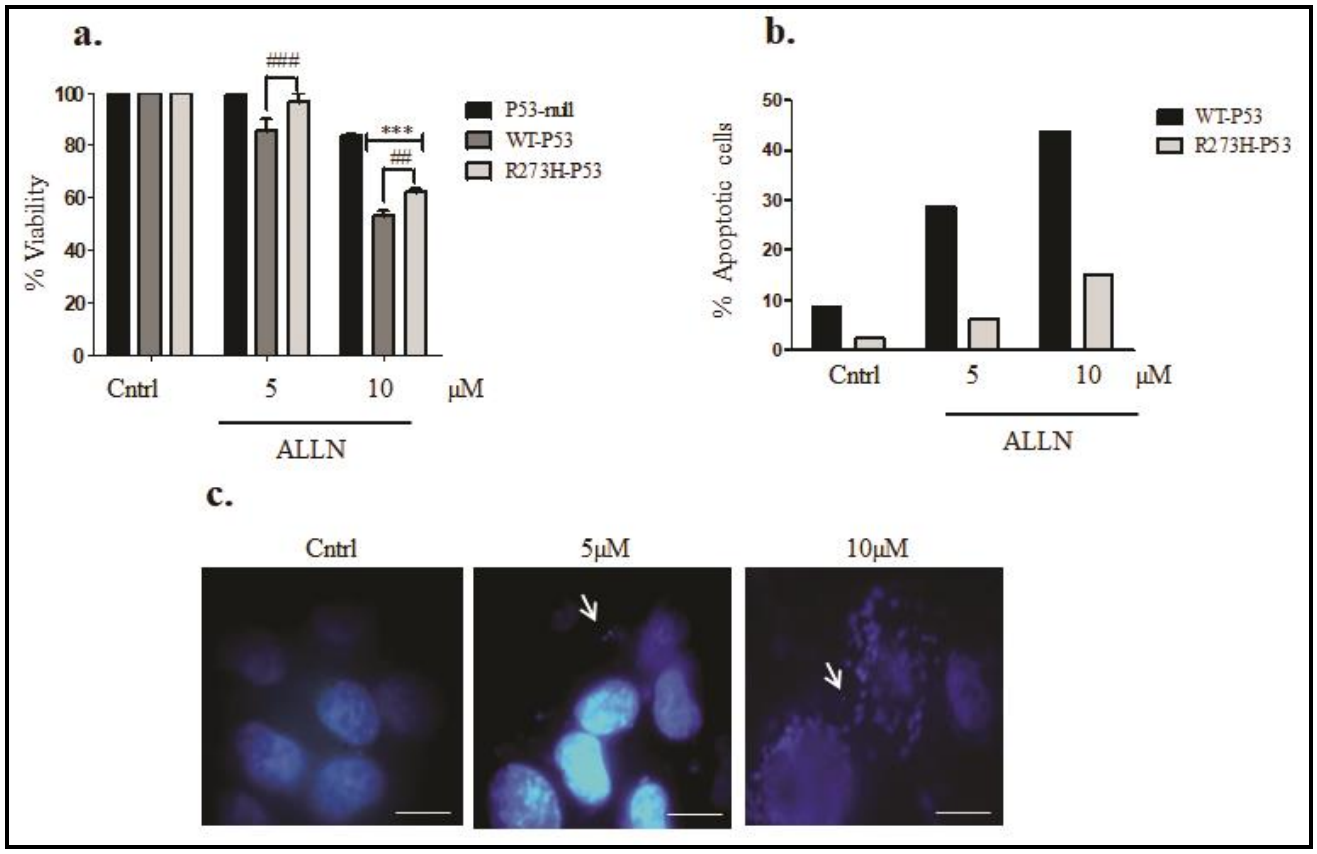

Figure 3.2.3. Proteasomal inhibitor (ALLN) induces apoptosis. a P53-null, WT-P53, and R273H-P53 cells were exposed to varying doses of ALLN. After 48 h of exposure, cell viability was measured through MTT assay. Untreated samples were taken as control. '*' and '#' indicate significant difference compared to P53-null and R273H-P53 cells, respectively. **b** The percentage of apoptotic cells was measured through flow cytometry using Annexin V/PI staining and compared between WT-P53 and R273H-P53 cells upon ALLN treatment. **c** R273H-P53 cells were either untreated or treated with ALLN for 48 h and then stained with DAPI. Nuclear fragmentation or condensation after treatment is marked with white arrows. The scale bar represents 100 μm.

3.2.4 Proteasomal inhibitor, ALLN, induces autophagy in R273H-P53 cells

Two major pathways of degradation maintain protein homeostasis, the UPS, responsible for degrading the majority of proteins including many short-lived, denatured, or, in general, damaged proteins, and autophagy, which, by contrast, is mostly responsible for the degradation of long-lived proteins [215]. Although UPS and autophagy were initially considered to be largely disconnected pathways, recent advances in the understanding of UPS and autophagy have highlighted a strong connection between them. To examine the effect of ALLN on autophagy, R273H-P53 cells were treated with 10 μM ALLN for different time points, and LC3B-II (marker for autophagy) protein

expression was analyzed. An increase in LC3B-II expression levels indicative of enhanced autophagy was observed with ALLN treatment **(Fig. 3.2.4a)**. However, an increase in LC3B-II protein levels can be resultant of increased autophagy or inhibition of the final step of autophagosome-lysosomal fusion [216]. Hence, to confirm autophagic flux, we checked for the changes in LC3B-II protein levels with or without the lysosomotropic agent, chloroquine, CQ. An increased expression of LC3B-II was observed in ALLN+CQ treated samples when compared to only independent treatments indicative of enhanced autophagic flux with ALLN **(Fig. 3.2.4b)**. Autophagy induction was further validated through MDC staining; MDC preferentially accumulates in acidic autophagic vacuoles. MDC fluorescence, represented by the green punctate dots, increased with ALLN treatment in a dose-dependent manner, suggesting an increase in autophagy **(Fig. 3.2.4c)**. Furthermore, an increase in the number of lysosomes is often associated with increased autophagy. We observed an increase in LTG staining with ALLN **(Fig. 3.2.4d)**. The above results are supportive of the fact that proteasomal inhibition by ALLN in R273H-P53 cells activates autophagy. However, in tumor cells, autophagy can act as both a prodeath or prosurvival mechanism in a context-dependent manner [162].

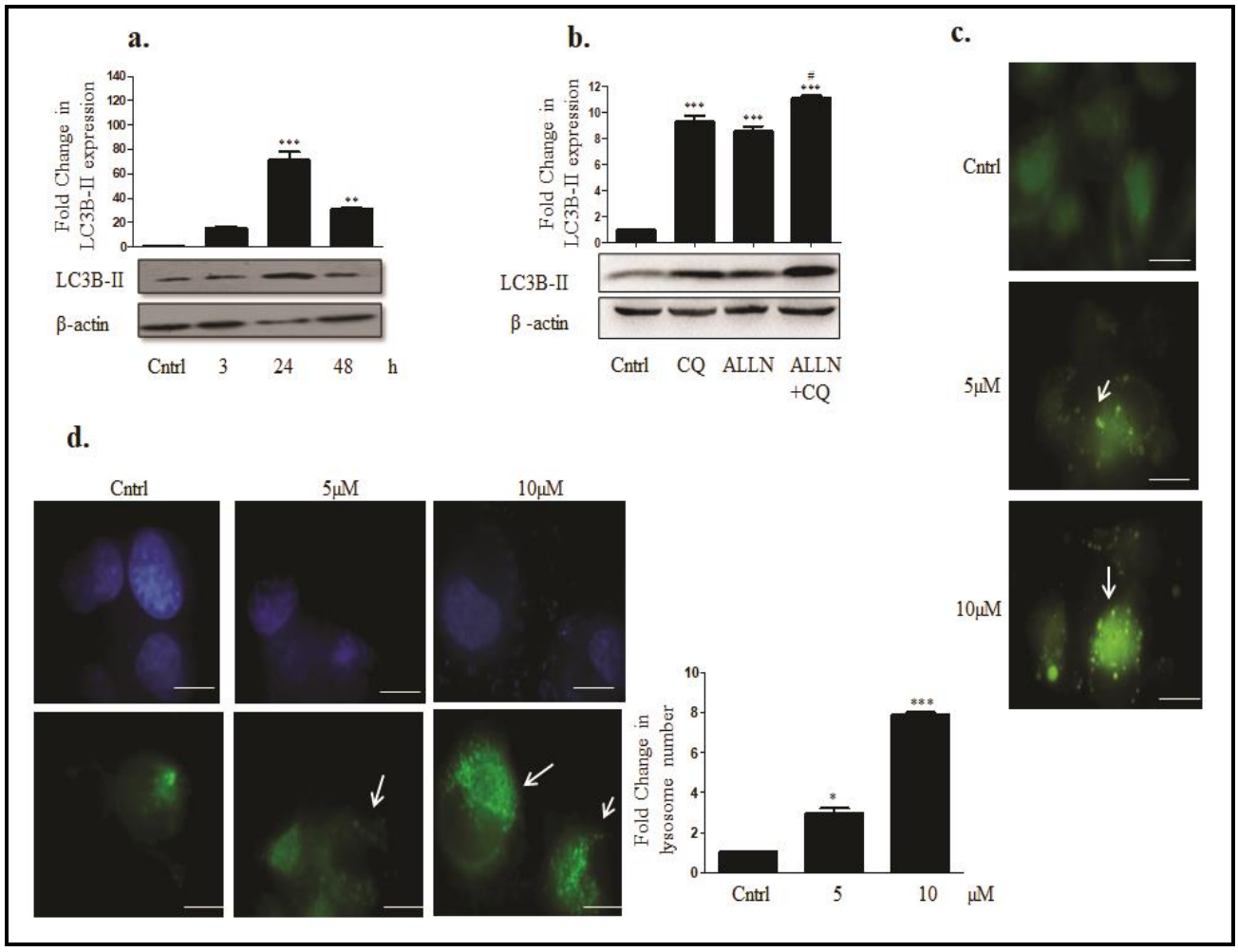

Figure 3.2.4. ALLN induces autophagy in R273H-P53 cells. **a** R273H-P53 cells were treated with 10 μM ALLN for different time points and expression of LC3B-II was analyzed through immunoblotting. **b** Immunoblot analysis showing expression of LC3B-II upon 48 h of exposure to CQ, ALLN, and ALLN+CQ in R273H-P53 cells. **c** Fluorescent microscopic images of MDC fluorescence in ALLN-treated (0, 5, and 10 μM; 48 h) R273H-P53 cells. The scale bar represents 100 μm. **d** R273H-P53 cells were treated with ALLN for 48 h and then stained with LTG dye. Green dots representing the lysosomes were counted and represented as a bar graph. The scale bar represents 100 μm.

3.2.5 R273H-P53 cells are sensitive to autophagy induction

Enhanced autophagy has recently been implicated in multiple studies facilitating cancer cell survival under physiological stresses. Hence, we hypothesized that combination treatment with ALLN (being an autophagy inducer) with CQ (an agent that inhibits autophagy) might lead to accumulation of acidic vesicles, thereby blocking autophagic flux, and can act as a potent strategy to sensitize R273H-P53 cells. We initially checked for the cytotoxicity-inducing property of CQ alone. CQ even at 50 μM was not able to impart any significant cytotoxic effect on R273H-P53 cells as analyzed by MTT assay and also Annexin V/PI staining **(Fig. 3.2.5a-b)**. Since CQ is a late-stage autophagy inhibitor, we thought of exploring the effect of an early-stage autophagy inhibitor, 3-methyl adenine (3-MA). Interestingly, on the contrary, 3-MA treatment was able to sensitize R273H-P53 cells. As depicted in **supplementary figure 3e**, only 3-MA treatment reduced cell viability to less than 50% in R273H-P53 cells. However, as we analyzed the expression of autophagic markers upon 3-MA exposure, we noticed an increased expression of LC3B-II and Atg-5 protein levels **(Fig. 3.2.5c.i-ii)**. We assumed that 3-MA might have autophagy-inducing effects as well. Indeed, in corroboration to above, there are previous reports suggesting that prolonged 3-MA treatment can inhibit PI3K-class-I, in turn inhibiting mTOR and activating autophagy [217]. However, results obtained with 3-MA provided us with a hint that, rather than autophagy inhibition, these cells might be more sensitive to autophagy induction. Accordingly, the effect of rapamycin (Rapa), a widely used mTOR inhibitor, and serum starvation (SS), which are known to elicit an autophagic response, was investigated in R273H-P53 cells [218, 219]. Interestingly, R273H-P53 cells treated with autophagy inducers like Rapa or exposed to SS alone or in combination with ALLN had significantly enhanced cytotoxic effects when compared to autophagy inhibition with CQ alongside ALLN **(Fig. 3.2.5d-h)**. Autophagy inhibition with CQ was found to moderately decrease the sensitivity of cells to ALLN **(Fig. 3.2.5i and Supplementary Fig. 3f)**. Hence, in this study, we suggest that although

physiologically relevant levels of autophagy are required for cellular homeostasis maintenance, enhanced autophagy can in turn induce autophagy-dependent cell death. Excessive autophagy has been previously observed in association with various forms of cell death and the term "autophagic cell death" was originally introduced to describe cell death associated with autophagy. However, evidences associating autophagy to cell death in these reports were more circumstantial, and the nature of such death occurring in cancer cells remains poorly defined. We were hence interested in analyzing the modus operandi of cell death observed upon autophagy enhancement.

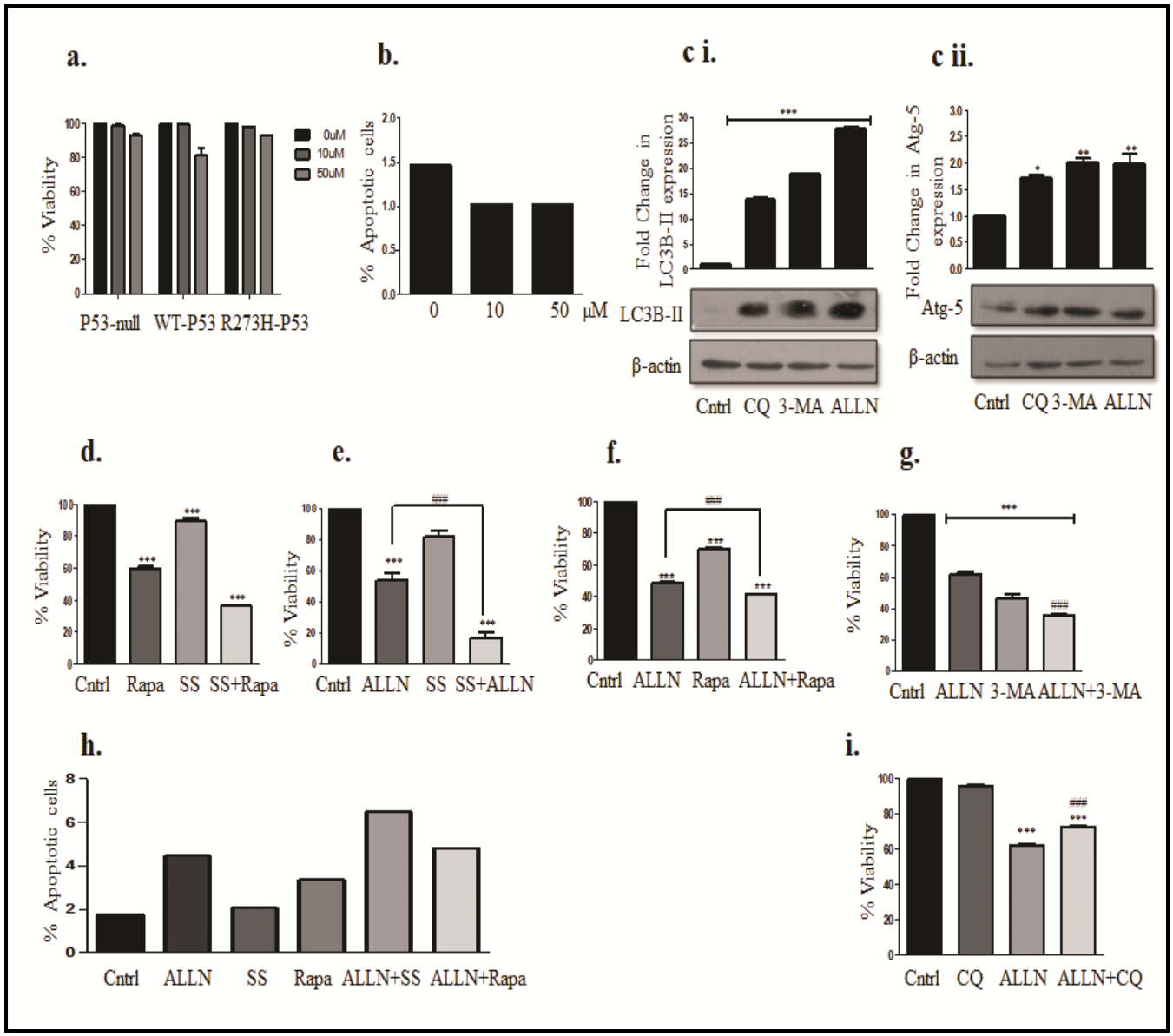

Figure 3.2.5. Autophagy induction promotes cell death in R273H-P53 cells. **a** P53-null, WT-P53, and R273H-P53 cells were exposed to varying doses of CQ. After 48 h of exposure, cell viability was measured through MTT assay. **b** CQ-treated R273H-P53 cells were analyzed for apoptosis

induction through Annexin V/PI staining followed by flow cytometry. Fold change is represented through a bar graph. **c** R273H-P53 cells were exposed to CQ (10 μM), 3-MA (5 mM), and ALLN (10 μM) for 48 h, and immunoblot analysis was performed for LC3B-II and Atg-5. '*' indicates a significant difference to untreated control. Cell viability in R273H-P53 cells was measured through MTT assay after 48 h of treatments at various combinations, **d** Rapa (500 nM), Rapa + SS, **e** SS, ALLN+SS, **f** Rapa, ALLN+Rapa, **g** 3-MA, 3-MA+ALLN and represented in the form of bar graph. **h** Apoptosis was analyzed through flow cytometry using Annexin V/PI staining in R273H-P53 cells, after treatment with various autophagy inducers. The percentage of apoptotic cells is represented through a bar graph. **i** Cell viability was measured through MTT assay in R273H-P53 cells after autophagy inhibition in the presence or absence of ALLN. '*' indicates a significant difference compared to untreated control, while '#' indicates a significant difference compared to ALLN-treated cells.

3.2.6 ALLN-induced autophagy facilitates cell sensitization by regulating ROS levels

Generation of ROS through oxidative stress is known to cause cell death; however, the role of oxidative stress in autophagy-induced cell death is relatively unexplored. Conventionally, autophagy serves as a buffer system to control the level of ROS in cells and reduce their toxic effects [220]. However, in our experimental context the intracellular ROS levels measured by DCFDA dye followed by fluorimetric analysis showed a prominent increase with ALLN treatment in R273H-P53 cells **(Fig. 3.2.6a)**. A profound increase in ROS levels was observed upon ALLN treatment in SS condition **(Fig. 3.2.6a)**. Interestingly, pretreatment of cells with the ROS scavenger-NAC resulted in a substantial increase in cell viability with only ALLN, ALLN plus SS, or ALLN plus Rapa treated cells, suggesting a direct positive correlation of increase in ROS with cell death **(Fig. 3.2.6b)**. **Figure 3.2.6c-d** represents the status of ROS level and cell viability on Rapa or SS exposure. The experiment was performed with or without NAC pretreatment. The above experiments also confirm that ALLN-induced cytotoxicity is not only autophagy-dependent but is also regulated by an increase in ROS levels. Interestingly, R273H-P53 cells when pretreated with NAC resulted in a decrease in autophagic marker expression, Atg-3 or LC3B-II, suggesting that, in this context, ROS is upstream to autophagy and quenching of ROS reduces autophagy-induced cell death as well **(Fig. 3.2.6ei-iii)**.

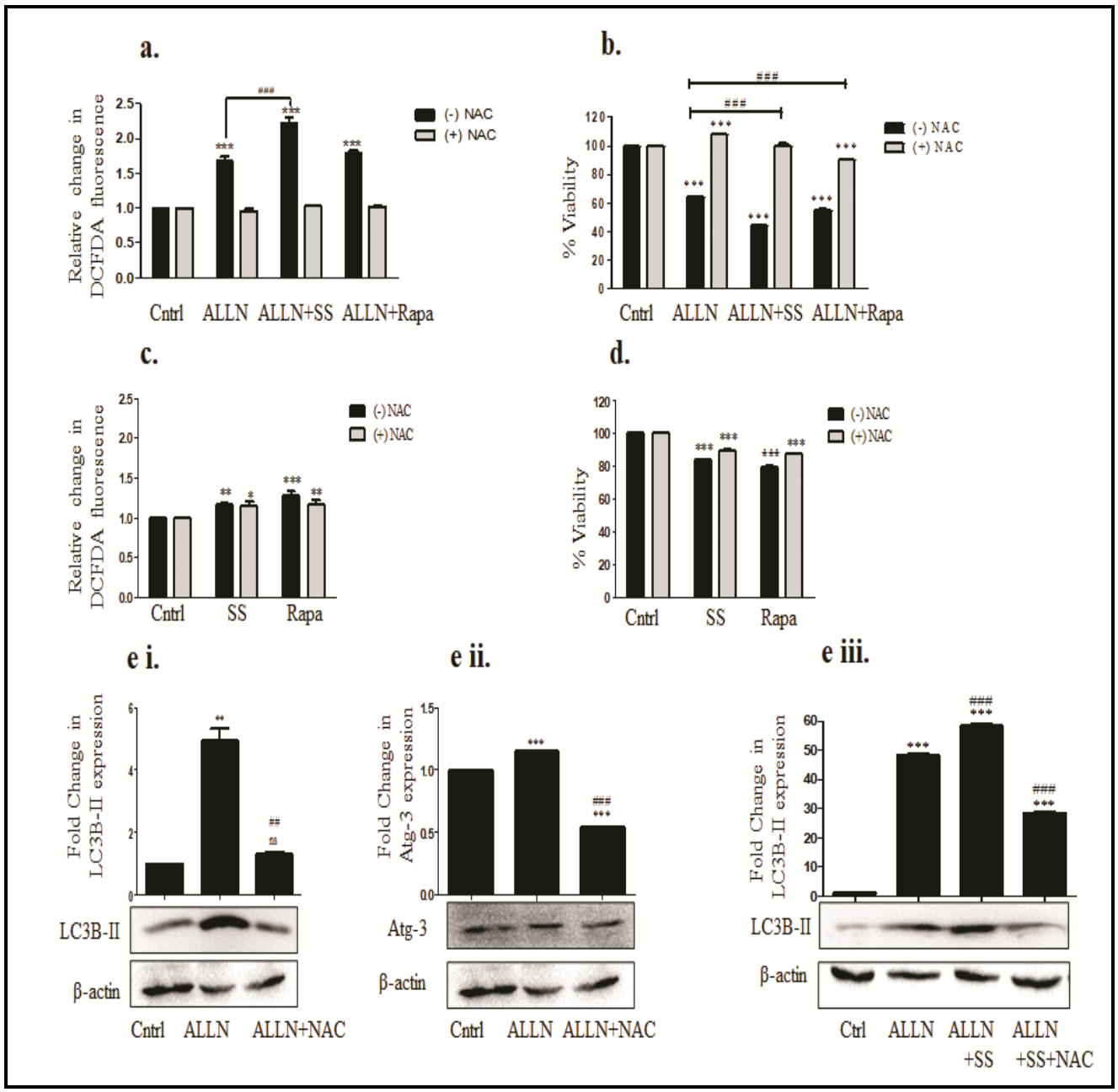

Figure 3.2.6. ALLN-induced autophagy sensitizes R273H-P53 cells by increasing ROS levels. a R273H-P53 cells were exposed to ALLN, ALLN+SS, and ALLN+Rapa for 48 h. NAC (5 mM) was applied 1 h before treatment wherever mentioned. Fold change in ROS levels is represented through bars; untreated control was taken as an arbitrary unit '1'. **b** MTT assay was performed to analyze cell viability following exposure of R273H-P53 cells to ALLN and other autophagy inducers; data is represented through bar graph. **c** R273H-P53 cells were exposed to serum-starved media or Rapa (500 nM) for 48 h. Fold change in ROS levels is represented. **d** MTT assay was performed to check cell viability following exposure of R273H-P53 cells to autophagy inducers with/without NAC. '*' indicates a significant difference compared to untreated control, while '#' indicates a significant

difference compared to ALLN-treated cells. **e (i-iii)** R273H-P53 cells were treated with ALLN or ALLN plus SS for 48 h. NAC was given 1 h before treatment wherever mentioned. Immunoblotting was thereafter performed for LC3B-II and Atg-3. '*' indicates a significant difference compared to untreated control, while '#' indicates a significant difference compared to ALLN-treated cells.

3.2.7 Sensitization of R273H-P53 cancer cells is mediated by ERK along with ROS accumulation

Previous reports show that mitogen-activated protein kinase (MAPK) signaling pathways can modulate autophagy and determine cell fate [221]. There are also a growing number of reports stating that, in certain conditions, the MAPK-ERK can promote cell death [222, 223]. Interestingly, an increase in phospho-ERK indicative of its activation was observed in cells treated with ALLN, which went down with autophagy inhibition by CQ **(Fig. 3.2.7a)**. To confirm the role of ERK in cell death, U0126, a widely used selective inhibitor of the upstream MAP kinase pathway, was used and cell viability was measured in presence of ALLN or ALLN plus SS. Importantly, inhibition of the ERK pathway by U0126 significantly reduced cell death induced by ALLN alone or ALLN plus autophagy induction. This implicates that ERK signaling acts as a pro-death mechanism **(Fig. 3.2.7b)**. ROS, such as hydrogen peroxide, are reported to regulate ERK phosphorylation as ERK-specific phosphatases are sensitive to ROS. Hence, ROS-mediated prolonged ERK activation might be a crucial mechanism regulating cell death [224]. Interestingly, a significant decrease in phospho-ERK levels was observed when ALLN-treated cells were predisposed to NAC **(Fig. 3.2.7ci-ii)**. We also checked for the reverse effect, that is, ROS production upon ERK inhibition. R273H-P53 cells were pretreated with U0126 for 2 h before the addition of ALLN or ALLN plus autophagy inducers. Interestingly, a drastic decline in the level of ROS was observed with ERK inhibition **(Fig. 3.2.7d)**. Collectively, the above findings highlight that R273H-P53 cell sensitization is regulated by ROS-autophagy-ERK signaling loop upon ALLN or ALLN plus autophagy induction.

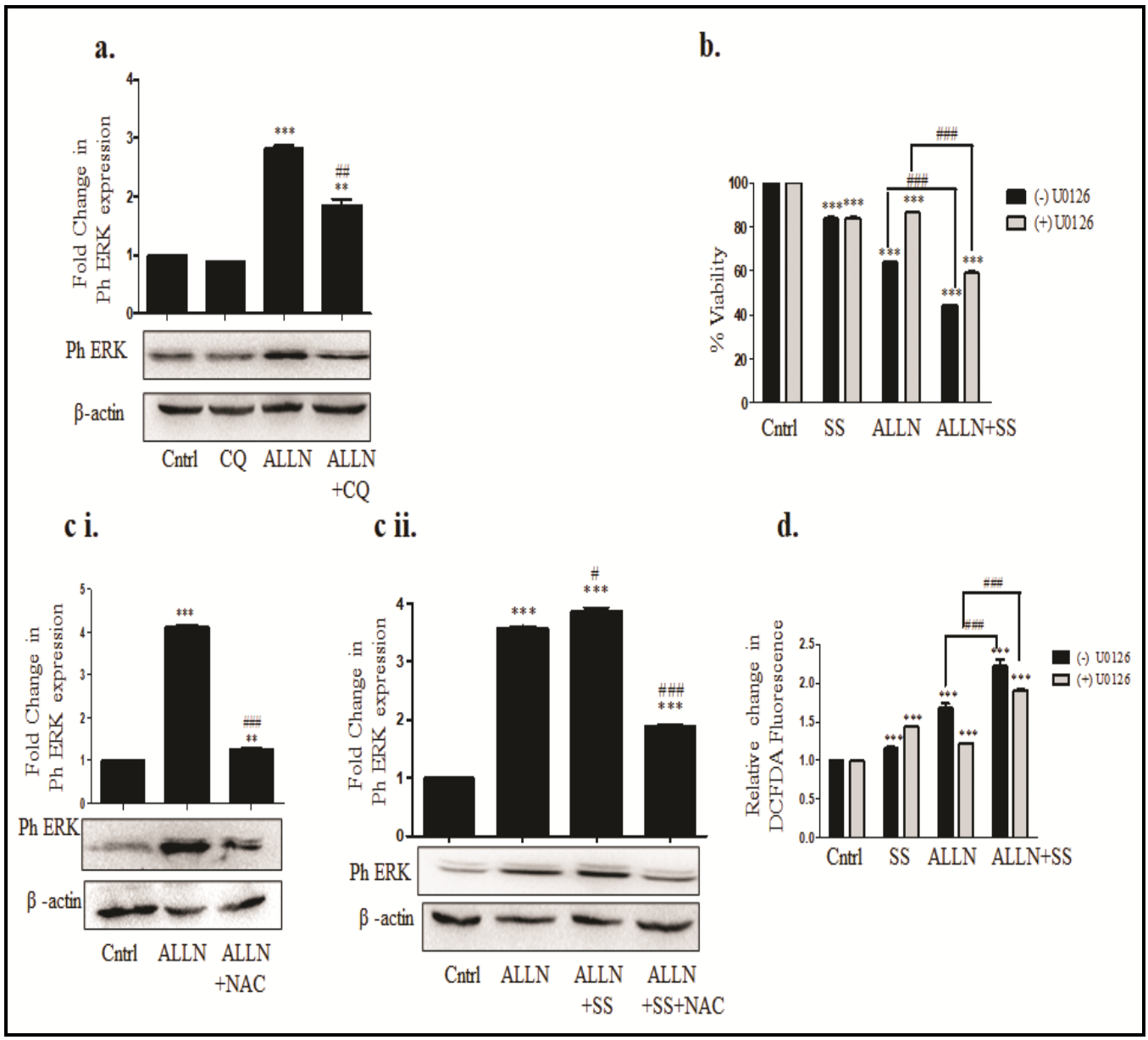

Figure 3.2.7. The sensitization of R273H-P53 cells is mediated by ERK signaling and ROS. a Immunoblot analysis representing Ph ERK expression upon ALLN and/or CQ treatment in R273H-P53 cells. **b** MTT assay was performed to analyze ALLN and/or serum starvation-induced cell death in the presence or absence of ERK inhibitor, U0126, given 2 h before treatment. Percentage viability is represented in the form of a bar graph. **c** Immunoblot analysis was performed for Ph ERK expression upon ALLN and/or serum starvation in R273H-P53 cells. NAC was given 1 h before treatment wherever mentioned. **d** DCFDA fluorimetric assay measuring intracellular levels of ROS after treatment of R273H-P53 cells with or without U0126, given 2 h before ALLN and/or serum starvation for 48 h. '*' indicates a significant difference compared to untreated control, while '#' indicates a significant difference compared to ALLN-treated cells.

3.2.8 Induction of prodeath autophagy in R273H-P53 cells is a P53-dependent process

Although many links connect autophagy with P53, molecular crosstalk between them is still incompletely understood [225]. One of the earliest studies describing the relationship between mutant P53 and autophagy states that the subcellular localization of mutant P53 is the major determinant of autophagy and it is conventionally accepted that P53 inhibits autophagy [172]. On the other hand, in many cells, it is observed that prolonged inhibition of the proteasome leads to its autophagy-mediated degradation of P53, suggesting that autophagy, in turn, can regulate the stability of P53 protein [200]. In this study, we inhibited P53 with a well-known P53 inhibitor, pifithrin-α (PFT-α) **(Fig. 3.2.8a)**. Interestingly, a significantly decreased cell viability was obtained with PFT-α plus ALLN treatment compared to only ALLN **(Fig. 3.2.8b)**. This suggests that R273H-P53 inhibition had a positive impact on cell sensitization. We were hence curious to analyze the effects of PFT-α on autophagy levels as well. Interestingly, pretreatment of PFT-α followed by ALLN exposure caused an increase in Atg-5 levels and a decrease in sequestrosome P62 levels, indicating an enhancement of autophagy **(Fig. 3.2.8ci-ii)**. Enhanced autophagy induction on ALLN plus PFT-α treatment was further confirmed by MDC staining which showed an additive effect as well **(Fig. 3.2.8d)**. Furthermore, an increased ROS accumulation was observed with ALLN plus PFT-α treatment associated with enhanced cell death **(Fig. 3.2.8e-f)**. ROS scavenger, NAC, successfully reversed the effect substantiating a ROS-dependent phenomenon. Further, as evident from **figure 3.2.8g**, U0126 pretreatment followed by ALLN plus PFT-α exposure increased the cell viability and decreased accumulated ROS **(Fig. 3.2.8h)**. A significantly increased phospho-ERK level was also observed with ALLN plus PFT-α treatment **(Fig. 3.2.8i)**. Taken together, we postulate that GOF-P53 inhibition facilitates cell sensitization by upregulating autophagy and by enhancing ROS and ERK activation.

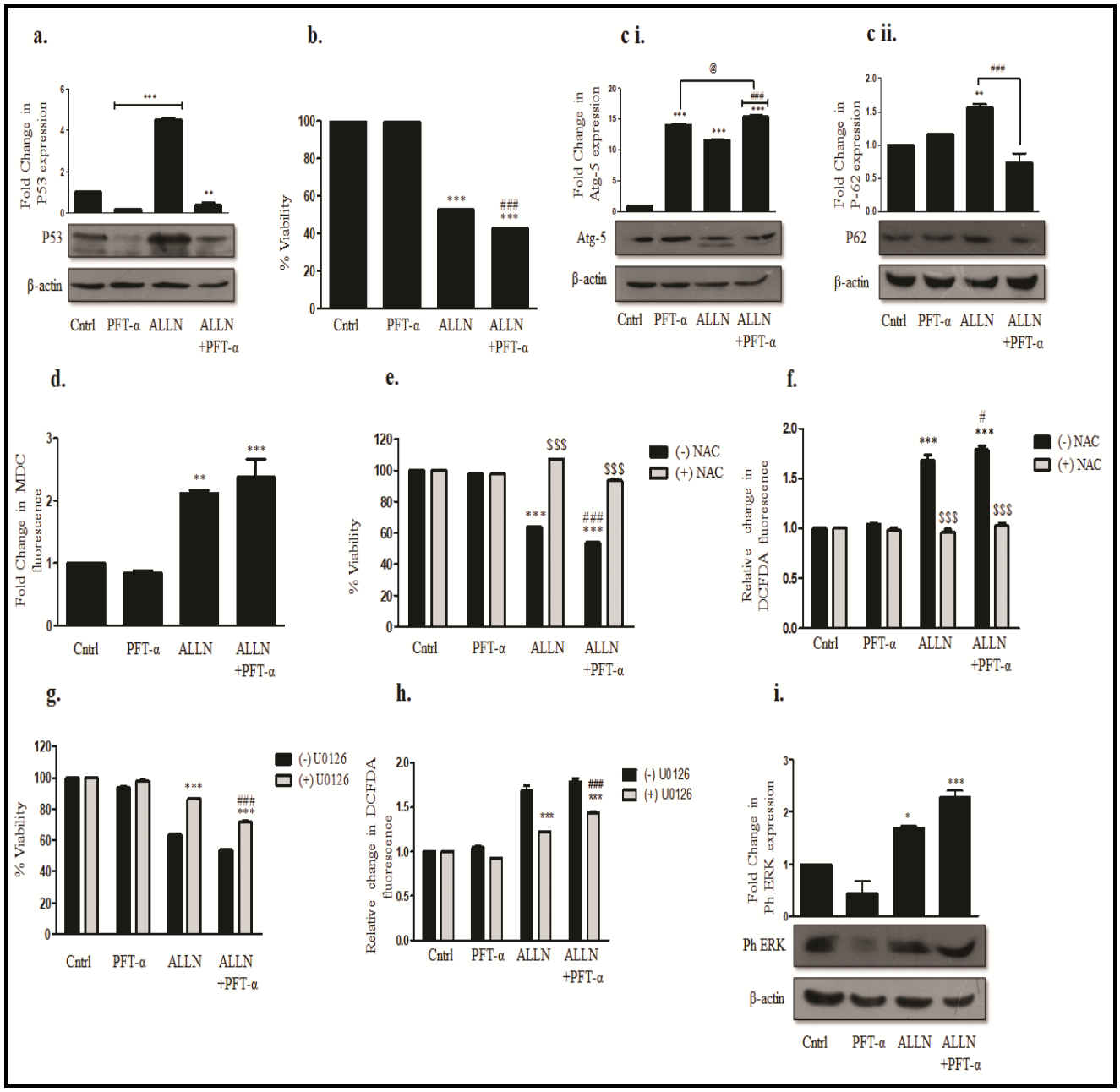

Figure 3.2.8. P53 regulates the induction of pro-death autophagy in R273H-P53 cells. **a** Immunoblot analysis depicting P53 expression upon ALLN treatment with or without 30 min of prior PFT-α exposure. **b** MTT assay was performed after ALLN and/or PFT-α treatment for 48 h and percentage viability represented in the form of a bar graph. **c(i)** R273H-P53 cells were exposed to ALLN and/or PFT-α for 48 h and autophagy was checked through immunoblot analysis of Atg-5 and **(ii)** P62. **d** MDC fluorescence assay was conducted after R273H-P53 cells were exposed to ALLN or PFT-α or in combination for 48 h. '*' indicates a significant difference compared to untreated control, while '#' indicates a significant difference compared to ALLN-treated cells. '@' indicates significant difference compared to PFT-α-treated cells. R273H-P53 cells were exposed to ALLN

and/or PFT-α (30 min before ALLN treatment) with and without NAC (1h before ALLN treatment) for 48 h and then cell viability and ROS levels were measured through **e** MTT assay and **f** DCFDA fluorimetric assay. **g** Cell viability and **h** ROS levels were analyzed with/without 2 h prior treatment of U0126 and the result is shown in the form of a bar graph. **i** Immunoblot analysis showing Ph ERK expression on ALLN and/or PFT-α treatment in R273H-P53 cells. '*' indicates a significant difference compared to untreated control and '#' indicates a significant difference compared to ALLN-treated cells, while $$$ indicates the statistical difference compared to minus (-) NAC.

3.3 Discussion and conclusion

For decades, the majority of previous studies have focused on understanding protein synthesis, particularly their transcriptional and translational control. While the aspects of protein degradation have been largely overlooked, it is a natural way by which cells clean up proteins that are redundant or have been misfolded or damaged [226, 227]. Inhibition of this protein degradation machinery has been useful previously for the treatment of autoimmune diseases and cancer [209, 228]. Especially in particular types of cancer, where protein production is much higher than normal, primarily to meet their over proliferative or secretary demand, an inhibition of proteasomes can cause proteins to pile up, eventually killing the cancer cell [229, 230]. There are already proteasome inhibitors like bortezomib in the clinics for treating Kahler's disease (multiple myeloma). However, the proteasomal inhibitors not only affect the proteasome but also can significantly alter the functioning of another cellular homeostatic machinery, like autophagy. The latter is primarily devoted towards maintaining the cellular balance of organelles, proteins, and other macromolecules. For example, cancer cells that produce excess unfolded proteins generate high endoplasmic reticulum stress leading to protein removal via either the proteasome or autophagy, suggesting that both pathways may be specifically exploited therapeutically. This is further relevant because proteasome inhibition, as in our study, with ALLN leads to compensatory upregulation of autophagy for clearance of proteins, which may provide a survival advantage to cells. Given the intense interest in targeting proteasomal degradation and the promise they hold for a multitude of cancer types, it is therefore important to precisely understand the consequences of autophagy induction after inhibition of proteasomal degradation as a cancer therapeutic strategy. In this study, we have demonstrated that cells transfected with GOF mutant P53 show resistance to not only conventional drugs like cisplatin or 5-FU but also to ALLN when compared to WT-P53. There was induction of autophagy upon ALLN treatment as well. Since ALLN induces autophagy and the latter may be a tumor survival response, we initially hypothesized that blocking autophagy with CQ, along with ALLN, may initiate

cell death or apoptosis. However, despite the proven benefits of lysosomotropic agents in cancer clinics in conjunction to autophagy inducers or drugs, in our study, CQ rather than enhancing ALLN-induced cytotoxicity reduced its sensitivity in GOF-R273H-P53 cells. Hence, from these studies, we concluded that, in this context, autophagy does not serve as a mechanism that prolongs cell survival.

It is increasingly getting recognized that the well-conserved autophagic machinery may be essential for cell death, at least in certain settings. However, it is controversially discussed in literature whether cells truly die "by autophagy" or in dying cells autophagy is just a bystander or programmed mechanism facilitating apoptosis [231]. Few studies in the past have indeed provided evidence that cells can possess a novel death mechanism that may depend on autophagy [232-234]. However, the nature of stimulus leading to autophagy-dependent cell death has remained poorly defined till date. In this study, we showed that R273H is one of the most prevalent mutations in NSCLCs. Further, the R273H harboring NSCLC P53 cells can be better sensitized to proteasomal inhibition by ALLN, by enhancement of autophagy rather than its inhibition. Though autophagy is predominantly thought to play an important protective role in sustaining homeostasis of cancer cells supporting their proliferation, we provide evidence of autophagy as a death promoter in the resistant lung cancer cells. This death was characterized by an enhanced ROS and ERK signaling. We further prove that inhibition of GOF-mutant-P53 can enhance cell death in lung cancer cells. **Figure 3.3.1** schematically represents the summary of our findings. Currently, there are very few literatures available which identifies molecular mechanisms where autophagy is a death enhancer. This signifies the importance of our study. However, more broadly, it still remains to be investigated whether the cell death observed was autosis (that represents a subtype of autophagic cell death) or whether a bona fide cell death by autophagy also requires the core apoptotic machinery. Together, our results reveal a novel mechanism through which mutant P53 harboring lung cancer cells can be sensitized by exploiting the crosstalk between the cellular homeostatic protein degradation machineries.

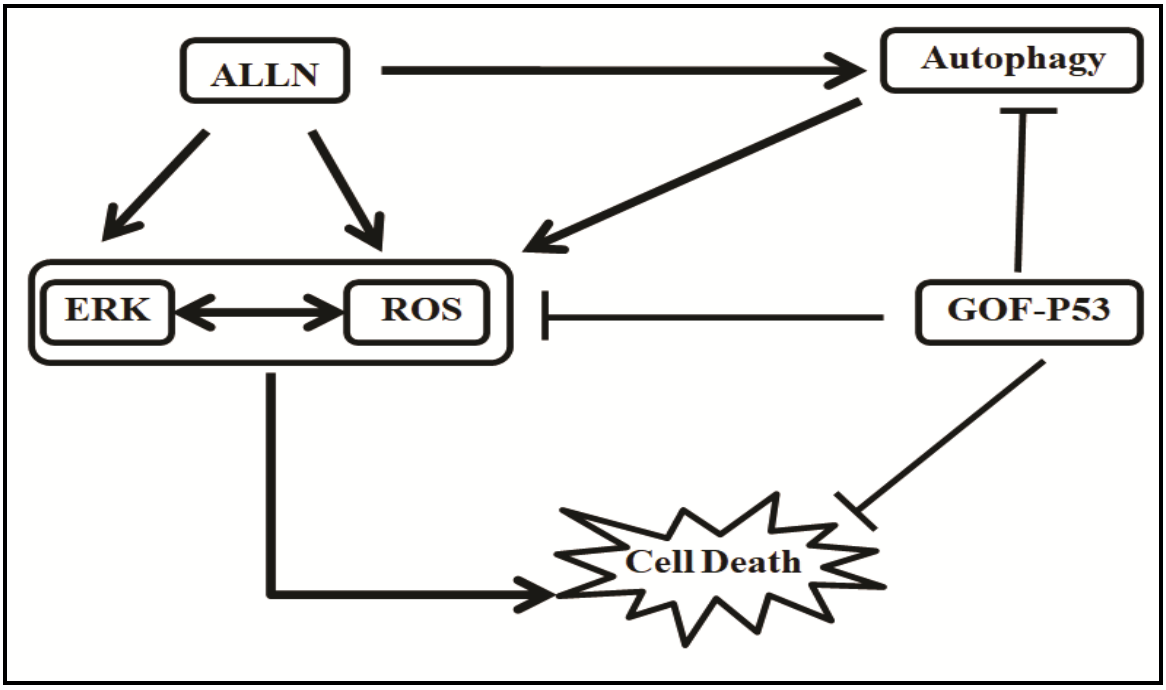

Figure 3.3.1. Schematic representation of the probable mechanism involved in proteasomal inhibitor, ALLN induced cell death in R273H-P53 cells.

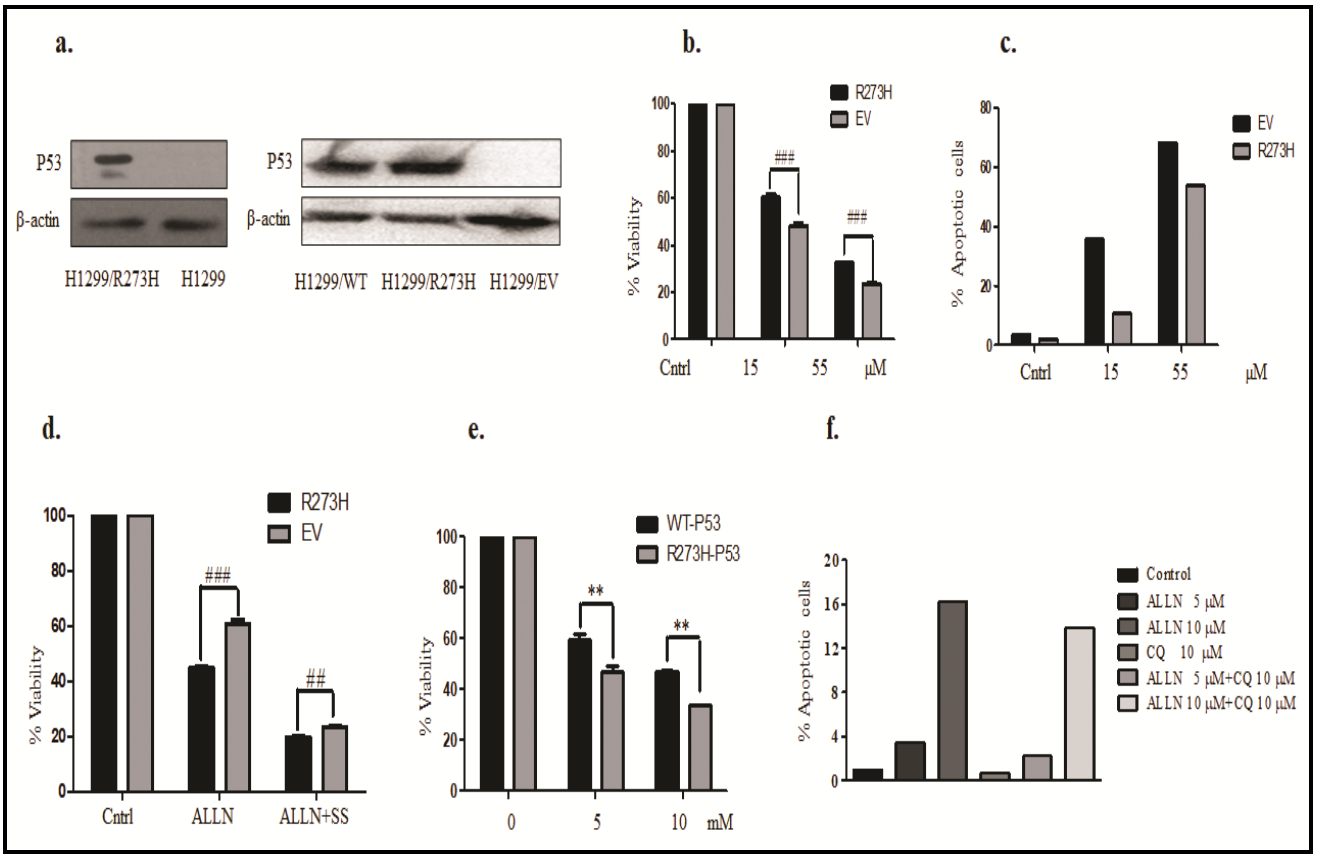

Supplementary Figure 3. a Stable transfection of WT, R273H-P53, and EV plasmids was

confirmed by immunoblotting against P53. **b** R273H-P53 and EV transfected cells were exposed to different doses of cisplatin followed by an MTT assay to analyze the viability. '#' indicates a significant difference compared to R273H-P53. **c** Annexin V/PI staining was performed to compare the percentage of apoptotic cells between R273H-P53 and EV transfected cells upon cisplatin treatment. **d** MTT assay was performed to check for viability between R273H-P53 and EV transfected cells upon ALLN treatment. '#' indicates a significant difference compared to R273H-P53. **e** WT-P53 and R273H-P53 cells were exposed to different doses of 3-MA for 48 h and cell viability was analyzed through MTT assay. '*' indicates a significant difference compared to R273H-P53. **f** Annexin V/PI staining was performed to compare the percentage of apoptotic cells upon exposure to varying doses of ALLN and/or CQ in R273H-P53 cells.

Chapter-4

Autophagy inhibitor, chloroquine induces a transitory attenuation of proliferation through regulation of cytoskeletal organization, mutant P53, and YAP in NSCLCs

4.1 Overview

A vast majority of P53 mutations have been observed to impart unique properties to the protein that are hitherto absent in its wild-type form. Mechanistic insights reveal that a GOF mutation can allow the P53 protein to associate with other novel interacting protein partners. This enables a transcriptional program unique to the GOF mutant form promoting oncogenic traits [19, 101, 196]. In this regard, the master transcription regulator Yes-associated protein (YAP) is reported to be a potent P53 partner enabling tumor-promoting function [49]. While the canonical function of YAP is mostly restricted to the activation of the TEAD family of transcription factors that control organ growth [84], however, dysregulation of YAP and its signalling can promote tumor growth, proliferation, and metastasis *via* selective transcription of genes like, connective tissue growth factor (CTGF) [88], amphiregulin (AREG) [89], cysteine-rich angiogenic inducer 61 (Cyr61) [90], axl [91], birc-5 [92], ankyrin repeat domain 1 (ANKRD1) [93] and others. Given the imperative effect of GOF-P53 and YAP in tumor growth, further studies are required to precisely understand their co-operative function in a cellular context and design appropriate strategies to attenuate their effect.

Interestingly, there are burgeoning reports for GOF-P53 [235-238] and YAP [239-242] regulating autophagy, or being regulated by autophagy. The latter is a highly conserved catabolic process that maintains cellular protein and organelle homeostasis through lysosome-mediated degradation [199]. Recent research highly implicates the role of autophagy in the regulation of multiple events associated with cancer, however, it is thought to be a dual-edged sword with both tumor-promoting or attenuating function in a cellular or context-dependent manner [243]. Therefore, while autophagy can recycle intracellular macromolecules to meet up to the colossal demand of tumor growth [244], on contrary, prolonged activation of autophagy can also lead to autophagy-induced cell death in cancer cells [245]. Strikingly, autophagy is reported to facilitate the growth of lung cancers bearing mutations in BRAF or RAS [246, 247] and it is also involved in EGFR-TKI induced resistance in NSCLCs [248]. Hence, there is an urgent need to understand the interplay between these critical molecular factors and thereafter design an appropriate strategy targeting them in cancers like NSCLC.

In this study, we established the cross-talk between R273H-P53, YAP, and autophagy *in vitro*. Furthermore, we observed that the well-known autophagy inhibitor and the FDA-approved drug, chloroquine (CQ) can induce proliferative arrest in lung cancer cells through the regulation of P53 and YAP. We propose an independent strategy to regulate lung cancer cell proliferation which can be of future therapeutic benefit.

4.2 Results

4.2.1 GOF-P53 and YAP co-operatively regulate NSCLC progression

As mentioned before, the acquisition of GOF mutations allows P53 protein to interact with other proteins present in the intracellular milieu, increasing its pro-oncogenic properties [49, 101]. To identify probable interacting partners, we extracted and analyzed publicly available RNA sequencing data from H1299 cells over-expressing R273H-P53 [249]. Interestingly, ChIP-seq analysis revealed that TEAD1 promoter, the binding partner of the potent transcription regulator-YAP, is a direct target of R273H-P53, and RNA-seq data further showed an increased expression of TEAD1 in cells over-expressing R273H-P53 compared to cells stably transfected with empty vector control **(Fig. 4.2.1a)**. Additionally, several well-known downstream targets of YAP, like CTGF, CYR61 etc. also showed a significant up-regulation in R273H transfected cells compared to empty vector transfected control **(Fig. 4.2.1b)**. Importantly, a high expression of YAP downstream targets was found to be associated with decreased 5-year survival of patients with lung cancer (source-The Human Protein Atlas) **(Fig. 4.2.1c)**. The above indications were suggestive of a probable crosstalk between GOF-R273H-P53 and YAP in regulation of oncogenesis in lung cancer cells. To validate the same, we stably transfected the lung cancer H1299 cells with R273H-P53 and performed an RNAi-mediated ablation of P53. Interestingly, we observed a decreased expression of YAP and its downstream target- CYR61 upon inhibition of P53 in H1299 cells **(Fig. 4.2.1d)**. Conversely, a YAP over-expression in SW-480 cells, naturally harboring a R273H-P53 mutant, showed an enhanced p53 transcription **(Fig. 4.2.1e)**. Additionally, an increased P53 protein level was also observed upon YAP over-expression in another tumor cell type- HOS expressing a different GOF mutant-R156P **(Fig. 4.2.1f)**. These findings strongly indicate of a possible transcriptional feedback loop existing between YAP and different variants of GOF mutants irrespective of the cell type. Given the functional relevance of GOF-P53 and YAP in NSCLCs, we analyzed cell viability post treatment with verteporfin (VP) and pifithrin-alpha (PFT-α), the pharmacological inhibitors for YAP and P53 respectively [250, 251], or post siRNA-mediated ablation of the above transcripts. Importantly, independent pharmacological inhibition **(Fig. 4.2.1g)** or siRNA-mediated ablation of YAP or P53 **(Fig. 4.2.1h)** result in a significant cell death, however, a simultaneous knock-down of both P53 and YAP resulted in considerably enhanced sensitization of H1299 cells **(Fig. 4.2.1h)**. The above data are indicative of the probable regulatory feedback loop existing between R273H-P53 and YAP and the functional significance of these proteins in NSCLCs.

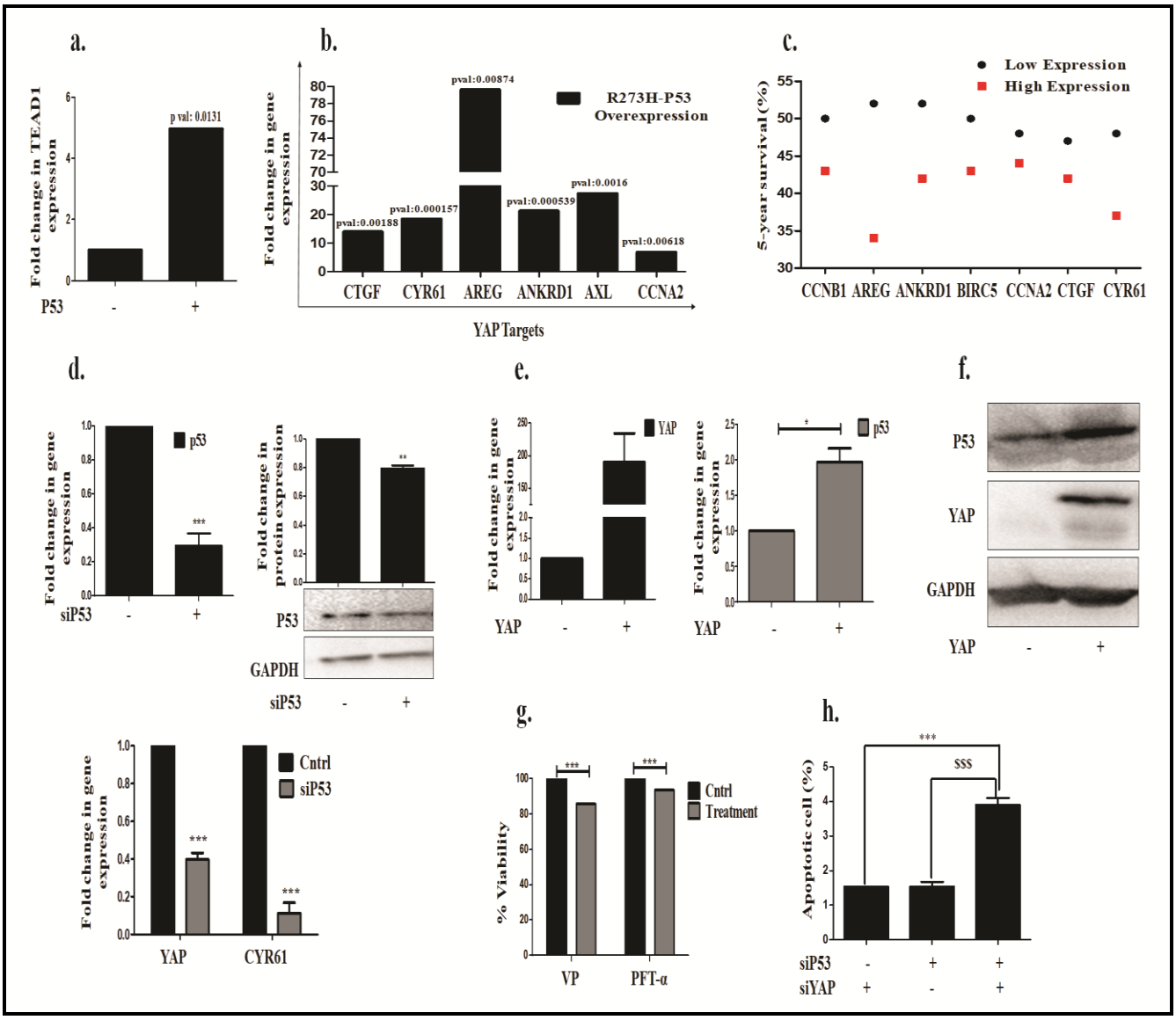

Figure 4.2.1. Crosstalk and functional relevance of GOF-P53 and YAP in NSCLCs. Bar graph representing significant (p value ≤ 0.05) difference in expression of **a** TEAD1 and **b** YAP downstream targets in R273H-P53 overexpressing H1299 cells compared to empty vector transfected control (arbitrary unit '1'). **c** Graph showing relation between expressions of YAP downstream targets and 5-year survival (%) of NSCLC patients. **d** Bar graph showing transcript level of YAP and its downstream target - CYR61 upon siP53-mediated ablation of GOF-R273H-P53 in H1299 cells. **e** Bar graph representing transcript level of p53, upon overexpression of YAP in GOF-R273H-P53 harboring SW480 cells. **f** Immunoblot representing level of P53, upon overexpression of YAP in GOF-R156P-P53 harboring HOS cells. **g** Cell viability, as measured through MTT assay after exposure to verteporfin (VP) or Pifithrin-alpha (PFT-α) at 10μM dose for 48 hour. '∗' indicates a significant difference compared to untreated cells. **h** Bar graph showing percentage apoptosis post siYAP and/or siP53 treatment for 24 hour in R273H-P53 harboring H1299 cells. '∗' or '$'' indicates

a significant difference compared to only siYAP or siP53 treated cells respectively.

4.2.2 Autophagy is highly dysregulated in NSCLC patients and has crosstalk with R273H-P53 and YAP

Interestingly, the cellular homeostatic process autophagy is reported to be involved in the regulation of proteostasis. Also, existing reports suggest that P53 and YAP can either regulate autophagy or can be regulated by autophagy as well. Moreover, interactome studies have also indicated a strong correlation between hippo signaling components and vesicle-trafficking [252]. Given the importance of GOF-P53 and YAP in NSCLCs we wanted to explore the role of autophagy in lung cancers, dissect any crosstalk with R273H-P53 and YAP and finally identify a vulnerability of GOF-R273H harboring cells by modulating this proteostasis mechanism. We analyzed gene expression data of NSCLC patients extracted from the GDC portal. Interestingly, genes involved in different stages of autophagy were found to be significantly differentially regulated and a positive correlation in their expression was observed with a poor survival rate of NSCLC patients **(Fig. 4.2.2a)**. Thereafter, the autophagy genes de-regulated in NSCLC patients were evaluated for their differential expression in the publicly available transcriptomic data of R273H-P53 overexpressing H1299 cells. Interestingly, a striking 21.6% of the genes were identical in both patient data-set and R273H-P53 over-expressed cells **(Fig. 4.2.2b.i)**. Some of the key genes showing an increased up-regulation (log2 fold >2) and p-value significance (< 0.05) are represented in **figure 4.2.2b.ii.** Interestingly, an over-expression of YAP in H1299 cells **(Supplementary Fig. 4a)** resulted in increased LC3B-II, a hallmark of autophagy induction **(Fig. 4.2.2c)**. On a similar note, in R273H-P53 stable transfected cells **(Supplementary Fig. 4b)** an enhanced basal level of LC3B-II was observed compared to parental H1299 cells **(Fig 4.2.2d).** While, a knockdown of YAP or P53 in turn led to decreased transcript levels of ATG-5, crucial for autophagic vesicle formation **(Fig. 4.2.2e)**. Interestingly, inhibition of autophagy through RNAi-mediated knock-down of ATG-5 resulted in reduced expression of YAP and its downstream targets **(Fig. 4.2.2f)**. The above experiments indicate towards the intricate crosstalk and probable interdependence existing between autophagy, P53 and YAP in lung cancer cells.

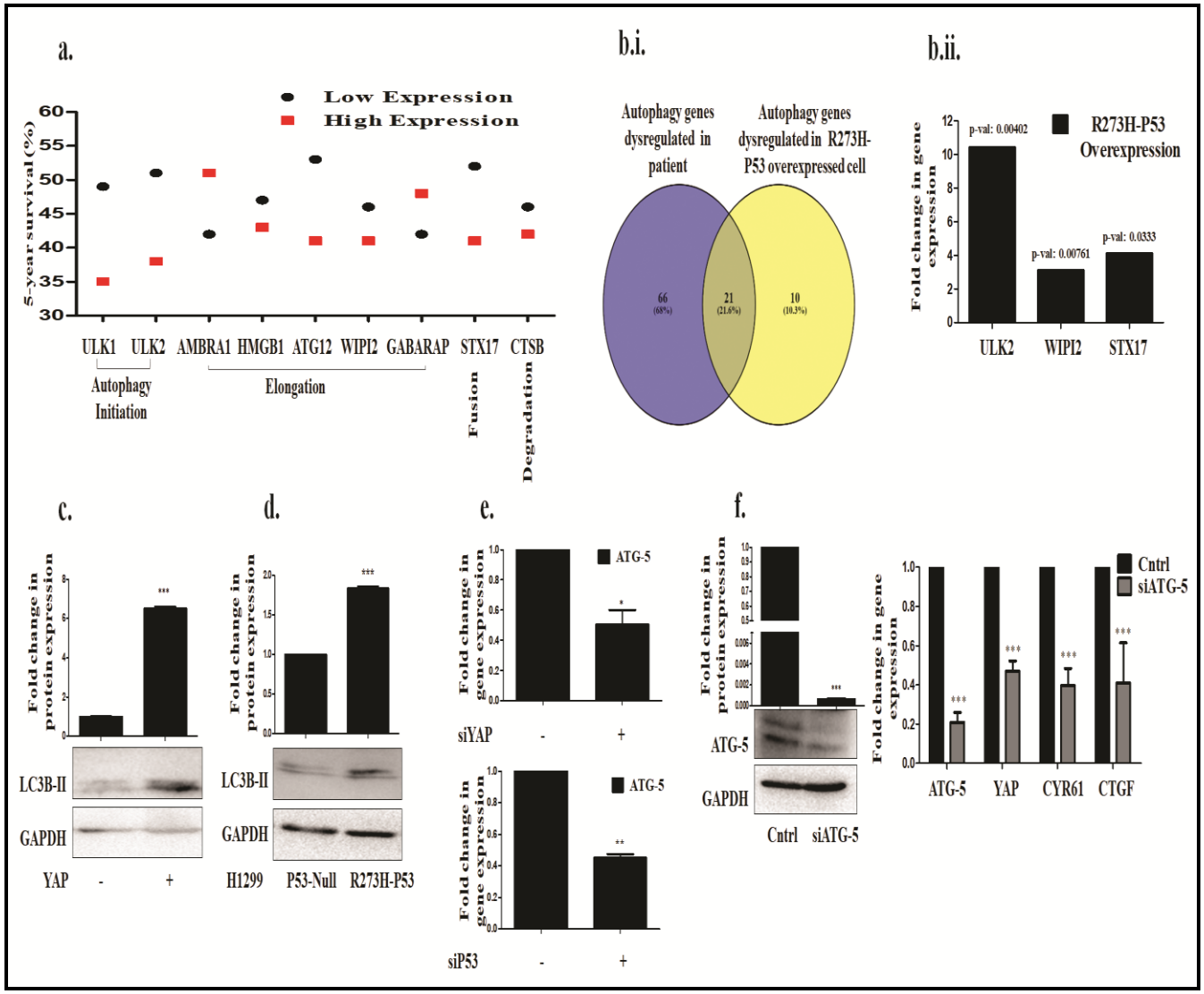

Figure 4.2.2. Autophagy dysregulation and its association with R273H-P53 and YAP in NSCLCs. a Graph showing relation between expressions of autophagy associated genes and 5-year survival (%) of NSCLC patients. **b(i)** Venn diagram showing number of autophagy associated genes dysregulated in NSCLC patients and/or in R273H-P53 overexpressing H1299 cells. **b(ii)** Bar graph representing significant difference in expression of autophagy associated genes in R273H-P53 overexpressing H1299 cells compared to empty vector transfected control (arbitrary unit '1') **c** Immunoblot showing LC3B-II expression post 48-hour transfection of YAP. **d** Immunoblot showing difference in LC3B-II expression between p53-null and R273H-P53 expressing H1299 cells. **e** Expression level of ATG-5 transcripts post siYAP or siP53 transfection. **f** Bar graph representing transcript levels of downstream targets of YAP post siATG-5 transfection. Unless otherwise mentioned experiments were performed in R273H-P53 harboring H1299 cells. '∗' indicates a significant difference compared to untreated cells.

4.2.3 A high dose of CQ disrupts YAP and GOF-P53 localization

The implication of autophagy in the regulation of GOF-P53 and YAP prompted us to further explore the efficacy of the FDA-approved drug and an autophagy inhibitor, chloroquine (CQ) against lung cancer cells [157]. The addition of CQ to the cells resulted in an impairment of autophagic flux indicated by the accumulation of LC3B-II **(Fig. 4.2.3a)**. Interestingly, CQ at the stipulated dose induced a decrease in expression of YAP and its downstream target-CYR61 suggesting regulation at the transcriptomic level **(Fig.4.2.3b)**. To further validate the same, H1299 cells were transfected with YAP/TAZ-responsive promoter-driven luciferase construct with TEAD binding sites. Importantly, with an increase of CQ dose, we observed a reduced luciferase activity; Verteporfin (VP), a YAP inhibitor was used as a positive control **(Fig. 4.2.3c)**. Reduced transcriptional activity of YAP can also be attributed to the differential localization of the protein. Strikingly, immuno-fluorescence microscopy showed a prominent cytoplasmic accumulation of YAP after CQ exposure **(Fig. 4.2.3d)**. The R273H-P53 also showed a similar pattern of accumulation after CQ exposure and was found to co-localize with YAP **(Fig. 4.2.3e)**. Importantly, an RNAi-mediated ablation of ATG-5 or inhibition of autophagy with another autophagy inhibitor- bafilomycin (Baf), though led to a comparative increase in cytoplasmic YAP or P53, however, the accumulation was not as prominent as observed with CQ **(Supplementary Fig. 4c-d)**. Furthermore, to understand whether the CQ-specific accumulation of P53/YAP is dependent on each other we exposed P53-null H1299 cells to CQ. An increase in accumulation of YAP was still observed indicating a P53 independent effect **(Supplementary Fig. 4e)**. Exposure of CQ to another cell type-HOS harboring a GOF-R156P-P53 mutation also showed similar results suggesting a cell-type independent effect of CQ **(Fig. 4.2.3f)**. An earlier study by Liang *et al* 2014 indicated that YAP can be a cargo for lysosomal degradation; similarly, P53 is also known to undergo degradation through autophagy [237, 253]. In corroboration to above, we observed co-localization of YAP with Lysotracker Red (LTR) **(Fig. 4.2.3g)** and additionally, both YAP and P53 were found to co-localize with the lysosomal membrane-associated glycoprotein- LAMP-2a after CQ exposure **(Fig. 4.2.3h-i)**. Existing reports suggest probable involvement of chaperons in translocation of specific proteins with KFERQ motif to the lysosomes, via LAMP-2a when macro-autophagy is inhibited [254]. The chaperone- HSC-70 is known to facilitate this process often described as chaperone-mediated autophagy (CMA) [147]. Interestingly, YAP was found to possess a KFERQ motif (while P53 is already reported to have the same) as analyzed through KFERQ motif finder [255] and was also found to co-localize with HSC-70 **(Fig. 4.2.3j)** after CQ treatment. The above findings indicate towards the preferential lysosomal accumulation of YAP/P53 after CQ exposure resulting in a concomitant decrease in their

transcriptional activity.

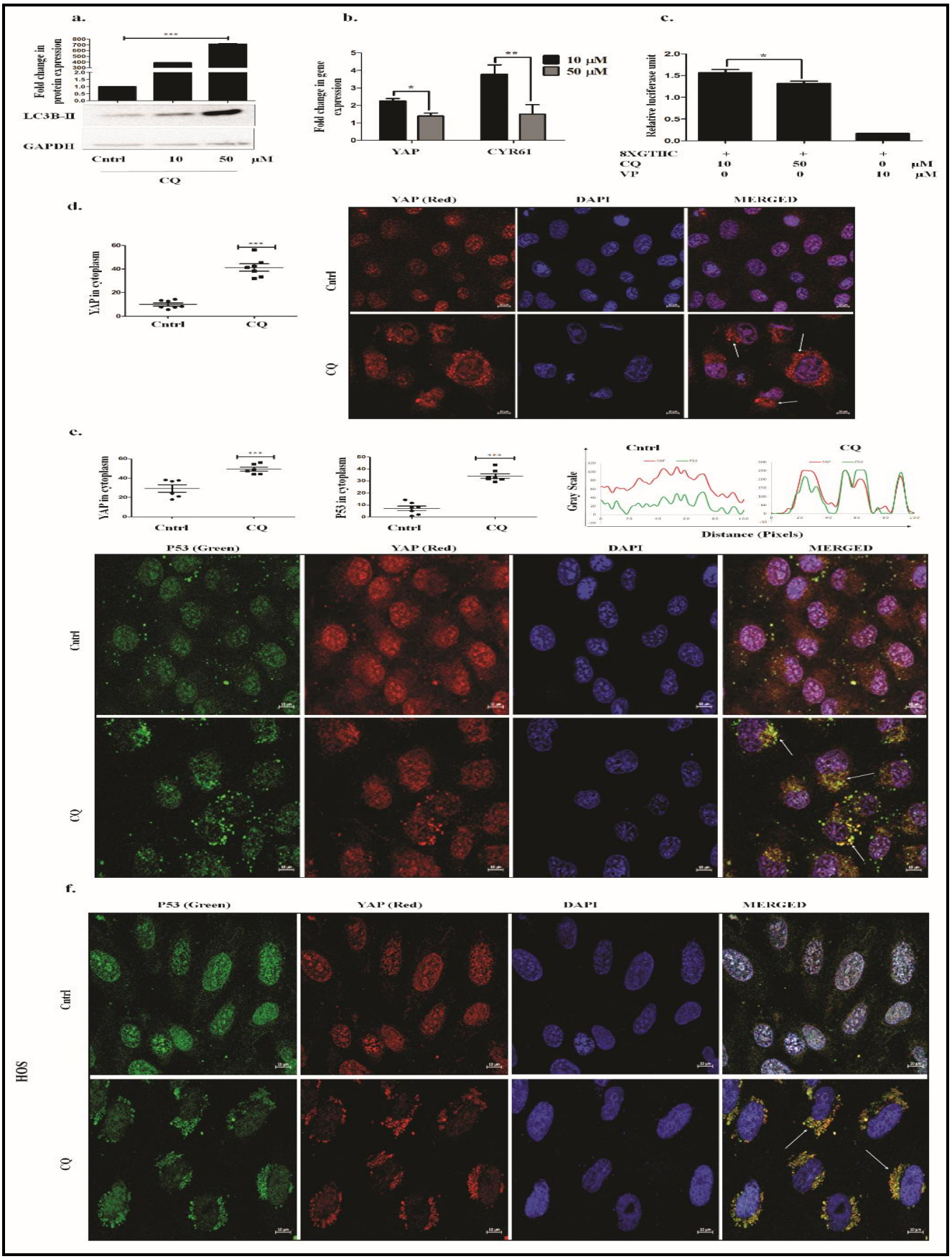

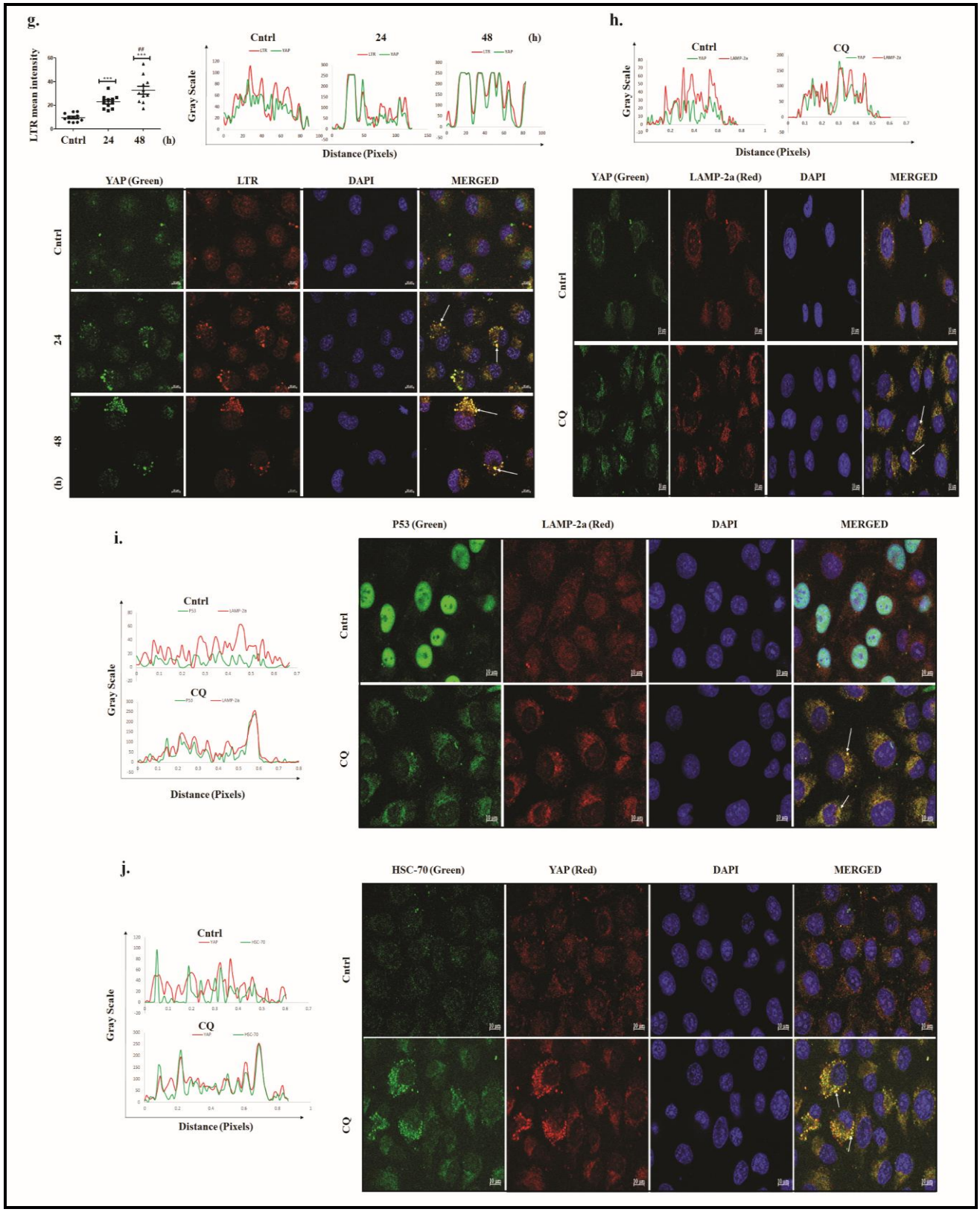

Figure 4.2.3. Effect of CQ on YAP and R273H-P53 in NSCLC cells. a Immunoblot showing LC3B-II expression post CQ exposure. **b** Transcript levels of YAP and CYR61 after CQ treatment. **c** YAP responsive promoter luciferase activity upon CQ treatment; VP (10μM) served as a positive

control. **d** Immunofluorescence for YAP post CQ exposure. **e** Immunofluorescence and fluorescence intensity profiling showing P53 and YAP localization after CQ exposure. **f** Immunofluorescence showing YAP and P53 localization post CQ treatment in HOS cells. **g** Immunofluorescence and fluorescence intensity profiling indicating YAP and LTR; **h** YAP and LAMP-2a; **i** P53 and LAMP-2a; **j** HSC-70 and YAP localization post CQ exposure. White arrows indicate accumulation and co-localization. The experiments were performed in R273H-P53 harboring H1299 cells unless otherwise mentioned. CQ was administered at 50μM dose for 48 hour, unless otherwise mentioned. DAPI (Blue) was used to stain the nucleus. Scale bar: 10 μm. Objective: Plan Apochromat 63x/1.40 oil M27. '∗' indicates a significant difference compared to untreated cells or 10μM CQ treated cells.

4.2.4 CQ induces a dynamic alteration of cellular architecture and cytoskeletal pattern

A plethora of existing reports suggests that various mechanical cues can converge upon actin cytoskeleton organization resulting in regulation of YAP localization and its transcriptional activity [93, 256]. To evaluate the underlying causes to CQ-mediated cytoplasmic accumulation of YAP or GOF-P53, we analyzed F-actin distribution through phalloidin staining after CQ exposure. Interestingly, a distinctive difference in F-actin staining with appearance of punctate structures, and a re-modeling of cortical actin cytoskeleton was observed upon treatment with CQ **(Fig. 4.2.4a)**. The cell morphology, as observed through bright-field microscopy was also distinctively altered after CQ treatment with respect to untreated control **(Fig. 4.2.4b)**. To have better insights we further performed SEM analysis. Multiple, large pits predominantly in the perinuclear region was observed after CQ treatment, but not with Baf **(Fig. 4.2.4c-d)**. The change in morphology was also coupled to an increase in MDC-labeled autophagic vesicles **(Fig 4.2.4e)**, a probable outcome of inhibition of vesicular fusion or disruption of trafficking after CQ exposure [257]. To the best of our understanding, we assume that CQ results in an overall re-modeling of cellular morphology and F-actin organization, which might be an important factor responsible for the cytoplasmic accumulation of the potent transcriptional regulators- YAP and P53. Importantly, a withdrawal of CQ from the culture medium resulted in reversal of features characterized by reduced cytoplasmic pits, decreased cytoplasmic accumulation, and increased nuclear localization of YAP and P53 suggesting a dynamic effect imparted by CQ on the tumor cells **(Fig. 4.2.4f-g)**. Simultaneously, an increased transcription of YAP and its target was observed after CQ withdrawal **(Fig. 4.2.4h)**. These findings suggest that CQ induces a transitory alteration of cellular phenotype through cytoskeletal remodeling and associated regulation of potent transcription regulators, like YAP and GOF-P53.

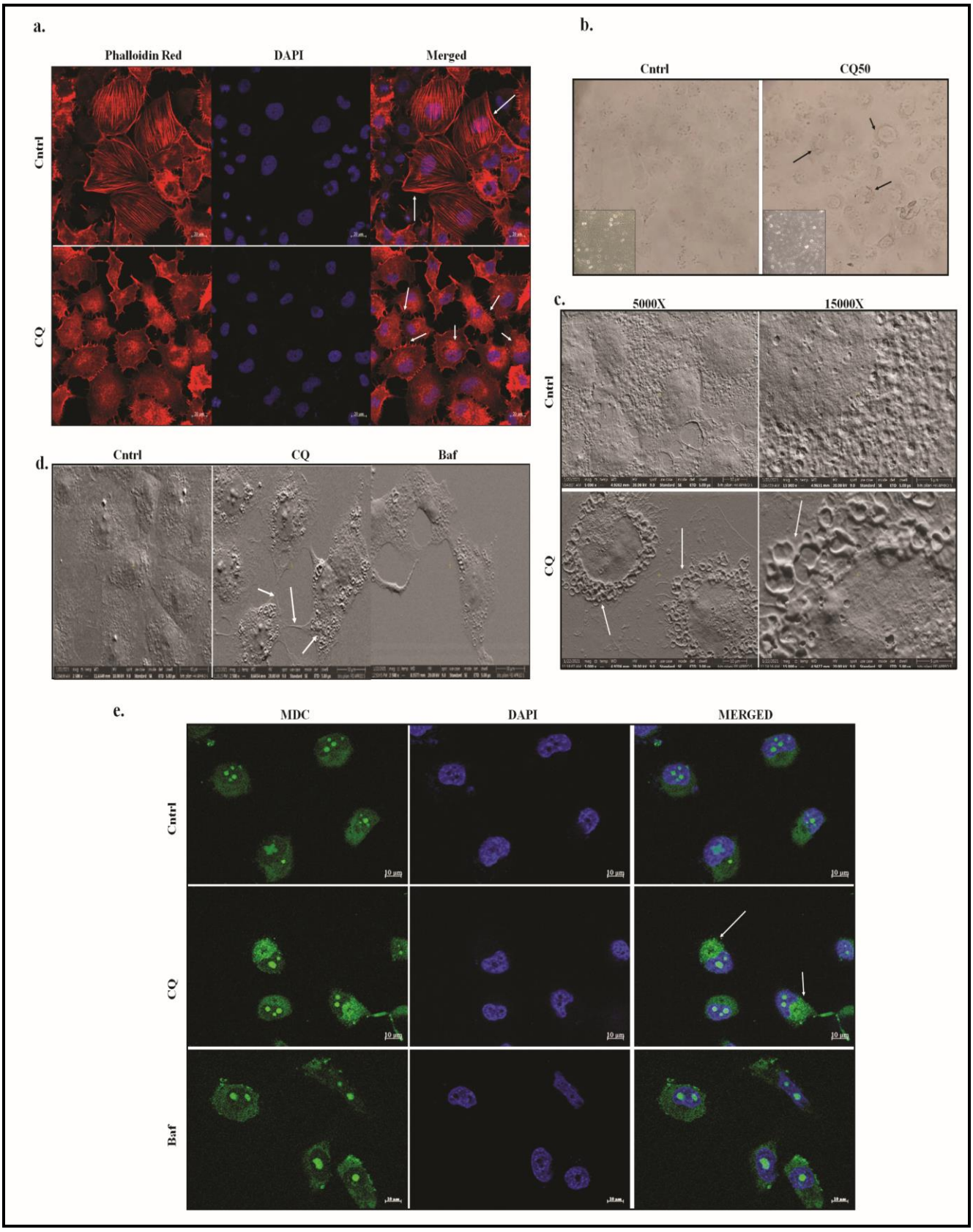
a.
Phalloidin Red
DAPI
Merged
Cntrl
CQ
b.
Cntrl
CQ50
c.
5000X
15000X
Cntrl
CQ
d.
Cntrl
CQ
Baf
e.
MDC
DAPI
MERGED
Cntrl
CQ
Baf

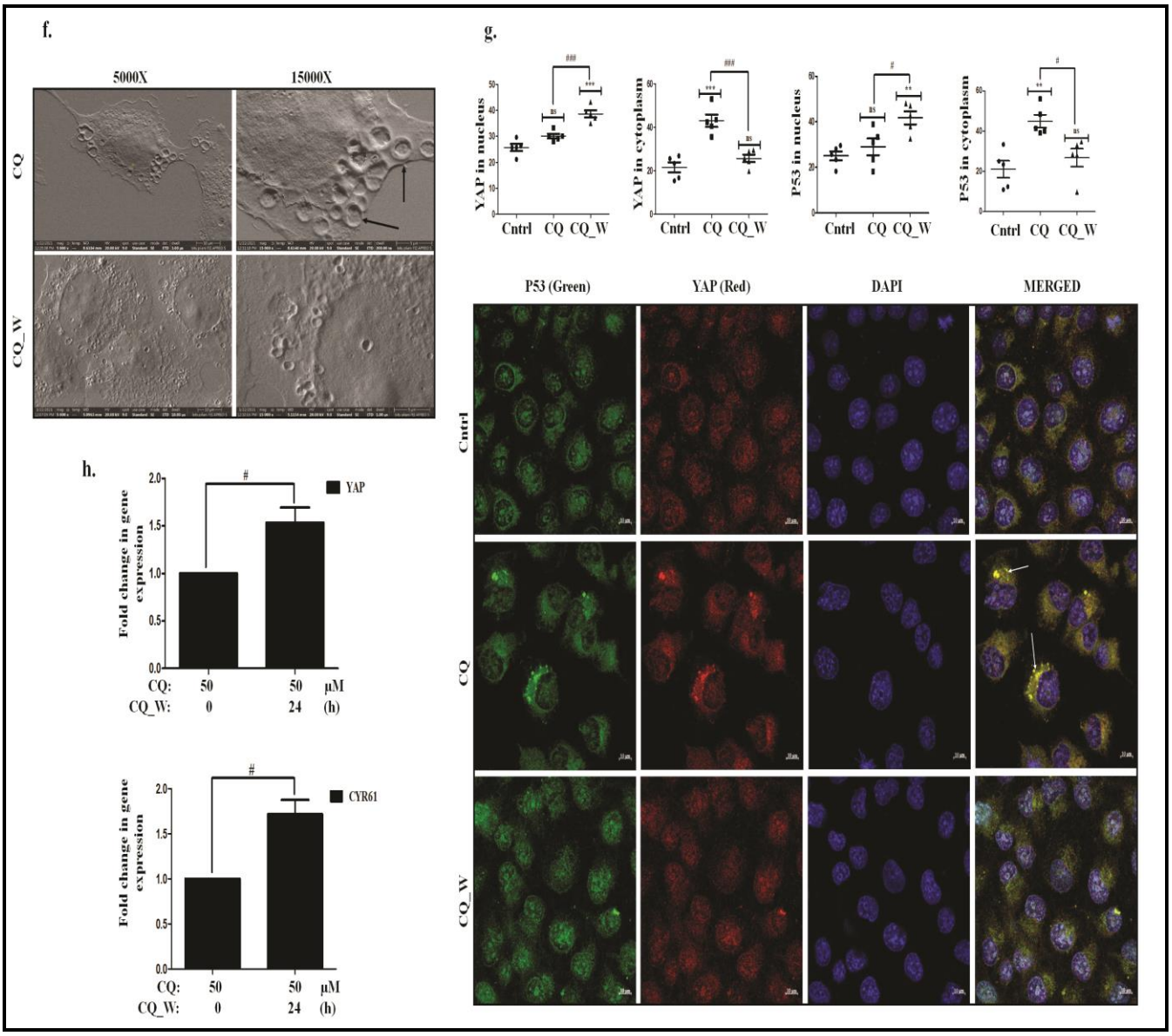

Figure 4.2.4. Effect of CQ on cellular architecture of NSCLC cells. a Phalloidin staining showing cytoskeletal alterations post CQ treatment. Scale bar: 20 µm. Objective: Plan Apochromat 40x/1.3 oil M27. White arrows indicate change in cortical and punctate structures. **b** Phase contrast image representing cytoplasmic alterations (black arrows) after CQ exposure. **c-d** Scanning electron microscope (SEM) images at different magnifications (X) showing cytoplasmic pits (white arrows) after treatment with CQ or Baf (10 nM). **e** Microscopic analysis of MDC fluorescence after treatment with CQ or Baf. White arrows indicate accumulation of green fluorescence observed. **f** SEM images showing comparative cytoplasmic changes in cells cultured in CQ-free media (withdrawal; W). **g** Immunofluorescence image of YAP and P53 post CQ withdrawal. Scale bar: 10 µm. Objective: Plan Apochromat 63x/1.40 oil M27. White arrows indicate accumulation and co-localization. '∗' indicates a significant difference compared to untreated cells. **h** Transcript levels of YAP and CYR61 after CQ

withdrawal. The experiments were performed in R273H-P53 harboring H1299 cells. CQ treatment (50µM) was for 48 hour; however, for withdrawal experiments cells were exposed to CQ for 24 hour followed by culture in CQ free media for 24 hour. '∗' or '#' indicates a significant difference compared to untreated and CQ treated cells respectively.

4.2.5 CQ induces a transitory arrest and inhibits proliferation of R273H-P53 harboring NSCLC cells

A cytoplasmic accumulation of the transcription regulators was found to be associated with a decreased expression of the cellular proliferation markers- PCNA and Ki67 after CQ treatment **(Fig. 4.2.5a)**. Interestingly, crystal violet staining showed fewer colonies of cells after CQ exposure compared to untreated control. However, the cells resumed proliferation after a CQ withdrawal, as evident from an increase in crystal violet stained colonies, indicating a temporary state and a dynamic regulation **(Fig. 4.2.5b)**. We hypothesized that the cells might attain a transitory non or minimally dividing state when exposed to CQ which might be associated with senescence-like features. Interestingly, an increase in Beta-galactosidase activity, often associated with senescent cells was indeed observed after CQ treatment **(Fig. 4.2.5c).** Simultaneously, flow cytometric analysis showed that the cells enter a cell cycle arrest when exposed to CQ, which is reverted after a CQ withdrawal **(Fig. 4.2.5d)**. From the clinical perspective, it is important to sensitize the persister cells adapting to a non-dividing transitory state thus surviving the CQ exposure. Herein, further studies are required to identify susceptibility of CQ exposed cells that can be utilized to eradicate the surviving non-dividing tolerant cells.

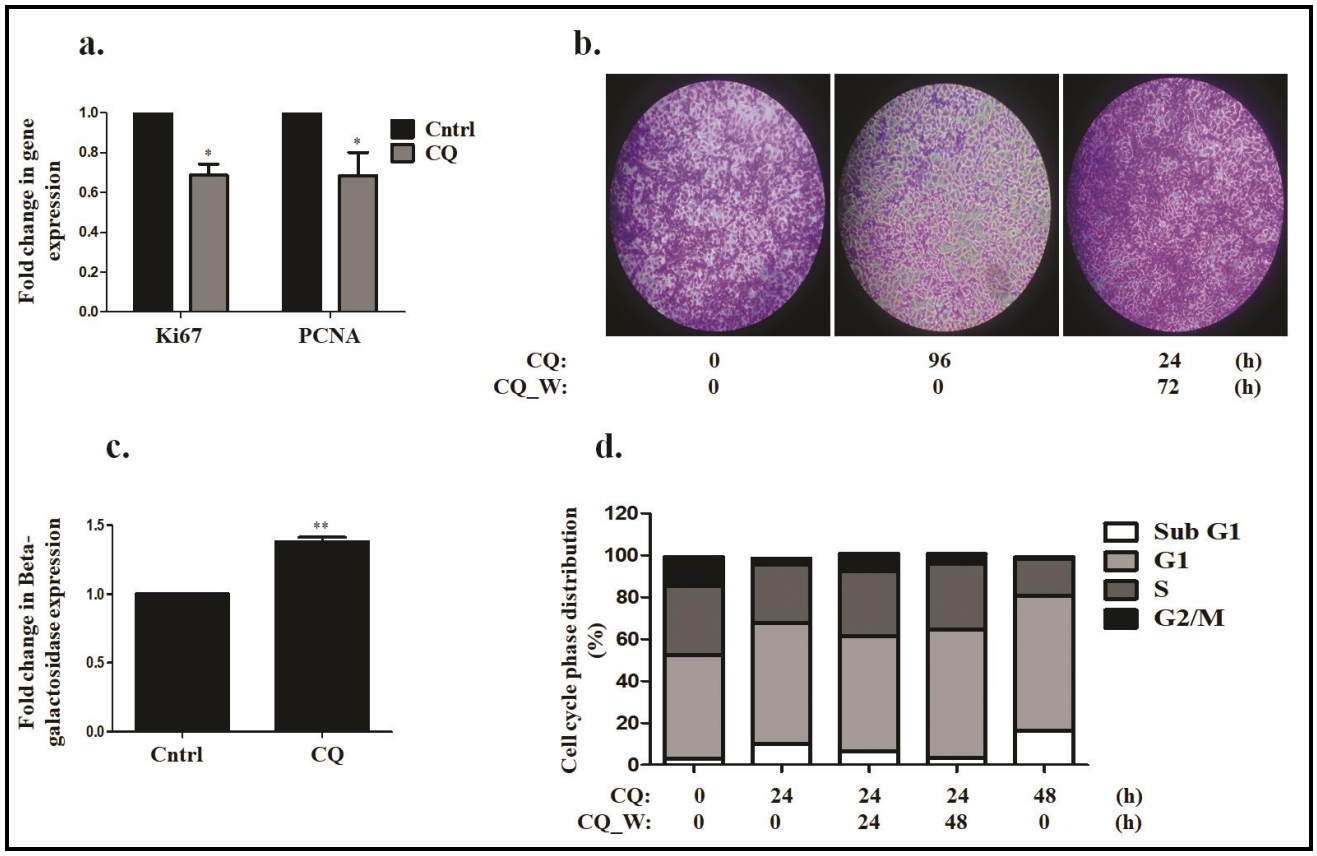

Figure 4.2.5. Effect of CQ on proliferation of R273H-P53 harboring NSCLC cells. a Transcript levels of Ki67 and PCNA post CQ treatment for 48 hour. **b** Crystal violet staining showing surviving cells after CQ treatment for 96 hour. **c** Bar graph representing fold change in Beta-galactosidase expression after CQ exposure for 48 hour. **d** Flow cytometric analysis representing cells at different phases of cell cycle post CQ treatment. '∗' indicates a significant difference compared to untreated cells.

4.3 Discussion and conclusion

Over the past few years, there has been extensive interest in understanding the role of the cellular homeostatic process, autophagy in cancer. Predominantly, targeting pro-survival autophagy has been the prime focus of autophagy-directed therapeutic strategies. In this regard, several clinical trials have been in progress demonstrating the potential of the autophagy inhibitor, chloroquine, or its derivatives [258, 259]. This anti-malarial drug has been a promising candidate for re-purposing against hematological or solid tumors, driven primarily by its various attributes like efficacy, cost-effectiveness, and oral administration. Importantly, till date, CQ and its derivatives remain the only autophagy inhibitory drugs that are approved by FDA against cancer. However, despite the considerable success of CQ in cancer, its precise mechanism of action remains equivocal [259]. The

conventional theory has been that CQ being a weak base, it increases the pH of intra-cellular compartments leading to inhibition of autophagic flux, following mechanisms analogous to Baf [260]. However, very recently Mauthe et al 2018, reported that CQ might not be interchangeable with Baf. Rather, the bona fide modus operandi of CQ is an impairment of autophagosome-lysosome fusion [157]. Furthermore, recent research also reveals the functions of CQ that extend beyond its canonical role as a flux inhibitor. For example, it can cause the dis-organization of Golgi or endo-lysosomal networks [157]. Nevertheless, CQ is primarily thought of as an exclusive autophagy inhibitor, and that concept has persisted. In this study, we show that the cellular effects of chloroquine extend from inhibition of flux to cytoskeletal disorganization and cytoplasmic sequestration of potent transcription regulators leading to compromise of tumor cell proliferative functions.

In this regard, we demonstrate the potential of CQ as an anti-proliferative agent in NSCLC cells. We observed that in contrary, to the conventional model, CQ was not found to be overtly cytotoxic to the lung cancer cells, even after 48h of exposure. However, it showed profound cellular effects that might extended beyond its autophagy inhibitory function. The cells when exposed to CQ went into a transitory non-proliferative state marked by growth arrest and showed senescence-like features as well. But, CQ withdrawal from the culture medium led to a rescue of cellular proliferation indicating dynamic adoption of survival strategies acquired by the cells in response to the drug. Interestingly, chloroquine induced a cytoskeletal remodeling marked by the punctate distribution of F-actin filaments, a substantial loss of cellular stress fibers, and re-organization of the cortical cytoskeleton. This remodeling was further associated with cytoplasmic, preferentially lysosomal accumulation of GOF-P53 and YAP proteins **(Fig. 4.3.1)**.

We observed that GOF-P53 mutations and the expression of YAP or its downstream targets are inversely correlated with NSCLC patient survival. Further, there exists crosstalk between these two proteins, and autophagy regulating NSCLC proliferation. Given the importance of GOF-P53 and YAP in NSCLC biology, CQ-induced cytoplasmic accumulation and attenuation of a pro-proliferative function of these key proteins can have a profound impact on the development of future therapeutic strategies against NSCLCs. Importantly, a knockdown of an autophagy-associated gene, ATG-5, or pharmacological inhibition of autophagy through Baf failed to show such a pronounced effect as CQ. However, transcription of YAP and its targets revived after withdrawal of CQ indicating transitory adaptation of the cells to attain a non-dividing state. How to effectively target these non-dividing cells still remains a pertinent question, that is yet to be addressed. However, we

believe that strategies often undertaken to eliminate the ‘drug-tolerant persisters (DTPs)' might be useful. The DTPs are often described in the literature as non-dividing cells surviving a drug shock which re-acquire its proliferative abilities over time to re-populate the tumor [261, 262]; to our understanding, CQ treated cells shared partly similar features. Overall, our data provides valuable insights into the diverse effects that chloroquine might have on cellular architecture, physiology, transcriptional regulation and proliferation of NSCLC cells which might be critically relevant for consideration of an appropriate treatment regimen.

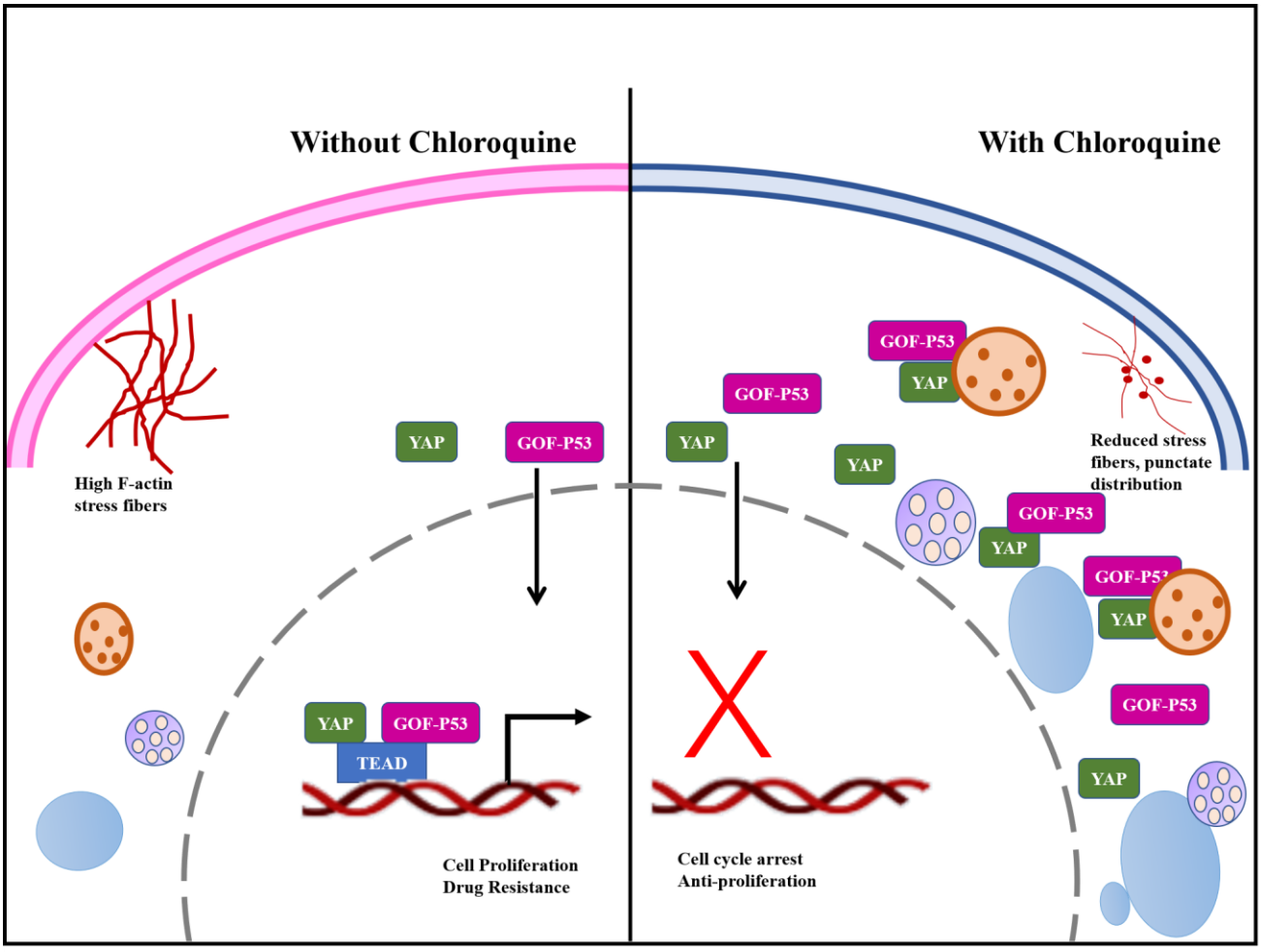

Figure 4.3.1. Schematic representation of CQ induced effects in GOF-P53 harboring cells.

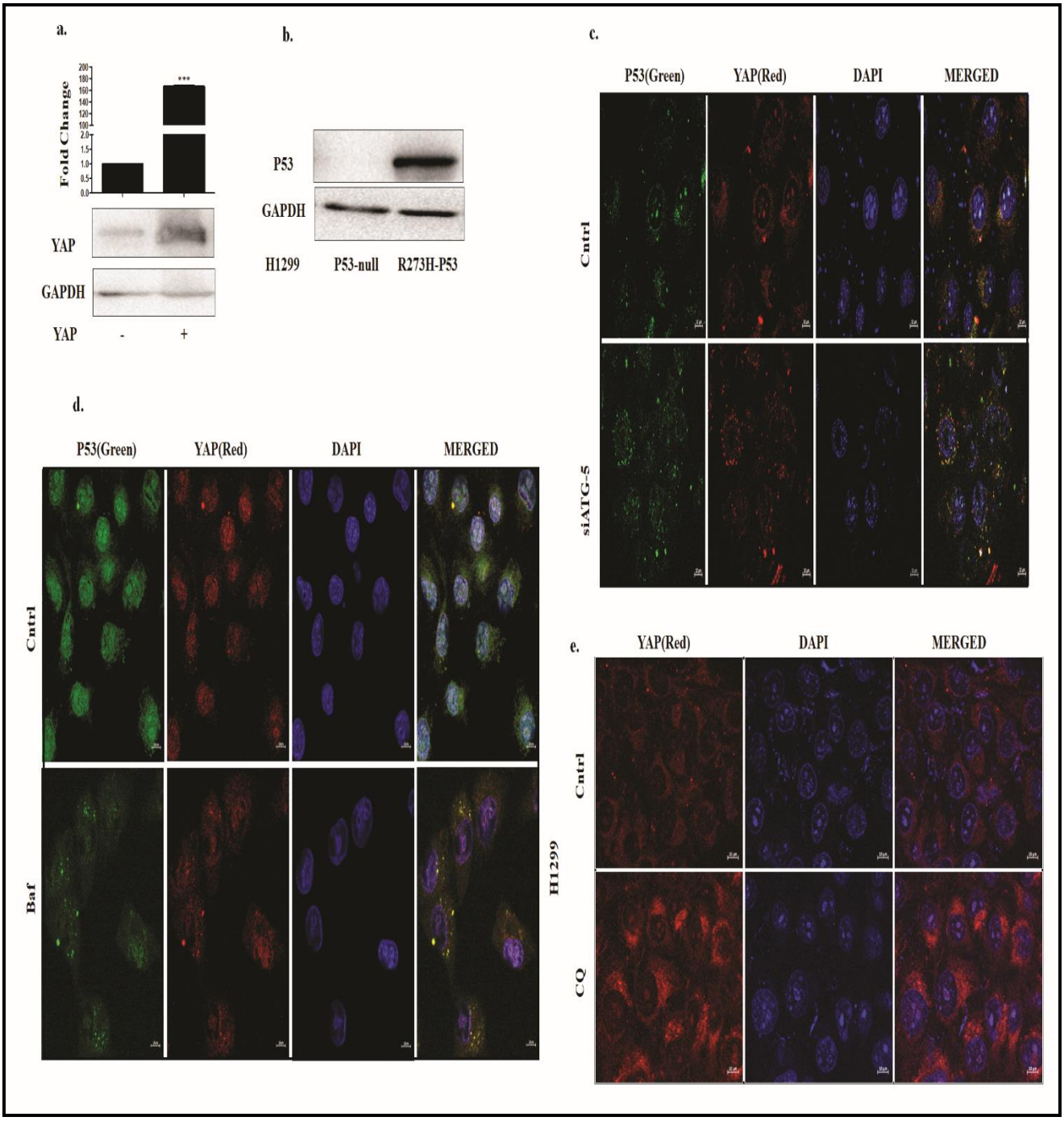

Supplementary Figure 4. a-b Immunoblots post overexpression of YAP and P53 in NSCLC cells. **c** Immunofluorescence image showing YAP and P53 localization 48 hour after si-ATG-5 transfection and **d** Baf treatment in R273H-P53 harboring H1299 cells. **e** Immunofluorescence image showing YAP localization post CQ treatment (50µM) for 48 hour in P53 null H1299 cells. Scale bar: 10 µm. Objective: Plan Apochromat 63x/1.40 oil M27.

Chapter-5

Verteporfin disrupts multiple steps of autophagy and induces gain of function mutant P53 oligomerization leading to cancer cell sensitization

5.1 Overview

Several reports suggest the connection between ubiquitin-proteasome system (UPS) and autophagy in cancer cell growth. Studies have demonstrated the dependence of UPS and autophagy mechanistically and functionally, and a blockage to one can lead to compensatory regulation of the other in a way that remains yet to be fully clarified [201]. Proteins like GOF-P53 critically regulate or are themselves get regulated by these protein homeostatic pathways. In previous chapters, we have established the importance of GOF-P53 mutations in cancer progression and explored the disruption of the protein homeostasis machinery and its impact on GOF-P53 harboring cancer cells. We have also established that a feedback regulatory loop exists between GOF-P53 and the potent transcription regulator YAP. Based on these connections, we planned to target GOF-P53 harboring cancer cells with an FDA-approved drug – Verteporfin (VP) which is known to inhibit autophagy by inducing oligomerization of proteins like P62 which plays a critical role in autophagy, and also has functional implications in UPS [263]; additionally, VP is known to inhibit YAP and its interaction with TEAD leading to inhibition of its transcriptional activity and subsequent proteasomal degradation of YAP [264].

The effect of VP was studied on GOF-P53 cells of two different origins, primarily Osteosarcoma (OS) and further its effects were validated in NSCLC cells as well. OS is an aggressive malignancy of the bone [265]; and interestingly, the overall frequency of P53 mutation in people with OS is as high as 22% [266]. Further, GOF mutations in P53 imposes an eminent problem in OS sensitization and remain a significant challenge to address [40]. Additionally, analysis of the existing literature indicates a plausible role of the cellular homeostatic process- autophagy in OS pathogenesis as well [222, 261, 267, 268]. For example, inhibition of autophagy, with the early autophagy inhibitor, 3-methyladenine (3-MA) was found to increase paclitaxel-induced apoptotic cell death [269]. In another study, an HSP90AA1 and HMGB1-mediated autophagy was found to induce drug resistance [267, 268]. Importantly, cumulative evidence indicates a probable pro-survival role of autophagy in OS cells. Since both autophagy and GOF-P53 are implicated in OS pathogenesis we included osteosarcoma as part of our analysis and apprehended that molecules that can modulate autophagy and can simultaneously neutralize GOF-P53 induced effects might be critical to successful therapy.

Herein, we analyzed differential gene expression data from the GEO database. Autophagy-associated processes were found to be highly dysregulated in OS. Subsequently, we re-purposed the FDA-approved drug, VP to inhibit autophagy and explore its potential in sensitizing GOF-R156P-P53 harboring OS cells and GOF-R273H-P53 harboring NSCLC cells. We observed that VP was

predominantly effective in disrupting multiple steps of autophagy and was cytotoxic to the cells. An enhanced cytotoxic effect was observed with the addition of a proteasomal inhibitor. VP also caused an accumulation of high molecular weight-P53 protein in both OS and NSCLC cells. Taken together, our study provides critical insights into effective sensitization of GOF-P53 harboring cells with VP and proteasomal inhibitor.

5.2 Results

5.2.1 Autophagy associated pathways are frequently dysregulated in cancer patients

In our previous chapters, we have shown the significance of autophagy in NSCLC progression. We have also validated its connection with other degradation pathways like UPS, and several cancers associated proteins including GOF-P53 and YAP. To further extend our understanding of autophagy playing a crucial role, we analyzed the gene expression data of OS patients, extracted from GEO. Our objective was to identify probable set of pathways that are maximally de-regulated, and controlled by significantly differentially expressed genes. As evident from **figure 5.2.1a**, functionally linked pathways like cellular autophagy, phagosome, lysosome, protein processing, and ribosome were amongst the significant deregulated pathways. **Figure 5.2.1a** represents some of the top pathways found to be deregulated, based on gene expression data. Furthermore, autophagy, endocytosis, and phagosome were found to harbor a high percentage of differentially expressed genes implicating their probable involvement in the disease **(Fig. 5.2.1b)**. Additionally, several supportive studies are also there that reveal the pro-survival role of autophagy in multiple cancers [222, 243, 261, 270]. The above evidences persuaded us to explore potential inhibitors of autophagy in regulating cell proliferation and GOF-P53 function.

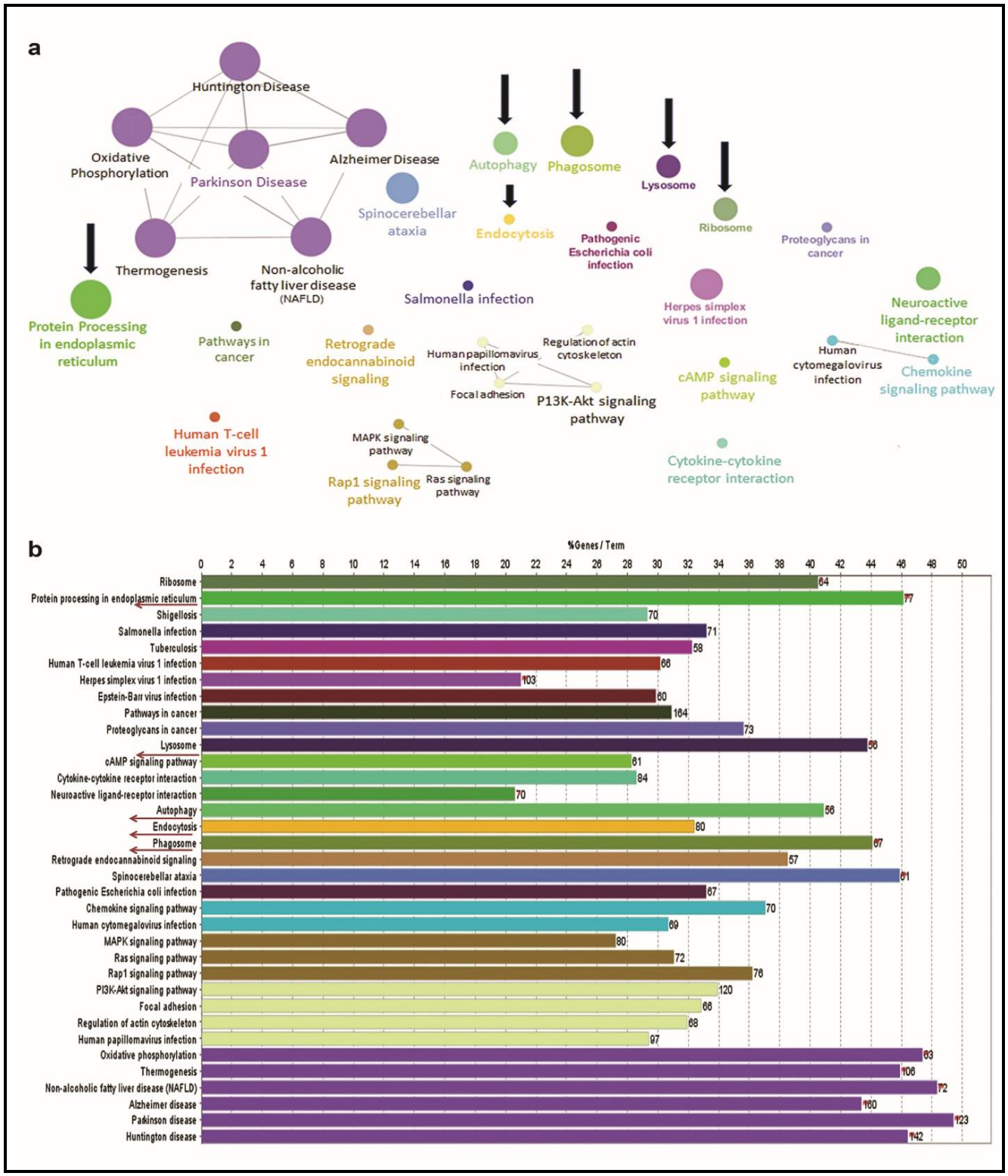

Figure 5.2.1. Autophagy-associated pathways are dysregulated in the cancer patients. a ClueGo pathway map showing majorly dysregulated pathways and their connections in OS patients. **b** Bar graph representing the number of genes in each dysregulated pathway in OS patients.

5.2.2 VP, repurposed for autophagy inhibitory role sensitizes GOF-P53 harboring cancer cells

We selected an FDA-approved drug VP, known to possess potent light-independent autophagy inhibitory functions [264]. Cells were exposed to different doses of VP (1, 5, and 10 µM) for a varied period (1, 6, 24, and 48 h) and cytotoxicity was analyzed. Interestingly, a dose and time-dependent cytotoxicity was observed with VP treatment in GOF-P53 harboring OS cells **(Fig. 5.2.2a)**. VP induced sensitization was also observed in NSCLC cells. We further performed a VP uptake analysis in HOS cells. As depicted in **figure 5.2.2b**, a consistent increase in uptake of VP was observed over time. We thereafter chose a 10 µM dose of VP for a period of 24 h for experiments in the rest of our study. Further, the investigation into molecular mechanisms leading to VP-induced cytotoxic effect showed a decrease in expression of the total caspase-3 protein **(Fig. 5.2.2c)**; an increase in caspase-3 activity **(Fig. 5.2.2d)**, and a down-regulation of mesenchymal markers, like, N-cadherin and Vimentin after VP treatment **(Fig. 5.2.2e)**.

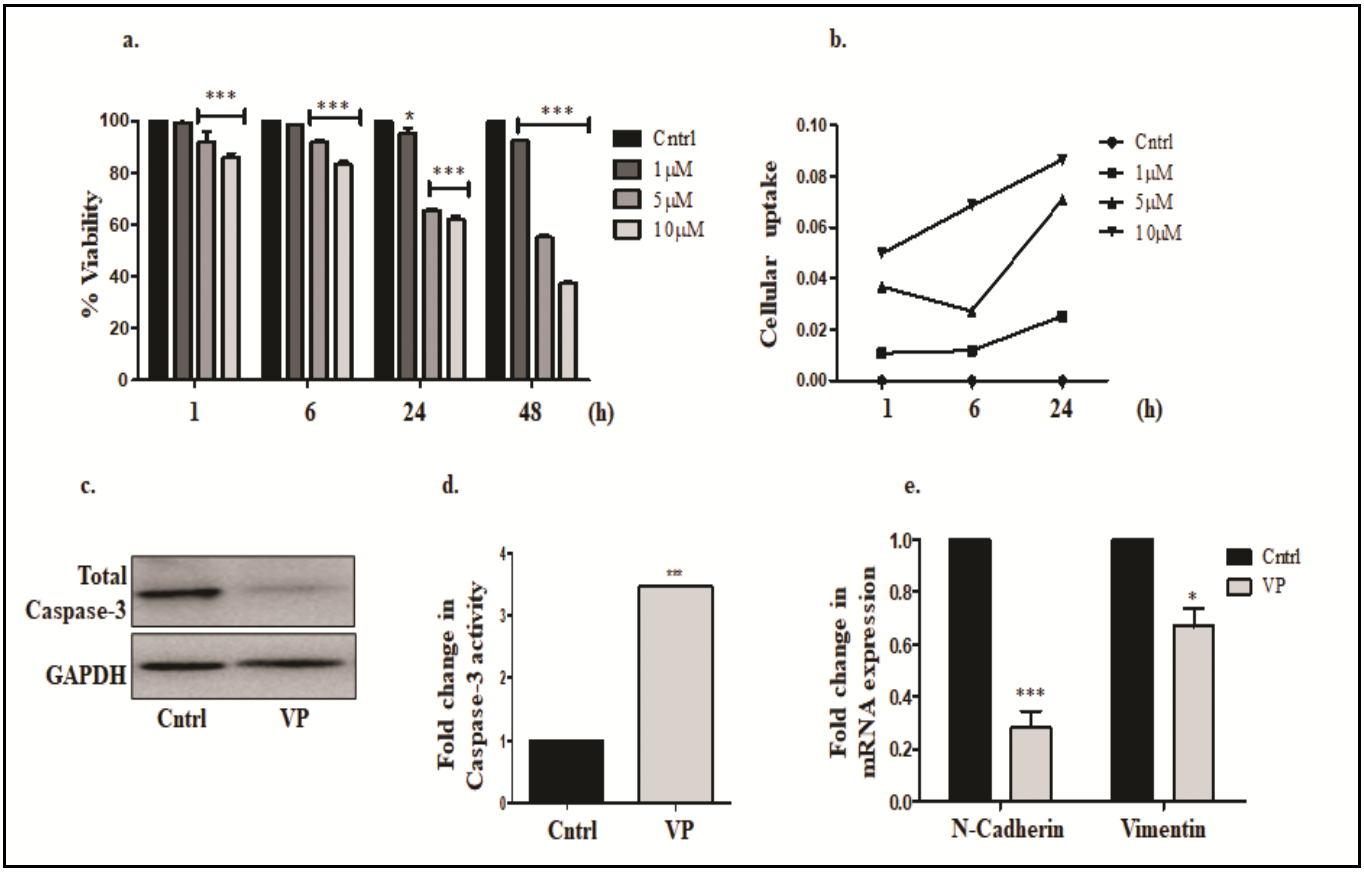

Figure 5.2.2. Effect of VP on GOF-P53 harboring cancer cells. **a** Cell viability analysis, measured through MTT assay upon exposure to VP. **b** Cellular uptake after exposure to VP for different time points. **c** Immunoblot showing expression of total caspase-3 after VP exposure (10 µM) for 24 h.

GAPDH is used as a loading control. **d** Fold change in caspase-3 enzyme activity after VP treatment (10 μM) for 24 h. Enzyme activity in untreated control is taken as '1'. **e** Gene expression of EMT markers was analyzed using RT-PCR after VP exposure (10 μM) for 24 h. Fold change is plotted taking gene expression of the untreated sample as '1'. '∗' indicates a significant difference compared to untreated cells.

5.2.3 VP disrupts both early and late autophagic processes

We thereafter investigated whether VP has the potential to modulate the cellular homeostatic process autophagy in OS cells. While VP is reported as an autophagy inhibitor, a detailed report exploring its effect on different steps involved in autophagy is least explored. VP-mediated inactivation of P62 protein is one of the most widely accepted effects on autophagy. Herein, we initially analyzed the expression of early autophagy markers required for the initiation of the autophagic process and extension of the phagophoric membranes. As evident in **figure 5.2.3a**, VP exposure showed a decrease in ATG-5 and Beclin-1 protein expression indicating disruption of early autophagic processes. We further analyzed the expression of LC3B-II. The level of lipidated form of LC3, popularly called LC3-II, is commonly used to monitor the number of autophagosomes present in a cell; LC3 is also required for autophagosome membrane expansion and fusion [271]. Importantly, the protein levels of LC3B-II decreased with VP treatment suggesting a probable reduction in autophagosome biogenesis after treatment **(Fig. 5.2.3b)**. Furthermore, P62 showed the formation of high molecular weight (HMW) band after VP treatment **(Fig. 5.2.3c)**. P62 binds to LC3-II and facilitates autophagic cargo degradation [272]; a loss of P62 function is often associated with ubiquitinated protein accumulation, impaired autophagic trafficking, and cell death [273]. Therefore, the HMW-P62 band, as observed after VP exposure, reflects compromised autophagy. Inhibition of autophagic vacuole formation after VP treatment was further confirmed using MDC staining. MDC is a fluorescent dye that preferentially accumulates in autophagic vacuoles [257]. The fluorometric analysis revealed a decreased MDC fluorescence after VP exposure indicating a probable diminished number of cellular vesicles **(Fig. 5.2.3d)**. On the contrary, CQ which is known to block autophagosome-lysosome fusion [157] showed an enhanced MDC fluorescence due to probable accumulation of vesicles and hence served as a positive control. Further, Rab7 protein, known to have an important role in autophagic vacuole maturation [138], showed a drastic decrease in expression after VP treatment, suggesting that VP regulates the expression of endosomal or autophagosomal trafficking markers as well **(Fig. 5.2.3e)**. To further confirm that VP inhibits autophagy and reduces autophagosome-lysosome fusion, cells were transfected with the GFP-LC3-

RFP vector, which helps to monitor autophagy [274]. Importantly, we didn't observe an increase in RFP fluorescence, indicating that VP inhibits autophagic flux **(Fig. 5.2.3f)**. All the above suggests that the VP has a disruptive effect on the overall autophagic process.

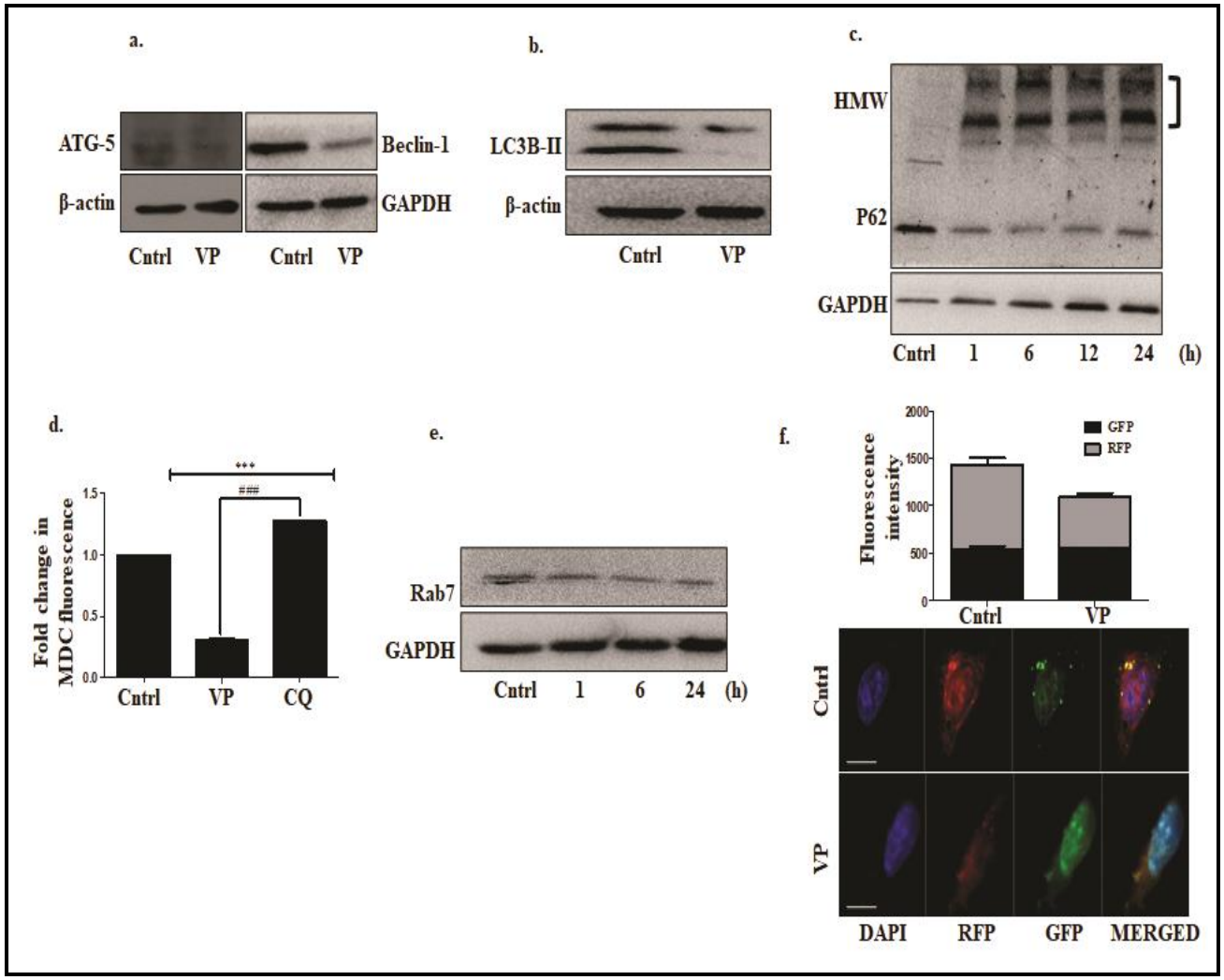

Figure 5.2.3. VP disrupts multiple steps of autophagy. **a, b** Immunoblots showing expression of ATG-5, Beclin-1 and LC3B-II after VP treatment for 24 h. **c** Immunoblot showing P62 protein expression after exposure to VP for different time points. The 'third bracket' represents the high molecular weight (HMW) band detected. **d** Fluorimetric analysis of MDC fluorescence in cells treated with VP or CQ (10 µM) for 24 h. **e** Immunoblot showing expression of Rab7 after VP exposure (10 µM). **f** GFP and RFP fluorescence intensity in cells transfected with GFP-RFP-LC3 vector followed by exposure to VP (10 µM) for 24 h. Scale bar: 10 µm. Objective: Plan Apochromat 63x/1.40 oil M27. '*' and '#' indicate the significant difference with respect to control and VP, respectively.

5.2.4 VP disrupts lysosomal stability

In the final step of autophagy, the cellular autophagic vesicles fuse with the lysosomes to degrade their contents. We observed that VP imparted a negative effect on the process of autophagy, however, its effect on the integrity of lysosomes was not known in this context. To analyze the same, we initially used the dye- acridine orange (AO), a lysosomotropic fluorochrome [275]. A flow cytometric analysis showed a decrease in red fluorescence after VP exposure, indicating disruption of lysosomal stability and probable lysosomal membrane permeabilization (LMP) **(Fig. 5.2.4a)**. Lysosomal membrane proteins, such as LAMP-1, are also indicative of lysosomal integrity [276]. Interestingly, as evident from **figure 5.2.4b**, a decrease in LAMP-1 protein expression was observed after VP treatment. Heat-shock proteins like HSP70 are reported to act as an endogenous inhibitor of lysosome-mediated cell death [277]. We also observed a decrease in HSP70 expression upon VP exposure **(Fig. 5.2.4c)**. Hydrolytic enzymes can leak out of lysosomes upon massive lysosomal breakdown, which in turn can lead to cellular stress [278]. Importantly, herein, a perturbation of lysosomal function was also associated with a noticeable increase in ROS, as measured through DCFDA assay **(Fig. 5.2.4d.i)**. Pre-treatment of cells with the ROS scavenger- N-acetyl cysteine (NAC), resulted in a substantial decrease in VP-induced cytotoxicity, suggesting a positive correlation between enhanced ROS and cell death **(Fig. 5.2.4d.ii)**. The assimilation of all the above results proposes VP to be a prototypical agent, with cytotoxic potential against OS, through inhibition of multiple steps involved in autophagy, including lysosomal de-stability; hence, its action is not just restricted to P62-HMW complex formation. CQ has often been found to enhance the cytotoxic effects of many chemotherapeutic agents [187]. It is known to inhibit the autophagosome-lysosome fusion process [157] leading to enhanced accumulation of vesicles, which often triggers cell death. Hence, we assumed that CQ might have an additive effect with VP and can be considered in combination for augmented benefit against OS. However, as shown in **figure 5.2.4e**, CQ and VP co-treatment showed no cumulative cytotoxic effect. Additionally, CQ either alone or in combination with VP had minimal effect on intracellular ROS levels at the dose studied further suggesting the ineffectiveness of this combination **(Fig. 5.2.4f)**. We assume that, since both the compounds inhibit autophagic flux, they did not manifest an additive effect. In addition, the fact that only CQ exposure, at the dose studied, did not impart a significant cytotoxicity in the HOS cells might have contributed to the observed ineffectual effect of the combination. We further checked for the difference in expression of the autophagic markers like, LC3B-II and P62 with VP plus CQ treatment, and in corroboration to the above results it failed to show a significant difference in expression compared to independent treatments **(Supplementary Fig. 5 a.i. and a.ii)**.

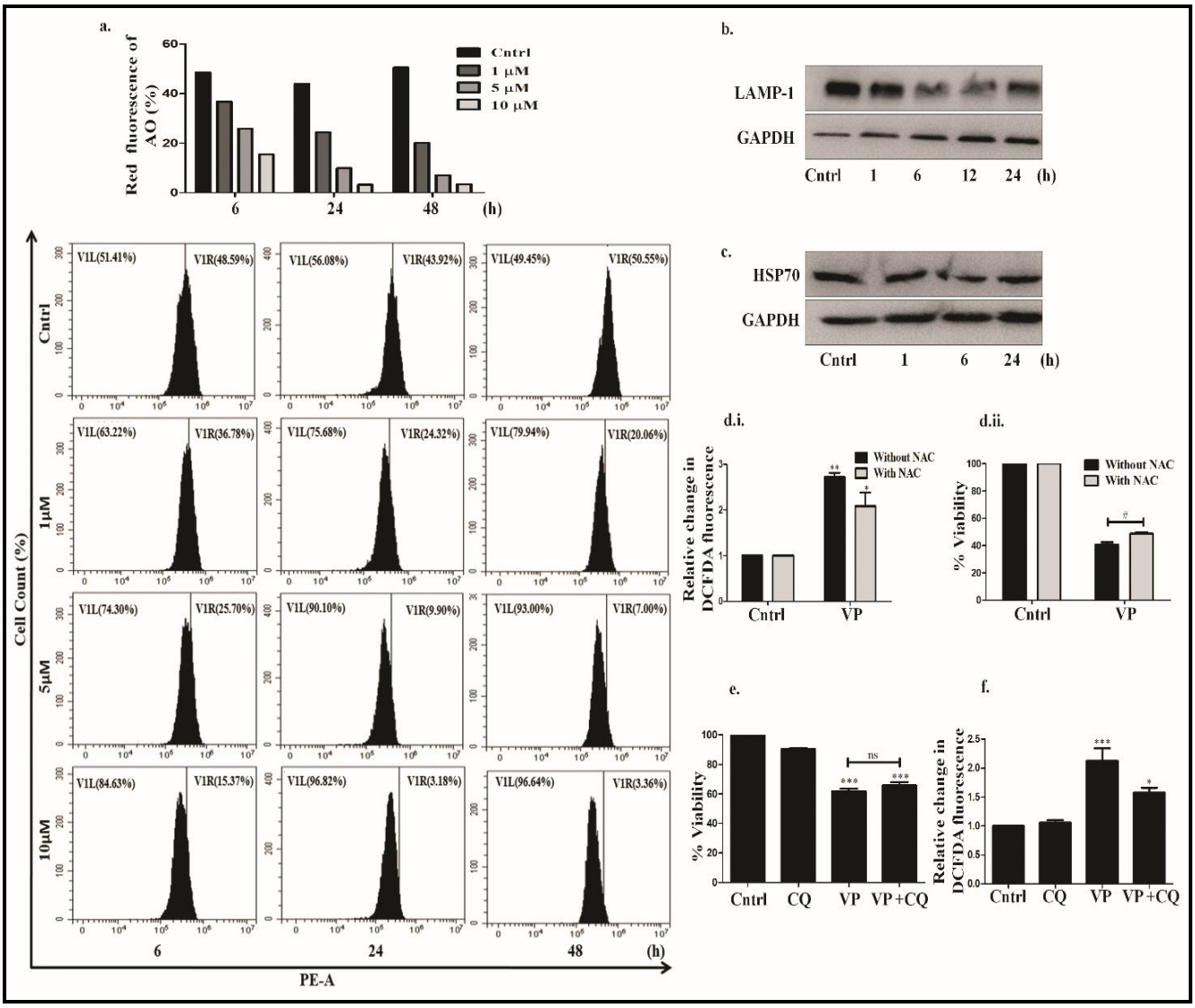

Figure 5.2.4. VP disrupts lysosomal stability. **a** Flow cytometric analysis representing a shift in AO fluorescence after VP treatment with respect to dose and time. **b, c** Immunoblots showing expression of LAMP-1 and HSP70 after VP exposure (10 µM). **d(i)** Bar graph representing fold change in intracellular ROS levels post-exposure to VP (10 µM) for 24 h as measured through DCFDA assay; **(ii)** MTT assay after 24 h of VP treatment, in presence or absence of NAC (20 mM). '#' indicates a significant difference compared to NAC treated cells. **e** MTT assay showing cell viability after treatment with CQ only (10 µM), or after VP (10 µM) plus CQ treatment for 24 h. CQ was added 1 h before VP treatment. **f** Fluorimetric analysis representing ROS levels in CQ only, or on VP plus CQ treatment. '*' indicates a significant difference compared to untreated control.

5.2.5 Proteasomal inhibitor enhances VP-induced cytotoxicity

While we were in search of a molecule that can enhance VP-induced effects, we came across existing literature that points towards the functional crosstalk existing between the cellular ubiquitin proteasomal degradation pathway (UPS) and autophagy that together maintains cellular proteostasis [215]. In this regard, autophagy impairment is known to hinder proteasomal substrate delivery due to excess accumulation of P62, thus compromising UPS function [138, 272]. This allowed us to apprehend that a simultaneous blocking of UPS alongside VP can further enhance VP-induced effects. Explicitly, with autophagy dysregulated and P62 forming HMW protein aggregate, the addition of a proteasomal inhibitor might further disrupt protein clearance leading to increased cytotoxicity. To explore a probable perturbation of protein homeostasis after VP exposure, we analyzed the formation of GFP-Ub punctae after VP treatment. As evident from **figure 5.2.5a**, an increase in green punctate dots was visible with VP exposure indicating Ub protein accumulation. We thereafter exposed cells to the proteasomal inhibitor- MG132 along with VP and analyzed RFP-Ub fluorescence microscopically. As expected, enhanced accumulation of RFP-Ub puncta was observed in cells treated with VP and MG compared to only VP exposure **(Fig. 5.2.5b)** showing an additive accumulation of Ub proteins. Additionally, ROS levels showed a significant elevation **(Fig. 5.2.5c.i)** along with a correlative increase in cytotoxicity in the combination treatment, as measured through MTT assay **(Fig. 5.2.5c.ii)**. Importantly, NAC reduced the cytotoxic effect suggesting a role of ROS in imparting the cytotoxic response in osteosarcoma cells **(Fig. 5.2.5c.ii)**. A similar cytotoxic effect was also observed when lung cancer cells- H1299 were exposed to VP and MG **(Supplementary Fig. 5b- d)**. An enhanced ROS and associated decreased cell viability were observed in the H1299 cells with different P53 protein status **(Supplementary Fig. 5b-d)**. Application of another proteasomal inhibitor- ALLN in combination with VP **(Supplementary Fig. 5e**) also showed an enhanced cytotoxic effect in HOS cells, compared to only VP or ALLN. To further confirm enhanced cytotoxicity with MG and VP treatment, we also measured the percentage of PI +ve cells after exposure to both the compounds. The PI dye is impermeable to live cells but stains dead cells; therefore, an increase in PI +ve cells, as observed, confirmed more cell death after combination treatment **(Fig. 5.2.5d)**. From the above experiments, it can be inferred that a proteasomal inhibitor increases VP-induced cellular stress leading to enhanced cell death.

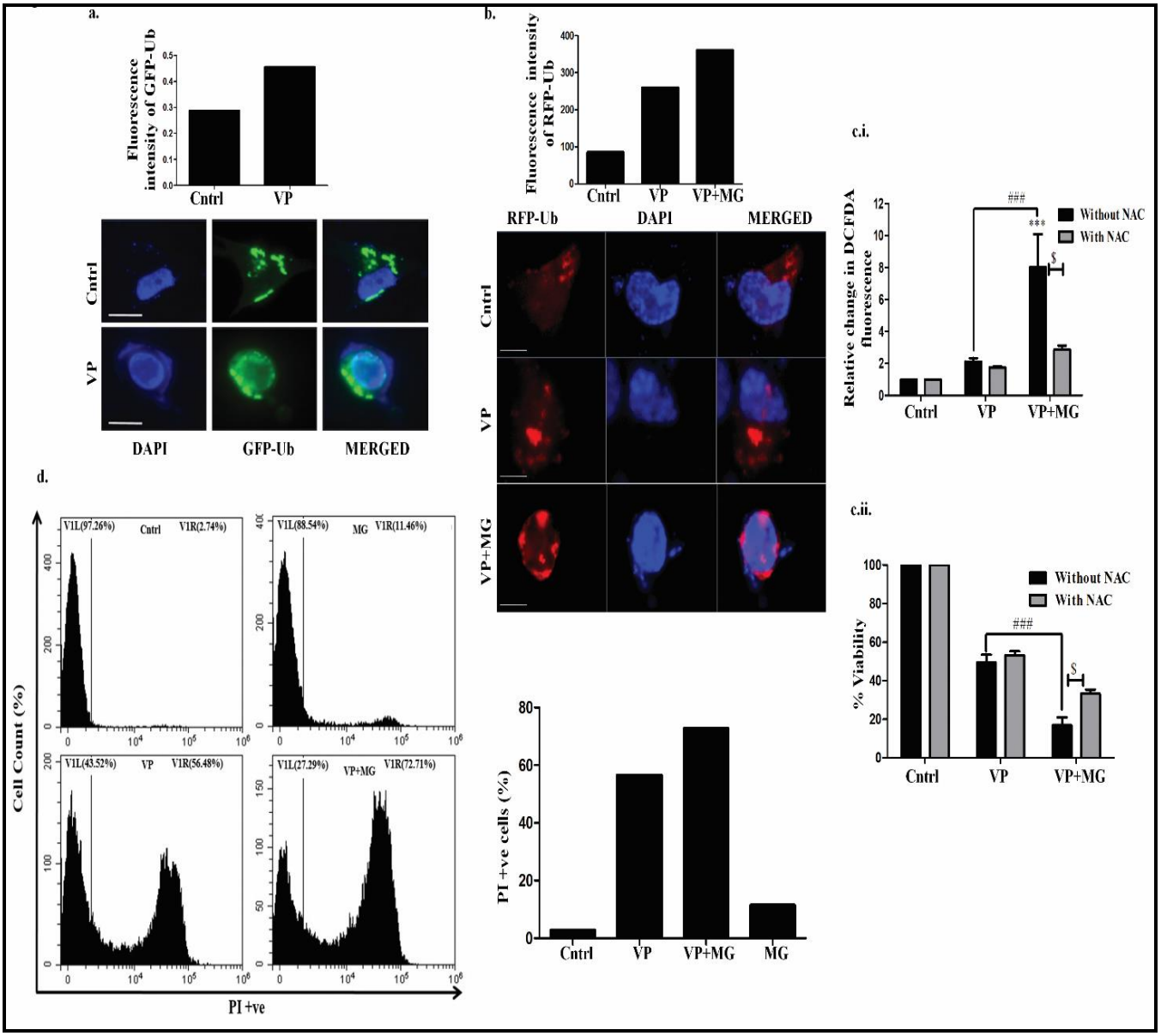

Figure 5.2.5. MG co-treatment enhances cytotoxicity in GOF-P53 cells. **a** Fluorescence microscopy showing GFP-Ub after VP exposure (10 µM) for 24 h. Scale bar: 100 µm. **b** Fluorescence microscopy showing RFP-Ub upon VP (10 µM) only, or VP and MG (0.5 µM) treatment for 24 h. **c (i)** Bar graph representing fold change in intracellular ROS levels post-exposure to VP only, or VP plus MG for 24 h. **(ii)** MTT assay analyzing cell viability after 24 h of VP or VP plus MG treatment in the presence or absence of NAC. '*', '#' and '$' indicate the significant difference with respect to control, VP with VP+MG, or between NAC+ and NAC− cells, respectively**. d** Flow cytometric analysis showing PI +ve cells after VP (10 µM) and/or VP plus MG (0.5 µM) treatment for 24 h

5.2.6 VP induces ROS-dependent HMW P53 band

As discussed earlier, mutations in P53 play a pivotal role in development of cancers like OS and NSCLC. We were therefore interested in investigating whether VP regulates the stability of the P53 protein. Interestingly, as shown in **figure 5.2.6 a.i-a.ii**., similar to what was observed for P62 protein, VP exposure at different doses or escalating time showed a HMW band in HOS cells when probed for P53 by immunoblot. To confirm the same, we performed immunofluorescence analysis of P53 protein in the HOS cells (harboring a GOF-mutant-P53) **(Fig. 5.2.6b.i)** [279] and also in H1299 P53 null NSCLC cells stably transfected with GOF-P53. Predominantly, cytoplasmic accumulation of green fluorescence of P53 protein was observed in both the cell types, more distinctly in the stably transfected P53 overexpressing cells **(Fig. 5.2.6b.ii)**. Thereafter, we analyzed HMW aggregate formation in the H1299 cells stably transfected with either empty vector (EV), or WT-P53, or GOF R273H-P53 after VP exposure. As expected, no HMW band was observed in the EV transfected cells, but importantly, cells stably transfected with wild-type or GOF-R273H-P53 showed a HMW band when probed for P53 **(Fig. 5.2.6c)**; however, the HMW band intensity was more for the GOF cell type, though HMW-P62 did not follow a similar trend. Interestingly, upon pull-down of P53 protein in VP-treated cells, P62 was not found to be co-immuno-precipitated, specifying that P53 and P62 proteins were not part of the same HMW complex in this study (data not shown). The HMW-protein band for P53 was also confirmed in two other cell types, MCF7 (WT-P53) and MDA-MB-468 (GOF-R273H-P53) **(Fig. 5.2.6d)** [280]. Earlier studies depict that protein oxidation by ROS can play a significant role in the formation of high molecular weight protein aggregates [281]. Therefore, to further understand whether the generation of ROS has a role in the VP-induced formation of HMW protein aggregates, we treated the cells with the ROS quencher- NAC. As evident from **figure. 5.2.6e**, a decrease in both VP-induced P62 and P53 HMW bands was observed with the addition of NAC, suggesting that ROS plays a critical role in HMW complex formation.

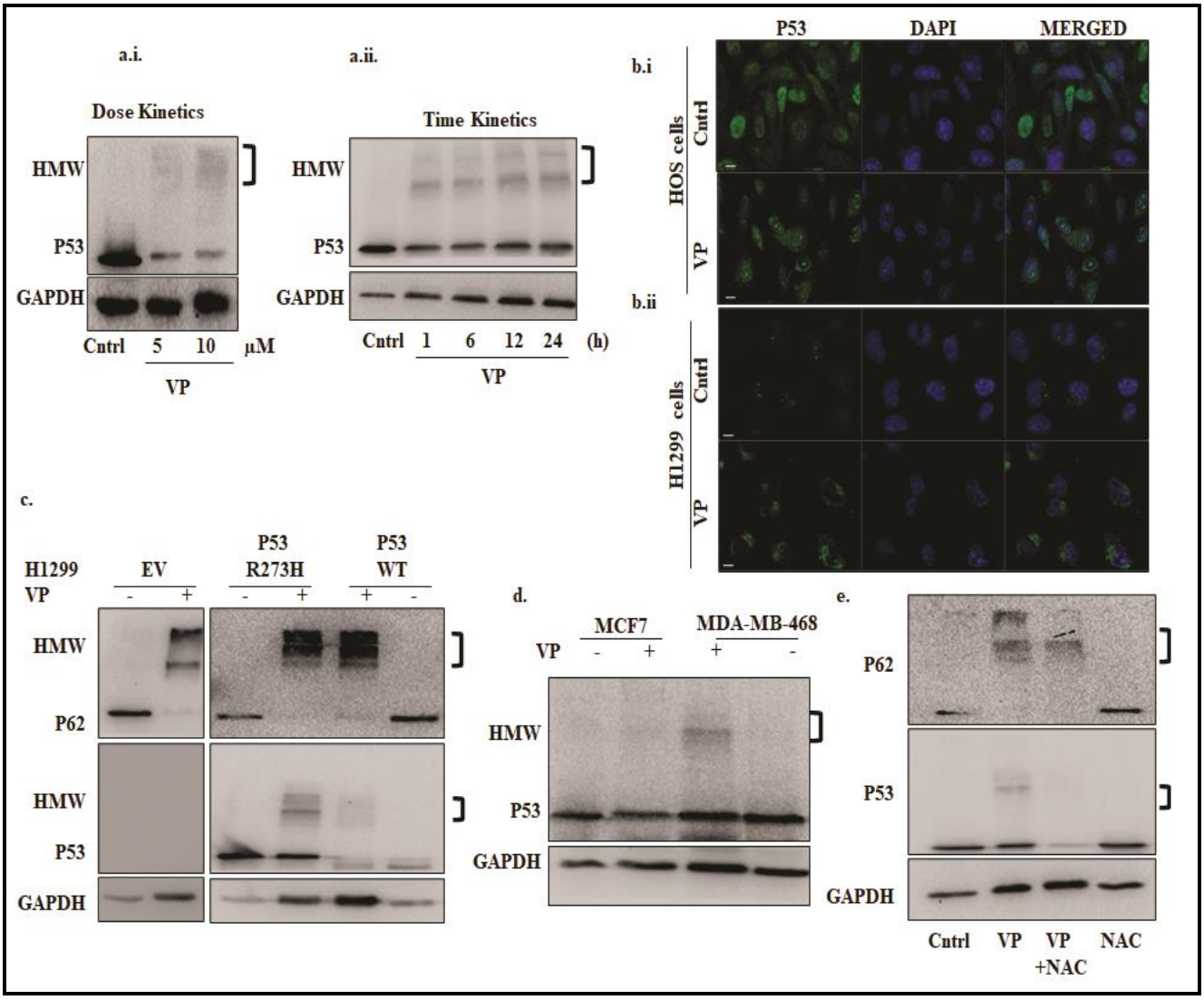

Figure 5.2.6. VP induces HMW band of P53. a(i-ii) Immunoblots showing P53 expression after VP treatment (10 μM) at different doses and different time points in HOS cells. **b(i)** Immunofluorescence images showing P53 protein upon VP exposure in HOS, and **b(ii)** H1299 cells stably transfected with GOF-R273H-P53 cells. Scale bar: 10 μm. Objective: Plan Apochromat 63x/1.40 oil M27. **c** Immunoblots showing P62 and P53 expression upon VP treatment in H1299 cells stable transfected with EV or GOF-R273H-P53 or WT-P53**. d** Immunoblots showing P53 expression after VP treatment in MCF-7 and MDA-MB-468 cells. **e** Immunoblots showing P62 and P53 expression upon VP treatment with or without NAC in HOS cells. The 'third bracket' indicates the high molecular weight (HMW) band detected.

5.2.7 MG co-treatment induces lysosomal targeting of selected proteins

There are existing studies that hint at an increase in the autophagic process after proteasomal inhibition [202, 282]. On a similar note, an increased LC3B-II protein level was observed in MG plus VP treated cells compared to only VP **(Fig. 5.2.7a)**. Simultaneously, an increase in red fluorescence of AO **(Supplementary Fig. 5f)** and TFEB protein expression was also seen in the combination treatment **(Fig. 5.2.7b)**; TFEB is reported to be involved in lysosomal biogenesis [283]. Collectively, these observations suggest that MG can partly salvage autophagy-like phenomena. Interestingly, as we further analyzed P62 and P53 protein expression in the combination treatment, we observed an intense HMW-P62 band in the presence of both MG and VP, compared to the only VP. However, in contrast, the P53-HMW protein did not show an increase in the combination treatment **(Fig. 5.2.7c.i and ii)**. Kaushik et al. in 2008, earlier reported that impairment of macroautophagy could lead to an accompanying activation of a special branch of autophagy, like, the chaperone-mediated autophagy (CMA) that can contribute to selective protein degradation [254]. Also, a recent study suggests that reduced macroautophagy can activate CMA leading to clearance of P53 [284]. During CMA, selected cytoplasmic proteins are recognized by chaperones and directed to lysosomes via lysosomal membrane-protein (LAMP-2A) [285]. As we analyzed protein expression, we found an increase in the expression of LAMP-2A in VP plus MG exposed cells **(Fig. 5.2.7d)**. Additionally, HSC70- an important CMA marker that recognizes specific KFERQ-like sequence motifs on CMA substrates also showed an increased expression in the combination treatment **(Fig. 5.2.7e)**. Importantly, P53 is reported to be a CMA substrate with a KFERQ motif [147]. Next, we analyzed co-localization of P53 with LTR; an increased co-localization of P53 with LTR was observed in VP plus MG-treated cells **(Fig. 5.2.7f.i)**. We then probed for P53 protein and observed its co-localization with LAMP-2A through immune-staining which also followed a similar pattern **(Fig. 5.2.7f.ii.)**. We hence propose that the combination of VP and MG targets P53, and not P62, to the lysosomes, possibly through a special branch of autophagy.

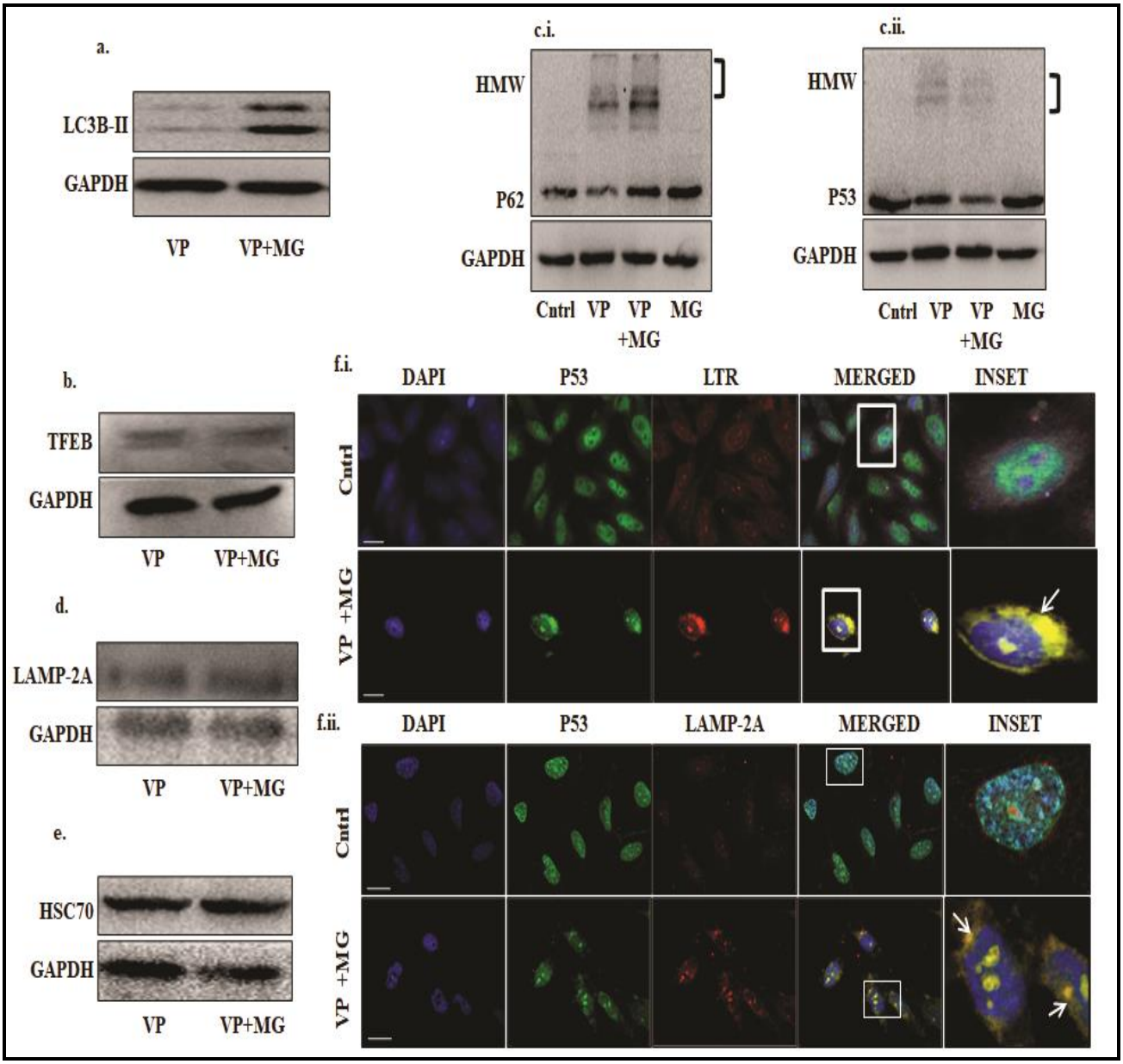

Figure 5.2.7. VP plus MG co-treatment targets P53 to lysosomes. Immunoblots showing **a** LC3B-II, **b** TFEB, **c(i)** P62, and **c(ii)** P53 expressions after VP (10 µM) or VP plus MG treatment for 24 h. The 'third bracket' represents an HMW band detected. **d** and **e** Immunoblots showing LAMP-2A and HSC70 expression after VP or VP plus MG treatment. **f(i)** Immunofluorescence image showing P53 (FITC-green) and Lysotracker-Red; **f(ii)** or P53 (FITC-green) and LAMP-2A (TRITC-red) post VP and MG treatment. The white arrow indicates co-localization. Scale bar: 10 µm. Objective: Plan Apochromat 63x/1.40 oil M27.

5.3 Discussion and conclusion

In this part of the study, we explored repurposing the FDA approved drug and widely accepted photosensitizer- verteporfin against tumor cells harboring GOF-P53. VP exposure resulted in a significant accumulation of ubiquitinated proteins coupled to P62 accumulation and associated autophagy inhibition. **Figure 5.3.1a-b** schematically represents the effect of VP on autophagy. Herein, previous studies report cross-linked HMW complex formation with VP, predominantly for P62 [281, 286]. We however observed that upon VP exposure, a HMW band is also observed when lysates are probed with an anti-P53 antibody in OS and NSCLC cells. A possible explanation for a P62-HMW complex formation with VP is often credited to the presence of the PB1 (Phox and Bem1p-1) domain with a scaffold-like grasping fold that might facilitate its homo- and hetero-oligomerization [281]. However, the P53 protein is not known to have a similar PB1 domain. It prompted us to explore any structural similarity existing between P53 and P62. However, amino acid alignment of P53 with P62 failed to reveal by far any particular shared sequence among them, which might contribute to its HMW complex formation. But it is important to mention here that, P53 protein is reported to be naturally 'sticky' and to undergo multiple oligomeric states and higher-order aggregates by virtue of its oligomerization domain [287]. Further, mutation in P53 protein can make them even more susceptible to oligomerization as it can facilitate interaction with other stabilizing proteins thus increasing their overall stability [57]. Here, we assume that VP most likely stimulates this already existing oligomerization potential resulting in HMW band formation; however, precise mechanisms involved in such phenomenon are required to be further explored. Importantly, we also identified that the average hydropathicity score of P62 is about 17% lower than that of P53, indicating that P62 protein is more hydrophobic than P53. Hence, we assume that P62 is more likely to show an enhanced oligomerized state than P53 [288]. Importantly, in our study, P53 was not found to be part of the P62-HMW aggregate; however, the HMW bands for both the proteins reduced with NAC suggesting a role of ROS in its formation, independent of the type of proteins oligomerized. In corroboration to above, Donohue et al. in 2014 showed HMW-P62 crosslinks to be formed resultant of ROS, especially singlet oxygen (1 O2) generated after VP treatment [281]. Furthermore, we observed that the P62-HMW protein band, but not P53 enhanced with the addition of a proteasomal inhibitor, MG. The proteasomal inhibitors are known to enhance a selective branch of autophagy, that is chaperone mediated autophagy (CMA) [289]; also, P53 is a probable substrate for CMA [147, 284]. In corroboration to above, we observed that P53 co-localized with LTR and with LAMP-2A upon VP plus MG exposure indicating a probable targeting to lysosomes. Furthermore, with autophagy inhibited by VP, we planned to explore whether inhibition of the other

intracellular protein turnover machinery, the UPS can aggravate cytotoxicity in the tumor cells. As expected, an increased cytotoxicity accompanied by enhanced ROS was observed with VP plus MG not only in OS cells studied but also in lung cancer cells, suggesting that it might not be a cell type dependent event. **Figure 5.3.1c** shows a schematic representation of effect of VP and MG.

To the best of our knowledge, we are the first to report VP-induced sensitization of cancer cells through inhibition of multiple steps of autophagy. Given the significant implication of autophagy in cancer, the strategy can have significant therapeutic implications. We also show that VP exposure results in HMW band formation for P53 protein. This is important in cancer therapy as mutant P53 is highly prevalent in OS and NSCLCs, which can hence be aggregated by VP, associated with cell sensitization. We also show that a proteasomal inhibitor- MG can enhance VP-mediated cytotoxicity. According to NCI's information on clinical trials, VP is re-purposed as a PDT drug for Phase II trials in multiple cancers. In addition, several reports portray VP to be a potent anti-cancer agent [290, 291]. Given our observations, further exploration of anti-cancer properties of VP can be promising from future therapeutic perspective.

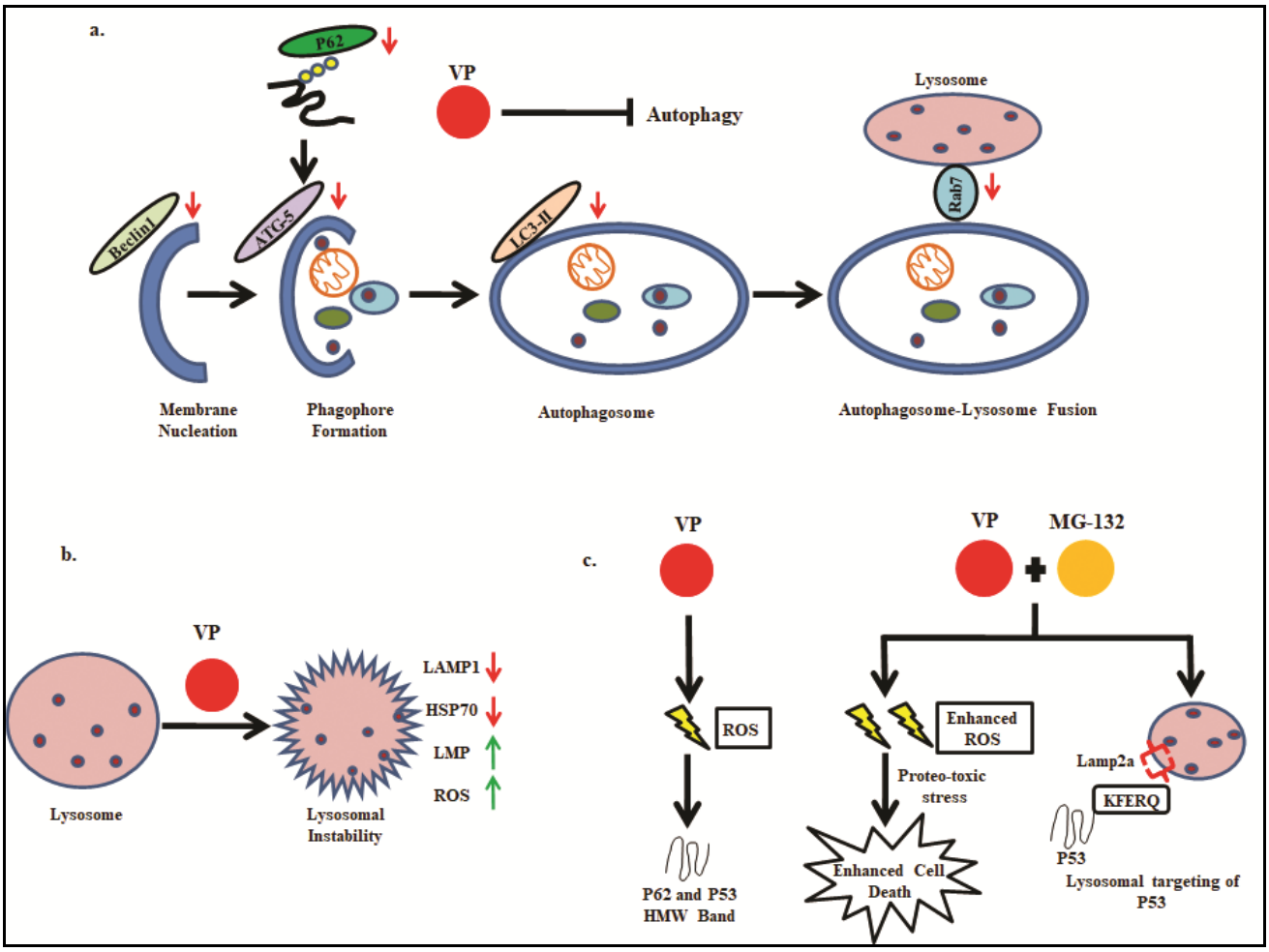

Figure 5.3.1. Schematic representation of VP-induced effects. a and b Effects of VP on the autophagic pathway in GOF-P53 cells. Down (↓) pointing red arrow and up (↑) pointing green arrow represents a down-regulation or up-regulation respectively after VP treatment. **c** The overall effect of VP and MG combination on GOF-P53 cells.

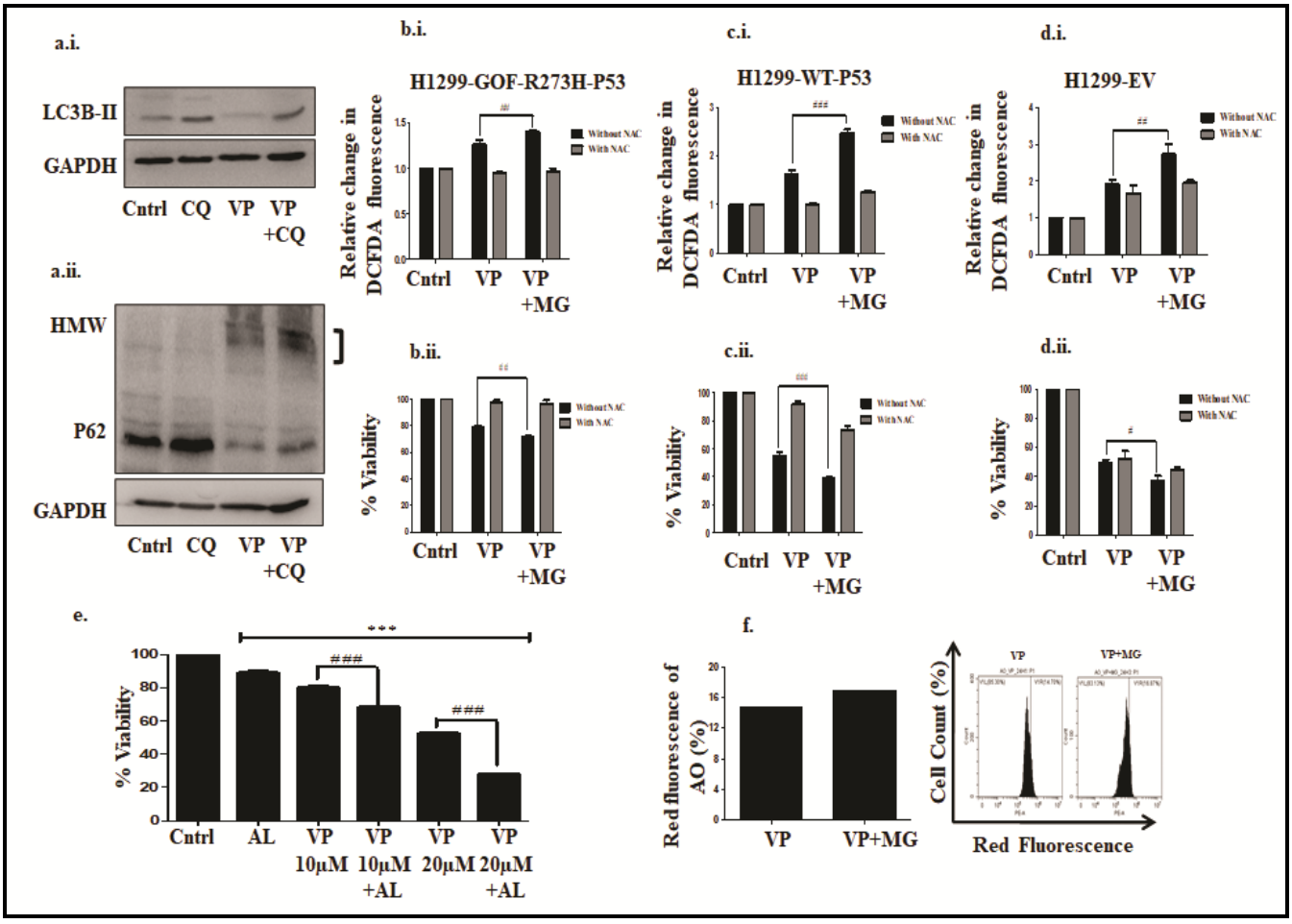

Supplementary Figure 5 a(i-ii) Immunoblots showing expression of LC3B-II and P62 upon VP (10 µM) and/or CQ (10 µM) treatment for 24 h in HOS cells. **b- d** Bar graph representing fold change in intracellular ROS levels, and MTT assay analyzing cell viability after 24 h of VP or VP plus MG treatment in the presence or absence of NAC in H1299- GOF-R273H-P53 **b(i-ii),** WT-P53 **c(i-ii.)** and EV **d(i-ii)** cells. '#' indicates a significant difference with respect to VP. **e** MTT assay showing cell viability after ALLN (10 µM) and/or VP (10 µM) treatment for 24 h in HOS cells. '*', '#' represents a significant difference with respect to untreated control and VP treated cells, respectively. **f** Flow cytometry images showing fluorescence of AO upon treatment with VP (10 µM) only or VP plus MG (0.5 µM) in HOS cells.

Chapter-6

Conclusion, limitations, and future prospects

6.1 Conclusion

With the advent of modern technologies, there has been progressive evolution of treatment options for multiple cancers, NSCLCs are no exception. However, despite significant advances in the therapeutic arsenal, the prognosis of cancer has improved marginally. Refractoriness to conventional and targeted chemotherapy still stands as a major hindrance. In this regard, we assumed that extensive exploration of the genomic data from cancer patients might provide valuable insights into unaccounted causative factors and may lead to alternative modes of approach towards therapy. As part of this study, we initially explored the publicly available patient databases for cancer and primarily analyzed the cancer with the highest mortality rate- NSCLCs. Interestingly, the tumor suppressor and the extensively studied p53 was identified to be the top mutated gene in NSCLC patients, and this was associated with poor patient survival. Interestingly a vast majority of p53 mutations in NSCLCs was found to be of missense type, with R273H being amongst the top nucleotide alterations. A vast majority of these mutations, including R273H can impart a 'gain of function' property to the mutant-P53 protein inclusive of its pro-tumorigenic role, hitherto absent in its wild-type form. The consideration of the importance of p53 status, the type of mutation, the site of the mutation, and its gain of function effects, if any thus represent a key factor to prognosis. Therefore, to understand the molecular effects imparted by GOF-P53 and design an appropriate therapeutic strategy, we prepared a stably transfected model of R273H-P53, WT-P53, and EV control in a P53 null NSCLC cell line, H1299; we also performed experiments in cancer cells harboring endogenous GOF-P53. Interestingly, the presence of R273H-P53 imparted comparative insensitivity to the first-line chemotherapeutic drugs not only in NSCLCs but also in the other cancer cell types establishing its role in therapy resistance.

Regulation of protein turnover has been used previously for the treatment of cancer. One of the conventional theories has been that, in particular types of cancer, where protein production is much higher than normal, primarily to meet their over-proliferative or secretary demand, inhibition of protein turnover can lead proteins to accumulate, eventually killing the tumor cell. We hypothesized that the fact that UPS control P53 protein turnover, and importantly GOF-P53 proteins are reported to have higher stability resulting in an increased half-life; this can open up possible therapeutic opportunity based on interference of protein degradation. We observed that proteasome inhibitors (PIs) induce cytotoxic stress in R273H cells primarily by virtue of over-accumulated protein response. It simultaneously induced a compensatory activation of the other cellular homeostatic and protein turnover process- autophagy. An increase in autophagy through serum starvation or rapamycin enhanced PI-induced cell death. In this context, autophagy induced by PI when enhanced was found to play a pro-death role through enhancement of cellular reactive oxygen

species (ROS) and *via* ERK signaling in the NSCLC cells. Though autophagy has been mostly discussed in the literature for its pro-survival role, herein we show its contrasting character and our results demonstrate a probable strategy of sensitizing R273H-P53 lung cancer cells.

Furthermore, to understand the transcriptomic alterations associated with GOF-P53, we extracted RNA sequencing and ChiP-seq data available over web source for H1299 cells transfected with R273H-P53. Further analysis revealed an increased expression of the potent transcription factor-TEAD1, the binding partner of YAP and its downstream targets, in R273H cells. Furthermore, we observed that the expression of the latter was correlated with poor survival of NSCLC patients. Importantly, inhibition of R273H-P53 and/or YAP resulted in reduced cell viability of NSCLC cells. Additionally, an *in vitro* analysis showed that a probable mutual feedback exists between R273H-P53 and YAP in GOF-P53 harboring cancer cells. Given the importance of these two proteins in overall tumor biology including NSCLCs, we were therefore interested in identifying a potent molecule that can hinder their activity. Herein, P53 and YAP can regulate or can be regulated by autophagy as well. We observed that the autophagy inhibitor, CQ induced a significant inhibition of proliferation coupled to growth arrest of the NSCLC cells. Importantly, CQ resulted in cytoplasmic accumulation of both GOF-P53 and YAP. The cytoplasmic co-localization of these proteins upon CQ exposure might be attributed to the non-dividing state of the CQ exposed cells. Importantly, a knockdown of an autophagy-associated gene, ATG-5, or pharmacological inhibition of autophagy through Bafilomycin failed to show such a pronounced effect as observed with CQ. This implied that the observed effect of CQ, at the stipulated dose and time can be because of its autophagy-independent role as well. However, a withdrawal of CQ from culture medium resulted in reversal of features characterized by decreased cytoplasmic accumulation of P53/YAP and reversal of non-dividing state suggesting a dynamic effect imparted by CQ. Overall, our data provides valuable insights into the critical effect that chloroquine might have on NSCLC cell proliferation through spatial regulation of YAP and GOF-P53 which might be relevant for consideration of a future treatment regimen.

Given the connection of UPS and autophagy in regulation of GOF-P53, and the success of modulation of these two pathways in sensitizing NSCLC cells, we further decided to explore the effectiveness of another FDA approved drug, verteporfin (VP) that is reported to inhibit autophagy as well. VP is known to impair the function of P62, a protein critical to autophagy, through induction of P62-high molecular weight (HMW) oligomerization complex. Importantly, we observed that VP disrupted not only autophagic flux but also multiple steps of autophagy. Further, VP treatment resulted in a ROS-dependent high molecular weight band formation, of not only P62, but of GOF-P53 protein as well. It was also associated with ROS dependent sensitization of the cancer cells. This

was observed in cells of various origin, extending from osteosarcoma to NSCLCs. Herein, a simultaneous addition of a proteasomal inhibitor (MG132), resulted in increased ROS and associated cytotoxicity, further enhancing VP induced cytotoxic effects. Also, the combinatorial treatment led to selective targeting of P53 to the lysosomes. In summary, our study provides critical insights into disruption of protein homeostasis-based strategies as an effective approach against GOF-mutant-P53 harboring tumor cells **(Fig. 6.1).**

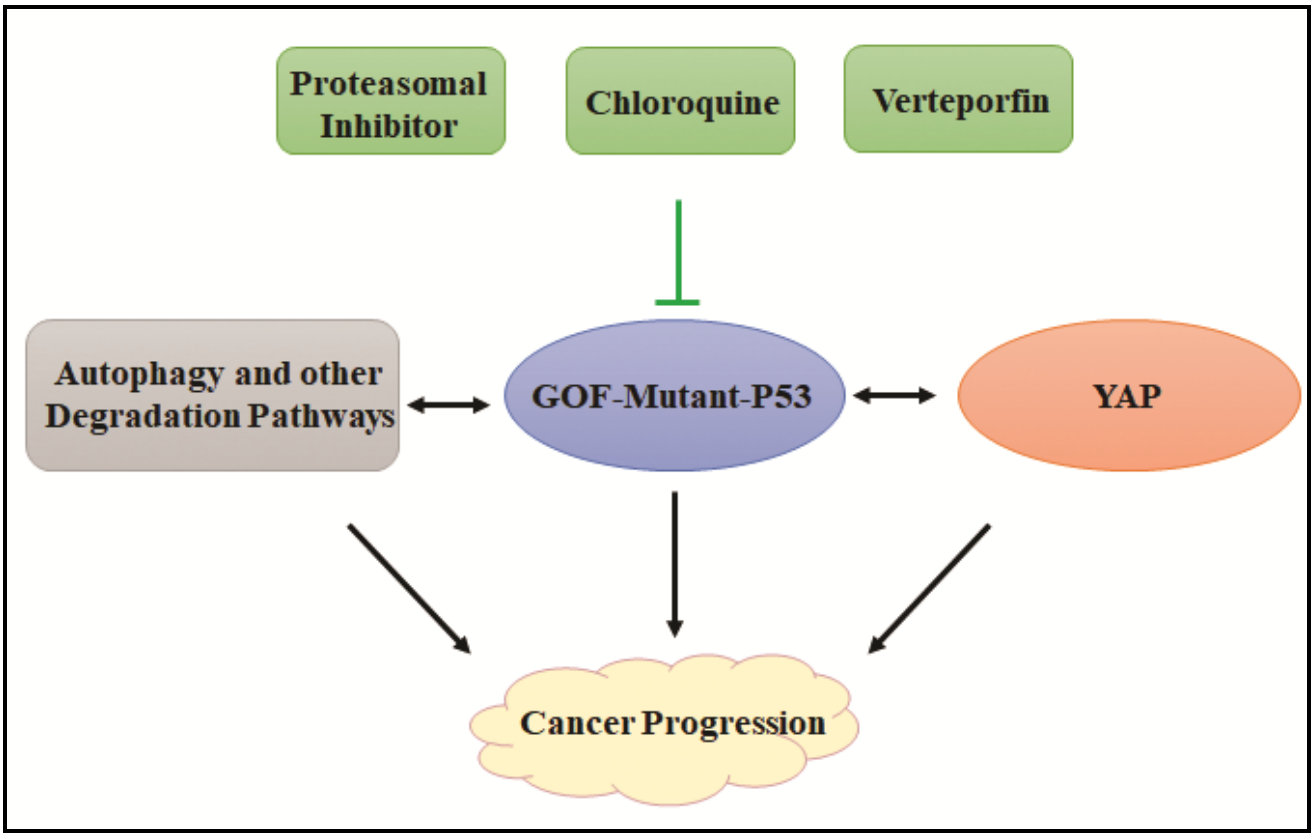

Figure 6.1. Schematic diagram highlighting major findings from the thesis.

6.2 Limitations and future prospects

1. The present study is restricted to *in vitro* analysis; however, further *in vivo* analysis is required to establish the therapeutic strategies proposed.
2. The majority of the current study is performed with respect to GOF-R273H-P53. The current study can be extended to other prevalent GOF mutant forms, like R175H, R248W etc.
3. Mutant P53 oligomerizes with VP exposure. It would be of keen interest to trace the proteins co-oligomerized with mutant P53 upon VP treatment. This finding would help in better understand the binding partners of mutant P53 and its effect on the regulation of cellular death program.
4. We discussed selective clearance of proteins or the involvement of chaperons in autophagy. However, further experimental clarifications are required to confirm the involvement of chaperone mediated autophagy.
5. We have observed CQ exposure results in a non-dividing cellular state. Recent literature suggests the existence of drug-tolerant persisters through adaptation of epigenetic strategies. The possible involvement of epigenetic regulation in this regard is still unknown.
6. Finally, how regulation of cytoskeletal dynamics results in cytoplasmic sequestration of GOF-P53 or YAP; the proteins involved in the transportation of YAP/GOF-P53 to the cytoplasm under the given condition; and any cytoplasmic role of the localized proteins requires further analysis.
7. GOF-P53 imparts resistance in cancer cell; does it vary with different dose of cisplatin is yet to be explored

References

1. Colotta, F., et al., *Cancer-related inflammation, the seventh hallmark of cancer: links to genetic instability*. 2009. **30**(7): p. 1073-1081.
2. Negrini, S., et al, *Genomic instability—an evolving hallmark of cancer.* 2010. **11**(3): p. 220-228.
3. Sung, H., et al., *Global cancer statistics 2020: GLOBOCAN estimates of incidence and mortality worldwide for 36 cancers in 185 countries.* CA Cancer J Clin, 2021.
4. Ferlay, J., et al., *Estimating the global cancer incidence and mortality in 2018: GLOBOCAN sources and methods.* 2019. **144**(8): p. 1941-1953.
5. Inamura, K.et al, *Lung cancer: understanding its molecular pathology and the 2015 WHO classification.* 2017. **7**: p. 193.
6. Cheng, L., et al., *Molecular pathology of lung cancer: key to personalized medicine.* 2012. **25**(3): p. 347-369.
7. Lane, D.P. and L.V.J.N. Crawford, *T antigen is bound to a host protein in SY40-transformed cells.* 1979. **278**(5701): p. 261-263.
8. Linzer, D.I. and A.J.J.C. Levine, *Characterization of a 54K dalton cellular SV40 tumor antigen present in SV40-transformed cells and uninfected embryonal carcinoma cells.* 1979. **17**(1): p. 43-52.
9. DeLeo, A.B., et al., *Detection of a transformation-related antigen in chemically induced sarcomas and other transformed cells of the mouse.* 1979. **76**(5): p. 2420-2424.
10. Rotter, V. et al., *p53, a transformation-related cellular-encoded protein, can be used as a biochemical marker for the detection of primary mouse tumor cells.* 1983. **80**(9): p. 2613-2617.
11. Levine, A.J. et al., *The first 30 years of p53: growing ever more complex.* 2009. **9**(10): p. 749-758.
12. Hinds, P., et al., *Mutation is required to activate the p53 gene for cooperation with the ras oncogene and transformation.* 1989. **63**(2): p. 739-746.
13. Hinds, P.W., et al., *Mutant p53 DNA clones from human colon carcinomas cooperate with ras in transforming primary rat cells: a comparison of the" hot spot" mutant phenotypes.* 1990. **1**(12): p. 571-580.
14. Finlay, C.A., P.W. Hinds, and A.J.J.C. Levine, *The p53 proto-oncogene can act as a suppressor of transformation.* 1989. **57**(7): p. 1083-1093.
15. Soussi, T., et al., *Cloning and characterization of a cDNA from Xenopus laevis coding for a protein homologous to human and murine p53.* 1987. **1**(1): p. 71-78.
16. Candau, R., et al., *Two tandem and independent sub-activation domains in the amino terminus of p53 require the adaptor complex for activity.* 1997. **15**(7): p. 807-816.
17. El-Deiry, W.S., et al., *Definition of a consensus binding site for p53.* 1992. **1**(1): p. 45-49.
18. Funk, W.D., et al., *A transcriptionally active DNA-binding site for human p53 protein complexes.* 1992. **12**(6): p. 2866-2871.
19. Petitjean, A., et al., *TP53 mutations in human cancers: functional selection and impact on cancer prognosis and outcomes.* Oncogene, 2007. **26**(15): p. 2157-2165.
20. Chene, P.J.O., *The role of tetramerization in p53 function.* 2001. **20**(21): p. 2611-2617.
21. Pluquet, O. and P.J.C.l. Hainaut, *Genotoxic and non-genotoxic pathways of p53 induction.* 2001. **174**(1): p. 1-15.
22. Shieh, S.-Y., et al., *DNA damage-induced phosphorylation of p53 alleviates inhibition by MDM2.* 1997. **91**(3): p. 325-334.
23. Pomerantz, J., et al., *The Ink4a tumor suppressor gene product, p19Arf, interacts with MDM2 and neutralizes MDM2's inhibition of p53.* 1998. **92**(6): p. 713-723.
24. Laptenko, O., et al., *Transcriptional regulation by p53: one protein, many possibilities.* 2006. **13**(6): p. 951-961.
25. Harper, J.W., et al., *The p21 Cdk-interacting protein Cip1 is a potent inhibitor of G1 cyclin-dependent kinases.* 1993. **75**(4): p. 805-816.
26. Wang, X.W., et al., *GADD45 induction of a G2/M cell cycle checkpoint.* 1999. **96**(7): p. 3706-3711.
27. Gallagher, W. and R.J.A.o.o. Brown, *p53-oriented cancer therapies: current progress.* 1999. **10**(2): p. 139-150.
28. Cadwell, C. and G.P.J.G. Zambetti, *The effects of wild-type p53 tumor suppressor activity and mutant p53 gain-of-function on cell growth.* 2001. **277**(1-2): p. 15-30.
29. Harms, K., et al., *The common and distinct target genes of the p53 family transcription factors.* 2004. **61**(7): p. 822-842.

30. Oren, M. and V. Rotter, *Mutant p53 gain-of-function in cancer.* 2010. **2**(2): p. a001107.
31. Soussi, T. and G. Lozano, *p53 mutation heterogeneity in cancer.* Biochemical and biophysical research communications, 2005. **331**(3): p. 834-842.
32. Sigal, A. and V. Rotter, *Oncogenic mutations of the p53 tumor suppressor: the demons of the guardian of the genome.* Cancer research, 2000. **60**(24): p. 6788-6793.
33. Weisz, L., M. Oren, and V.J.O. Rotter, *Transcription regulation by mutant p53.* 2007. **26**(15): p. 2202-2211.
34. Gualberto, A., et al., *An oncogenic form of p53 confers a dominant, gain-of-function phenotype that disrupts spindle checkpoint control.* 1998. **95**(9): p. 5166-5171.
35. Talos, F., et al., *p73 suppresses polyploidy and aneuploidy in the absence of functional p53.* 2007. **27**(4): p. 647-659.
36. Song, H., M. Hollstein, and Y. Xu, *p53 gain-of-function cancer mutants induce genetic instability by inactivating ATM.* Nature cell biology, 2007. **9**(5): p. 573.
37. Tsang, W.p., et al., *p53-R175H mutant gains new function in regulation of doxorubicin-induced apoptosis.* 2005. **114**(3): p. 331-336.
38. Deb, S. et al., *Tumor-derived p53 mutants induce NF-kappaB2 gene expression.* 2005.
39. de la Vega, et al., *NRF2 and the hallmarks of cancer.* 2018. **34**(1): p. 21-43.
40. Wong, R.P.C., et al., *p53-R273H gains new function in induction of drug resistance through down-regulation of procaspase-3.* Molecular cancer therapeutics, 2007. **6**(3): p. 1054-1061.
41. Chee, J.L., et al., *Wild-type and mutant p53 mediate cisplatin resistance through interaction and inhibition of active caspase-9.* 2013. **12**(2): p. 278-288.
42. Liu, K., et al., *TopBP1 mediates mutant p53 gain of function through NF-Y and p63/p73.* 2011. **31**(22): p. 4464-4481.
43. Olivos, D.J., et al., *Emerging non-canonical functions and regulation by p53: p53 and stemness.* 2016. **17**(12): p. 1982.
44. Masciarelli, S., et al., *Gain-of-function mutant p53 downregulates miR-223 contributing to chemoresistance of cultured tumor cells.* 2014. **33**(12): p. 1601-1608.
45. Dong, P., et al., *Mutant p53 gain-of-function induces epithelial–mesenchymal transition through modulation of the miR-130b–ZEB1 axis.* 2013. **32**(27): p. 3286-3295.
46. Wang, S.-P., et al., *p53 controls cancer cell invasion by inducing the MDM2-mediated degradation of Slug.* 2009. **11**(6): p. 694-704.
47. Kogan-Sakin, I., et al., *Mutant p53 R175H upregulates Twist1 expression and promotes epithelial–mesenchymal transition in immortalized prostate cells.* 2011. **18**(2): p. 271-281.
48. Di Agostino, S., et al., *Gain of function of mutant p53: the mutant p53/NF-Y protein complex reveals an aberrant transcriptional mechanism of cell cycle regulation.* 2006. **10**(3): p. 191-202.
49. Di Agostino, S., et al., *YAP enhances the pro-proliferative transcriptional activity of mutant p53 proteins.* 2016. **17**(2): p. 188-201.
50. Verduci, L., et al., *The oncogenic role of circPVT1 in head and neck squamous cell carcinoma is mediated through the mutant p53/YAP/TEAD transcription-competent complex.* 2017. **18**(1): p. 1-24.
51. Zhu, J., et al., *Gain-of-function p53 mutants co-opt chromatin pathways to drive cancer growth.* 2015. **525**(7568): p. 206-211.
52. Wang, W., et al., *Mutant p53-R273H gains new function in sustained activation of EGFR signaling via suppressing miR-27a expression.* 2013. **4**(4): p. e574-e574.
53. Strano, S., et al., *Mutant p53: an oncogenic transcription factor.* 2007. **26**(15): p. 2212-2219.
54. Midgley, C.A. and D.P. Lane, *p53 protein stability in tumour cells is not determined by mutation but is dependent on Mdm2 binding.* Oncogene, 1997. **15**(10): p. 1179.
55. Lukashchuk, N., et al., *Ubiquitination and degradation of mutant p53.* 2007. **27**(23): p. 8284-8295.
56. Whitesell, L., et al., *The physical association of multiple molecular chaperone proteins with mutant p53 is altered by geldanamycin, an hsp90-binding agent.* 1998. **18**(3): p. 1517-1524.
57. Li, D., N.D. Marchenko, and U.M. Moll, *SAHA shows preferential cytotoxicity in mutant p53 cancer cells by destabilizing mutant p53 through inhibition of the HDAC6-Hsp90 chaperone axis.* Cell Death & Differentiation, 2011. **18**(12): p. 1904-1913.
58. Wiech, M., et al., *Molecular mechanism of mutant p53 stabilization: the role of HSP70 and MDM2.* 2012. **7**(12): p. e51426.

59. Chen, Y., et al., *Hot-spot p53 mutants interact specifically with two cellular proteins during progression of the cell cycle.* 1994. **14**(10): p. 6764-6772.
60. Gallagher, W.M., et al., *MBP1: a novel mutant p53-specific protein partner with oncogenic properties.* 1999. **18**(24): p. 3608-3616.
61. Haupt, S., et al., *Promyelocytic leukemia protein is required for gain of function by mutant p53.* 2009. **69**(11): p. 4818-4826.
62. Girardini, J.E., et al., *A Pin1/mutant p53 axis promotes aggressiveness in breast cancer.* 2011. **20**(1): p. 79-91.
63. Chicas, A., et al., *Mutant p53 forms a complex with Sp1 on HIV-LTR DNA.* 2000. **279**(2): p. 383-390.
64. Walerych, D., et al., *Proteasome machinery is instrumental in a common gain-of-function program of the p53 missense mutants in cancer.* 2016. **18**(8): p. 897-909.
65. Huang, X., et al., *A novel PTEN/mutant p53/c-Myc/Bcl-XL axis mediates context-dependent oncogenic effects of PTEN with implications for cancer prognosis and therapy.* 2013. **15**(8): p. 952-965.
66. Do, P.M., et al., *Mutant p53 cooperates with ETS2 to promote etoposide resistance.* 2012. **26**(8): p. 830-845.
67. Marin, M.C., et al., *A common polymorphism acts as an intragenic modifier of mutant p53 behaviour.* 2000. **25**(1): p. 47-54.
68. Dell'Orso, S., et al., *ChIP-on-chip analysis of in vivo mutant p53 binding to selected gene promoters.* 2011. **15**(5): p. 305-312.
69. Hwang, C., et al., *Wild-type p53 controls cell motility and invasion by dual regulation of MET expression.* 2011. **108**(34): p. 14240-14245.
70. Vaughan, C.A., et al., *Preferred binding of gain-of-function mutant p53 to bidirectional promoters with coordinated binding of ETS1 and GABPA to multiple binding sites.* 2014. **5**(2): p. 417.
71. Milner, J. and E.J.C. Medcalf, *Cotranslation of activated mutant p53 with wild type drives the wild-type p53 protein into the mutant conformation.* 1991. **65**(5): p. 765-774.
72. Pfister, N.T., et al., *Mutant p53 cooperates with the SWI/SNF chromatin remodeling complex to regulate VEGFR2 in breast cancer cells.* 2015. **29**(12): p. 1298-1315.
73. Vogiatzi, F., et al., *Mutant p53 promotes tumor progression and metastasis by the endoplasmic reticulum UDPase ENTPD5.* 2016. **113**(52): p. E8433-E8442.
74. Strano, S., et al., *Physical interaction with human tumor-derived p53 mutants inhibits p63 activities.* 2002. **277**(21): p. 18817-18826.
75. Freed-Pastor, et al., *Mutant p53: one name, many proteins.* 2012. **26**(12): p. 1268-1286.
76. Sampath, J., et al., *Mutant p53 cooperates with ETS and selectively up-regulates human MDR1 not MRP1.* 2001. **276**(42): p. 39359-39367.
77. Bossi, G., et al., *Conditional RNA interference in vivo to study mutant p53 oncogenic gain of function on tumor malignancy.* 2008. **7**(12): p. 1870-1879.
78. Frazier, M.W., et al., *Activation of c-myc gene expression by tumor-derived p53 mutants requires a discrete C-terminal domain.* 1998. **18**(7): p. 3735-3743.
79. Ludes-Meyers, J.H., et al., *Transcriptional activation of the human epidermal growth factor receptor promoter by human p53.* 1996. **16**(11): p. 6009-6019.
80. Freed-Pastor, W.A., et al., *Mutant p53 disrupts mammary tissue architecture via the mevalonate pathway.* 2012. **148**(1-2): p. 244-258.
81. Buganim, Y., et al., *p53 Regulates the Ras circuit to inhibit the expression of a cancer-related gene signature by various molecular pathways.* 2010. **70**(6): p. 2274-2284.
82. Fontemaggi, G., et al., *The execution of the transcriptional axis mutant p53, E2F1 and ID4 promotes tumor neo-angiogenesis.* 2009. **16**(10): p. 1086.
83. Zhao, B., et al., *Cell detachment activates the Hippo pathway via cytoskeleton reorganization to induce anoikis.* 2012. **26**(1): p. 54-68.
84. Pan, D.J.D.c., *The hippo signaling pathway in development and cancer.* 2010. **19**(4): p. 491-505.
85. Varelas, X., et al., *The Crumbs complex couples cell density sensing to Hippo-dependent control of the TGF-β-SMAD pathway.* 2010. **19**(6): p. 831-844.
86. Bai, N., et al., *Yes-associated protein (YAP) increases chemosensitivity of hepatocellular carcinoma cells by modulation of p53.* 2013. **14**(6): p. 511-520.
87. Matallanas, D., et al., *RASSF1A elicits apoptosis through an MST2 pathway directing proapoptotic transcription by the p73 tumor suppressor protein.* 2007. **27**(6): p. 962-975.

88. Zhao, B., et al., *TEAD mediates YAP-dependent gene induction and growth control.* 2008. **22**(14): p. 1962-1971.
89. Zhang, J., et al., *YAP-dependent induction of amphiregulin identifies a non-cell-autonomous component of the Hippo pathway.* 2009. **11**(12): p. 1444-1450.
90. Gibault, F., et al., *Molecular features of the YAP inhibitor verteporfin: synthesis of hexasubstituted dipyrrins as potential inhibitors of YAP/TAZ, the downstream effectors of the Hippo pathway.* 2017. **12**(12): p. 954-961.
91. Xu, M., et al., *AXL receptor kinase is a mediator of YAP-dependent oncogenic functions in hepatocellular carcinoma.* 2011. **30**(10): p. 1229-1240.
92. Zhu, C., et al., *The regulation and function of YAP transcription co-activator.* 2015. **47**(1): p. 16-28.
93. Dupont, S., et al., *Role of YAP/TAZ in mechanotransduction.* 2011. **474**(7350): p. 179-183.
94. Meinhardt, G., et al., *Pivotal role of the transcriptional co-activator YAP in trophoblast stemness of the developing human placenta.* 2020. **117**(24): p. 13562-13570.
95. Dai, Y., et al., *YAP1 regulates ABCG2 and cancer cell side population in human lung cancer cells.* 2017. **8**(3): p. 4096.
96. Xia, Y., et al., *YAP/TEAD co-activator regulated pluripotency and chemoresistance in ovarian cancer initiated cells.* 2014. **9**(11): p. e109575.
97. Song, S., et al., *The Hippo coactivator YAP1 mediates EGFR overexpression and confers chemoresistance in esophageal cancer.* 2015. **21**(11): p. 2580-2590.
98. Yuan, Y., et al., *YAP overexpression promotes the epithelial-mesenchymal transition and chemoresistance in pancreatic cancer cells.* 2016. **13**(1): p. 237-242.
99. Dai, X.-Y., et al., *Nuclear translocation and activation of YAP by hypoxia contributes to the chemoresistance of SN38 in hepatocellular carcinoma cells.* 2016. **7**(6): p. 6933.
100. Steinhardt, A.A., et al., *Expression of Yes-associated protein in common solid tumors.* 2008. **39**(11): p. 1582-1589.
101. Kim, M.P., G.J.C.D. Lozano, and Differentiation, *Mutant p53 partners in crime.* 2018. **25**(1): p. 161-168.
102. Escoll, M., et al., *Mutant p53 oncogenic functions in cancer stem cells are regulated by WIP through YAP/TAZ.* 2017. **36**(25): p. 3515-3527.
103. Ferraiuolo, M., et al., *Mutant p53 protein and the hippo transducers YAP and TAZ: a critical oncogenic node in human cancers.* 2017. **18**(5): p. 961.
104. Lee, Y., et al., *Dishevelled has a YAP nuclear export function in a tumor suppressor context-dependent manner.* 2018. **9**(1): p. 1-16.
105. Bykov, V.J., et al., *Targeting mutant p53 for efficient cancer therapy.* 2018. **18**(2): p. 89.
106. Zhang, Q., et al., *Correction: APR-246 reactivates mutant p53 by targeting cysteines 124 and 277.* 2019. **10**(10): p. 1-2.
107. Liu, D.S., et al., *APR-246 potently inhibits tumour growth and overcomes chemoresistance in preclinical models of oesophageal adenocarcinoma.* 2015. **64**(10): p. 1506-1516.
108. Lindemann, A., et al., *COTI-2, a novel thiosemicarbazone derivative, exhibits antitumor activity in HNSCC through p53-dependent and-independent mechanisms.* 2019. **25**(18): p. 5650-5662.
109. Synnott, N.C., et al., *COTI-2 reactivates mutant p53 and inhibits growth of triple-negative breast cancer cells.* 2020. **179**(1): p. 47-56.
110. Proia, D.A. and R.C.J.C.r. Bates, *Ganetespib and HSP90: translating preclinical hypotheses into clinical promise.* 2014. **74**(5): p. 1294-1300.
111. Alexandrova, E.M., et al., *Improving survival by exploiting tumour dependence on stabilized mutant p53 for treatment.* 2015. **523**(7560): p. 352-356.
112. Foggetti, G., et al., *Autophagy induced by SAHA affects mutant P53 degradation and cancer cell survival.* 2019. **39**(2).
113. Wang, Z., et al., *Histone deacetylase inhibitors suppress mutant p53 transcription via HDAC8/YY1 signals in triple negative breast cancer cells.* 2016. **28**(5): p. 506-515.
114. Portugal, J., et al., *Mechanisms of drug-induced mitotic catastrophe in cancer cells.* 2010. **16**(1): p. 69-78.
115. Osman, A.A., et al., *Wee-1 kinase inhibition overcomes cisplatin resistance associated with high-risk TP53 mutations in head and neck cancer through mitotic arrest followed by senescence.* 2015. **14**(2): p. 608-619.

116. Tanaka, N., et al., *Replication stress leading to apoptosis within the S-phase contributes to synergism between vorinostat and AZD1775 in HNSCC harboring high-risk TP53 mutation.* 2017. **23**(21): p. 6541-6554.
117. Batır, M.B., et al., *Evaluation of the CRISPR/Cas9 directed mutant TP53 gene repairing effect in human prostate cancer cell line PC-3.* 2019. **46**(6): p. 6471-6484.
118. Zhang, Y., et al., *Therapeutic potential of ReACp53 targeting mutant p53 protein in CRPC.* 2020. **23**(1): p. 160-171.
119. Soragni, A., et al., *A designed inhibitor of p53 aggregation rescues p53 tumor suppression in ovarian carcinomas.* 2016. **29**(1): p. 90-103.
120. Sobhani, N., et al., *Mutant p53 as an Antigen in Cancer Immunotherapy.* 2020. **21**(11): p. 4087.
121. Low, L., et al., *Targeting mutant p53-expressing tumours with a T cell receptor-like antibody specific for a wild-type antigen.* 2019. **10**(1): p. 1-14.
122. Kocaturk, N.M. and D. Gozuacik, *Crosstalk between mammalian autophagy and the ubiquitin-proteasome system.* Frontiers in cell and developmental biology, 2018. **6**: p. 128.
123. Groll, M., et al, *Substrate access and processing by the 20S proteasome core particle.* 2003. **35**(5): p. 606-616.
124. Dikic, I., et al., *Proteasomal and autophagic degradation systems.* 2017. **86**: p. 193-224.
125. Heinemeyer, W., et al., *Ubiquitin-proteasome system.* 2004. **61**(13): p. 1562-1578.
126. Collins, G.A. and A.L.J.C. Goldberg, *The logic of the 26S proteasome.* 2017. **169**(5): p. 792-806.
127. Benanti, J.A. *Coordination of cell growth and division by the ubiquitin–proteasome system*. in *Seminars in cell & developmental biology*. 2012. Elsevier.
128. Delgado, M.E., et al., *Modulation of apoptosis sensitivity through the interplay with autophagic and proteasomal degradation pathways.* 2014. **5**(1): p. e1011-e1011.
129. Park, J., J. Cho, and E.J.J.A.o.p.r. Song, *Ubiquitin–proteasome system (UPS) as a target for anticancer treatment.* 2020: p. 1-18.
130. Kisselev, A.F., et al., *Proteasome inhibitors: an expanding army attacking a unique target.* 2012. **19**(1): p. 99-115.
131. Hideshima, T., et al., *Molecular mechanisms mediating antimyeloma activity of proteasome inhibitor PS-341.* 2003. **101**(4): p. 1530-1534.
132. Shen, M., et al., *Targeting the ubiquitin–proteasome system for cancer therapy.* 2013. **17**(9): p. 1091-1108.
133. Adams, J., et al., *Proteasome inhibitors: a novel class of potent and effective antitumor agents.* 1999. **59**(11): p. 2615-2622.
134. Klionsky, D., et al., *Autophagy: from phenomenology to molecular understanding in less than a decade.* 2007. **8**(11): p. 931-937.
135. Hosokawa, N., et al., *Nutrient-dependent mTORC1 association with the ULK1–Atg13–FIP200 complex required for autophagy.* 2009. **20**(7): p. 1981-1991.
136. Mercer, T.J., et al., *A molecular perspective of mammalian autophagosome biogenesis.* 2018. **293**(15): p. 5386-5395.
137. Tsuboyama, K., et al., *The ATG conjugation systems are important for degradation of the inner autophagosomal membrane.* 2016. **354**(6315): p. 1036-1041.
138. Jäger, S., et al., *Role for Rab7 in maturation of late autophagic vacuoles.* Journal of cell science, 2004. **117**(20): p. 4837-4848.
139. Khaminets, A., et al., *Regulation of endoplasmic reticulum turnover by selective autophagy.* 2015. **522**(7556): p. 354-358.
140. An, H.,et al., *Systematic analysis of ribophagy in human cells reveals bystander flux during selective autophagy.* 2018. **20**(2): p. 135-143.
141. Lamark, T., et al., *Aggrephagy: selective disposal of protein aggregates by macroautophagy.* 2012. **2012**.
142. Lane, J.D., et al., *Autophagy as a defence against intracellular pathogens.* 2013. **55**: p. 153-163.
143. Okamoto, K., et al., *Mitochondria-anchored receptor Atg32 mediates degradation of mitochondria via selective autophagy.* 2009. **17**(1): p. 87-97.
144. Till, A., et al., *Pexophagy: the selective degradation of peroxisomes.* 2012. **2012**.
145. Huang, H., et al., *Bulk RNA degradation by nitrogen starvation-induced autophagy in yeast.* 2015. **34**(2): p. 154-168.

146. Mijaljica, D., et al., *Microautophagy in mammalian cells: revisiting a 40-year-old conundrum.* 2011. **7**(7): p. 673-682.
147. Tang, Y., et al., *Chaperone-mediated autophagy substrate proteins in cancer.* Oncotarget, 2017. **8**(31): p. 51970.
148. Singh, S.S., et al., *Dual role of autophagy in hallmarks of cancer.* 2018. **37**(9): p. 1142-1158.
149. Takamura, A., et al., *Autophagy-deficient mice develop multiple liver tumors.* 2011. **25**(8): p. 795-800.
150. Kimmelman, A., et al., *The dynamic nature of autophagy in cancer.* 2011. **25**(19): p. 1999-2010.
151. Mathew, R., et al., *Autophagy suppresses tumorigenesis through elimination of p62.* 2009. **137**(6): p. 1062-1075.
152. Bellot, G., et al., *Hypoxia-induced autophagy is mediated through hypoxia-inducible factor induction of BNIP3 and BNIP3L via their BH3 domains.* 2009. **29**(10): p. 2570-2581.
153. Wei, H., et al., *Suppression of autophagy by FIP200 deletion inhibits mammary tumorigenesis.* 2011. **25**(14): p. 1510-1527.
154. Cook, K.L., et al., *Autophagy and endocrine resistance in breast cancer.* 2011. **11**(8): p. 1283-1294.
155. Jain, K., et al., *Autophagy in breast cancer and its implications for therapy.* 2013. **3**(3): p. 251.
156. Wang, J., et al., *Role of autophagy in cisplatin resistance in ovarian cancer cells.* 2014. **289**(24): p. 17163-17173.
157. Mauthe, M., et al., *Chloroquine inhibits autophagic flux by decreasing autophagosome-lysosome fusion.* Autophagy, 2018. **14**(8): p. 1435-1455.
158. Hu, Y., et al., *Hypoxia-induced autophagy promotes tumor cell survival and adaptation to antiangiogenic treatment in glioblastoma.* 2012. **72**(7): p. 1773-1783.
159. Milano, V., et al., *Dasatinib-induced autophagy is enhanced in combination with temozolomide in glioma.* 2009. **8**(2): p. 394-406.
160. Liu, Y., et al., *Autophagy potentiates the anti-cancer effects of the histone deacetylase inhibitors in hepatocellular carcinoma.* 2010. **6**(8): p. 1057-1065.
161. Guba, M., et al., *Rapamycin inhibits primary and metastatic tumor growth by antiangiogenesis: involvement of vascular endothelial growth factor.* 2002. **8**(2): p. 128-135.
162. Ge, P., et al., *Inhibition of autophagy induced by proteasome inhibition increases cell death in human SHG-44 glioma cells.* Acta pharmacologica Sinica, 2009. **30**(7): p. 1046.
163. Tannous, P., et al., *Intracellular protein aggregation is a proximal trigger of cardiomyocyte autophagy.* 2008. **117**(24): p. 3070.
164. Korolchuk, V.I., et al., *Autophagy inhibition compromises degradation of ubiquitin-proteasome pathway substrates.* 2009. **33**(4): p. 517-527.
165. Marshall, R.S., et al., *Autophagic degradation of the 26S proteasome is mediated by the dual ATG8/ubiquitin receptor RPN10 in Arabidopsis.* 2015. **58**(6): p. 1053-1066.
166. Cohen-Kaplan, V., et al., *p62-and ubiquitin-dependent stress-induced autophagy of the mammalian 26S proteasome.* 2016. **113**(47): p. E7490-E7499.
167. Marshall, R.S., et al., *Proteasome storage granules protect proteasomes from autophagic degradation upon carbon starvation.* 2018. **7**: p. e34532.
168. Shi, Y., et al., *Mutant p53 as a Regulator and Target of Autophagy.* 2020. **10**: p. 3300.
169. Tasdemir, E., et al., *Regulation of autophagy by cytoplasmic p53.* 2008. **10**(6): p. 676-687.
170. Bensaad, K., et al., *TIGAR, a p53-inducible regulator of glycolysis and apoptosis.* 2006. **126**(1): p. 107-120.
171. Hoshino, A., et al., *Cytosolic p53 inhibits Parkin-mediated mitophagy and promotes mitochondrial dysfunction in the mouse heart.* 2013. **4**(1): p. 1-12.
172. Morselli, E., et al., *Mutant p53 protein localized in the cytoplasm inhibits autophagy.* Cell cycle, 2008. **7**(19): p. 3056-3061.
173. Cordani, M., et al., *Mutant p53 proteins counteract autophagic mechanism sensitizing cancer cells to mTOR inhibition.* 2016. **10**(7): p. 1008-1029.
174. Tomita, Y., et al., *WT p53, but not tumor-derived mutants, bind to Bcl2 via the DNA binding domain and induce mitochondrial permeabilization.* 2006. **281**(13): p. 8600-8606.
175. Sakanashi, F., et al., *Apoptosis, necroptosis and autophagy in colorectal cancer: Associations with tumor aggressiveness and p53 status.* 2019. **215**(7): p. 152425.
176. Guo, J.Y., et al., *Activated Ras requires autophagy to maintain oxidative metabolism and tumorigenesis.* 2011. **25**(5): p. 460-470.

177. Cerami, E., et al., *The cBio cancer genomics portal: an open platform for exploring multidimensional cancer genomics data*. 2012, AACR.
178. Gao, J., et al., *Integrative analysis of complex cancer genomics and clinical profiles using the cBioPortal*. 2013. **6**(269): p. pl1-pl1.
179. Uhlen, M., et al., *A pathology atlas of the human cancer transcriptome.* 2017. **357**(6352).
180. Ho, X.D., et al., *Whole transcriptome analysis identifies differentially regulated networks between osteosarcoma and normal bone samples.* Experimental Biology and Medicine, 2017. **242**(18): p. 1802-1811.
181. Love, M.I., W. Huber, and S. Anders, *Moderated estimation of fold change and dispersion for RNA-seq data with DESeq2.* Genome biology, 2014. **15**(12): p. 550.
182. Bindea, G., et al., *ClueGO: a Cytoscape plug-in to decipher functionally grouped gene ontology and pathway annotation networks.* Bioinformatics, 2009. **25**(8): p. 1091-1093.
183. Chowdhury, R., et al., *Arsenic induced apoptosis in malignant melanoma cells is enhanced by menadione through ROS generation, p38 signaling and p53 activation.* Apoptosis, 2009. **14**(1): p. 108-123.
184. Sengupta, P., et al., *Evaluation of Apoptosis and Autophagy Inducing Potential of Berberis aristata, Azadirachta indica, and Their Synergistic Combinations in Parental and Resistant Human Osteosarcoma Cells.* Frontiers in oncology, 2017. **7**.
185. Pfaffl, M.W., *A new mathematical model for relative quantification in real-time RT–PCR.* Nucleic acids research, 2001. **29**(9): p. e45-e45.
186. Chowdhury, R., et al., *Nitric oxide produced endogenously is responsible for hypoxia-induced HIF-1α stabilization in colon carcinoma cells.* Chemical research in toxicology, 2012. **25**(10): p. 2194-2202.
187. Lohitesh, K., et al., *Autophagy inhibition potentiates SAHA-mediated apoptosis in glioblastoma cells by accumulation of damaged mitochondria.* Oncology reports, 2018. **39**(6): p. 2787-2796.
188. Maemondo, M., et al., *Gefitinib or chemotherapy for non–small-cell lung cancer with mutated EGFR.* 2010. **362**(25): p. 2380-2388.
189. Mitsudomi, T., et al., *Gefitinib versus cisplatin plus docetaxel in patients with non-small-cell lung cancer harbouring mutations of the epidermal growth factor receptor (WJTOG3405): an open label, randomised phase 3 trial.* 2010. **11**(2): p. 121-128.
190. Yoh, K., et al., *Vandetanib in patients with previously treated RET-rearranged advanced non-small-cell lung cancer (LURET): an open-label, multicentre phase 2 trial.* 2017. **5**(1): p. 42-50.
191. Shaw, A.T., et al., *Crizotinib in ROS1-rearranged non–small-cell lung cancer.* 2014. **371**(21): p. 1963-1971.
192. Shaw, A.T., et al., *Crizotinib versus chemotherapy in advanced ALK-positive lung cancer.* 2013. **368**(25): p. 2385-2394.
193. Socinski, M.A., et al., *Treatment of stage IV non-small cell lung cancer: Diagnosis and management of lung cancer: American College of Chest Physicians evidence-based clinical practice guidelines.* 2013. **143**(5): p. e341S-e368S.
194. Liu, W., et al., *Drug resistance to targeted therapeutic strategies in non-small cell lung cancer.* 2020. **206**: p. 107438.
195. Perri, F., et al., *P53 mutations and cancer: a tight linkage.* 2016. **4**(24).
196. Harris, C.C. and M. Hollstein, *Clinical implications of the p53 tumor-suppressor gene.* New England Journal of Medicine, 1993. **329**(18): p. 1318-1327.
197. Cho, Y., et al., *Crystal structure of a p53 tumor suppressor-DNA complex: understanding tumorigenic mutations.* Science, 1994. **265**(5170): p. 346-355.
198. Blandino, G., A.J. Levine, and M. Oren, *Mutant p53 gain of function: differential effects of different p53 mutants on resistance of cultured cells to chemotherapy.* Oncogene, 1999. **18**(2): p. 477.
199. Høyer-Hansen, M. and M. Jäättelä, *Autophagy: an emerging target for cancer therapy.* Autophagy, 2008. **4**(5): p. 574-580.
200. Choundhury, S., et al., *Dissecting the pathways that destabilize mutant p53: the proteasome or autophagy?*, in *Cell Cycle*. 2013. p. 1022-1029.
201. Ebrahimi-Fakhari, D., et al., *Distinct roles in vivo for the ubiquitin–proteasome system and the autophagy–lysosomal pathway in the degradation of α-synuclein.* Journal of Neuroscience, 2011. **31**(41): p. 14508-14520.
202. Bao, W., et al., *Induction of autophagy by the MG-132 proteasome inhibitor is associated with endoplasmic reticulum stress in MCF-7 cells.* Molecular medicine reports, 2016. **13**(1): p. 796-804.

203. Yonekawa, T. and A. Thorburn, *Autophagy and cell death.* Essays in biochemistry, 2013. **55**: p. 105-117.
204. Martincorena, I., et al., *Universal patterns of selection in cancer and somatic tissues.* 2017. **171**(5): p. 1029-1041. e21.
205. Pant, S., et al., *Clinical update on K-Ras targeted therapy in gastrointestinal cancers.* 2018. **130**: p. 78-91.
206. Goldstein, I., et al., *Understanding wild-type and mutant p53 activities in human cancer: new landmarks on the way to targeted therapies.* Cancer gene therapy, 2011. **18**(1): p. 2.
207. Momose, I., et al., *A new proteasome inhibitor, TP-110, induces apoptosis in human prostate cancer PC-3 cells.* Bioscience, biotechnology, and biochemistry, 2007. **71**(4): p. 1036-1043.
208. Yang, H., et al., *Natural compounds with proteasome inhibitory activity for cancer prevention and treatment.* Current Protein and Peptide Science, 2008. **9**(3): p. 227-239.
209. Fan, W., et al., *Proteasome inhibitor MG-132 induces C6 glioma cell apoptosis via oxidative stress.* Acta Pharmacologica Sinica, 2011. **32**(5): p. 619.
210. Nagata, Y., et al., *The stabilization mechanism of mutant-type p53 by impaired ubiquitination: the loss of wild-type p53 function and the hsp90 association.* Oncogene, 1999. **18**(44): p. 6037.
211. Peng, Y., et al., *Stabilization of the MDM2 oncoprotein by mutant p53.* Journal of Biological Chemistry, 2001. **276**(9): p. 6874-6878.
212. Peng, Y., et al., *Inhibition of MDM2 by hsp90 contributes to mutant p53 stabilization.* Journal of Biological Chemistry, 2001. **276**(44): p. 40583-40590.
213. Esser, C., M. Scheffner, and J. Höhfeld, *The chaperone-associated ubiquitin ligase CHIP is able to target p53 for proteasomal degradation.* Journal of Biological Chemistry, 2005. **280**(29): p. 27443-27448.
214. Atencio, I.A., et al., *Calpain inhibitor 1 activates p53-dependent apoptosis in tumor cell lines.* Cell Growth and Differentiation-Publication American Association for Cancer Research, 2000. **11**(5): p. 247-254.
215. Lilienbaum, A., *Relationship between the proteasomal system and autophagy.* International journal of biochemistry and molecular biology, 2013. **4**(1): p. 1.
216. Klionsky, D.J., et al., *Guidelines for the use and interpretation of assays for monitoring autophagy.* Autophagy, 2016. **12**(1): p. 1-222.
217. Wu, Y., et al., *Dual role of 3-methyladenine in modulation of autophagy via different temporal patterns of inhibition on class I and III phosphoinositide 3-kinase.* Journal of Biological Chemistry, 2010. **285**(14): p. 10850-10861.
218. Li, J., S.G. Kim, and J. Blenis, *Rapamycin: one drug, many effects.* Cell metabolism, 2014. **19**(3): p. 373-379.
219. Shang, L., et al., *Nutrient starvation elicits an acute autophagic response mediated by Ulk1 dephosphorylation and its subsequent dissociation from AMPK.* Proceedings of the National Academy of Sciences, 2011. **108**(12): p. 4788-4793.
220. Li, L., et al., *ROS and autophagy: interactions and molecular regulatory mechanisms.* Cellular and molecular neurobiology, 2015. **35**(5): p. 615-621.
221. Son, Y., et al., *Reactive oxygen species in the activation of MAP kinases*, in *Methods in enzymology*. 2013, Elsevier. p. 27-48.
222. Mukherjee, S., et al., *The dynamic role of autophagy and MAPK signaling in determining cell fate under cisplatin stress in osteosarcoma cells.* PloS one, 2017. **12**(6): p. e0179203.
223. Fageria, L., et al., *Biosynthesized Protein-Capped Silver Nanoparticles Induce ROS-Dependent Proapoptotic Signals and Prosurvival Autophagy in Cancer Cells.* ACS Omega, 2017. **2**(4): p. 1489-1504.
224. Cagnol, S. and J.C. Chambard, *ERK and cell death: Mechanisms of ERK-induced cell death–apoptosis, autophagy and senescence.* The FEBS journal, 2010. **277**(1): p. 2-21.
225. Mujumdar, N. and A.K. Saluja, *Autophagy in pancreatic cancer.* Autophagy, 2010.
226. Ciechanover, A., *Intracellular protein degradation: from a vague idea thru the lysosome and the ubiquitin–proteasome system and onto human diseases and drug targeting.* Cell death and differentiation, 2005. **12**(9): p. 1178.
227. Ding, W.-X. and X.-M. Yin, *Sorting, recognition and activation of the misfolded protein degradation pathways through macroautophagy and the proteasome.* Autophagy, 2008. **4**(2): p. 141-150.
228. Rock, K.L., et al., *Inhibitors of the proteasome block the degradation of most cell proteins and the generation of peptides presented on MHC class I molecules.* Cell, 1994. **78**(5): p. 761-771.

229. Adams, J., *The development of proteasome inhibitors as anticancer drugs.* Cancer cell, 2004. **5**(5): p. 417-421.
230. Goldberg, A., *Functions of the proteasome: from protein degradation and immune surveillance to cancer therapy.* Biochemical Society Transactions, 2007. **35**(1): p. 12-17.
231. Liu, Y. and B. Levine, *Autosis and autophagic cell death: the dark side of autophagy.* Cell death and differentiation, 2015. **22**(3): p. 367.
232. Shimizu, S., et al., *Role of Bcl-2 family proteins in a non-apoptotic programmed cell death dependent on autophagy genes.* Nature cell biology, 2004. **6**(12): p. 1221.
233. Shimizu, S., et al., *Involvement of JNK in the regulation of autophagic cell death.* Oncogene, 2010. **29**(14): p. 2070.
234. Yu, L., et al., *Regulation of an ATG7-beclin 1 program of autophagic cell death by caspase-8.* Science, 2004. **304**(5676): p. 1500-1502.
235. Saini, H., et al., *Autophagy Regulated by Gain of Function Mutant p53 Enhances Proteasomal Inhibitor-Mediated Cell Death through Induction of ROS and ERK in Lung Cancer Cells.* Journal of oncology, 2019. **2019**.
236. Tang, J., et al., *p53-mediated autophagic regulation: A prospective strategy for cancer therapy.* 2015. **363**(2): p. 101-107.
237. Cordani, M., et al., *Molecular interplay between mutant p53 proteins and autophagy in cancer cells*. 2017. **1867**(1): p. 19-28.
238. Liu, G., et al., *Role of autophagy and apoptosis in non-small-cell lung cancer.* 2017. **18**(2): p. 367.
239. Totaro, A., et al., *Cell phenotypic plasticity requires autophagic flux driven by YAP/TAZ mechanotransduction.* 2019. **116**(36): p. 17848-17857.
240. Xu, W., et al., *YAP manipulates proliferation via PTEN/AKT/mTOR-mediated autophagy in lung adenocarcinomas.* 2021. **21**(1): p. 1-13.
241. Zhou, Y., et al., *YAP promotes multi-drug resistance and inhibits autophagy-related cell death in hepatocellular carcinoma via the RAC1-ROS-mTOR pathway.* 2019. **19**(1): p. 1-15.
242. Pavel, M., et al., *Contact inhibition controls cell survival and proliferation via YAP/TAZ-autophagy axis.* 2018. **9**(1): p. 1-18.
243. Yun, C.W. and S.H. Lee, *The roles of autophagy in cancer.* International journal of molecular sciences, 2018. **19**(11): p. 3466.
244. Guo, J.Y. and E. White. *Autophagy, metabolism, and cancer*. *Cold Spring Harbor symposia on quantitative biology*. 2016.
245. Ye, M.-X., et al., *Curcumin: updated molecular mechanisms and intervention targets in human lung cancer.* 2012. **13**(3): p. 3959-3978.
246. Guo, J.Y. and E.J.A. White, *Autophagy is required for mitochondrial function, lipid metabolism, growth, and fate of KRASG12D-driven lung tumors.* 2013. **9**(10): p. 1636-1638.
247. Strohecker, A.M., et al., *Autophagy sustains mitochondrial glutamine metabolism and growth of BrafV600E–driven lung tumors.* 2013. **3**(11): p. 1272-1285.
248. Wang, X., et al., *Opportunities and challenges of co-targeting epidermal growth factor receptor and autophagy signaling in non-small cell lung cancer.* 2019. **18**(1): p. 499-506.
249. Vaughan, C.A., et al., *Gain-of-function p53 activates multiple signaling pathways to induce oncogenicity in lung cancer cells.* 2017. **11**(6): p. 696-711.
250. Zucchini, C., et al., *ROCK2 deprivation leads to the inhibition of tumor growth and metastatic potential in osteosarcoma cells through the modulation of YAP activity.* Journal of Experimental & Clinical Cancer Research, 2019. **38**(1): p. 1-14.
251. Bassi, L., et al., *Pifithrin-α, an inhibitor of p53, enhances the genetic instability induced by etoposide (VP16) in human lymphoblastoid cells treated in vitro.* 2002. **499**(2): p. 163-176.
252. Kwon, Y., et al., *The Hippo signaling pathway interactome.* 2013. **342**(6159): p. 737-740.
253. Liang, N., et al., *Regulation of YAP by mTOR and autophagy reveals a therapeutic target of tuberous sclerosis complexYAP is required for tumorigenesis of TSC.* 2014. **211**(11): p. 2249-2263.
254. Kaushik, S., et al., *Constitutive activation of chaperone-mediated autophagy in cells with impaired macroautophagy.* Molecular biology of the cell, 2008. **19**(5): p. 2179-2192.
255. Kirchner, P., et al., *Proteome-wide analysis of chaperone-mediated autophagy targeting motifs.* 2019. **17**(5): p. e3000301.

256. Zhang, C., et al., *AMOT 130 linking F-actin to YAP is involved in intervertebral disc degeneration.* 2018. **51**(6): p. e12492.
257. Mizushima, N., *Methods for monitoring autophagy.* The international journal of biochemistry & cell biology, 2004. **36**(12): p. 2491-2502.
258. Wang, C., et al., *Pharmacological inhibitors of autophagy as novel cancer therapeutic agents.* 2016. **105**: p. 164-175.
259. Kimura, T., et al., *Chloroquine in cancer therapy: a double-edged sword of autophagy.* 2013. **73**(1): p. 3-7.
260. Redmann, M., et al., *Inhibition of autophagy with bafilomycin and chloroquine decreases mitochondrial quality and bioenergetic function in primary neurons.* 2017. **11**: p. 73-81.
261. Niveditha, D., et al., *A global transcriptomic pipeline decoding core network of genes involved in stages leading to acquisition of drug-resistance to cisplatin in osteosarcoma cells.* Bioinformatics, 2019. **35**(10): p. 1701-1711.
262. Niveditha, D., et al., *Transcriptomic analysis associated with reversal of cisplatin sensitivity in drug resistant osteosarcoma cells after a drug holiday.* 2019. **19**(1): p. 1-14.
263. Zhang, H., et al., *Tumor-selective proteotoxicity of verteporfin inhibits colon cancer progression independently of YAP1.* Sci. Signal., 2015. **8**(397): p. ra98-ra98.
264. Gibault, F., et al., *Non-photoinduced biological properties of verteporfin.* Current medicinal chemistry, 2016. **23**(11): p. 1171-1184.
265. Bielack, S.S., et al., *Bone tumors in adolescents and young adults.* Current treatment options in oncology, 2008. **9**(1): p. 67.
266. McIntyre, J.F., et al., *Germline mutations of the p53 tumor suppressor gene in children with osteosarcoma.* Journal of Clinical Oncology, 1994. **12**(5): p. 925-930.
267. Xiao, X., et al., *HSP90AA1-mediated autophagy promotes drug resistance in osteosarcoma.* Journal of Experimental & Clinical Cancer Research, 2018. **37**(1): p. 201.
268. Huang, J., et al., *Targeting HMGB1-mediated autophagy as a novel therapeutic strategy for osteosarcoma.* Autophagy, 2012. **8**(2): p. 275-277.
269. Kim, H.J., et al., *Cytoprotective role of autophagy during paclitaxel-induced apoptosis in Saos-2 osteosarcoma cells.* International journal of oncology, 2013. **42**(6): p. 1985-1992.
270. Chen, Z., et al., *NPRL2 enhances autophagy and the resistance to Everolimus in castration-resistant prostate cancer.* The Prostate, 2019. **79**(1): p. 44-53.
271. Hansen, T.E. and T. Johansen, *Following autophagy step by step.* BMC biology, 2011. **9**(1): p. 39.
272. Pankiv, S., et al., *p62/SQSTM1 binds directly to Atg8/LC3 to facilitate degradation of ubiquitinated protein aggregates by autophagy.* Journal of biological chemistry, 2007. **282**(33): p. 24131-24145.
273. Liu, W.J., et al., *p62 links the autophagy pathway and the ubiqutin–proteasome system upon ubiquitinated protein degradation.* Cellular & molecular biology letters, 2016. **21**(1): p. 29.
274. Kimura, S., T. Noda, and T. Yoshimori, *Dissection of the autophagosome maturation process by a novel reporter protein, tandem fluorescent-tagged LC3.* Autophagy, 2007. **3**(5): p. 452-460.
275. Antunes, F., et al., *Apoptosis induced by exposure to a low steady-state concentration of H2O2 is a consequence of lysosomal rupture.* Biochemical Journal, 2001. **356**(2): p. 549-555.
276. Eskelinen, E., *Roles of LAMP-1 and LAMP-2 in lysosome biogenesis and autophagy.* Molecular aspects of medicine, 2006. **27**(5-6): p. 495-502.
277. Nylandsted, J., et al., *Heat shock protein 70 promotes cell survival by inhibiting lysosomal membrane permeabilization.* Journal of Experimental Medicine, 2004. **200**(4): p. 425-435.
278. Boya, P. and G. Kroemer, *Lysosomal membrane permeabilization in cell death.* Oncogene, 2008. **27**(50): p. 6434.
279. Ganjavi, H., et al., *Adenovirus-mediated p53 gene therapy in osteosarcoma cell lines: sensitization to cisplatin and doxorubicin.* Cancer gene therapy, 2006. **13**(4): p. 415-419.
280. Yi, Y.W., et al., *Targeting mutant p53 by a SIRT1 activator YK-3-237 inhibits the proliferation of triple-negative breast cancer cells.* Oncotarget, 2013. **4**(7): p. 984.
281. Donohue, E., et al., *Induction of covalently crosslinked p62 oligomers with reduced binding to polyubiquitinated proteins by the autophagy inhibitor verteporfin.* PloS one, 2014. **9**(12): p. e114964.
282. Ye, S., et al., *p53 overexpression increases chemosensitivity in multidrug-resistant osteosarcoma cell lines.* Cancer chemotherapy and pharmacology, 2016. **77**(2): p. 349-356.

283. Settembre, C., et al., *TFEB links autophagy to lysosomal biogenesis.* science, 2011. **332**(6036): p. 1429-1433.
284. Vakifahmetoglu-Norberg, H., et al., *Chaperone-mediated autophagy degrades mutant p53.* Genes & development, 2013. **27**(15): p. 1718-1730.
285. Cuervo, A.M. and J. Dice, *Unique properties of lamp2a compared to other lamp2 isoforms.* Journal of cell science, 2000. **113**(24): p. 4441-4450.
286. Konstantinou, E.K., et al., *Verteporfin-induced formation of protein cross-linked oligomers and high molecular weight complexes is mediated by light and leads to cell toxicity.* Scientific reports, 2017. **7**: p. 46581.
287. de Oliveira, G.A., et al., *The status of p53 oligomeric and aggregation states in cancer.* Biomolecules, 2020. **10**(4): p. 548.
288. Gasteiger, E., et al., *Protein identification and analysis tools on the ExPASy server*, in *The proteomics protocols handbook*. 2005, Springer. p. 571-607.
289. Koga, H., et al., *A photoconvertible fluorescent reporter to track chaperone-mediated autophagy.* Nature communications, 2011. **2**(1): p. 1-10.
290. Ma, Y.-W., Y.-Z. Liu, and J.-X. Pan, *Verteporfin induces apoptosis and eliminates cancer stem-like cells in uveal melanoma in the absence of light activation.* American journal of cancer research, 2016. **6**(12): p. 2816.
291. Al-Moujahed, A., et al., *Verteporfin inhibits growth of human glioma in vitro without light activation.* Scientific reports, 2017. **7**(1): p. 1-8.
292. Glickman, M.S. and C.L.J.C. Sawyers, *Converting cancer therapies into cures: lessons from infectious diseases.* 2012. **148**(6): p. 1089-1098.
293. Lipinski, K.A., et al., *Cancer evolution and the limits of predictability in precision cancer medicine.* 2016. **2**(1): p. 49-63.
294. Caulin, A.F., et al., *Peto's Paradox: evolution's prescription for cancer prevention.* 2011. **26**(4): p. 175-182.
295. Marusyk, A., et al., *Tumor heterogeneity: causes and consequences.* 2010. **1805**(1): p. 105-117.
296. Michor, F., et al., *The origins and implications of intratumor heterogeneity.* 2010. **3**(11): p. 1361-1364.
297. Bashashati, A., et al., *Distinct evolutionary trajectories of primary high-grade serous ovarian cancers revealed through spatial mutational profiling.* 2013. **231**(1): p. 21-34.
298. Gerlinger, M., et al., *Intratumor heterogeneity and branched evolution revealed by multiregion sequencing.* 2012. **366**: p. 883-892.
299. Navin, N., et al., *Inferring tumor progression from genomic heterogeneity.* 2010. **20**(1): p. 68-80.
300. Landau, D.A., et al., *Evolution and impact of subclonal mutations in chronic lymphocytic leukemia.* 2013. **152**(4): p. 714-726.
301. Burrell, R.A., et al., *Tumour heterogeneity and the evolution of polyclonal drug resistance.* 2014. **8**(6): p. 1095-1111.
302. Sharma, S.V., et al., *A chromatin-mediated reversible drug-tolerant state in cancer cell subpopulations.* 2010. **141**(1): p. 69-80.
303. Zhan, Z., et al., *Resistance to paclitaxel mediated by P-glycoprotein can be modulated by changes in the schedule of administration.* 1997. **40**(3): p. 245-250.
304. De Souza, R., et al., *Continuous docetaxel chemotherapy improves therapeutic efficacy in murine models of ovarian cancer.* 2010. **9**(6): p. 1820-1830.
305. Lopes, N.M., et al., *Cell kill kinetics and cell cycle effects of taxol on human and hamster ovarian cell lines.* 1993. **32**(3): p. 235-242.
306. Jordan, M.A., et al., *Mitotic block induced in HeLa cells by low concentrations of paclitaxel (Taxol) results in abnormal mitotic exit and apoptotic cell death.* 1996. **56**(4): p. 816-825.
307. Bray, F., et al., *Global cancer statistics 2018: GLOBOCAN estimates of incidence and mortality worldwide for 36 cancers in 185 countries.* 2018. **68**(6): p. 394-424.
308. Herraez, E., et al., *Cisplatin-induced chemoresistance in colon cancer cells involves FXR-dependent and FXR-independent up-regulation of ABC proteins.* 2012. **9**(9): p. 2565-2576.
309. Saber, M.M., et al., *Targeting colorectal cancer cell metabolism through development of cisplatin and metformin nano-cubosomes.* 2018. **18**(1): p. 1-11.
310. Cree, I.A., et al., *Molecular chess? Hallmarks of anti-cancer drug resistance.* 2017. **17**(1): p. 1-8.

311. Haider, T., et al., *Drug resistance in cancer: Mechanisms and tackling strategies.* 2020: p. 1-27.
312. Amaravadi, R.K., et al., *Principles and current strategies for targeting autophagy for cancer treatment.* 2011. **17**(4): p. 654-666.

Appendix-I

Deciphering transcriptomic alterations associated with cisplatin treatment in cancer cells with varied P53 status

AI.1 Overview:

The emergence of drug resistance is one of the major hurdles in cancer therapy today [292, 293]. For more than a decade researcher all around the world are looking for the cause of cancer drug resistance. With the advancement in research, we have filtered out several factors like intrinsic resistance, acquired resistance, change in the tumor microenvironment, genetic or non-genetic changes, and activation of several molecular pathways [294-296] as key players in drug refractoriness. However, the precise mechanism of resistance is still unclear as cancer is a very complex multistage process comprising of a heterogeneous population of cells with different genomic profiles [295, 296]. Many studies have reported the co-existence of different genetic signatures in the subpopulation of single tumor types including, ovarian cancer, renal cell carcinoma, breast cancer, and chronic lymphocytic leukemia [297-300]. These subpopulations show different sensitivity to chemotherapy or targeted drug therapy so that a portion of cells would survive after initial drug treatment. Once these portions of cells start proliferating again, the tumor would come back with a different set of genetic signatures that might show enhanced drug resistance to the initial therapy. This drug treatment-inspired evolution of genomic heterogeneity presumably follows a Darwinian selection process and shows different subclonal compositions at different stages [300, 301].

Due to this heterogeneous nature of cancer cells, many researchers are working on combinatorial therapy and trying to standardize the dose and time for killing the majority of this subclonal population. This resilient subpopulation surviving a drug pressure is often termed as “Drug Tolerant Persisters” (DTPs). Many groups have adopted different mechanisms to target DTPs. For instance, some researchers believe that a drug holiday can better sensitize persister cells while others have shown efficacy with epigenetic modulators [262, 302]. Previous studies have also suggested that a prolonged drug exposure and a short drug holiday might have the potential to evade the development of drug resistance [303]. Similarly, other reports suggest a low and prolonged exposure of cell cycle-specific drugs such as taxanes could show an enhanced cancer cell sensitization [304-306]. There is also existing controversy on the stipulated drug dose, whether to go for a single toxic dose or multiple low doses of chemotherapy.

Importantly, the knowledge of genetic signatures with different doses of drugs given for similar time duration is poorly understood. To understand this, we planned a study to compare the expression profile of cancer cells exposed to a low dose (LD) or a high dose (HD) of drug treatment for the same period. We selected colorectal cancer (CRC) cells for this study as CRC is one of the most occurring cancers which expresses rapid metastasis and relapse leading to high mortality [307]. Also, CRC is a prime example of drug resistance-induced mortality. In our study, we treated WT or GOF-

R273H-P53 harboring colorectal cancer cell lines, with a LD or HD of drug for 48 hours and performed transcriptomic profiling. We compared the transcriptomic data of LD group with respect to untreated control (Cntrl), HD group with respect to Cntrl or HD group with respect to LD group and denoted them as Cntrl vs LD, Cntrl vs HD, and LD vs HD respectively. Interestingly, we observed a very different set of genes or pathways getting dysregulated suggesting differential adaptation of cells to the drug doses. Though this study is at its preliminary stage, yet, we believe, that further analysis would help in understanding the cellular molecular adaptations, which can help in designing a better strategy for future treatment.

AI.2 Result and Discussion

AI.2.1 CRC cells survive a high dose of cisplatin treatment

Cisplatin is the first-line therapeutic agent against multiple cancers including CRC. However, it often results in the selection of resilient persisters that serve as a reservoir of cells surviving drug pressure leading to eventual recurrence [261, 308, 309]. In corroboration to above, we observed that though treatment of cisplatin to CRC cells resulted in a dose dependent cytotoxicity, yet, cells do survive even the highest dose of drug pressure as well **(Fig. AI.2.1a)**. We assume that the molecular response of cells to cisplatin at a low dose substantially varies when compared to the cells under acute drug pressure. Notably, IC-50 for HCT116-WT cells was comparatively lower than the other cells harboring endogenously expressing GOF-R273H-P53. We further selected two doses of cisplatin, 30 µM, low dose (LD), and a ten times higher dose, 300 µM, high dose (HD) and exposed the cells for 48 hours. Phase contrast images of the cells post treatment are presented in **figure AI.2.1b-d**. Further, we wanted to analyze the effect of repeated drug doses on the CRC cells. The HT-29 and SW480 cells were exposed to three treatment shots of LD and HD of cisplatin for 48 hours, each without any drug break; thereafter post 144 hours of drug exposure crystal violet (CV) assay was performed. As shown in **figure AI.2.1e** both HT-29 and SW480 cells survived the triple shock of LD and HD treatment suggesting that these cells are resilient to multiple chemotherapeutic shocks. Interestingly, we observed that the cells when exposed to LD tend to survive in colonies, unlike a HD exposure. This might be associated with differential survival strategy adapted by cells under varied drug pressure.

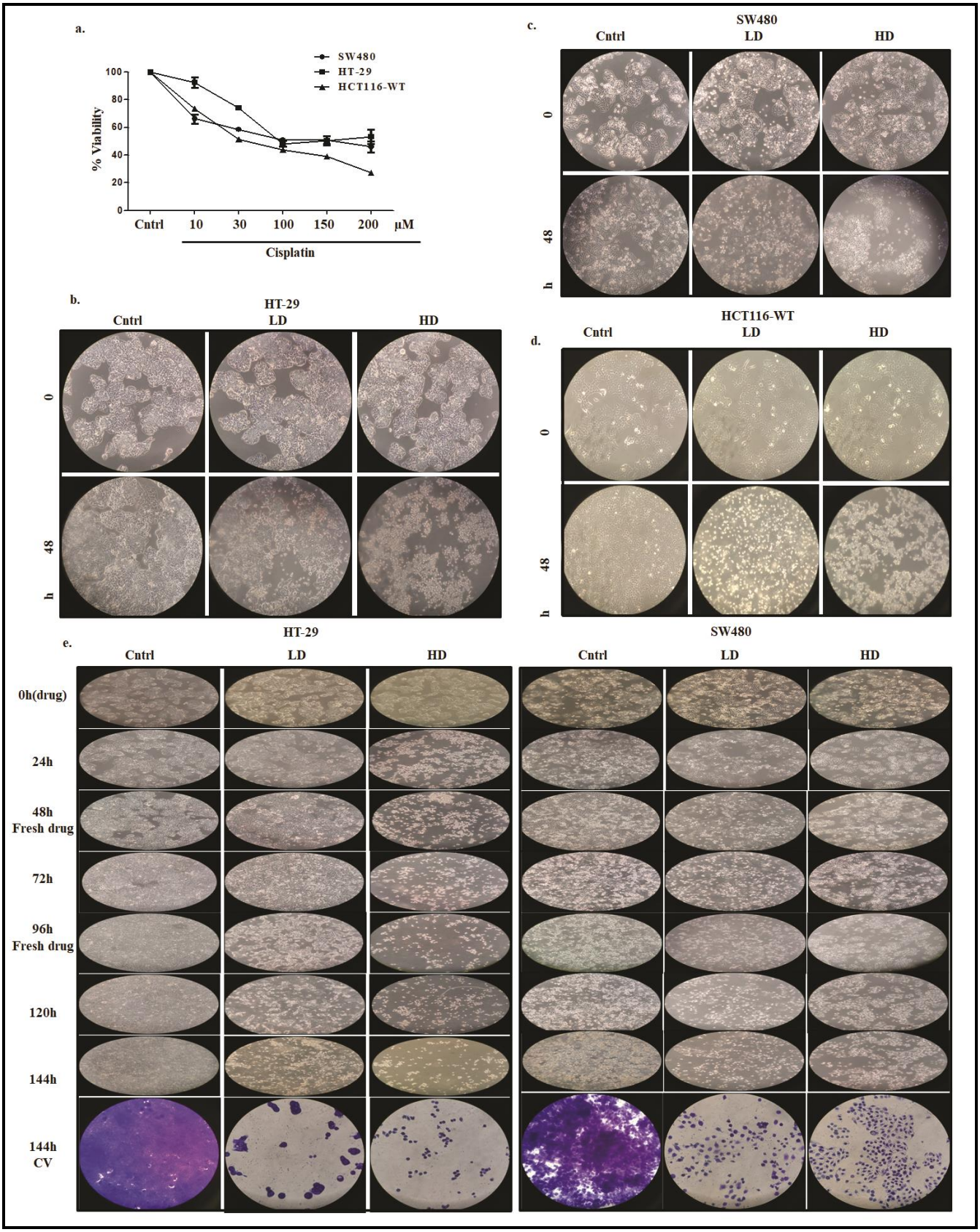

Figure AI.2.1. CRC cells survive a high dose of cisplatin treatment. a Cell viability as measured through MTT assay upon exposure to cisplatin for 48 hours. Phase contrast image showing cell viability and morphology post 48 hour of cisplatin treatment in **b** HT-29 cell, **c** SW480 cells and **d**

HCT116-WT cells. **e** Phase contrast image showing cell viability post three repetitive doses of cisplatin for 48 hours, followed up by crystal violet (CV) assay. Here, LD is low dose (30 µM) and HD is high dose (300 µM) of cisplatin.

AI.2.2 Comparative analysis of transcriptomic signatures between different groups of cisplatin-treated HT-29 cells

To understand the difference in gene expression under LD or HD of cisplatin we performed deep sequencing of mRNA. For this, HT-29 cells were treated with LD or HD of cisplatin for 48 hours, the total RNA was isolated, and further deep sequencing of mRNA was performed and the transcriptomic data was analyzed. The number of total transcripts in Cntrl vs LD, Cntrl vs HD, and LD vs HD is shown in **figure AI.2.2a**. Interestingly, a high dose treatment resulted in a reduced number of transcripts indicating a probable transcriptomic shutdown. In addition, the number of differentially regulated transcripts was much higher in high dose drug treatment compared to low dose **(Fig. AI.2.2b)**. However, an increased number of protein coding transcripts were found to be downregulated in high dose treatment **(Fig. AI.2.2c)**, suggesting that a high dose can result in a shutdown of transcripts as an effect of acute drug stress and/or putatively as a survival strategy. Several mechanisms have been reported for cancer drug resistance including, enhanced expression of ABC transporters, drug metabolism, apoptosis or autophagy induction, cancer stemness, DNA repair, and epigenetic regulation [310, 311]. We analyzed the transcripts obtained from our data for categorization into established mechanisms of drug resistance. As shown in **figure AI.2.2d**, genes involved in ABC transporters, drug metabolism, and apoptosis showed differential expression pattern. Also, the number of transcripts involved in platinum drug resistance were found to be more in Cntrl vs HD compared to Cntrl vs LD expressing the possibility of activation of specific mechanisms of survival [310, 311]. Additionally, the ABC transporters showed a trend of up-regulation in LD compared to control and was primarily down-regulated in high dose treatment **(Fig. AI.2.2e)**. Our preliminary analysis suggests differential expression of transcripts at high dose compared to low dose; however, further studies are required to validate the functional significance of the same.

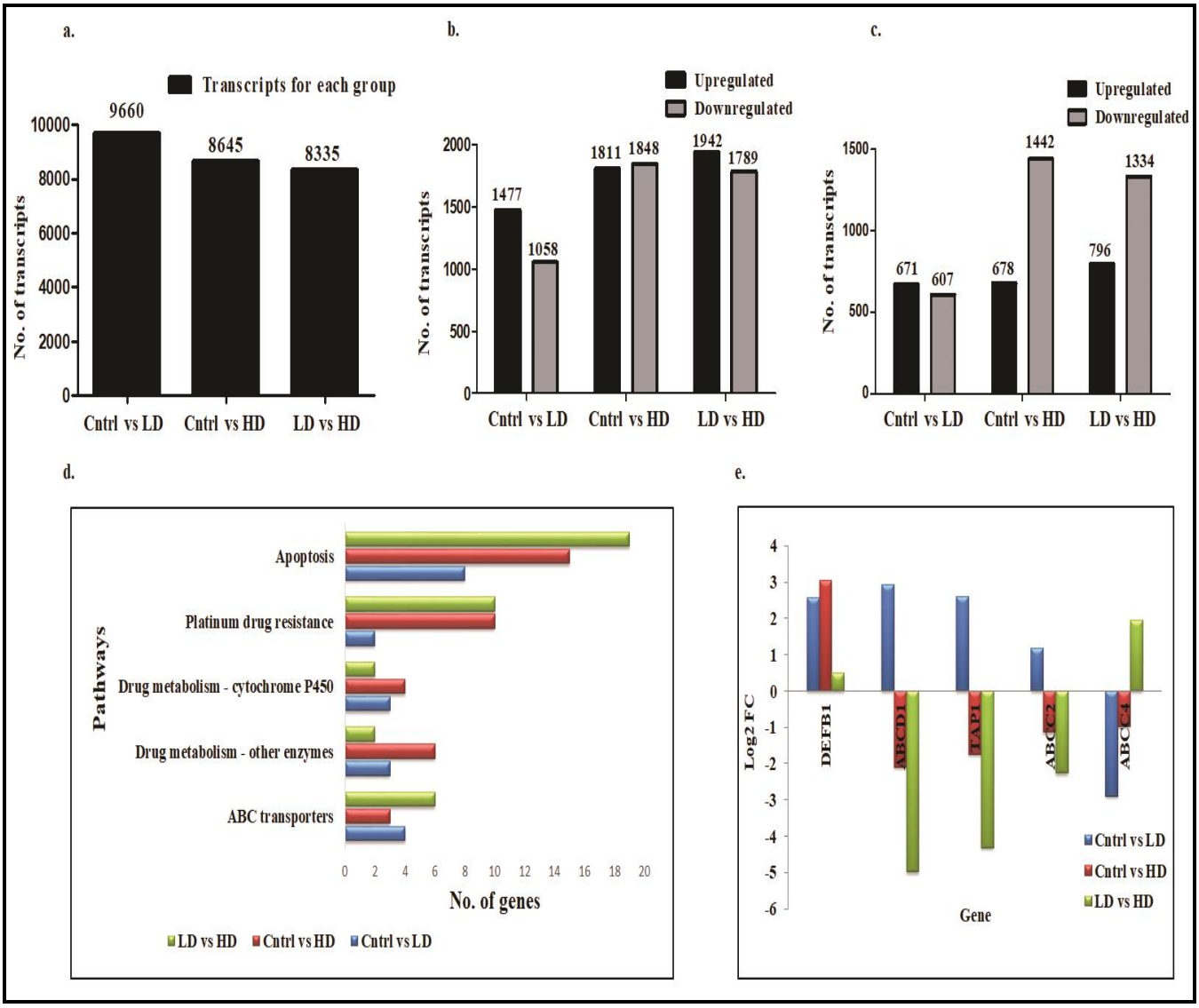

Figure AI.2.2 Comparative analysis of transcriptomic signatures upon cisplatin treatment in HT-29 cells. a Comparison of the total number of transcripts in each set. **b** Bar graph representing differentially regulated transcripts in each comparative set. **c** Bar graph representing differentially regulated protein coding transcripts in each set. Here, LD is low dose (30 µM) and HD is high dose (300 µM) of cisplatin. Genes with log2 Fold value ± 1.5 were considered differentially expressed (up or down regulated). **d** Bar graph representing number of genes dysregulated in drug resistance associated pathways. **e** Bar graph showing the expression of ABC transporter genes.

AI.2.3 Transcriptomic comparison of degradation pathways with varied drug dose

The involvement of autophagy and other cellular degradation pathways in imparting drug resistance has been extensively discussed in the literature [199, 222, 312]. However, there is hardly any report depicting their regulation under different drug doses. Hence, we next checked for transcriptomic regulation of various degradation associated pathways and as shown in **figure AI.2.3a**, a vast

majority of transcripts involved in cellular degradation pathways were dys-regulated in high dose treatment compared to low dose. Herein, we analyzed the autophagy associated genes after low dose and high dose treatment and mapped them using autophagy KEGG pathway. Interestingly, 11 autophagy genes were de-regulated in LD **(Fig. AI.2.3b)**, however as many as 25 genes were de-regulated in HD **(Fig. AI.2.3c)** of cisplatin treatment implicating a probable dys-regulation of autophagy after cisplatin treatment. Importantly, the genes- HMGB1 and UVRAG were downregulated in LD however showed an increased expression after acute dose of cisplatin treatment. Notably, HMGB1 has been reported to induce drug resistance in highly resistant cancers like osteosarcoma [268]. Additionally, the selective autophagy- mitophagy has been implicated in cellular homeostasis and prevention of oncogenesis. However, contrasting reports are there as well, which suggest involvement of mitophagy in cancer cell survival through degradation of damaged mitochondria and a reduced mitochondrial reactive oxygen species. Hence, we further checked for the regulation of mitophagy genes, and interestingly, as evident from **figure AI.2.3d**, some of the mitophagy genes showed significant upregulation in LD treatment, while a different set showed a reverse trend **figure AI.2.3e**. The above data is just a preliminary analysis, which indicates towards different transcriptomic signature of cells at high dose compared to low dose; however, further functional validation is required to establish their role. We are currently analyzing the contribution of individual pathways in survival under differential drug stress.

a.

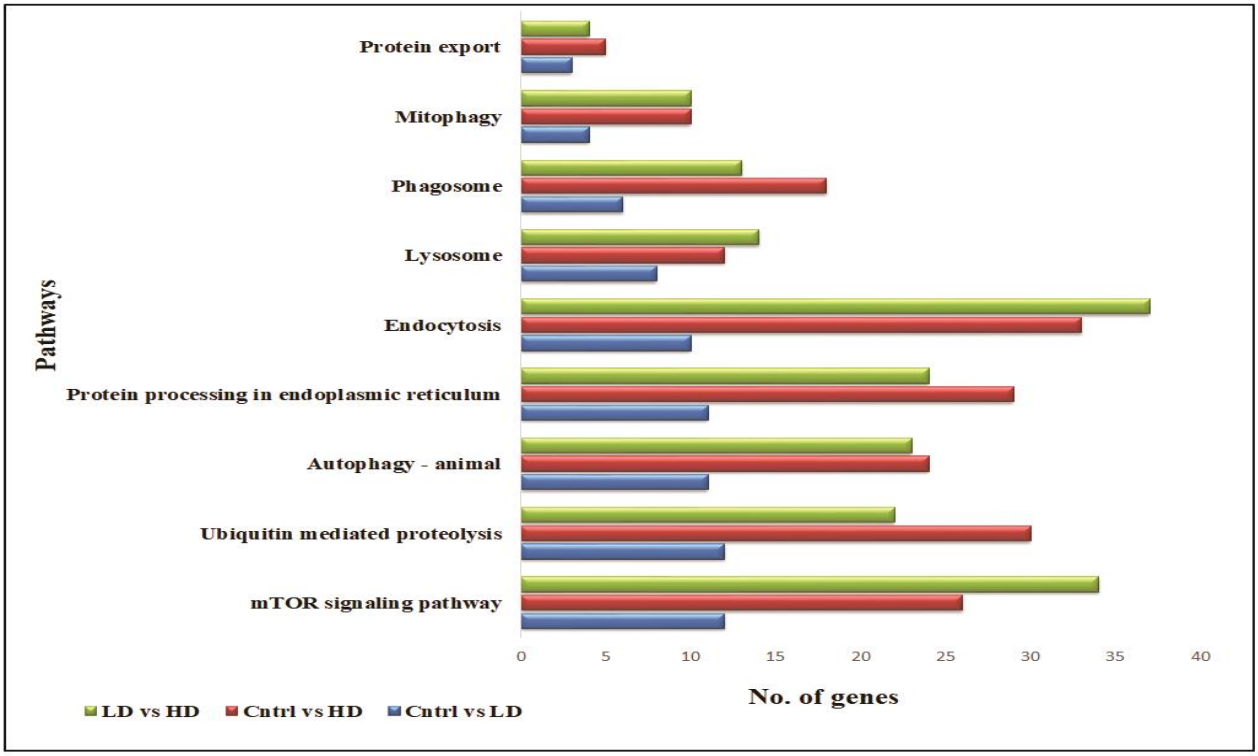

b.

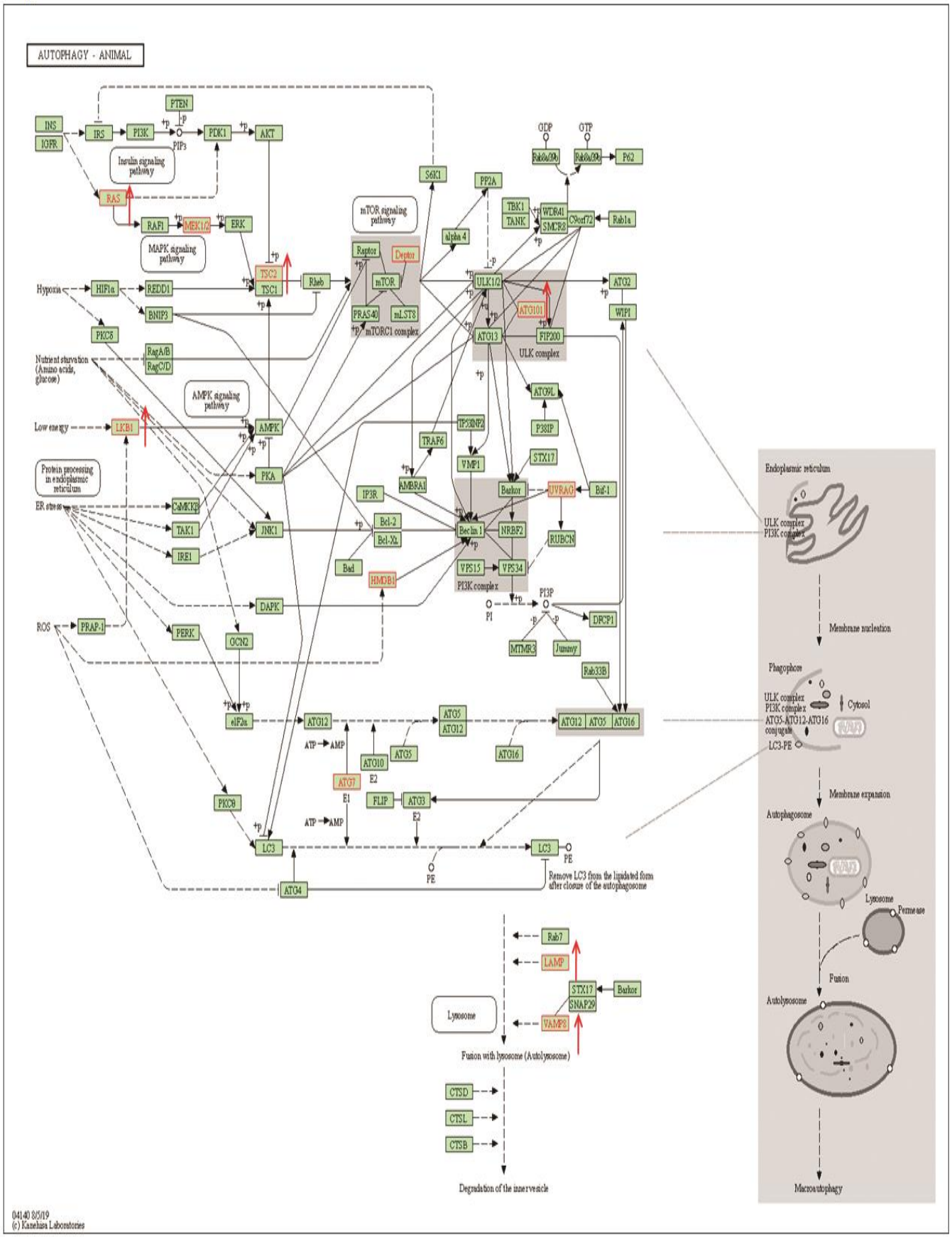
AUTOPHAGY - ANIMAL
PTEN
INS
IGFR
IRS
PI3K
PIP3
PDK1
AKT
Insulin signaling pathway
RAS
RAF1
MEK1/2
ERK
MAPK signaling pathway
TSC2
TSC1
Rheb
Hypoxia
HIF1α
REDD1
BNIP3
PKCδ
RagA/B
RagC/D
Nutrient starvation (Amino acids, glucose)
AMPK signaling pathway
Low energy
LKB1
AMPK
Protein processing in endoplasmic reticulum
ER stress
CaMKKβ
TAK1
IRE1
PKA
JNK1
DAPK
ROS
PRAP-1
PERK
GCN2
eIF2α
PKCθ
LC3
ATG4
mTOR signaling pathway
Raptor
Deptor
mTOR
PRAS40
mLST8
mTORC1 complex
S6K1
alpha 4
PP2A
ULK1/2
ATG13
FIP200
ULK complex
ATG101
ATG2
WIPI
ATG9L
P38IP
TP53INP2
STX17
VMP1
TRAF6
AMBRA1
IP3R
Bad
Bcl-2
Bcl-XL
HMGB1
Beclin 1
Barkor
UVRAG
Bif-1
NRBF2
RUBCN
VPS15
VPS34
PI3K complex
PI3P
PI
DRCP1
MTMR3
Jumonji
Rab33B
ATG12
ATG5
ATG16
ATG10
ATG7
ATG3
FLIP
E1
E2
ATP
AMP
PE
Remove LC3 from the lipidated form after closure of the autophagosome
GDP
GTP
Rab9a/9b
Rab9a/9b
P62
TBK1
TANK
WDR41
SMCR8
C9orf72
Rab1a
Endoplasmic reticulum
ULK complex
PI3K complex
Membrane nucleation
Phagophore
Cytosol
ATG5-ATG12-ATG16 conjugate
LC3-PE
Membrane expansion
Autophagosome
Lysosome
Permease
Fusion
Autolysosome
Macroautophagy
Rab7
LAMP
STX17
SNAP29
VAMP8
Barkor
Lysosome
Fusion with lysosome (Autolysosome)
CTSD
CTSL
CTSB
Degradation of the innervesicle
04140 8/5/19
(c) Kanehisa Laboratories

c.

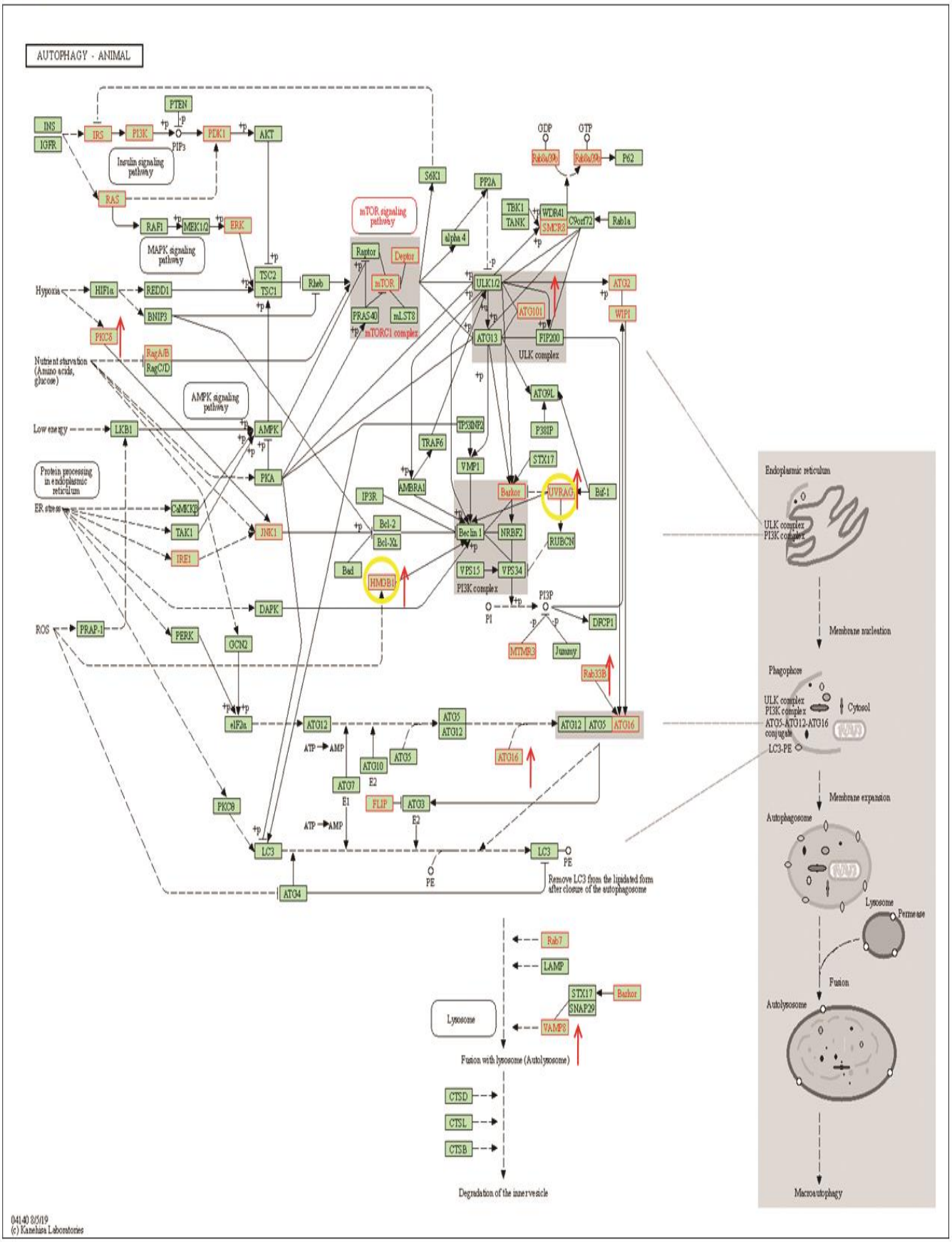
AUTOPHAGY - ANIMAL
INS
IGFR
IRS
PI3K
PIP3
PTEN
PDK1
AKT
Insulin signaling pathway
RAS
RAF1
MEK1/2
ERK
MAPK signaling pathway
TSC2
TSC1
Rheb
mTOR signaling pathway
Raptor
Deptor
mTOR
PRAS40
mLST8
mTORC1 complex
S6K1
PP2A
alpha 4
TBK1
TANK
WDR41
SMCR8
C9orf72
Rab1a
GDP
GTP
Rab8a/9b
Rab8a/9b
P62
ULK1/2
ATG101
ATG13
FIP200
ULK complex
ATG2
WIPI
ATG9L
Hypoxia
HIF1α
REDD1
BNIP3
PKC8
RagA/B
RagC/D
Nutrient starvation (Amino acids, glucose)
AMPK signaling pathway
Low energy
LKB1
AMPK
PKA
IPS3INP2
P38IP
TRAF6
VMP1
STX17
AMBRA1
Barkor
UVRAG
Bif-1
Protein processing in endoplasmic reticulum
ER stress
CaMKKβ
TAK1
IRE1
JNK1
IP3R
Bcl-2
Bcl-Xl
Bad
HMGB1
Beclin 1
NRBF2
RUBCN
VPS15
VPS34
PI3K complex
PI
PI3P
DRCP1
MTMR3
Jumpy
Rab33B
DAPK
ROS
PRAP-1
PERK
GCN2
eIF2α
ATG12
ATG5
ATG12
ATG5
ATG16
ATG16
ATP
AMP
ATG10
E2
ATG7
E1
FLIP
ATG3
E2
PKC8
LC3
LC3
PE
PE
ATG4
Remove LC3 from the lipidated form after closure of the autophagosome
Rab7
LAMP
STX17
SNAP29
Barkor
VAMP8
Lysosome
Fusion with lysosome (Autolysosome)
CTSD
CTSL
CTSB
Degradation of the innervesicle
041140 8/5/19
(c) Kanehisa Laboratories
Endoplasmic reticulum
ULK complex
PI3K complex
Membrane nucleation
Phagophore
ULK complex
PI3K complex
ATG5-ATG12-ATG16 conjugate
Cytosol
LC3-PE
Membrane expansion
Autophagosome
Lysosome
Permease
Fusion
Autolysosome
Macroautophagy

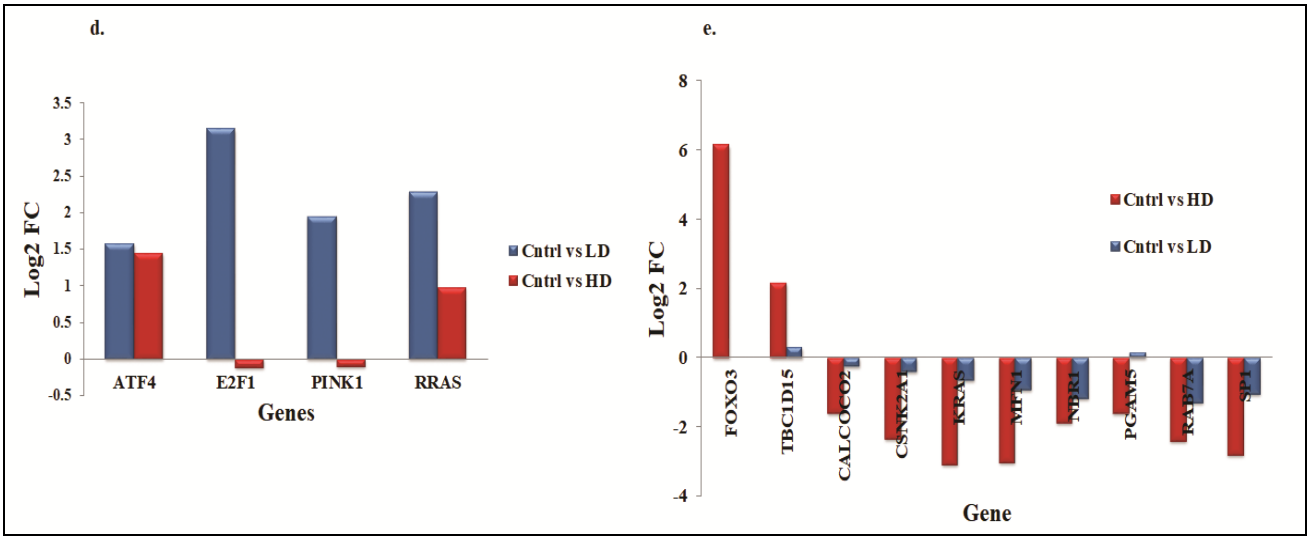

Figure AI.2.3 Comparative analysis of transcripts associated with degradation pathways. a Bar graph representing the number of differentially regulated transcripts associated with degradation related pathways upon cisplatin treatment in HT-29 cells. Autophagy KEGG pathway highlighting (red) the dysregulated genes in **b** Cntrl vs LD and **c** Cntrl vs HD set in HT-29 cells. Bar graph representing the differentially regulated mitophagy genes in **d** Cntrl vs LD and **e** Cntrl vs HD treatment set. Here, LD is low dose (30 µM) and HD is high dose (300 µM) of cisplatin. Genes with log2 Fold value ± 1.5 were considered as differentially regulated (up or down regulated).

AI.3 Conclusion

To the best of our knowledge, we are the first group to analyze dose-dependent comparison of transcriptomic profile of CRC cells after exposure to cisplatin. We also propose that varied dose of the drug results in differential transcriptomic response and hence a putatively diverse survival strategy. Overall, our preliminary study provides an understanding of distinct molecular signatures exhibited by the CRC cells after exposure to contrasting doses of the drug, which along with further deeper analysis, might facilitate the design of tailored therapy in future for maximum efficacy against resilient tumors like, CRC.

Appendix-II

AII.1. List of publications

AII.1.1 From the thesis

i. **Saini H.,** Sharma H, Mukherjee S, Chowdhury S, Chowdhury R. Verteporfin disrupts multiple steps of autophagy and regulates p53 to sensitize osteosarcoma cells. *Cancer Cell Int* **21,** 52 2021. **(Published)**

ii. **Saini H,** Hakeem I, Mukherjee S, Chowdhury S, Chowdhury R. Autophagy regulated by gain of function mutant p53 enhances proteasomal inhibitor-mediated cell death through induction of ROS and ERK in Lung cancer cells. J Oncol. 2019. **(Published)**

iii. **Saini H.,** Choudhary M, Sharma H, Mukherjee S, Chowdhury S, Chowdhury R. Chloroquine induces a transitory attenuation of proliferation through regulation of cytoskeletal organization, mutant P53 and YAP in NSCLCs. **(Submitted-under review)**

iv. **Saini H.,** Mukherjee S, Chowdhury S, Chowdhury R. Deciphering transcriptomic alterations associated with varied dose of cisplatin in drug resistant colorectal carcinoma. **(In pipeline)**

AII.1.2 Other Publications

i. K. Lohitesh, **H. Saini,** A. Srivastava, S. Mukherjee, A. Roy, and R. Chowdhury, "Autophagy inhibition potentiates SAHA-mediated apoptosis in glioblastoma cells by accumulation of damaged mitochondria," *Oncology Reports*, vol. 39, no. 6, pp. 2787–2796, 2018. **(Published)**

ii. P. Sengupta, S. Raman, R. Chowdhury, K. Lohitesh, **H. Saini**, S. Mukherjee, A. Paul "Evaluation of apoptosis and autophagy inducing potential of berberis aristata, Azadirachta indica, and their synergistic combinations in parental and resistant human osteosarcoma cells," *Frontiers in Oncology*, vol. 7, 2017. **(Published)**

iii. Leena Fageria, Vikram Pareek, R. Venkataramana Dilip, Arpit Bhargava, Sheik Saleem Pasha, Inamur Rahaman Laskar, **Heena Saini**, Subhra Dash, Rajdeep Chowdhury, and Jitendra Panwar, Biosynthesized protein-capped silver nanoparticles induce ROS-dependent pro-apoptotic signals and pro-survival autophagy in cancer cells. ACS Omega 2017, 2 (4): 1489-1504. **(Published)**

AII.2 List of conferences (Poster presented)

1. Saini H, Mukherjee S, Chowdhury S, Chowdhury R. Porphyrin Drug in combination with proteasomal inhibitor disrupts autophagy and protein homeostasis to sensitize cancer cells in a P53 dependent manner. **EMBO Workshop**, Autophagy: From molecular principles to human diseases in Crieff, Scotland**, United Kingdom** (2019)
2. Saini H, Hakeem I, Mukherjee S, Chowdhury S, Chowdhury R. Proteasomal Inhibitor mediated cell death in lung cancer cells with onset of ROS and ERK is enhanced by gain of function mutant P53 directed autophagy. International Conference on Life Science Research and its interface with engineering and allied sciences **(LSRIEAS 2018**), **BITS Pilani**. (**Appreciation Award)**
3. Saini H, Hakeem I, Mukherjee S, Chowdhury S, Chowdhury R. Proteasomal Inhibitor mediated cell death in lung cancer cells with onset of ROS and ERK is enhanced by gain of function mutant P53 directed autophagy. First National Biomedical Research Competition-2018. AIIMS, **Rishikesh, Uttarakhand**, 15th October 2018.
4. Saini H, Hakeem I, Mukherjee S, Chowdhury S, Chowdhury R. Proteasomal Inhibitor mediated cell death in lung cancer cells with onset of ROS and ERK is enhanced by gain of function mutant P53directed autophagy. **EMBO event**, Autophagy: Cellular mechanism(s) and significance in health and disease in **Bhubaneswar, India** (2017)
5. Saini H, Nagraj J, Mukherjee S, Chowdhury R. Dysregulation of ncRNAs - miRNAs and lncRNAs associated with acquisition of drug resistance in cancer cells. National Symposium on Current Research in Cancer Biology and Therapy **(CRCBT-2016**), UIAR-**Gandhinagar, Gujarat**. **(Best Poster Award).**

AII.3. Biographies

AII.3.1 A brief biography of the Supervisor

Dr. Rajdeep Chowdhury is currently working as Associate Professor, Department of Biological Sciences, BITS Pilani, Pilani Campus, Rajasthan. He earned his Bachelor's and Master's degrees from Calcutta University. In 2003 he joined Indian Institute of Chemical Biology, Molecular & Human Genetics Department, Kolkata, for his Ph.D. (CSIR-NET). He made significant contributions in the field of Cancer Biology and Toxicology with special emphasis on arsenic-induced carcinogenesis and its remediation during his Ph.D. He was awarded DBT Post-Doctoral Research Fellowship in 2008. In 2009, he joined Massachusetts Institute of Technology (MIT), USA, Department of Bioengineering, as a postdoctoral researcher, where he studied the myriad set of genetic events following Nitric Oxide (NO) exposure; his project extended from understanding the effects of NO-induced posttranslational modifications to its cancer-promoting effect and also its role in cell death mechanisms like Autophagy. In Oct 2012, he joined BITS-Pilani as an Assistant Professor. He has expertise in the field of cancer biology and is currently investigating causes of cancer drug resistance, emphasizing on autophagy. He has received research grants from various government funding authorities like (i) Department of Science and Technology (DST) under fast-track scheme of young scientist (ii) Science and Engineering Research Board (SERB) under Extra-Mural Research Funding (iii) University Grants Commission (UGC) under Minor Research Project (iv) Department of Biotechnology under Pilot Project and (v) Life Sciences Research Board (LSRB, DRDO) (vi) Indian Council of Medical Research (ICMR) (vii) and several other projects as co-PI as well. The findings from his works have been published in more than 25 international scientific journals. He has supervised 2 PhD students as PI. Presently, he is guiding 4 Ph.D. students as PI and 5 as Co-PI.

AII.3.2 A brief biography of the Co-Supervisor

Dr. Shibasish Chowdhury is currently working as Associate Professor, Department of Biological Sciences, BITS Pilani, Pilani Campus, Rajasthan. He earned his Master's degree in physical Chemistry from Calcutta University. Then shifted to biophysics and obtained Ph.D. degree from Molecular Biophysics Unit (MBU) at Indian Institute of Science, Bangalore on "Computer modelling studies on G-rich unusual DNA structure". Subsequently, entered into protein folding field and worked as postdoctoral research fellow in the Department of Chemistry and Biochemistry, University of Delaware, USA for three years. Broad area of his research interest is Structure-Function relationship of biomolecules, Protein folding, Modeling and Evolution, Bioinformatics. In 2004, he joined BITS-Pilani as a lecturer. From2006-2012, he worked as assistant professor in BITS-Pilani. He has received research grants from various government funding authorities like DST, ICMR etc. He has more than 25 publications and 4 book chapters. He has supervised 4 PhD students as PI and one as Co-PI. Presently, he is guiding 3 Ph.D. students as PI and 3 as Co-PI.

AII.3.3 A brief biography of the Candidate

Ms. Heena Saini has completed her B.Tech degree in Biotechnology from Banasthali University, Rajasthan, India. She has earned her M.Tech degree in Biotechnology as first rank holder from Maharishi Markandeshwar University, Mullana-Ambala, Haryana in the year 2014. She had her formal research training from one of the premier institutes in India-CSIR- IGIB, Delhi as a trainee in 2011 and then in 2014. She has also worked as a Senior Research Fellow in CSIR-IGIB in the year 2015. She joined BITS-Pilani, Pilani campus as a Ph.D. student in the year 2016, under the supervision of Prof. Rajdeep Chowdhury and Co-supervision of Prof. Shibasish Chowdhury. Her doctoral research is in the field of cancer biology, mutant P53 protein and autophagy. She has been awarded with Senior Research Fellowship from CSIR (accepted) and ICMR (not availed). She has presented her research work as posters in three international conferences and two national conferences where she has won best poster award and appreciation award. She has been awarded an international travel grant from DST (accepted) and ICMR (not availed) for poster presentation in an EMBO conference on autophagy and human diseases, held in Crieff, United Kingdom. She has published 5 research articles in peer-reviewed journals. She has qualified CSIR-UGC-NET 2019 for assistant professor. During her Ph.D., she was also involved in the teaching activities of the department by taking courses for first- and higher-degree students of BITS Pilani campus.